

Table of Contents

Andersson, J. . . . .	1
Barr, G.E. . . . .	2
Beauheim, R.L. . . . .	4
Butcher, B.M. . . . .	30
Christian-Frear, G.L. . . . .	45
Corbet, T.F. . . . .	46
Cranwell, R.M. . . . .	49
Dale, T. . . . .	57
Davies, P.B. . . . .	58
Dotson, L.J. . . . .	61
Earth Technology Corporation . . . . .	62
EPA (U.S. Environmental Protection Agency) . . . . .	64
Freeze, G.A. . . . .	73
Goodwin, B.W. . . . .	74
Hodgkinson, D.P. . . . .	75
Holt, R.M. . . . .	76
IAEA (International Atomic Energy Agency). . . . .	88
Iman, R.L. . . . .	90
Kaplan, S. . . . .	92
Lappin, A.R. . . . .	96



**Compliance Certification Application Reference Expansion**

---

Luker, R.S. . . . . .	99
Mercer, J.W. . . . . .	110
Miller, W.M. . . . . .	112
NAGRA . . . . .	114
OECD Nuclear Energy Agency. . . . .	115
Popielak, R.S. . . . . .	116
Sandia National Laboratories . . . . .	122
State of New Mexico, . . . . .	140
Stenhouse, M.J. . . . . .	141
Thorne, M.C. . . . . .	142
Van Pelt, R.S. . . . . .	144
Vaughn, P. . . . . .	145
Wallace, M.G. . . . . .	146
Wang, Y. . . . . .	147
<b>BIBLIOGRAPHY DOCUMENTS . . . . .</b>	<b>152</b>
Adams, J.E. . . . . .	153
Anderson, R.Y. . . . . .	154
Argüello, J.G. . . . . .	157
Bachman, G.O. . . . . .	158
Baes, C.F. . . . . .	168
Barker, D.S. . . . . .	169

Compliance Certification Application Reference Expansion

Bear, J. . . . . 170

Beauheim, R.L. . . . . 175

Bechtel National. . . . . 182

Bell, J.T. . . . . 183

Bellin, A. . . . . 185

Berger, A. . . . . 186

Bertram-Howery, S.G. . . . . 188

Bird, R.B. . . . . 191

Borns, D.J. . . . . 194

Bredehoeft, J.D. . . . . 199

Brush, L.H. . . . . 201

Buddemeier, R.W. . . . . 202

Burton, P.L. . . . . 203

Cauffman, T.L. . . . . 204

Chapman, J.B. . . . . 205

Chappell, J. . . . . 207

Chaturvedi, L. . . . . 208

Choppin, G.R. . . . . 209

Chugg, J.C. . . . . 210

Coats, K.H. . . . . 211

Cooper, J.B. . . . . 212



Compliance Certification Application Reference Expansion

Corbet, T.F. . . . . 213

Cranwell, R.M. . . . . 214

Davies, P.B. . . . . 215

Dearlove, J.P.L. . . . . 218

Doctor, P.G. . . . . 219

DOE (U.S. Department of Energy) . . . . . 220

Dowding, C.H. . . . . 231

Eager, G.P. . . . . 232

EPA (U.S. Environmental Protection Agency) . . . . . 233

Francis, A.J. . . . . 234

Freeland, M.H. . . . . 235

Freeze, R.A. . . . . 236

Galson, D.A. . . . . 237

Gonzales, M.M. . . . . 238

Griswold, G.B. . . . . 239

Hays, J.D. . . . . 240

Helton, J.C. . . . . 241

Hiemenz, P.C. . . . . 245

Hill, A.C. . . . . 246

Hills, J.M. . . . . 247

Holcomb, D.J. . . . . 248



**Compliance Certification Application Reference Expansion**

---

Hora, S.C. . . . .	249
Houghton, J.T. . . . .	251
Howard, C.L. . . . .	252
Hunter, R.L. . . . .	253
IAEA (International Atomic Energy Agency). . . . .	255
Imbrie, J. . . . .	256
Izett, G.A. . . . .	261
Jones, C.L. . . . .	262
Jones, T.L. . . . .	263
Jung, Y. . . . .	265
Kazemi, H. . . . .	266
Kelley, V.A. . . . .	267
Kim, J.I. . . . .	269
Lambert, S.J. . . . .	270
Lenhardt, W.A. . . . .	272
Litvak, B.L. . . . .	276
Lowenstein, T.K. . . . .	277
Lyklema, J. . . . .	280
Lyon, M.L. . . . .	281
Machette, M.N. . . . .	282
Maiti, T.C. . . . .	283



**Compliance Certification Application Reference Expansion**

---

Mansure, A. . . . .	284
Marietta, M.G. . . . .	285
McGrath E.J. . . . .	286
McKay, M.D. . . . .	289
Mercer, J.W. . . . .	290
Mitchell, J.F.B. . . . .	292
Molecke, M.A. . . . .	293
Muehlberger, W.R. . . . .	294
Myers, J. . . . .	295
Nicholson, Jr., A. . . . .	296
Nowak, E.J. . . . .	297
OECD Nuclear Energy Agency. . . . .	298
Parry, G.W. . . . .	299
Paté-Cornell, M.E. . . . .	300
Pfeifer, M.C. . . . .	301
Powers, D.W. . . . .	302
Rechard, R.P. . . . .	304
Richey, S.F. . . . .	306
Robinson, J.Q. . . . .	307
Robinson, T.W. . . . .	308
Rosholt, J.N. . . . .	310



Compliance Certification Application Reference Expansion

Sandia National Laboratories. . . . . 311

Saulnier, G.J. . . . . 312

Schiel, K.A. . . . . 315

Schlesinger, M.E. . . . . 317

Sewards, T. . . . . 319

Shinta, A.A. . . . . 320

Silva, M. . . . . 321

Slezak, S. . . . . 324

Snyder, R.P. . . . . 325

Stensrud, W.A. . . . . 327

Stone, C.M. . . . . 329

Stormont, J.C. . . . . 330

Telander, M.R. . . . . 333

Thorne, B.J . . . . . 334

Tierney, M.S. . . . . 335

Tiller, C.L. . . . . 337

Tipping, E. . . . . 338

Tóth, L.M. . . . . 339

Van der Lee, J. . . . . 340

Van Sambeek, L.L. . . . . 341

Vesely, W.E. . . . . 342



**Compliance Certification Application Reference Expansion**

---

Vilks, P. . . . .	343
Vine, J.D. . . . .	344
Vlassopoulos, D. . . . .	346
Wallner, M. . . . .	347
Warrick, R. . . . .	348
Washington, W.M. . . . .	349
Weatherby, J.R. . . . .	351
Westinghouse Electric Corporation. . . . .	352
Wilson, C.A. . . . .	353
Wolery, T.J. . . . .	354
Wood, B.J. . . . .	356
Zoback, M.D. . . . .	357
INDEX . . . . .	358





Andersson, J., Ed. 1989. The Joint SKI/SKB Scenario Development Project. SKB Technical Report 89-35, Authors: J. Andersson, T. Carlsson, T. Eng, F. Kautsky, E. Söderman, and S. Wingefors. Swedish Nuclear Fuel and Waste Management Co., Stockholm, Sweden.

ABSTRACT; p. 1, para. 1;

" The Swedish Nuclear Power Inspectorate (SKI) and the Swedish Nuclear Waste Management Co. (SKB) have carried through a joint scenario development exercise of a hypothetical repository for spent nuclear fuel and high level waste based on the KBS-3 concept as disposal method.

The starting point of the scenario development strategy has been the "Sandia Methodology", but the actual implementation of the steps in this method has required new strategy development. The work started with a relatively large internationally composed group meeting, which identified an extensive list (approximately 150 items) of features, events and processes (FEPs) that might influence the long term performance of a repository. All these FEPs and a memo-text containing a description of the FEP as well as its possible causes and consequences have been entered into a computer database.

The next step in the development was to remove from the list approximately 30 FEPs of low probability or negligible consequence. In a following step a large number of the FEPs on the original list were assigned to the "PROCESS SYSTEM". The PROCESS SYSTEM comprises the complete set of "deterministic" chemical and physical processes that might influence the release from the repository to the biosphere. A scenario is defined by a set of external conditions which will influence the processes in the PROCESS SYSTEM.

Approximately 50 FEPs were left representing external conditions. These remaining FEPs have been grouped (lumped) into a few (10) primary FEPs of external conditions. The remaining FEPs could all be combined to form scenarios, but it is concluded that it is not meaningful to discuss combinations without first analyzing the consequence and probability of the individual conditions.

An important aspect of the work is that the developed strategy includes a framework for the documentation of the complete chain of scenario development. Such a transparent documentation makes possible an extensive review and updating of the set of scenarios. A reviewing process, open to very broad groups in the society, is probably the best means of assuring reasonable completeness and of building up a general consensus on what are the critical issues for the safe disposal of radioactive waste.

In conclusion, the strategy developed within the project appear to be a feasible approach to scenario development, but it must be stressed that the present project is a first stage and that the complete analysis must be reiterated several times."

Barr, G.E., Miller, W.B., and Gonzalez, D.D. 1983. Interim Report on the Modeling of the Regional Hydraulics of the Rustler Formation. SAND83-0391. Sandia National Laboratories, Albuquerque, NM, pp. 26-27. WPO 27557.

ABSTRACT, pp 3-4;

" The finite-element code ISOQUAD was used to simulate the head distribution within the two major water-bearing units of the Rustler Formation at the Waste Isolation Pilot Plant (WIPP), the Magenta and Culebra dolomites. The derived surfaces correlate well with those generated manually by the US Geological Survey (USGS) and Sandia National Laboratories (SNL). Calculated migration of a continuously injected contaminant from an assumed smeared point source at the center of the site was observed in terms of concentration relative to the initial input. Migration rates of specific concentration fronts decreased with increasing time. The average rate of movement of the  $10^{-3}$  relative concentration contour was less than 10 m/yr for the first 800 yr in the Culebra Dolomite. By 800 yr, the migration of this concentration front has essentially ceased. In the case of the Magenta Dolomite, the average rate of movement of the  $10^{-3}$  relative concentration contour was 0.44 m/yr for the first 676 yr of continuous contaminant injection; the contaminant plume in the Magenta shows little movement thereafter. For reasons of scale, the plume calculation overestimates the actual rate of movement of contaminants. Particle velocities for selected streamlines, more characteristic of contaminant movement, are calculated in Appendix B for comparison with the results of the FEIS. These particle velocities indicate groundwater travel times of ~130 000 yr from the center of the WIPP site to a distance of 12.9 km (8 mi).

The validity of the porous-medium approximation of the Rustler aquifers was examined by the evaluation of the drawdown portion of aquifer pump tests. Drawdown curves were successfully duplicated as a function of hydraulic conductivity, storativity, and well radius. Estimation of the effective radius examined in each well test indicates that there are no significant fluid-bearing fractures or channels within 60 m of tested wells. Because of variable test duration and in situ hydraulic properties, effective radii tested range from 37 to 1500 m (see Appendix A)."

Magenta Unit; p. 26, col. 2;

" The data for the Magenta for the 16 mi x 16 mi region modeled consist of water level measurements, slug tests, and pumptests at 10 different locations. The wells measured were H-1, H-2, H-3, H-4, H-5, H-6, H-9, H-10, W-25 and W-27. In addition there are two holes, W-26 and W-28, where the Magenta did not yield water to a well. At W-29 the Magenta Unit is not present due to erosion. The Magenta Unit is similar in character to the Culebra and is discussed by Gonzalez (1983a). This unit was not tested for anisotropy and so is presumed for the purposes here to be isotropic, although transport is so slight that this presumption is essentially irrelevant. Values for the hydraulic conductivity are assigned as shown in Figure 15, except for W-26 and W-28, which were dry and were given an extremely small value of conductivity. The initial head distribution calculated with a reflecting boundary and fixed well head values is shown in Figure 16. The corresponding



## Compliance Certification Application Reference Expansion

---

self-consistent head distribution or potentiometric surface derived in these calculations is shown in Figure 17, and the corresponding derived values for the hydraulic conductivity are listed in Table 2. The head potential exhibits the steepest gradients in the vicinity of Nash Draw, to the west of the site. The repository site is indicated by the 8-sided figure (Figure 16). The smaller square inside this figure is a cutout used for a plume calculation in the manner of that discussed for the Culebra with the same concentration input. The cutout is a 2.4 x 2.4 km (1.5 x 1.5 mi) block with 289, 150 x 150 m (492 x 492 ft) elements. A plume is assumed to have formed around a central continuous source of contaminant. The initial plume is shown in Figure 18. The extent of the plume 676 yr later is shown in Figure 19, amounting to less than 300 m (1000 ft) growth in that period (0.44 m/yr). There is so little movement in this long period, and much of that movement appears to be numerical dispersion, that it seems pointless to transfer the plume to subsequent cutouts as was done for the Culebra. To check this conclusion, we assigned to the large-size problem, 25.8 x 25.8 km (16 x 16 mi), so that the plume clearly overlapped the region of highest gradients. The results were similar; in effect, no movement on the 1610 x 1610 m (1 x 1 mi) grid scale of the calculations. This calculation is not shown. Unless the well data change substantially, or new data are added, it seems inappropriate to examine the Magenta Unit further."



Beauheim, R.L., 1987. Interpretations of Single-Well Hydraulic Tests Conducted At and Near the Waste Isolation Pilot Plant (WIPP) Site, 1983-1987. SAND87-0039. Sandia National Laboratories, Albuquerque, NM, pp. 110-118. WPO 27679.

ABSTRACT, p 3, para 1;

" Both single-well and multiple-well hydraulic tests have been performed in wells at and near the WIPP site as part of the site hydrogeologic-characterization program. The single-well tests conducted from 1983 to 1987 in 23 wells are the subject of this report. The stratigraphic horizons tested include the upper Castile Formation; the Salado Formation; the unnamed, Culebra, Tamarisk, Magenta, and Forty-niner Members of the Rustler Formation; The Dewey Lake Red Beds; and Cenozoic alluvium. Tests were also performed to assess the integrity of a borehole plug isolating a pressurized brine reservoir in the Anhydrite III unit of the Castile Formation. The types of tests performed included drillstem tests (DST's), rising-head slug tests, falling-head slug tests, pulse tests, and pumping tests."

The Castile and Solado testing was performed at well WIPP-12 to try to define the source of high pressures measured at the WIPP-12 wellhead between 1980 and 1985. The test of the plug above the Castile brine reservoir indicated that the plug may transmit pressure, but if so, the apparent surface pressure from the underlying brine reservoir is significantly lower than the pressure measured at the wellhead. The remainder of the upper Castile did not show a pressure response differentiable from that of the plug. All attempts at testing the Salado in WIPP-12 using a straddle-packer DST tool failed because of an inability to locate good packer seats. Four attempts to test large sections of the Salado using a single-packer DST tool and a bridge plug were successful. All zones tested showed pressure buildups, but none showed a clear trend to positive surface pressures. The result of the WIPP-12 testing indicate that the source of the observed high pressures is within the Salado Formation rather than within the upper Castile Formation and that this source must have a very low flow capacity and can only create high pressures in a well shut in over a period of days to weeks.

DST's performed on the lower siltstone portion of the unnamed lower member of the Rustler Formation at H-16 indicated a transmissivity for the siltstone of about  $2.4 \times 10^{-4}$  ft<sup>2</sup>/day. The formation pressure of the siltstone is higher than that of the overlying Culebra at H-16 (compensated for the elevation difference), indicating the potential for vertical leakage upward into the Culebra. However, the top of the tested interval is separated from the Culebra by over 50 ft of claystone, halite, and gypsum.

The Culebra Dolomite Member of the Rustler Formation was tested in 22 wells. In 12 of these wells (H-4c, H-12, WIPP-12, WIPP-18, WIPP-19, WIPP-21, WIPP-22, WIPP-30 P-15, P-17, ERDA-9, and Cabin Baby-1), falling-head slug tests were performed in H-1, and only a rising-head slug test was performed in P-18. DSTs were performed in conjunction with rising-head slug tests in wells H-14, H-15, H-16, H-17, and H-18. At all of these wells except H-18, the indicated transmissivities were 1 ft<sup>2</sup>/day or less and single-porosity models fit the data well. At H-18, the Culebra has a transmissivity of about 2 ft<sup>2</sup>/day. The apparent single-porosity behavior of the Culebra at H-18 may be due to the small spatial scale of the





tests rather than to the intrinsic nature of the Culebra at that location. Pumping tests were performed in the other 3 Culebra wells. The Culebra appears to behave hydraulically like a double-porosity medium at wells H-8b and DOE-1, where transmissivities are 8.2 and 11 ft<sup>2</sup>/day, respectively. The Culebra transmissivity is highest, 43 ft<sup>2</sup>/day, at the Engle well. No double-porosity behavior was apparent in the Engle drawdown data, but the observed single-porosity behavior may be related more to wellbore and near-wellbore conditions than to the true nature of the Culebra at that location.

The claystone portion of the Tamarisk Member of the Rustler Formation was tested in wells H-14 and H-16. At H-14, the pressure in the claystone failed to stabilize in three days of shut-in testing, leading to the conclusion that the transmissivity of the claystone is too low to measure in test performed on the time scale of days. Similar behavior at H-16 led to the abandonment of testing at that location as well.

The Magenta Dolomite Member of the Rustler Formation was tested in wells H-14 and H-16. At H-14, examination of the pressure response during DSTs revealed that the Magenta had taken on a significant overpressure skin during drilling and Tamarisk-testing activities. Overpressure-skin effects were less pronounced during the drillstem and rising-head slug tests performed on the Magenta at H-16. The transmissivity of the Magenta at H-14 is about  $5.5 \times 10^{-3}$  ft<sup>2</sup>/day, while at H-16 it is about  $2.7 \times 10^{-2}$  ft<sup>2</sup>/day. The static formation pressures calculated for the Magenta at H-14 and H-16 are higher than those of the other Rustler members.

The Forty-niner Member of the Rustler Formation was tested in wells H-14 and H-16. Two portions of the Forty-niner were tested at H-14: the medial claystone and the upper anhydrite. DST's and a rising-head slug test were performed on the claystone, indicating a transmissivity of about  $7 \times 10^{-2}$  ft<sup>2</sup>/day. A buildup test of the forty-niner anhydrite revealed a transmissivity too low to measure on a time scale of days. a pulse test, DST's, and a rising-head slug test of the Forty-niner clay at H-16 indicated a transmissivity of about  $5.3 \times 10^{-3}$  ft<sup>2</sup>/day. Formation pressures estimated for the Forty-niner at H-14 and H-16 are lower than those calculated for the Magenta (compensated for the elevation differences), indicating that water cannot be moving downwards from the Forty-niner to the Magenta at these locations. . . ."

Section 5.2.1 Unnamed Lower Member., p 50, col 1, para 4;

" The unnamed lower member of the Rustler was tested only at H-16. This testing had two objectives: 1)to determine the transmissivity of the unit; and 2) to determine the hydraulic head of the unit. The transmissivity is a parameter needed to calculate potential leakage rates from the unnamed lower member into the WIPP shafts. The hydraulic head is also needed for leakage calculations, as well as to evaluate directions of potential vertical movement of groundwaters within the Rustler Formation. . . ."

p 50, col 2, para 4;

" The simulation in Figure 5-12 is of a single-porosity medium with a transmissivity of  $2.7 \times 10^{-4}$  ft<sup>2</sup>/day (Table 5-2). Assuming a porosity of 30%, a total-system compressibility of

## Compliance Certification Application Reference Expansion

---

$1.0 \times 10^{-5} \text{ psi}^{-1}$ , and a fluid viscosity of 1.0 cp, the skin factor for the well in this simulation is -0.4, indicating a very slightly stimulated well. The dimensionless Horner plot of the FBU (Figure 5-13) shows an excellent fit of the simulation to the data, and indicates that the static formation pressure is about 213 psia.

The SLF lasted about 29 minutes, and was followed by a 50-hr SBU. The log-log plot of the SBU data (Figure 5-14) shows behavior similar to that seen in the FBU plot (Figure 5-12). The single-porosity simulation shown, however, uses a transmissivity of  $2.2 \times 10^{-4} \text{ ft}^2/\text{day}$ , and a skin factor of 0.2 (Table 5-2). These values imply a slightly less permeable formation and a slightly more damaged well than were indicated by the FBU analysis."

$$\frac{2.7 \times 10^{-4} \text{ft}^2}{\text{day}} \times \frac{12^2 \text{in}^2}{\text{ft}^2} \times \frac{\text{m}^2}{39.3^2 \text{in}^2} \times \frac{\text{day}}{24 \text{ hour}} \times \frac{\text{hour}}{3600 \text{ sec.}} = \frac{2.9 \times 10^{-10} \text{m}^2}{\text{second}}$$

$$\frac{2.2 \times 10^{-4} \text{ft}^2}{\text{day}} \times \frac{12^2 \text{in}^2}{\text{ft}^2} \times \frac{\text{m}^2}{39.3^2 \text{in}^2} \times \frac{\text{day}}{24 \text{ hour}} \times \frac{\text{hour}}{3600 \text{ sec.}} = \frac{2.4 \times 10^{-10} \text{m}^2}{\text{second}}$$



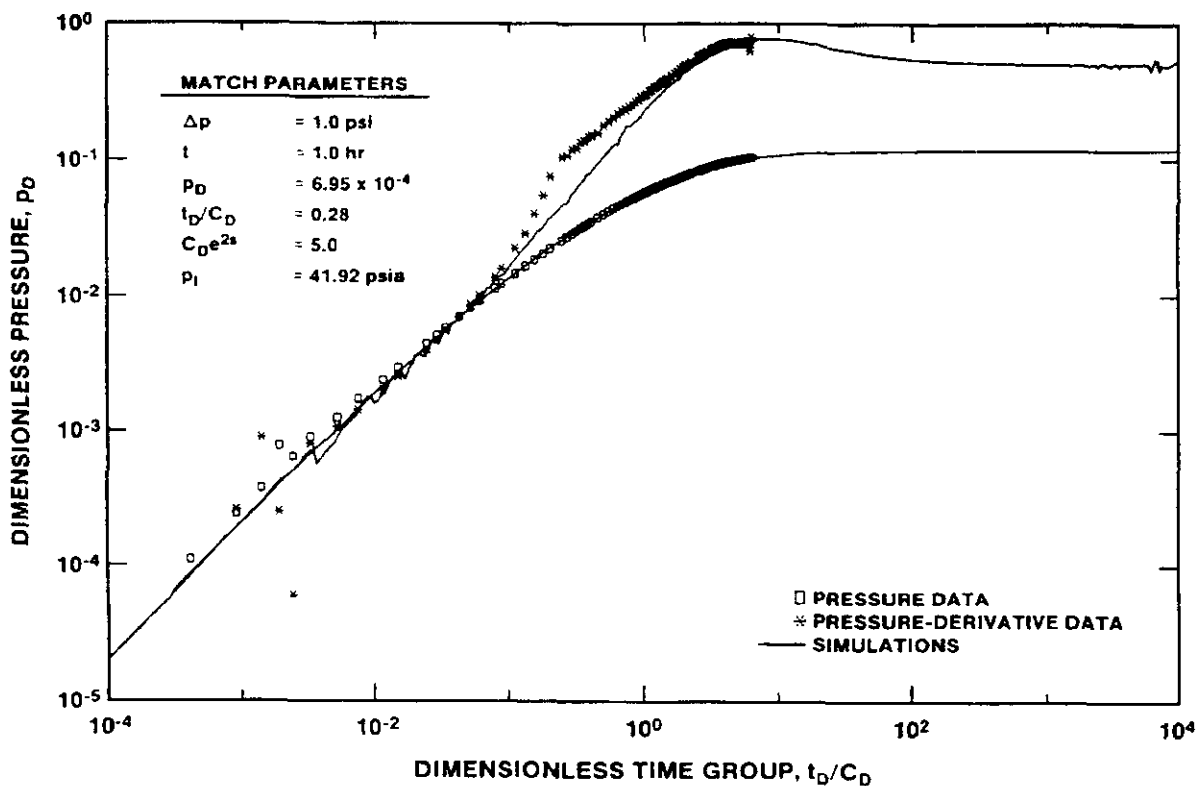


Figure 5-12. H-16/Unnamed Lower Member Siltstone First Buildup Log-Log Plot with INTERPRET Simulation



Compliance Certification Application Reference Expansion

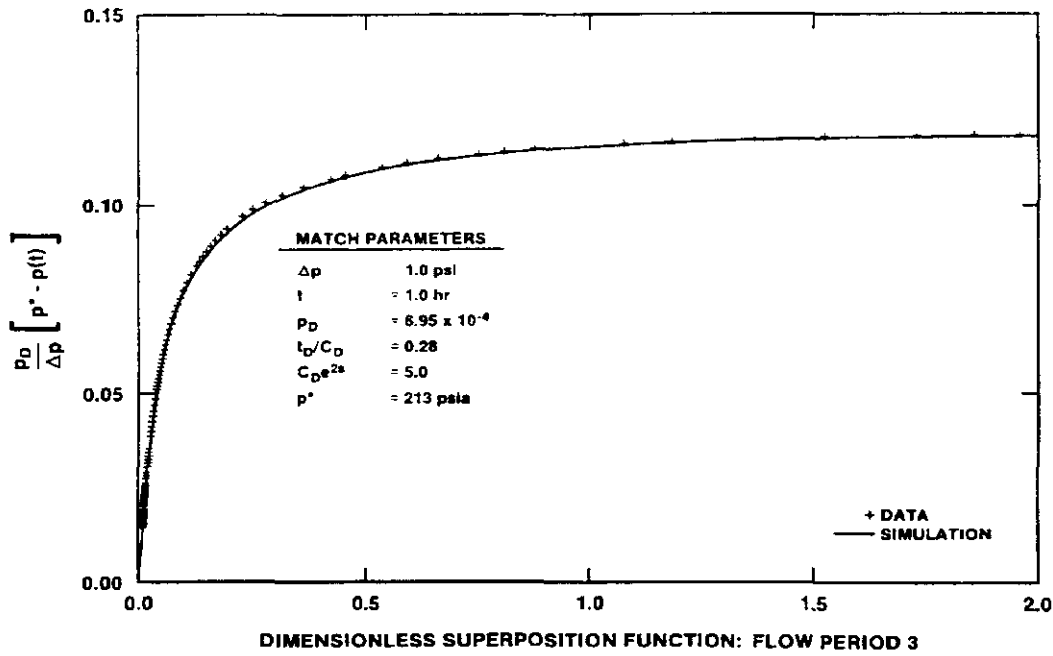


Figure 5-13. H-16/Unnamed Lower Member Siltstone First Buildup Dimensionless Horner Plot with INTERPRET Simulation

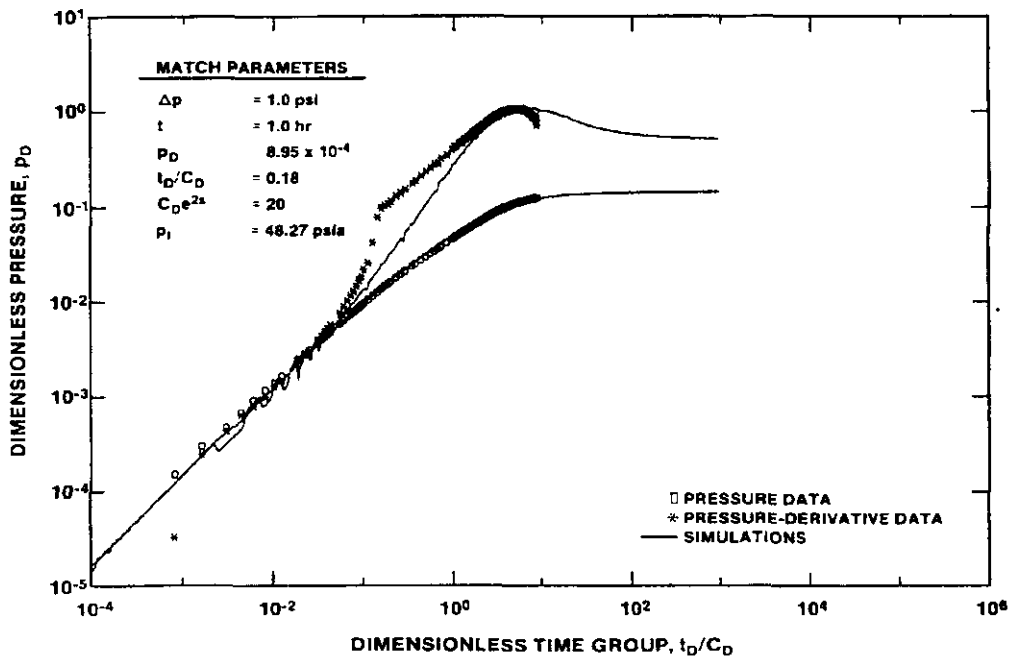


Figure 5-14. H-16/Unnamed Lower Member Siltstone Second Buildup Log-Log Plot with INTERPRET Simulation

**Compliance Certification Application Reference Expansion**

**TABLE 5-2  
SUMMARY OF NON-CULEBRA SINGLE-WELL TEST RESULTS**

<u>WELL</u>	<u>ZONE NAME</u>	<u>ZONE DEPTH INTERVAL (ft)</u>	<u>DEPTH INTERVAL TESTED (ft)*</u>	<u>TEST TYPE</u>	<u>TRANSMISSIVITY (ft<sup>2</sup>/day)</u>	<u>SKIN FACTOR</u>
H-16	Unnamed lower member siltstone	778-842	739-851	DST/FBU	2.7x10 <sup>-4</sup>	-0.4
				DST/SBU	2.2x10 <sup>-4</sup>	0.2
H-14	Magenta	424-448	420-448	DST/FBU	5.6x10 <sup>-3</sup>	0.5
				DST/SBU	5.6x10 <sup>-3</sup>	0.4
				DST/TBU	5.3x10 <sup>-3</sup>	0.3
H-16	Magenta	590-616	589-621	DST/FBU	2.8x10 <sup>-2</sup>	-0.4
				DST/SBU	2.8x10 <sup>-2</sup>	-0.8
				slug	2.4x10 <sup>-2</sup>	-
H-14	Forty-niner claystone	390-405	381-409	DST/FBU	7.1x10 <sup>-2</sup>	3.2
				DST/SBU	6.9x10 <sup>-2</sup>	3.3
				slug	3.0x10 <sup>-2</sup>	-
H-16	Forty-niner clay	563-574	560-581	pulse	2.2x10 <sup>-4</sup>	-
				DST/FBU	5.3x10 <sup>-3</sup>	0.7
				DST/SBU	5.6x10 <sup>-3</sup>	0.6
				slug	5.0x10 <sup>-3</sup>	-
Carper	Cenozoic alluvium	263-386	263-386	pumping	55	-

\*Actual intervals open to the wells.



p. 73;

"Conclusions: The Culebra is 26.5 ft thick at H-14. The transmissivity of the upper 5.8 ft is 0.10 ft<sup>2</sup>/day, while that of the entire unit is 0.30 ft<sup>2</sup>/day. Hence, the average hydraulic conductivity of the upper 5.8 ft of the Culebra appears to be about 1.8 times greater than that of the lower 20.7 ft. This difference does not represent a great degree of heterogeneity."

Section 5.2.3 Tamarisk Member, p. 108, col. 1, para 2;

" The Tamarisk Member of the Rustler Formation was tested in wells H-14 and H-16. The purposes of the Tamarisk testing were to: 1) define the hydraulic head of the unit; and 2) measure the transmissivity of the unit. Information on the hydraulic head of the Tamarisk is needed to evaluate potential direction of vertical movement of groundwater between the Rustler members. The transmissivity of the Tamarisk is a parameter needed for vertical cross-sectional or three-dimensional modeling of groundwater flow in the Rustler. The claystone/mudstone/siltstone portion of the Tamarisk (referred to hereafter simply as the claystone) is believed to be more permeable than the anhydrite/gypsum sections, and therefore easier to test. Consequently, tests were attempted only on the claystone portion of the Tamarisk at H-14 and H-16.

5.2.3.1 H-14.

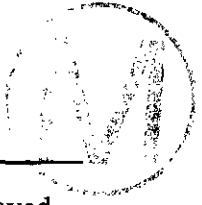
At H-14, the Tamarisk claystone extends from about 517 to 525 ft deep (Figure 3-6). The initial test was performed over an interval from the base of a packer at a depth of 494.5 ft to the then-bottom of the hole 533 ft deep. Thus, the test interval included the 8-ft thickness of claystone, and 30.5 ft of overlying and underlying anhydrite and gypsum. Descriptions of the test instrumentation and the test data are contained in Stensrud et al. (1987).

Testing began on October 7, 1986, by setting the packer, swabbing the tubing to decrease the pressure in the test interval, and closing the shut-in tool to isolate the test interval and allow the test-interval pressure to recover and equilibrate at the existing static formation pressure. The pressure response observed during the testing is shown in Figure 5-82. After being shut in for nearly 37 hr, the fluid pressure in the Tamarisk claystone test interval had still not stabilized, but was rising at an ever-decreasing rate. The pressure in the wellbore above the packer, in contrast, was dropping as fluid was apparently entering the exposed Magenta and Forty-niner Members. Because the Tamarisk pressure had not stabilized, and did not appear likely to stabilize for several days or weeks, no drillstem tests were performed.

To verify that the observed response during the shut-in period was representative of the Tamarisk claystone and not caused by a tool malfunction, the packer was deflated and the DST tool was reset 8 ft deeper in the hole on October 9, 1986. After swabbing and shutting in the new test interval, a pressure buildup similar to that observed at the previous depth was measured for 4.5 hr (Figure 5-82). At this point, we concluded that the permeability of the Tamarisk at H-14 is too low to allow testing on the time scale of a few days, and abandoned the effort.

No conclusions about the static formation pressure of the Tamarisk can be drawn





from the observed pressure buildups, because we have no way of evaluating the role played by the overpressure skin that was probably created during drilling. Subsequent testing of the Magenta and Forty-niner Members, discussed below, revealed fluid-pressure buildups to be significantly affected by overpressure skins.

#### 5.2.3.2 H-16

At H-16, the Tamarisk claystone extends from 677.5 to 690.1 ft deep (Figure 3-8). The interval tested extended from 674.5 to 697.9 ft, the bottom of the hole at that time, thus including 10.8 ft of overlying and underlying gypsum. Descriptions of the test instrumentation and the test data are presented in Stensrud et al. (1988).

Testing was performed on August 5, 1987. After the packer was set, the tubing was swabbed and the shut-in tool was opened to relieve the pressure that had been exerted on the formation by the column of drilling fluid in the well. The test interval was then shut in to allow the wellbore and formation pressures to equilibrate. Figure 5-83 shows the slow pressure rise that resulted over the next 10 hr. This pressure recovery was very similar to that observed for the Tamarisk claystone at H-14 (Figure 5-82). Based on the similarity to the H-14 response and the conclusion that the Tamarisk could not be tested on the time scale of a few days at H-14, the testing effort at H-16 was abandoned.

This decision was borne out by subsequent pressure measurements made by the transducer installed at the Tamarisk horizon as part of the 5-packer installation in H-16 (Figure 3-8). From August 31, 1987, 4 days after the 5-packer installation was completed, until December 15, 1987, the pressure in the Tamarisk interval declined from 204 psig to 169 psig (Stensrud et al., 1988 and in preparation), with complete stabilization apparently several months in the future. The Tamarisk transducer in the 5-packer system is mounted at a depth of 647.1 ft. IN a borehole containing brine with a specific gravity of 1.2, the pressure at the midpoint of the Tamarisk claystone 684 ft deep is about 19 psi higher than that measured by the transducer. Hence, the most that can be said at present is that the static formation pressure of the Tamarisk is less than 188 psig. The very slow pressure stabilization of the Tamarisk claystone likely indicates that its transmissivity is one or more orders of magnitude lower than that of the least-transmissive unit successfully tested in H-16, the unnamed lower member siltstone ( $2 \times 10^{-4}$  ft<sup>2</sup>/day; Table 5-2)."

Section 5.2.4 Magenta Dolomite Member, p. 110, col. 1, para. 2;

" The Magenta dolomite was tested in wells H-14 and H-16. The objectives of the Magenta testing were to obtain quantitative information on the hydraulic head and transmissivity of the unit."

Section 5.2.4.1 H-14, p 111, col 1, para 2, line 3;

" The simulation is representative of a single-porosity medium with a transmissivity of  $5.6 \times 10^{-3}$  ft<sup>2</sup>/day (Table 5-2). Assuming a porosity of 20%, a total-system compressibility of  $1.0 \times 10^{-5}$  psi<sup>-1</sup>, and a fluid viscosity of 1.0 cp, the skin factor of this simulation is about 0.5 indicating a well with very little wellbore damage. The simulation does not fit the observed early-time data very well, but it does fit the middle- and late-time pressure data adequately."

Section 5.2.4.2 H-16, page 115, col 2, para 2, line 3;

" The simulation is representative of a single-porosity medium with a transmissivity of  $2.8 \times 10^{-2} \text{ft}^2/\text{day}$  (Table 5-2). Assuming a porosity of 20%, a total system compressibility of  $1.0 \times 10^{-5} \text{psi}^{-1}$ , and a fluid viscosity of 1.0 cp, the skin factor for this simulation is -0.4, indicating a very slightly stimulated well. The pressure derivative shows oscillations similar, although with much lower amplitudes, to those observed in the H-14 Magenta SBU and TBU data (Figures 5-87 and 89)."

Section 5.2.5 Forty-niner Member, p. 119;

" The Forty-niner Member of the Rustler Formation was tested in wells H-14 and H-16. The objectives of the testing were to obtain hydraulic-head and transmissivity estimates. The hydraulic-head measurements are particularly important in helping to determine whether or not water from the Dewey Lake Red Beds, and by extension from the surface, can be recharging the Magenta and Culebra dolomites at the WIPP site. The transmissivity estimates allow an evaluation of the ability of the Forty-niner to provide water to the WIPP shafts, as well as providing data for cross-sectional or three-dimensional modeling of groundwater flow in the Rustler.

5.2.5.1 H-14.

Two sets of Forty-niner tests were performed at H-14, tests of the medial claystone/mudstone/siltstone unit (hereafter referred to simply as claystone) and tests of the upper anhydrite unit. The claystone tests were to provide data on the hydraulic head and transmissivity of the most permeable section of the Forty-niner. The anhydrite tests were intended to verify the assumptions that the Rustler anhydrites are much less permeable than the claystones, and that they cannot be tested on the time scale of days.

Forty-niner Claystone:

At H-14, the claystone portion of the Forty-niner lies between 390 and 405 ft deep (Figure 3-6). The claystone was tested in a DST straddle interval extending from 381.0 to 409.5 ft deep. Thus, about 13.5 ft of Forty-niner anhydrite and gypsum were included in the test interval. Descriptions of the test instrumentation and the test data are contained in Stensrud et al. (1987).

The Forty-niner claystone was tested on October 13 and 14, 1986. Testing consisted of two flow periods, two buildup periods, and a rising-head slug test (Figure 5-95). The FFL lasted about 18 minutes, and was followed by a 92-minute FBU. The SFL lasted about 32 minutes, and was followed by a SBU almost 16 hr long. To obtain equivalent constant-rate flow periods, each of the flow periods was divided into two shorter periods. The FFL was divided into two periods with flow rates of 0.028 and 0.021 gpm, and the SFL was divided into periods with flow rates of 0.022 and 0.017 gpm (Table 5-1). The slug test lasted slightly over 6 hr, by which time about 57% of the induced pressure differential had dissipated.

Overpressure skin effects were apparent during the Forty-niner claystone testing, just as they were during all other testing at H-14. The fluid pressure reached a maximum of 67.9 psia during the initial equilibration period, was essentially constant at 66.8 psia at the





end of the FBU, and peaked at 66.2 psia during the SBU (Figure 5-95). The superposition of pressure-skin effects manifested in the Magenta test data (see Section 5.2.4.1) was not apparent, however, in the Forty-niner claystone test data.

Figure 5-96 shows a log-log plot of the Forty-niner claystone FBU data with an INTERPRET-generated simulation. The late-time pressure derivative shows the decline indicative of overpressure skin. The simulation is representative of a single-porosity medium with a transmissivity of  $7.1 \times 10^{-2}$  ft<sup>2</sup>/day (Table 5-2). Assuming a porosity of 30%, a total-system compressibility of  $1.0 \times 10^{-5}$  psi<sup>-1</sup>, and a fluid viscosity of 1.0 cp, the skin factor for this simulation is about 3.2, indicating a damaged well.

The dimensionless Horner plot of the FBU data is shown in Figure 5-97. The simulation matches the observed data very well until late time, when the data deviate towards a static pressure lower than the 67.8 psia specified for the simulation. This discrepancy between the observed data and the simulation is entirely consistent with the effects of an overpressure skin.

The log-log plot of the SBU data is shown in Figure 5-98. Overpressure-skin effects are once again evident in the late-time pressure derivative. The simulation shown was generated by INTERPRET using a single-porosity model and a transmissivity of  $6.9 \times 10^{-2}$  ft<sup>2</sup>/day (Table 5-2). With the assumed parameter values listed above, the skin factor for this simulation is about 3.3, comparable to the value obtained from the FBU analysis.

A log-log early-time plot of the rising-head slug-test data is shown in Figure 5-99, along with the best-fit type curve. The fit is quite good until near the end, when the observed data oscillate for an unknown reason. The type-curve fit shown provides a transmissivity estimate of  $3.0 \times 10^{-2}$  ft<sup>2</sup>/day (Table 5-2), which is slightly less than half of the values provided by the FBU and SBU analyses. A slightly different type-curve fit might have been indicated had the late-time data been better behaved.

The static formation pressure for the Forty-niner claystone is difficult to estimate because of the overpressure-skin effects present during the buildup tests, and because of the nonideal behavior during the latter portion of the slug test. The static formation pressure must be less than the final pressure measured at the end of the SBU, 65.5 psia. The slug-test analysis relied on a static formation pressure estimate of 62 psia, although a reasonably good fit was also obtained using an estimate of 65 psia. Considering that the transducer during these tests was set 362.9 ft deep, that the transducer measured an atmospheric pressure of 12 psia before testing began, and that the borehole contained brine with a specific gravity of 1.2, 65 psia corresponds to a static formation pressure of 71 psig at the midpoint of the claystone 398 ft deep. This value is reliably a maximum.

#### Forty-niner Anhydrite.

The upper anhydrite and gypsum unit of the Forty-niner Member lies 359.5 to 390 ft deep at H-14 (Figure 3-6). The unit is roughly 75% anhydrite and 25% gypsum, based on interpretation of a neutron log. The unit was tested in a DST straddle interval extending from 356.0 to 384.5 ft deep. Thus, the bottom 3.5 ft of the Dewey Lake Red Beds and the Dewey Lake/Rustler contact were included in the test interval. Descriptions of the test instrumentation and the test data are contained in Stensrud et al. (1987).

The Forty-niner anhydrite was tested from October 14 to 15, 1986. Because the anhydrite was expected to have too low a permeability to allow quantitative testing the few days available for testing, no pressure-equilibration period preceded the testing. Instead, as soon as the packers were set, the tubing was swabbed with the shut-in tool open, and the test interval was left open to the tubing for about 16 minutes for a flow period (Figure 5-100). Very little fluid entered the tubing at this time. The test interval was then shut in for about 16.5 hr. The pressure increased by about 1 psi over the first 1.5 hr of the buildup, and by another psi over the last 1.5 hr. At that time, the testing was terminated. The Forty-niner anhydrite was judged to have a permeability much lower than that of the claystone, and quantitative testing of the anhydrite appeared to require weeks to months of effort."

Section 5.3 Dewey Lake Red Beds, p 128, col 1, para 2;

" Little testing of the Dewey Lake Red Beds near the WIPP site has ever been attempted, primarily because of the lack of evidence of continuous zones of saturation (Mercer, 1983). The Dewey Lake Red Beds are permeable, however, as evidenced by losses of circulation fluid during drilling of holes such as DOE-2 and H-3d, and therefore the unit remains of interest when considering groundwater-transport pathways in the event of a breach of the WIPP facility. Beauheim (1986) reported on unsuccessful attempts to test the lower Dewey Lake at DOE-2. The only other Dewey Lake testing attempted on behalf of the WIPP project was performed at well H-14. No information was obtained during the drilling of H-14 pertaining to the presence or absence of a water table in the Dewey Lake at that location. Nevertheless, limited testing of the lower portion of the Dewey Lake Red Beds was planned based on the supposition that either a water table did exist in the lower Dewey Lake, or sufficient water would have infiltrated into the Dewey Lake during drilling and Rustler testing to allow at least qualitative testing. . . ."

Section 6. DISCUSSION OF RUSTLER FLOW SYSTEM, p. 131;

" The single-well testing discussed in this report has provided significant information on the transmissivities and hydraulic-head relations of the five Rustler members. IN particular, our knowledge of the distribution of transmissivity within the Culebra dolomite has increased considerably. Section 6.1 attempts to explain the distribution of Culebra transmissivity in the context of geologic models of halite deposition and dissolution within the Rustler. Section 6.2 discusses the hydraulic-head relations among the Rustler members, and their implications regarding recharge to the Rustler Formation."



Section 6.1 Culebra Transmissivity, p. 131;

" Mercer (1983) reported values for Culebra transmissivity at 20 locations. The testing described in this report has provided values for Culebra transmissivity at 15 new locations, and new estimates at 7 locations for which values had previously been reported. Combined with other recent work performed at DOE-2 (Beauheim, 1986), H-3 (Beauheim, 1987a), H-11 (Saulnier, 1987), and WIPP-13 (Beauheim, 1987b), the WIPP project has tested 38 locations and the transmissivity values at each provided by this report or those referenced



above.

Figure 6-2 shows the areas around the WIPP site where halite is present in the non-dolomite Rustler members, as indicated by Snyder (1985 and personal communication) and Powers (personal communication). According to Snyder, halite was originally deposited in the unnamed lower, Tamarisk, and Forty-niner Members of the Rustler over the entire area covered by Figure 6-2. The present-day absence of halite from these members reflects the eastward progression of a dissolution front. This dissolution front apparently affects the uppermost Rustler halite, that in the Forty-niner, first, and works progressively downsection to the upper Salado Formation. Thus, the eastward extent of the Forty-niner dissolution front is greater than that of the Tamarisk dissolution front, which is in turn greater than the eastward extent of the dissolution front in the unnamed lower member (Figure 6-2). Dissolution of the upper Salado follows dissolution of halite from the unnamed lower member of the Rustler. Lagging behind the dissolution front in each member is a second front where anhydrite is being hydrated to gypsum. In Snyder's view, as halite is removed beneath the Rustler dolomites, the dolomites subside and fracture. Similar subsidence and fracturing may affect the anhydrites, allowing more groundwater flow through them which may effect their hydration to gypsum. Note that the areas shown on Figure 6-2 indicate that only some halite is present in the appropriate members, not that the full thicknesses originally deposited are present. For example, Snyder (1985) states that only about half of the halite originally present in the unnamed lower member at WIPP-21 is there today.

Alternatively, Holt and Powers (1988) believe that the different amounts of halite seen in the Rustler members at the WIPP site more likely represent original depositional differences and/or syndepositional dissolution that later progressive dissolution. They relate fracturing to stress relief caused by unloading of the Rustler, citing a preponderance of horizontal (as opposed to vertical) fractures within the Rustler as evidence. According to their hypothesis, fracturing would be expected to become less pronounced eastward as the depth of burial of the Rustler increases. Holt and Powers (1988) also do not believe that all of the gypsum present in the Rustler is related to the hydration of anhydrite, but that it is instead primary, pointing to the preservation of primary sedimentary structures as evidence. Hold and Powers do find evidence for late-stage dissolution of halite from the upper Salado in Nash Draw, however, and relate disruption of the overlying Rustler to this dissolution.

As can be seen on Figure 6-2, the highest values of Culebra transmissivity are found in areas in or close to Nash Draw where no halite is present in the Rustler. At DOE-2 and WIPP-13, which are very close to the boundary west of which no halite is present in the unnamed lower member, the transmissivity of the Culebra is also relatively high. Relatively high transmissivities are also found, however, at DOE-1 and H-11, where little or no halite is missing beneath the Culebra. WIPP-30, on the other hand, lies in an area of no Rustler halite, and yet the transmissivity of the Culebra is low at that location. Neither Snyder's (1985) nor Holt and Powers' (1988) model of halite deposition and dissolution can adequately explain the entire transmissivity distribution observed around the WIPP site.

If the absence of halite in the unnamed lower member is caused by dissolution and if this dissolution causes fracturing of the Culebra as Snyder (1985) suggests, then the high

transmissivities shown in the area of no halite on Figure 6-2 would be expected. Further, the high transmissivities at DOE-2 and WIPP-13 could be explained as the result of partial dissolution of halite from the unnamed lower member. The lower transmissivity at WIPP-30, however, cannot be explained by this hypothesis, nor can the low transmissivities at H-14 and P-15, which are closer to the no-halite boundary than is H-18. The relatively high transmissivities at DOE-1 and H-11 also cannot be related to dissolution of underlying halite.

Holt and Powers' (1988) model could predict the high transmissivities in Nash Draw by relating them to dissolution of the upper Salado. Their model further states that no Rustler halite was deposited and no dissolution of the Salado has occurred at WIPP-30, thus explaining the low Culebra transmissivity at that location. If their argument that fracturing is related to unloading is correct, then a correlation between the present-day depth of burial of the Culebra and the transmissivity of the Culebra might be expected to exist. Preliminary evaluation by Holt (personal communication) indicates that some correlation between depth of burial and Culebra transmissivity is evident, but that the correlation is not perfect. For example, despite the fact that the Culebra is approximately 200 ft shallower at WIPP-30 than at DOE-2, the Culebra transmissivity is over two orders of magnitude lower at WIPP-30 than at DOE-2. Other, as yet undefined, factors may be as important as depth of burial in controlling the transmissivity of the Culebra. The Holt and Powers (1988) model also fails to explain the relatively high transmissivities at DOE-1 and H-11.

Clearly, neither of the geologic models cited above provides a complete understanding of the distribution of transmissivity within the Culebra. The two models need not be considered completely mutually exclusive, however, and as discussed above, elements of both models provide reasonable explanations of some features observed in the Culebra. Nondeposition (or syndepositional dissolution) of halite may have been more widespread than believed by Snyder (1985), and late-stage dissolution may have occurred more than is believed by Holt and Powers (1988). The most significant problem area is in the vicinity of DOE-1 and H-11, where relatively high transmissivities would not be expected based on either model.

One additional observation that can be made from consideration of Figure 6-2 is that all measurements of Culebra transmissivity greater than 1 ft<sup>2</sup>/day coincide with areas having no halite in the Tamarisk. The simple dissolution of Tamarisk halite would not seem likely to affect the transmissivity of the Culebra. The lack of high Culebra transmissivity everywhere that halite has been removed from the Tamarisk further argues against a direct relationship between Culebra transmissivity and Tamarisk halite. Nevertheless, absence of Tamarisk halite appears to be a necessary, but not sufficient, condition for high Culebra transmissivity. Perhaps the removal of Tamarisk halite makes possible a second process that directly affects the transmissivity of the Culebra."



p. 137, col. 2, line 7;

" ... Attempts to collect representative data on the formation pressure of the Tamarisk have failed to date, but recent data from DOE-2, H-14, and H-16 support Mercer's observation of downward hydraulic gradients from the Magenta to the Culebra at the WIPP

site. Together these observations imply that the Culebra, the most transmissive member of the Rustler, acts as a drain on the overlying and underlying Rustler"

p 138, col 2, para 1;

" The unnamed lower member of the Rustler Formation was tested only in well H-16, where DST's were performed on the lower siltstone portion of the unit. The transmissivity of the siltstone is about  $2.4 \times 10^{-4}$  ft<sup>2</sup>/day (Table 5-2). . . ."

p 138, col 2, para 3;

" The claystone portion of the Tamarisk member of the Rustler Formation was tested in wells H-14 and H-16. At H-14, the pressure in the claystone failed to stabilize in three days of shut-in testing, leading to the conclusion that the transmissivity of the claystone is too low to measure in tests performed on the time scale of days. Similar behavior at H-16 led to the abandonment of testing at that location as well."

Section 7. SUMMARY AND CONCLUSIONS, p 139, col 1, para 3;

" The Forty-niner Member of the Rustler Formation was also tested in wells H-14 and H-16. Two portions of the Forty-niner were tested in H-14: the medial claystone and the upper anhydrite. DST's and a rising-head slug test were performed on the claystone. The transmissivity of the claystone is about  $7 \times 10^{-2}$  ft<sup>2</sup>/day (table 5-2). A prolonged buildup test performed on the Forty-niner anhydrite revealed a transmissivity too low to measure on a time scale of days. A pulse test, DST's, and a rising-head plug test were performed on the Forty-niner clay at H-16, indicating the clay has a transmissivity of about  $5 \times 10^{-3}$  ft<sup>2</sup>/day (Table 5-2). Formation pressures estimated for the Forty-niner at H-14 and H-16 are lower than those calculated for the Magenta (compensated for the elevation differences), indicating that water cannot be moving downwards from the Forty-niner to the Magenta at these locations."



Compliance Certification Application Reference Expansion

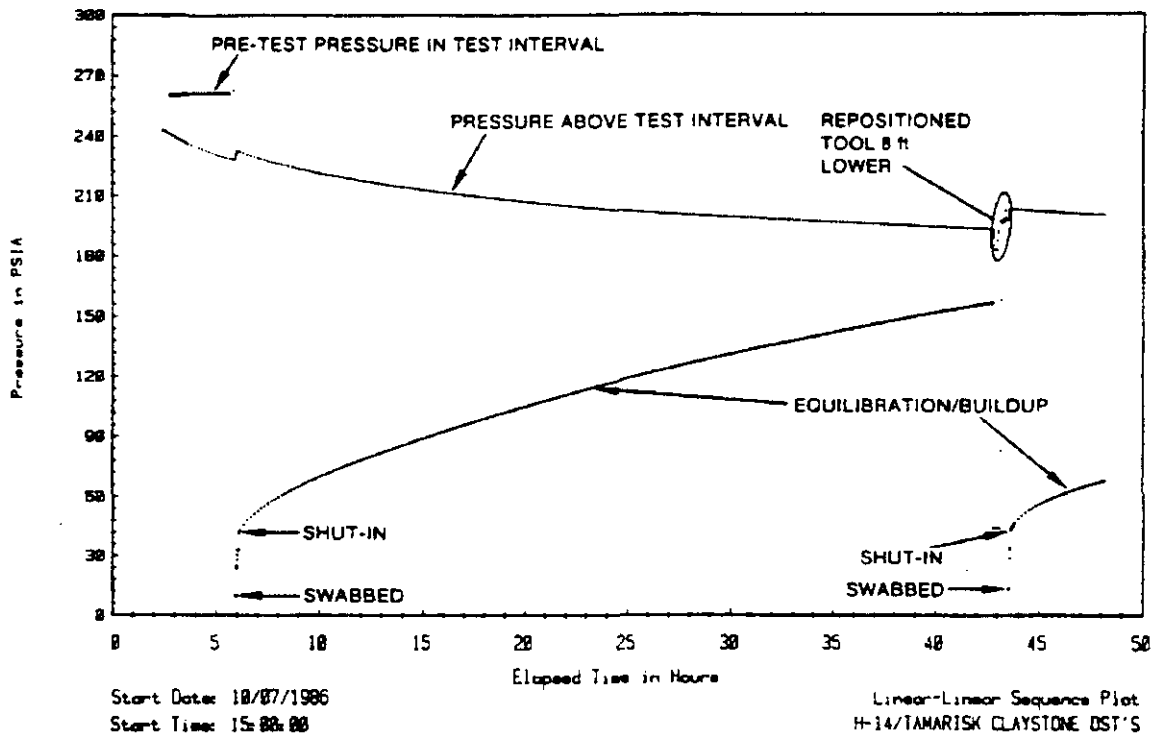


Figure 5-82. H-14/Tamarisk Claystone Shut-In Test Linear-Linear Sequence Plot



Compliance Certification Application Reference Expansion

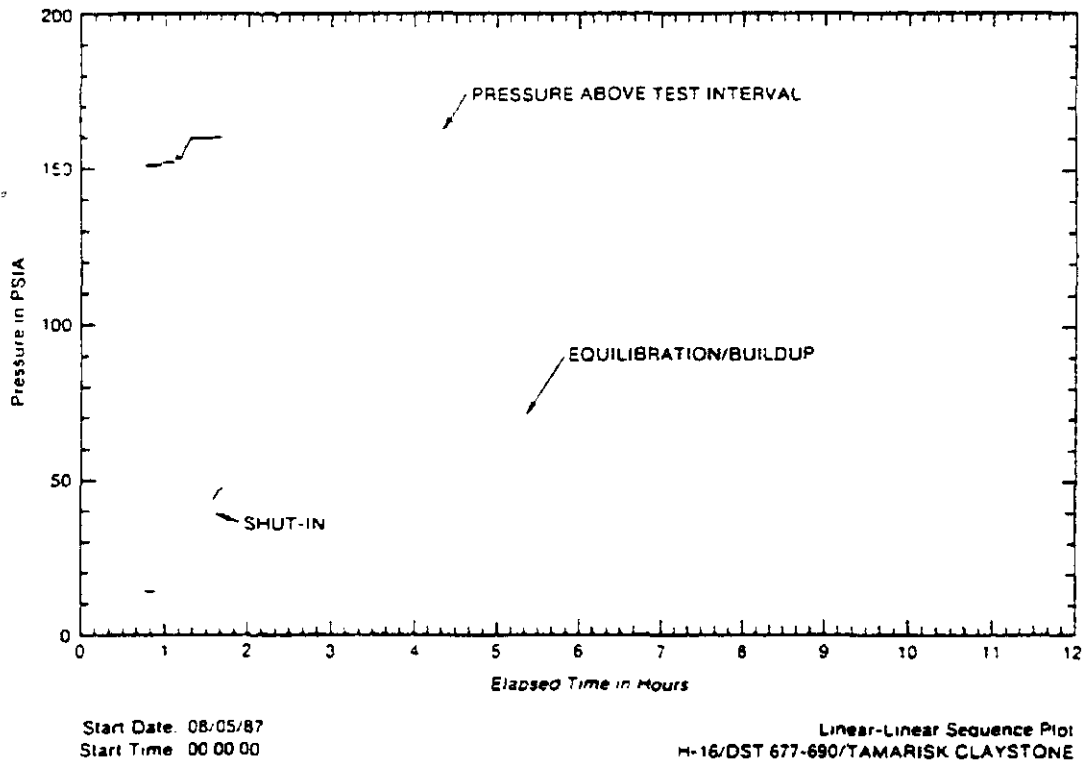


Figure 5-83. H-16/Tamarisk Claystone Shut-In Test Linear-Linear Sequence Plot



Compliance Certification Application Reference Expansion

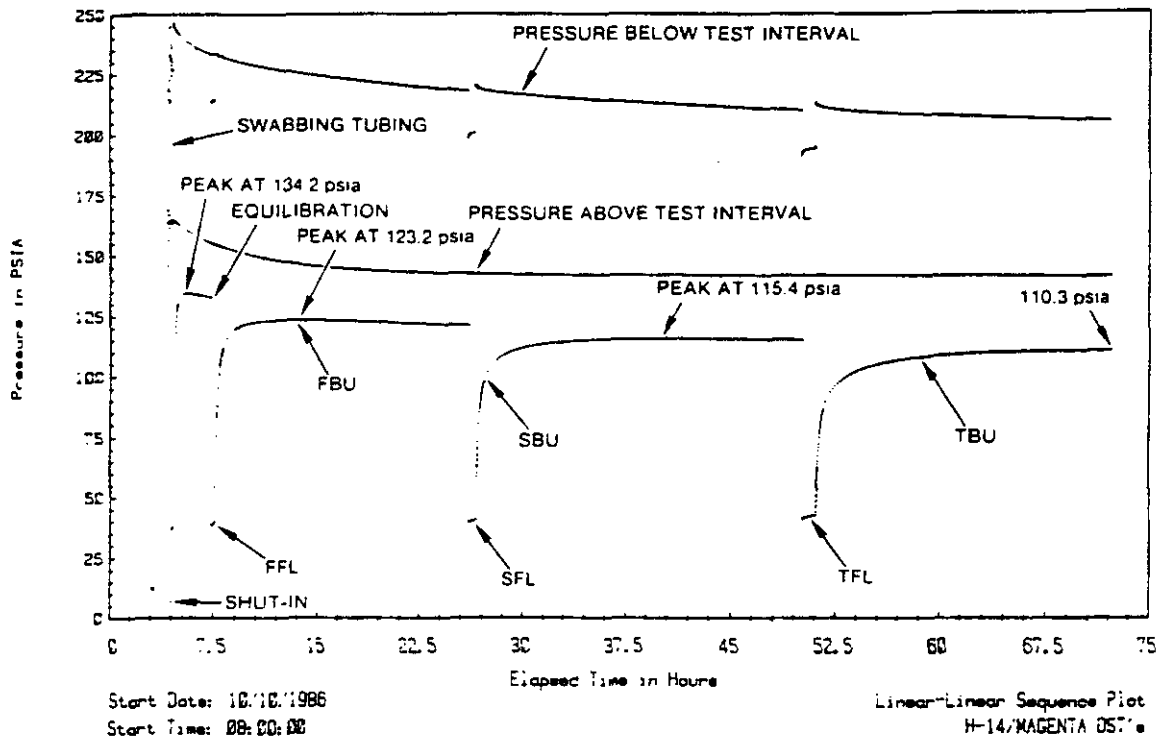


Figure 5-84. H-14/Tamarisk Claystone Shut-In Linear-Linear Sequence Plot



Compliance Certification Application Reference Expansion

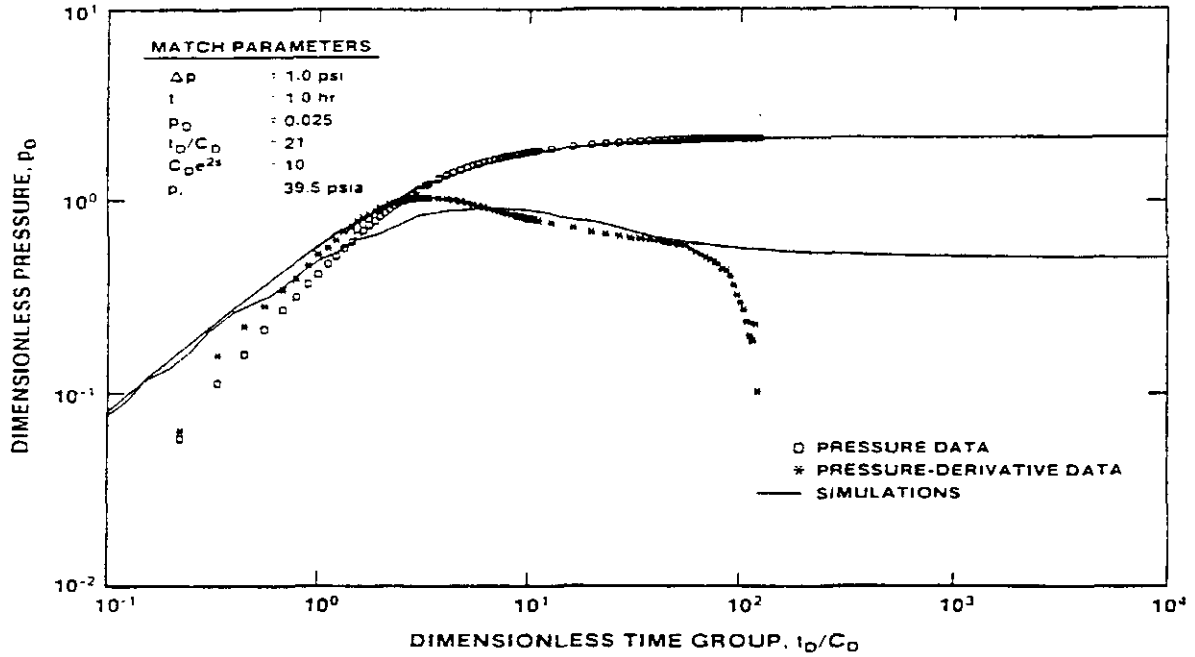


Figure 5-85. H-14/Magenta First Buildup Log-Log Plot with INTERPRET Simulation

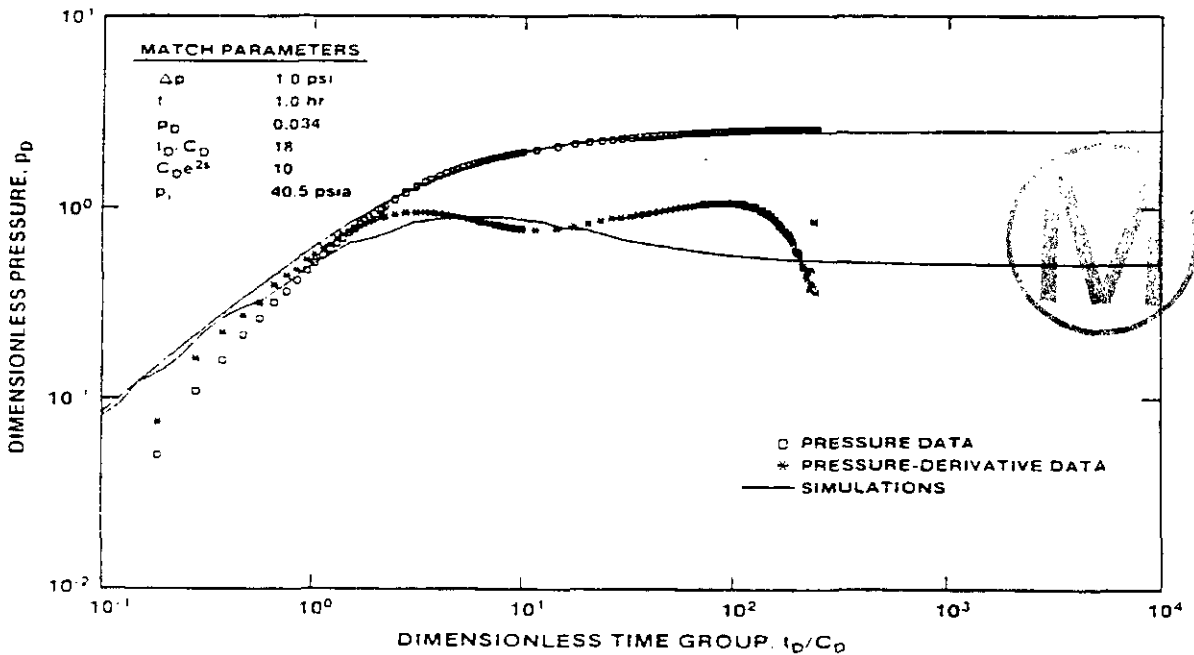


Figure 5-86. H-14/Magenta Second Buildup Log-Log Plot with INTERPRET Simulation

Compliance Certification Application Reference Expansion

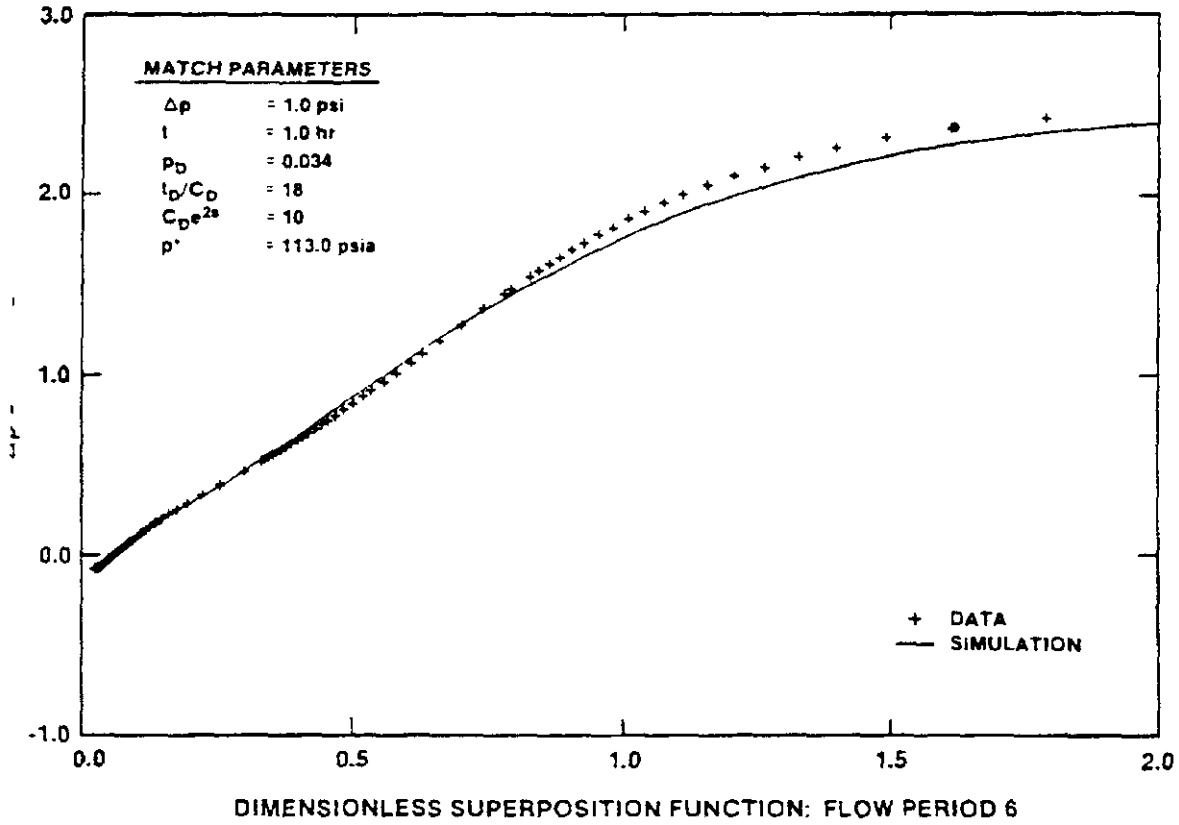


Figure 5-87. H-14/Magenta Second Buildup Dimensionless Horner Plot with INTERPRET Simulation



Compliance Certification Application Reference Expansion

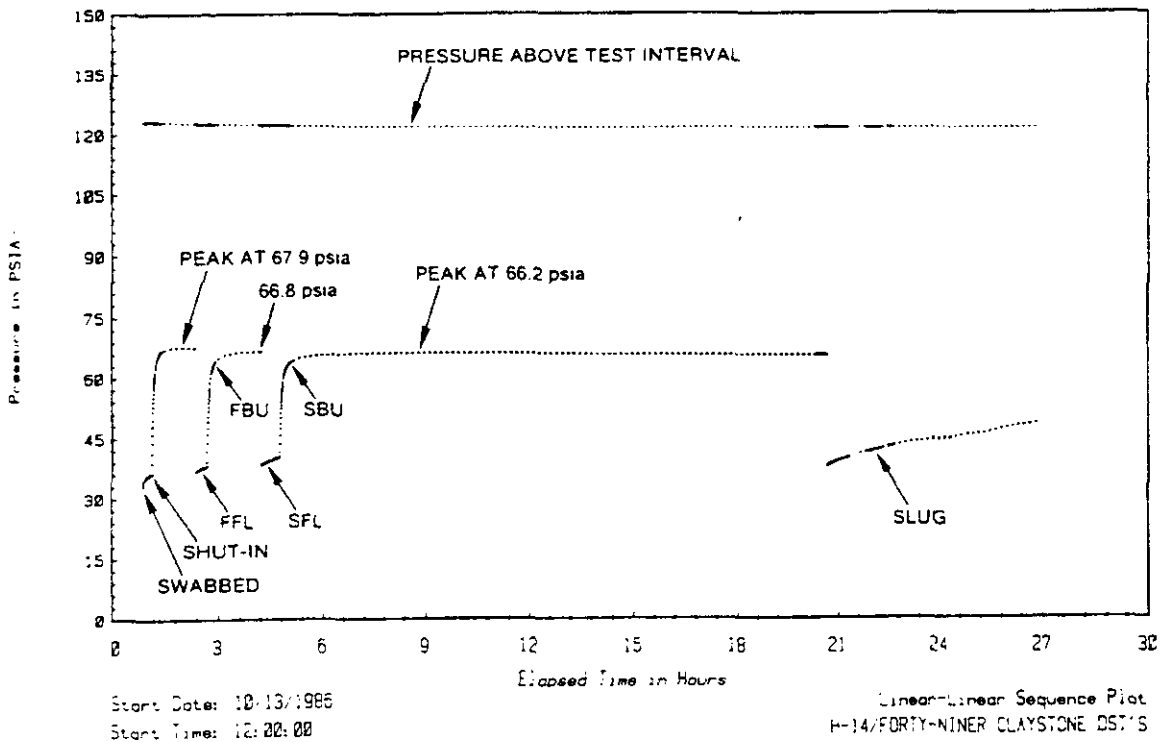


Figure 5-95. H-14/Forty-Niner Claystone Drillstem and Slug Testing Linear-Linear Sequence Plot



Compliance Certification Application Reference Expansion

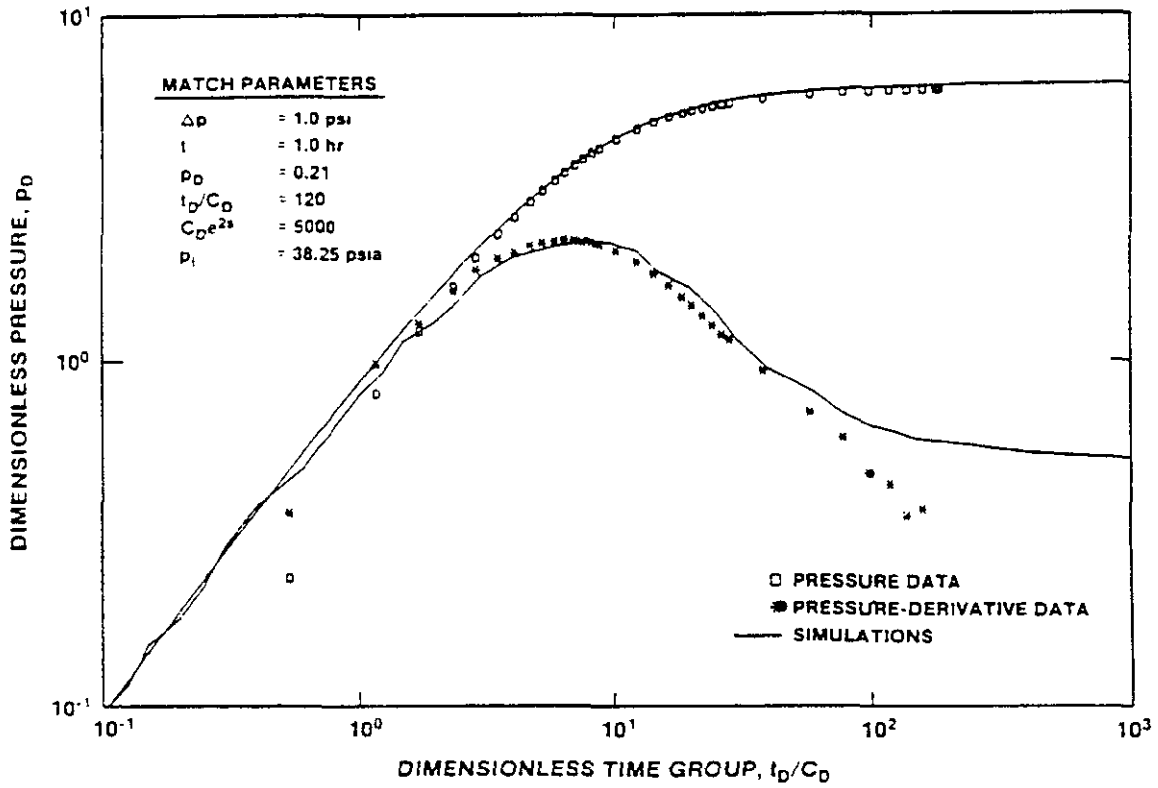
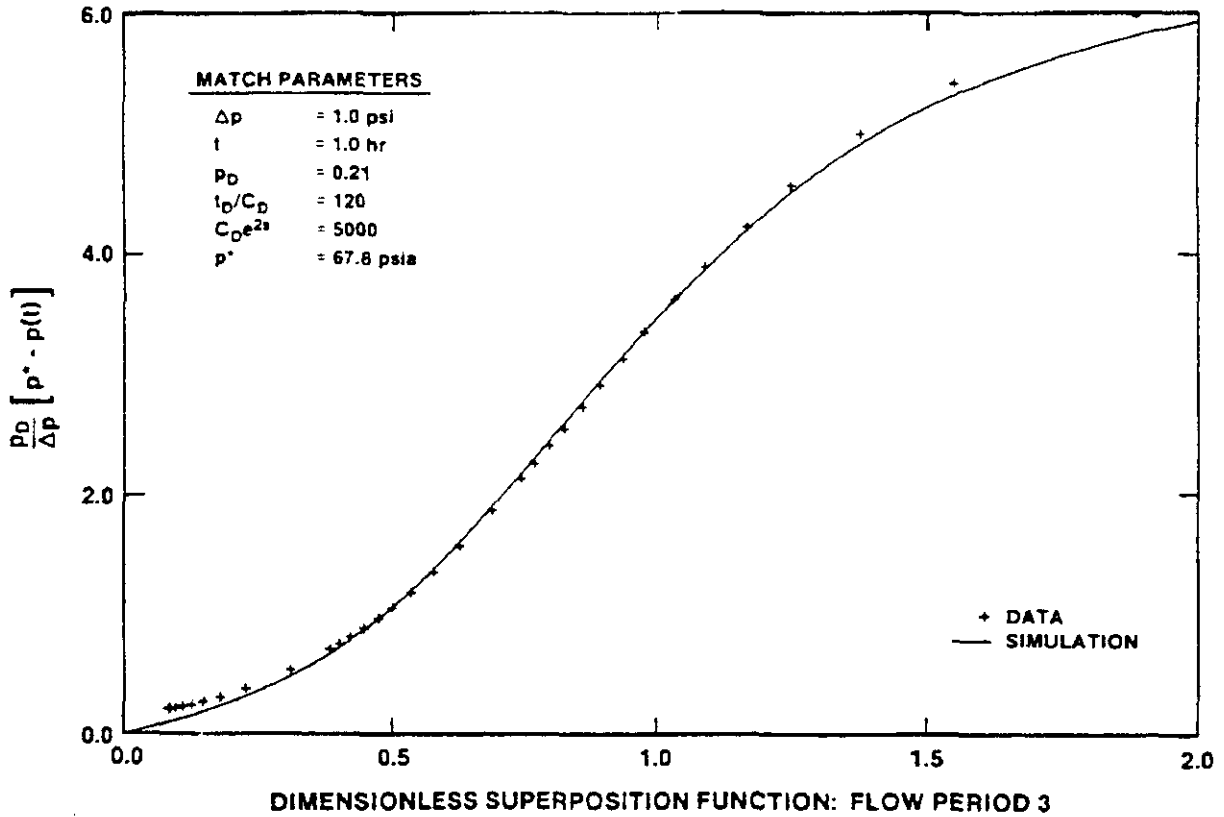


Figure 5-96. H-14/Forty-Niner Claystone First Buildup Log-Log Plot with INTERPRET Simulation



Compliance Certification Application Reference Expansion



Compliance Certification Application Reference Expansion

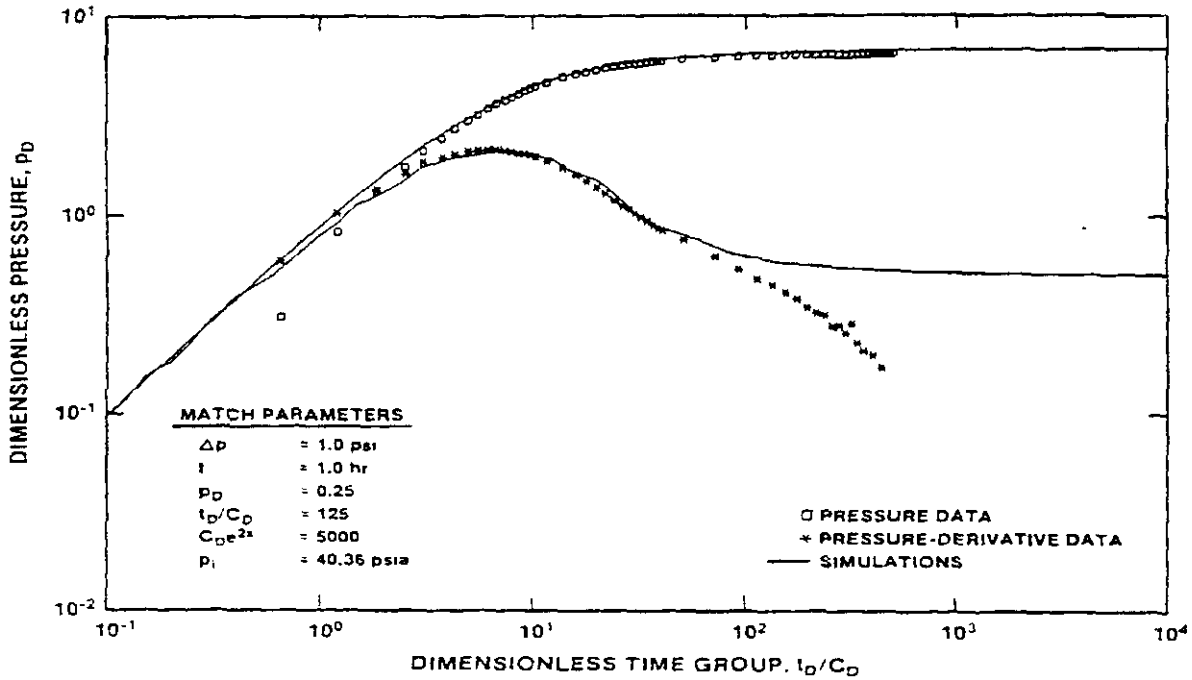


Figure 5-98. H-14/Forty-Niner Claystone Second Buildup Log-Log Plot with INTERPRET Simulation

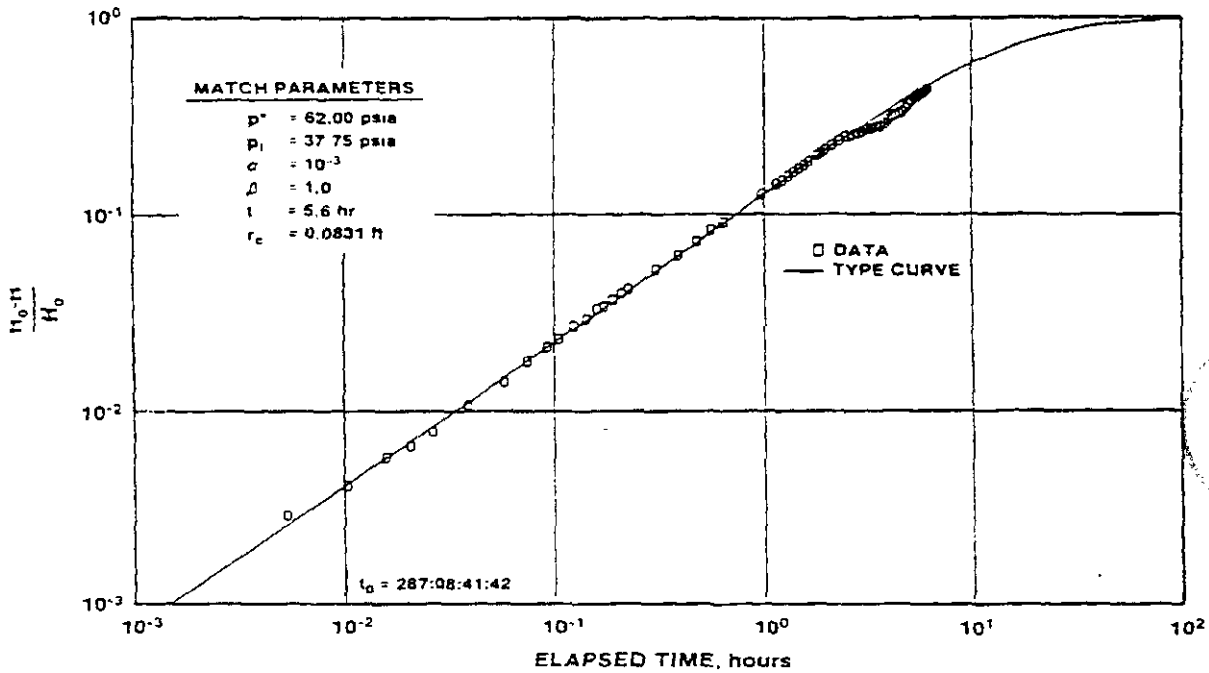


Figure 5-99. H-14/Forty-Niner Claystone Early-Time Slug-Test Plot

Compliance Certification Application Reference Expansion

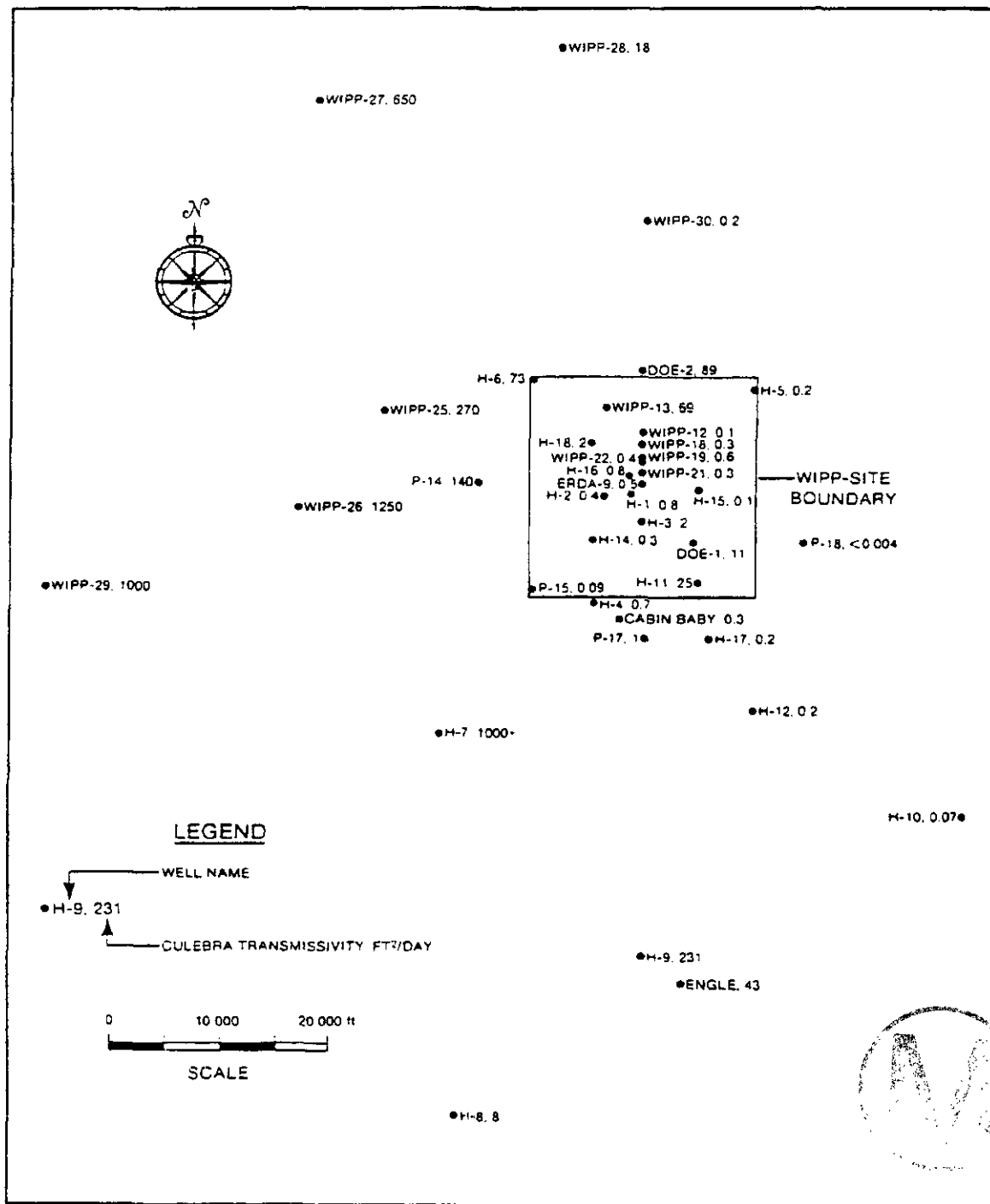


Figure 6-1. Culebra Wells Tested by the WIPP Project

Compliance Certification Application Reference Expansion

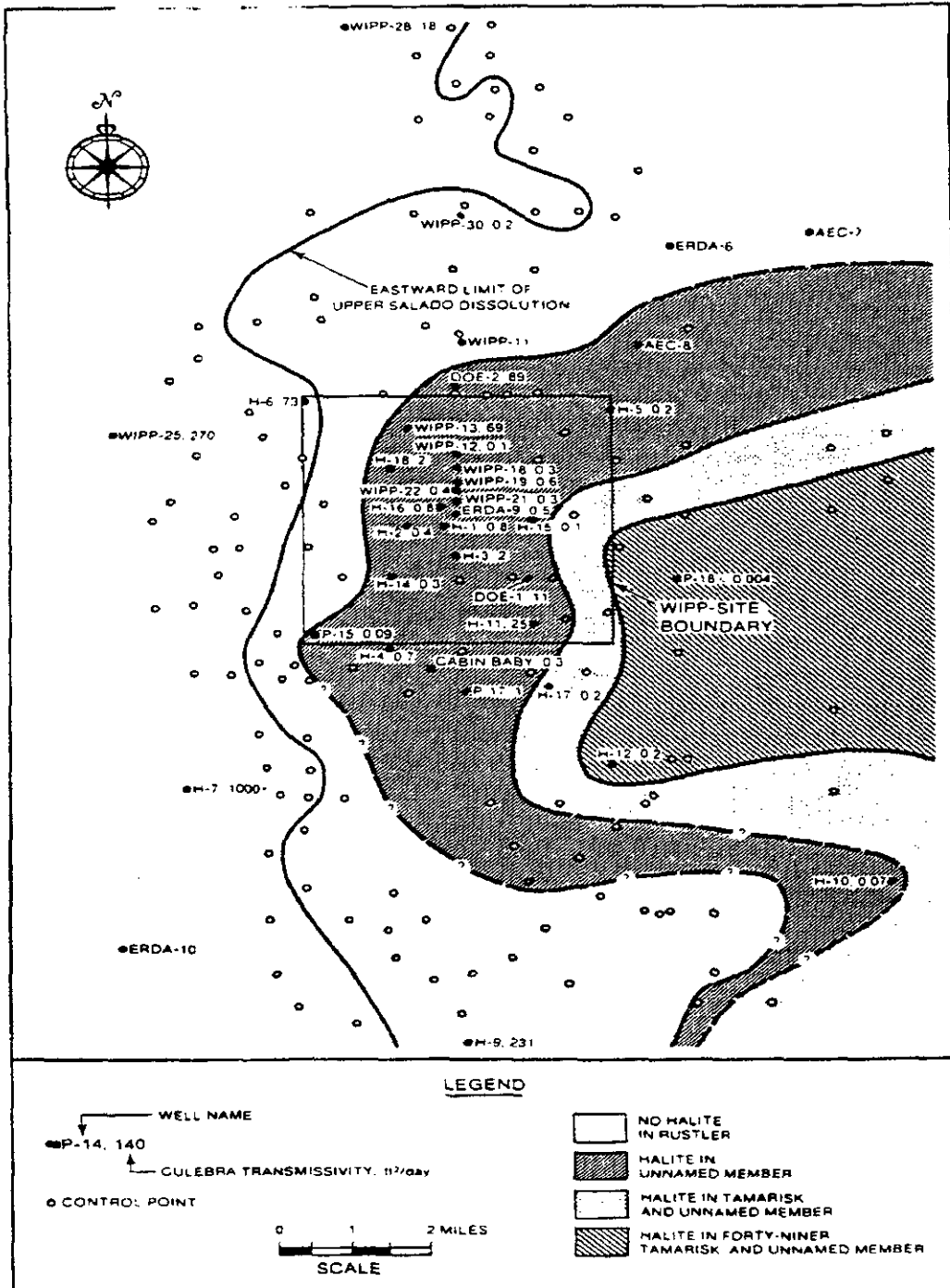


Figure 6-2. Distribution of Rustler Halite and Culebra Transmissivity Around the WIPP Site.

**Compliance Certification Application Reference Expansion**

---

Beauheim, R.L., Wawersik, W.R., and Roberts, R.M. 1993. "Coupled Permeability and Hydrofracture Tests to Assess the Waste-Containment Properties of Fractured Anhydrite." *Journal of Rock Mechanics*. Vol. 30, No. 7, pp. 1159-1163.

NOTE: The above listed document was not available for inclusion in the Reference Expansion as of the printing date. Page changes will be provided as the above document becomes available for inclusion.



**Compliance Certification Application Reference Expansion**

---

Butcher, B.M. 1996. Memo to M.S. Tierney, RE: QAP 9-1 Documentation of the Initial Waste Water Content for the CCA, January 29, 1996. WPO 30925.

NOTE: The above listed document was not available for inclusion in the Reference Expansion as of the printing date. Page changes will be provided as the above document becomes available for inclusion.

Butcher, B.M., Thompson, T.W., VanBuskirk, R.G., and Patti, N.C. 1991. Mechanical Compaction of Waste Isolation Pilot Plant Simulated Waste. SAND90-1206. Sandia National Laboratories, Albuquerque, NM. WPO 23968.

ABSTRACT, p i;

" The investigation described in this report acquired experimental information about how materials simulating transuranic (TRU) waste compact under axial compressive stress, and used these data to define a model for use in the Waste Isolation Pilot Plant (WIPP) disposal room analyses. The first step was to determine compaction curves for various simulant materials characteristic of TRU waste. Stress-volume compaction curves for various combinations of these materials were then derived to represent the combustible, metallic, and sludge waste categories. Prediction of compaction response in this manner is considered essential for the WIPP program because of the difficulties inherent in working with real (radioactive) waste.

Next, full-sized 55-gallon drums of simulated combustible, metallic, and sludge waste were axially compacted. These results provided data that can be directly applied to room consolidation and data for comparison with the predictions obtained in Part I of the investigation. Good agreement was obtained between prediction and test results.

Finally, compaction curves, which represent the combustible, metallic, and sludge waste categories, were determined, and a curve for the averaged waste inventory of the entire repository was derived. The results for axial compaction of combustible and metallic waste were found to be consistent with the assumptions used to estimate the final mechanical state of a typical disposal room, initially made as supporting information for the Draft Supplemental Environmental Impact Statement for WIPP."

Section 3.0 DRUM COMPACTION MEASUREMENTS, 3.1 Objectives, p 49;

" The objective of the second part of the testing program was to acquire collapse data for drums filled with different materials. These full-scale loading tests were conducted on single drums of waste by crushing them along their axis of symmetry with no restriction on lateral expansion. Loading continued until an axial stress of 13.8 MPa was exceeded. DOT-17C, 55-gallon drums with standard 90 mil polyethylene liners were used in all tests.

An empty drum was tested first for baseline information and to check out the mechanical systems and quality-assurance procedures. Next, a total of 10 waste-filled drums representing of combustible, metallic, and sludge waste were compacted. No lateral restraint was placed on the drums during the tests. Data acquired during compaction usually consisted of the force exerted on the top of the drum and its height.

A special feature of the tests incorporated both photographic and VCR coverage at prescribed time intervals to determine approximate drum volumes. Collapse was expected to be nonuniform, but only the sludge drums showed evidence of extensive bulging. Both the combustible and metallic waste drums were observed to compact uniformly with little indication of lateral deformation. Bulging was probably slight because tensile hoop stresses within the walls of the drums were sufficient to restrict any lateral movement of the waste."

Section 3.3.2 RING FORMATION IN THE DRUMS DURING COLLAPSE, p 52, para 2;

" The last information needed for drum collapse predictions was the way that the drums collapse during the tests. Cross-sections of the drums showed that they collapsed uniformly and independently of the drum contents, at least during the early parts of the tests, and formed crushed rings around the waste.<sup>1</sup> Because the drum appeared to crush straight down, without significant change in diameter, the assumption was made for data reduction purposes that a constant cross-section could be assumed in calculating drum densities.

To test this assumption, two test were performed by filling the voids in the filled waste drum with water before compaction. During the crush down, the water was allowed to move through tubing to another drum where the volume was measured to define the height versus volume of the waste relationship. These tests indicated that throughout most (about 2/3) of the crush down, the constant cross-section assumption was reasonable. For about the first half of the crush down, the cross-section was less than original, suggesting that the drum folded inward. Later, the volume reduction was less than assumed, showing that the drum was starting to bulge outward as compaction continued. The tendency of the curve of water-out versus drum height to reach a limit suggested that water would have eventually stopped coming out of the drum. This point was never reached in our tests; leaks either in the seal or the lid of the drum required an end to the water-collection portion of the test.

In contrast to the tests on simulated combustible and metallic waste, ring formation was not obvious during collapse of the sludge drums because both their total amount of collapse and the compressibility of the material was less. Compaction of the waste caused the drums to bulge outward slightly at the center, stretching the steel drums circumferentially and eventually causing them to break open at the seam, at which point some of the material near the seam would extrude from the drum and the tops of the drums would tilt downward towards the seam opening. However, the assumption was made, in reducing the sludge drum collapse data, that the drum crushed straight down without change in diameter. Therefore, the reduced data is truly representative of the early portions of the tests when bulging was minimal. The stress required to cause additional collapse rose so rapidly during the latter part of the test, however, that the constant cross-section assumption was probably adequate as a first approximation during the later portions of the tests."



4.0 REPOSITORY COMPACTIBILITY, p 65,

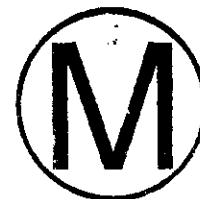
---

<sup>1</sup>Buckling patterns appearing along 'rolls' (strengthening hoops) in the drum were sinusoidal in shape, with five full sine waves at each roll. The sine wave pattern stayed stationary but grew in amplitude as the drum collapsed. After the pattern 'matured,' at a first ridge (generally the center of the drum), a second sinusoidal pattern would start at a second location on the drum (usually the bottom of the drum). The sine wave would contain five full waves as before, and the wave pattern would be a simple vertical translation from the wave pattern developed before. The third wave pattern would form like the second, at still another location on the drum.

#### 4.1 Method of Analysis;

" A composite compaction curve for the entire repository will be defined in this section. This calculation proceeds in the same manner as for the composite compaction curves (Section 2.3.4), but what should be a simple procedure becomes more uncertain when the data for the inventory of CH-TRU waste from the most current references are examined. The basic problem is that the inventory data from DOE/RW-0006, Rev 4, (1988), and Drez and James-Lipponer (1989), summarized in Table 4-1, are difficult to correlate. The first source reports only volume data, whereas the second source quotes only weight data and is incomplete.

#### 4.2 Repository Inventory



##### 4.2.1 METALS INVENTORY

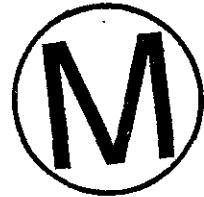
Definition of how much waste will eventually be stored in the repository (Table 4-1) started with metal waste. Metal and glass waste, according to Drez and James-Lipponer (1989), is composed of 2% by weight tantalum, 68% iron and steel, 17% lead (an upper bound), 4% Copper, and 9% aluminum. Using the theoretical solid densities listed in Table 2-2, and assuming that: (1) the weight assigned to leaded gloves in Drez's inventory was assumed to be entirely due to the lead, and (2) waste in the form of paint cans was added to the total weight of iron and steel waste, although the paint cans probably are filled with stabilized sludge, this mixture is estimated to have a theoretical solid density of 7110 kg/m<sup>3</sup>.

The total amount of steel waste reported by Drez also requires some adjustment because sometimes the weights of the containers were included in the totals for metallic waste given by INEL and the Los Alamos National Laboratory (LANL), and sometimes they were not separated out. Although Drez did not attempt to adjust his summary of results for this inconsistency, it was required for estimation of repository-wide averages, and was accomplished by estimating the volumes of INEL and LANL waste, finding the number of equivalent 55-gallon drums the volumes represented, and using this information to estimate the total weight of the containers. This procedure is a poor substitute for actual information, but it represents the best estimate that is possible at present. Thus, the estimates in this report that depend upon the separation of the total weight of the metal containers from the total weights of the waste categories must be redone as soon as more definitive information becomes available.

**Compliance Certification Application Reference Expansion**

TABLE 4-1. TRU WASTE INVENTORY ANALYSIS

	Weight kg	Volume m <sup>3</sup>	Volume Fraction <sup>1</sup>	Container steel, kg	Weight of Plastic liners & bags, kg	Wood contain- ers	Total Weight kg	Weight Fraction
Metals	7,330,000							
Glass	1,120,000							
<b>Metal/Glass</b>	<b>8,450,000</b>	<b>54,000</b>	<b>.40</b>	<b>4,400,000</b>	<b>744,000</b>	<b>596,000</b>	<b>14,190,000</b>	<b>.28</b>
Combustibles	8,590,000	55,400	.41	4,510,000	763,000	611,000	14,480,000	.28
Sludge	20,300,000 <sup>2</sup>	25,400	.19	2,090,000	353,000	283,000	23,030,000	.44
Steel Containers	11,000,000							
Polyethylene Liners	1,550,000							
PVC liners, bags	310,000							
Wood/Fiberboard	1,490,000							
	<b>51,700,000</b>	<b>134,800</b>	<b>1.00</b>	<b>11,000,000</b>	<b>1,860,000</b>	<b>1,490,000</b>	<b>51,700,000</b>	<b>1.00</b>



1. Values of the volume fraction were computed assuming the volume of the "other" category of waste to be proportionally distributed among the three major categories of waste.
2. Estimated value.

In the absence of any better information, the total weight of the INEL and LANL containers was estimated to be 7,350,000 kg, reducing the total weight of steel waste from the value of 9,170,000 kg quoted by Drez to 1,820,000 kg. The weight of iron in the Drez inventory remained unchanged at 2,620,000 kg. The total weight of metals in the inventory was 7,330,000 kg, and the weight of glass was estimated to be 1,120,000 kg.

A comparison of the new metallic waste inventory values by Drez with previous estimates by Clements and Kudera (1985) is also of interest. Clements and Kudera's study determined that the metals inventory was 4% tantalum, 64% steel, 7% lead, and 25% other metals such as aluminum and copper, by weight, with an average solid density of 6650 kg/m<sup>3</sup>. The principal difference between the two compilations is that there is a greater amount of lead, and less aluminum and copper in the Drez inventory.

#### 4.2.2 COMBUSTIBLES INVENTORY

For combustible waste, Drez reported that the total weight of cellulose was 4,350,000 kg, the weight of plastics was 4,180,000 kg, and other combustibles were present in the amount of 60,500 kg. In the absence of additional information, we will assume that the cellulose

are composed of about 60% wood and paper and 40% cloth (Butcher, 1989), with a solid density of 1100 kg/m<sup>3</sup> estimated from the densities quoted in Table 2-2. The category of "other" combustibles" was assumed to be 50% cellulose and 50% plastics, and a solid density of 1200 kg/m<sup>3</sup> was assumed for plastics.



#### 4.2.3 SLUDGE INVENTORY

The total weight of the sludges in the waste was not available at the time this report was prepared, nor was information available for estimating its solid density. Therefore, the weights of the sludge drum contents, estimated by Butcher (1989), from Clements and Kudera's (1985) data, were used to define the total weight of the sludge. These values were 170 kg for uncemented inorganic sludge, with an estimated solid density of 1330 kg/m<sup>3</sup> and 188 kg with an estimated solid density of 1480 kg/m<sup>3</sup> for uncemented organic sludge. For comparison, the mixture of water, quartz sand, and Portland cement for the tests used to simulate sludge in this investigation was estimated to have a no-void density of 2200 kg/m<sup>3</sup>. The sand-cement mixture was relatively unsaturated, however, and addition of water could have easily reduced its no-void density to the order of the densities computed for the Clements and Kudera results.

For an estimate of the total weight of sludges, the assumption was made that an average drum of sludge weighs approximately 180 kg. To obtain the number of equivalent drums of sludge-like material, the volumes of adsorbed liquids and sludges, concreted or cemented sludges, and dirt, gravel or asphalt categories, listed in Table 4-1, were added together. This sum, 23,700 m<sup>3</sup> was divided by 0.21 m<sup>3</sup>, the volume of an average 55-gallon drum, and the result multiplied by 180 kg to arrive at 20,300,000 kg for the total weight of sludge.

#### 4.2.4 CONTAINER MATERIALS

The total weights of the steel in the containers, the plastic liners, and the wood/plywood boxes were determined by Drez to be 11,000,000 kg of steel containers, 1,550,000 kg of polyethylene rigid liners, 1,490,000 kg of fiberboard liners or wood/plywood boxes, and 310,000 kg of PVC liners and bags.

#### 4.2.5 INVENTORY DISCREPANCIES

Discrepancies in the inventory data are best illustrated by using the weights and volumes given in Table 4-1 (257,000 equivalent drums assumed), and assuming a drum volume of 0.21 m<sup>3</sup>, to determine that the weight of an average drum of metal and glass combustible waste is 55.2 kg. Of this amount, the drum itself weighs about 29 kg, with the remaining 26 kg, or approximately 60 lb the weight of the contents. The computed value of 26 kg appears far too low, when compared with the average weight of the contents of INEL metallic waste drums of 64.5 kg (142 lb), estimated by Butcher (1989), even when the additional weight of

a liner (approximately 8 kg) is added to the weight of the waste. The computed value for the contents of combustible waste drums, using the data in Table 4-1, would also be 26 kg, versus 40 kg from the INEL survey. There is also no information from Drez's study for determining the average weight of sludge in a typical 55-gallon drum.

The differences in the weights of single drums of metallic waste obtained, computed from the results in Table 4-1 suggest that either the estimated volumes are too large by a factor of 2 or the weights are too small by a factor of 2 in Table 4-1. Attempts to reconcile such inconsistency are likely to be even more difficult in the future as waste volumes are constantly being revised downward because of greater utilization of pre- or supercompaction without being specific about how the weight of the waste will change.

Other methods of estimating the inventory of nonradioactive materials in the waste have been explored (Appendix A), because the inventory data is not consistent. The conclusion of this study is that the best current estimate is that 0.28 by weight of the inventory will be metallic waste, that the weight fraction of combustible waste will be 0.28, and the weight fraction of sludges will be 0.44. The initial porosity of the waste in the repository will be 0.79, its average theoretical solid density will be 2000 kg/m<sup>3</sup>, and the average initial density will be 426 kg/m<sup>3</sup>.

### 4.3 Repository Curves for Axial Drum Compaction

For axial compaction, the average compaction curve for the repository is estimated using the predicted compaction curves for the three major types of waste. These curves differ slightly from the experimental drum collapse curves and include the corrections for creep. The method of estimation was as follows: (1) For a given value of the compaction stress, the density of each category of waste was obtained; (2) the assumption was made that the weight fraction of combustible waste was 0.28, the weight fraction of metallic waste was 0.28, and the weight fraction of sludge was 0.44 (c.f. Table 4-1 and Appendix A). Using the simple mixture rule (Sections 2.3.2 and 2.3.4), the average compacted density and the average solid density of the waste in the repository were then estimated in a similar manner, assuming average solid densities of 3440 kg/m<sup>3</sup> for metallic waste, 1310 kg/m<sup>3</sup> for combustibles, and 2370 kg/m<sup>3</sup> for sludges (cf. Appendix I). (3) The porosity was then computed from quantity  $(1 - \rho/\rho_s)$ , where  $\rho$  is the compacted density at the given stress, and  $\rho_s$  is the solid density. Results are given in Figure 4-1. The initial density of the waste, derived in Appendix A, is 426 kg/m<sup>3</sup>, corresponding to a porosity of 0.787<sup>2</sup>.



The following extrapolations of the density curves for combustible and metallic waste were used to extend the respective curves in Figure 4-1 beyond lithostatic pressure (14.8 MPa):

Combustibles:  $\sigma = 0.392 \exp(0.001876 \rho)$ ,  $\sigma > 13.8 \text{ MPa}$ .

Compliance Certification Application Reference Expansion

---

Metallic:  $\sigma = 0.00867 \rho - 13.55$ ,  $\sigma > 13.8 \text{ MPa}$ .

Sludge:  $\sigma = 0.0379 \rho - 61.0$ ,  $\sigma > 13.8 \text{ MPa}$ .

While curve fitting of the data below these stress limits with simple functions did not provide a sufficient correlation to warrant their use for the individual components of waste, the average curve for the repository is approximately represented by:

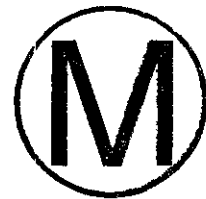
$$\sigma = 31.6772 - 118.511\eta + 161.808\eta^2 - 79.227\eta^3, \quad \sigma < 13.8 \text{ MPa},$$

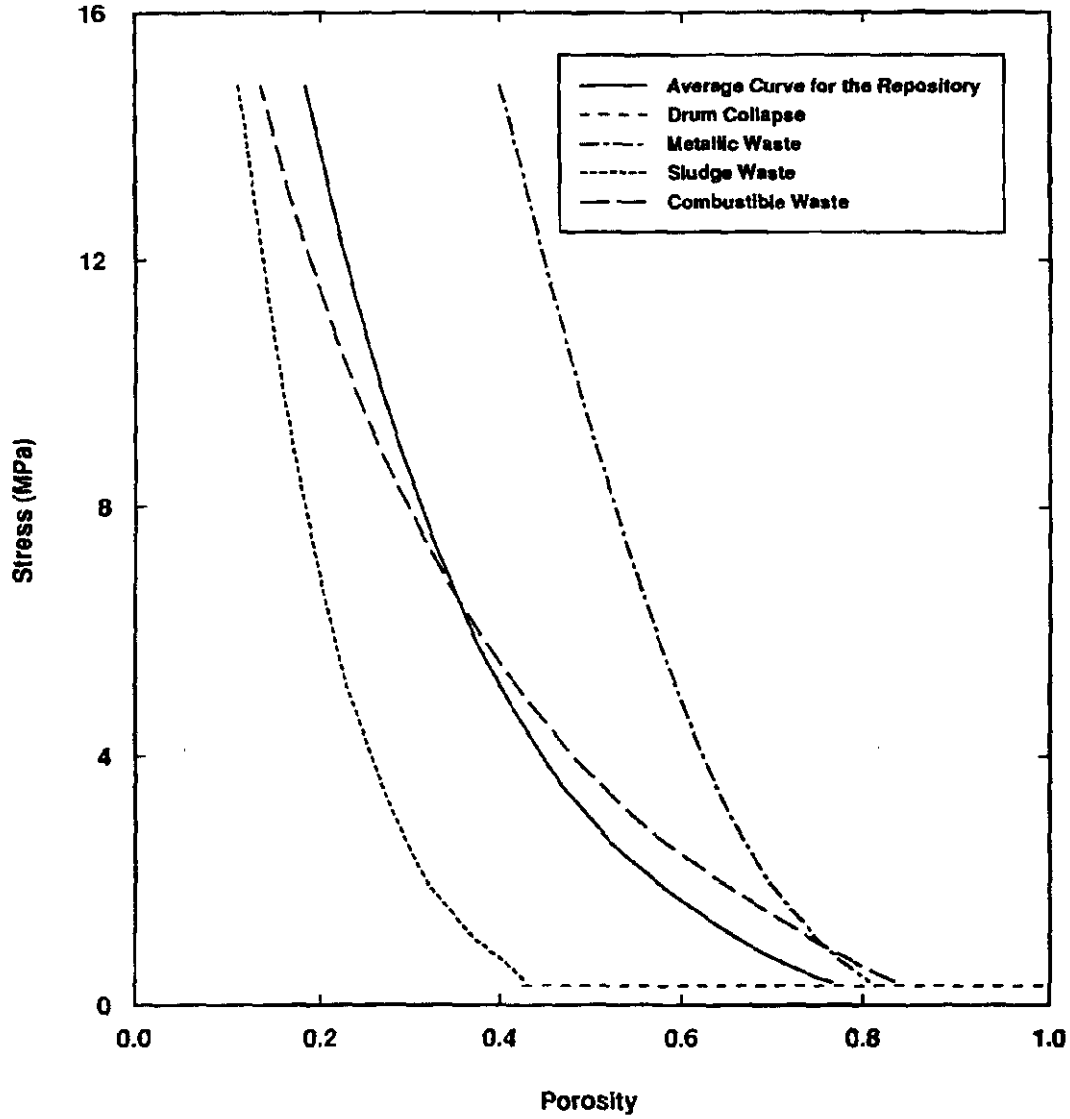
where  $\sigma$  is the stress in MPa and  $\eta$  is the porosity. The results, shown in Figure 4-1 and Table 3-2, indicate that the average drum would collapse to a minimum porosity of about 0.186.

1. For combustible waste, we assume 0.08 weight fraction metal with a solid density of 7110 kg/m<sup>3</sup>, 0.52 plastics with a solid density of 1200 kg/m<sup>3</sup>, 0.32 cellulose with a solid density of 1100 kg/m<sup>3</sup>, and 0.08 sorbents with a grain density of 3000 kg/m<sup>3</sup>. For metal waste, we assume a composition (waste + drums) of 0.75 weight fraction metal, 0.18 weight fraction plastics, 0.02 weight fraction cellulose, and 0.05 weight fraction sorbents (Portland cement). For sludge, we assume 0.134 weight fraction metals, 0.048 plastics, 0.058 sorbents, and 0.76 sludges. The sludge is assumed to have a solid density of 2200 kg/m<sup>3</sup>

2. Although the quality of the data does not warrant it, three significant figures are retained here to assure compatibility with an empirical fit of the repository consolidation curve defined below.

Finally, it is useful to compare the results for axial compaction of combustible and metallic waste in Table 3-2 with the assumptions for the final mechanical state of a typical disposal room made for analyses supporting the Draft Supplemental Environmental Impact Statement (DSEIS) (Lappin et al., 1989). The DSEIS assumptions were made prior to the availability of any test data. In the DSEIS analyses, the assumption was made that combustible waste would compact to a porosity of 0.1 or less. The results of this investigation predict a final porosity of 0.137 at 14.8 MPa (Table 3-2)





TRI-6345-44-0



Figure 4-1. A comparison between the predicted compaction curve for all the waste in the WIPP repository and the recommended compaction curves for combustible, metallic, and simulated sludge wastes.

For metallic waste, a porosity of 0.4 was assumed for the DSEIS analyses. The results of this investigation suggest that metallic waste will compact to the DSEIS porosity estimate of 0.4. For sludge, a porosity of 0.1 was assumed for the DSEIS, and the results of this investigation suggest that sludge waste will compact to 0.113 porosity. However, the assumptions of this last porosity were similar to the DSEIS assumptions; therefore, little difference should be expected between the two values.

#### 4.4 Repository Curves for Lateral Compaction of the Waste



##### 4.4.1 THE INFLUENCE OF SHEAR STRESS ON COMPACTION

All of the information up to this point in the report has been concerned with the axial stress that must be applied to achieve a given state of compaction. The axial stress is defined as the stress along the axis of symmetry of a drum. The axial representations were necessary because the simulated wastes were too heterogeneous to permit direct measurement of lateral stresses during testing and because of the impossibility of making such measurements during drum collapse. Limiting results to a one-dimensional description, was justified, therefore, because either the waste was contained in a rigid die and could not expand, or that little lateral expansion of the drums occurred during collapse. Shear stresses within the waste during drum collapse were believed to be small, because otherwise the outward lateral stresses exerted by the wastes against the walls of the drums would have exceeded the yield stress of the drums, expanding them outward during the tests. The exception was that the shear stresses in the simulated sludge material were sufficient to burst the drums.

Nevertheless, although the assumption that shear stresses could be ignored was convenient for data representation, the magnitude of shear stress that when exceeded will produce plastic deformation is one of the parameters that must be specified for a general mechanical description of the waste. Further, since measurement of shear stresses did not appear feasible, the alternative that was selected was to use computational means to determine how sensitive the results of closure analysis would be to various assumptions about the deviatoric (shear) behavior of the waste.

To illustrate the approach further, assume that a cylinder of waste with a yield stress  $Y$  is loaded axisymmetrically, under stresses  $\sigma_z, \sigma_r = \sigma_\theta$ , with  $\sigma_z > \sigma_r$  the axial stress, and that it is plastically deforming. For this state of stress, the mean stress,  $p$ , that is considered to have the same magnitude as the hydrostatic pressure, is:

$$p = (\sigma_z + 2\sigma_r)/3$$

and the yield point is the difference between the axial and lateral stress:

$$\text{Yield point } Y = \sigma_z - \sigma_r.$$

Therefore:

$$\sigma_z = p + 2/3 \star Y,$$

$$\sigma_r = p - Y/3,$$

and the extremes of possible experimental drum response are:

- 1) If  $\sigma_r = 0$ ; then  $p = Y/3 = \sigma_z/3$ ;  $Y = \sigma_z$ ,
- 2) If  $\sigma_r = \sigma_z$ ; then  $p = \sigma_z$ ;  $Y = 0$ ."

#### 4.4.2 CLOSURE OF A ROOM ENTIRELY FILLED WITH WASTE AND SALT/BENTONITE BACKFILL

This reasoning must now be implemented in a full-fledged numerical closure calculation. The room configuration selected for the calculations was approximately the same as the design configuration of a typical disposal room with the exceptions that a 0.61 m (2 ft) air gap at the top of the room was omitted, since its presence occasionally caused numerical stability problems. This omission is not likely to influence the results greatly because it simply implies that contact of the waste with the surrounding salt begins immediately, rather than after the short time predicted for closure of the 0.61 m (2 ft) gap. Gap closure is estimated to occur within less than ten years. Another major assumption was that the room was symmetric with regard to both its vertical center line and its horizontal center line (Figure 4-2). The calculation has the vertical symmetry plane common to these problems, but use of a horizontal symmetry plane differs from past investigations. The assumption of horizontal symmetry greatly reduces computer run time, and it is a close enough approximation of the actual configuration to justify its use.

The calculations were estimates of the closure of a room filled with TRU waste and salt/bentonite backfill, using the finite-element, finite strain code SANCHO (Stone et al., 1985). Salt/bentonite backfill was selected because closure times predicted for its consolidation are longer than those for pure crushed salt backfill; therefore, variations caused by different assumptions about the shear stress in the waste would be more apparent.

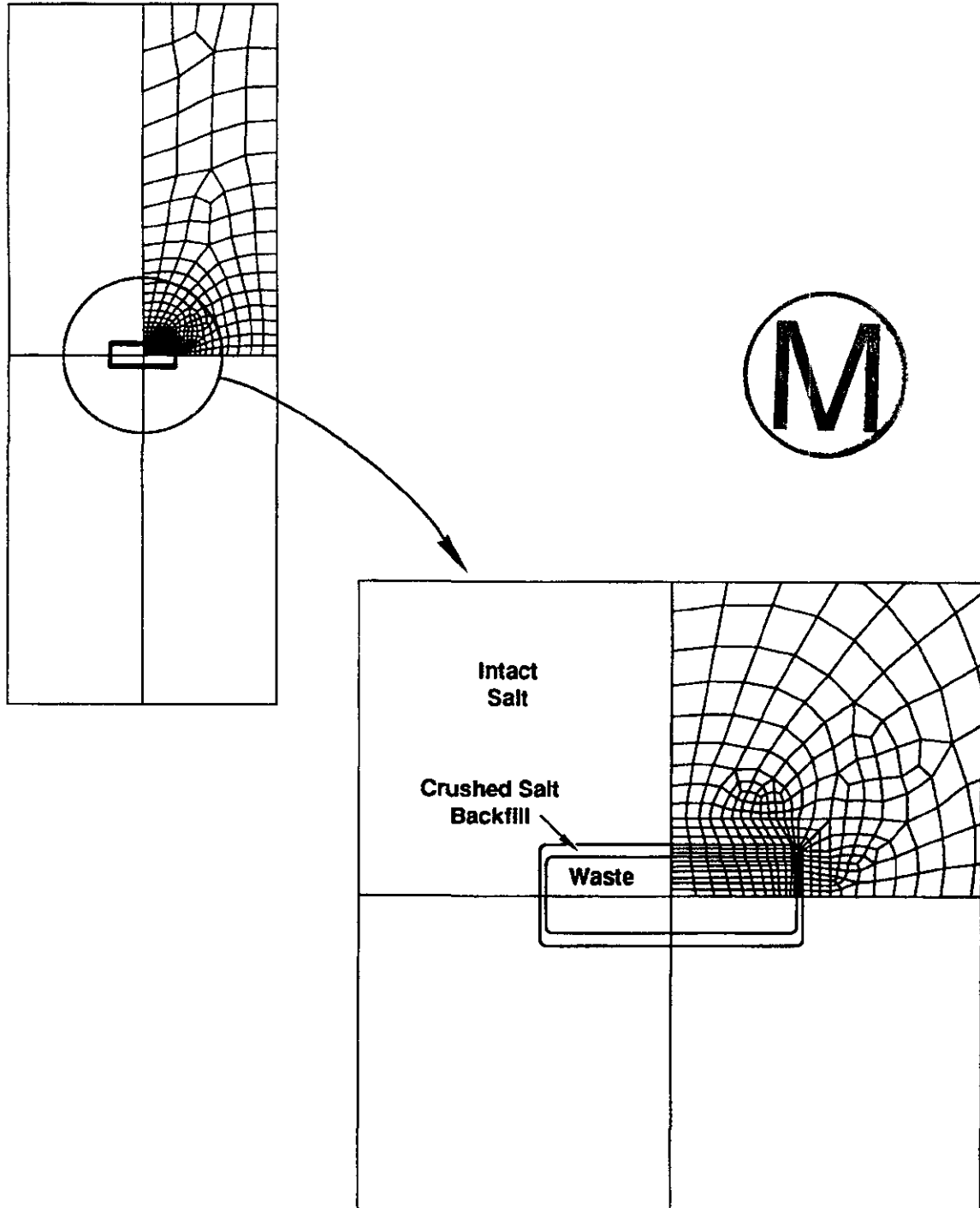


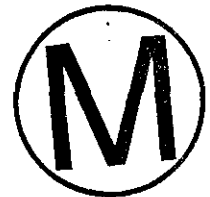
Figure 4-2. Plane strain-finite element model of a TRU storage room.

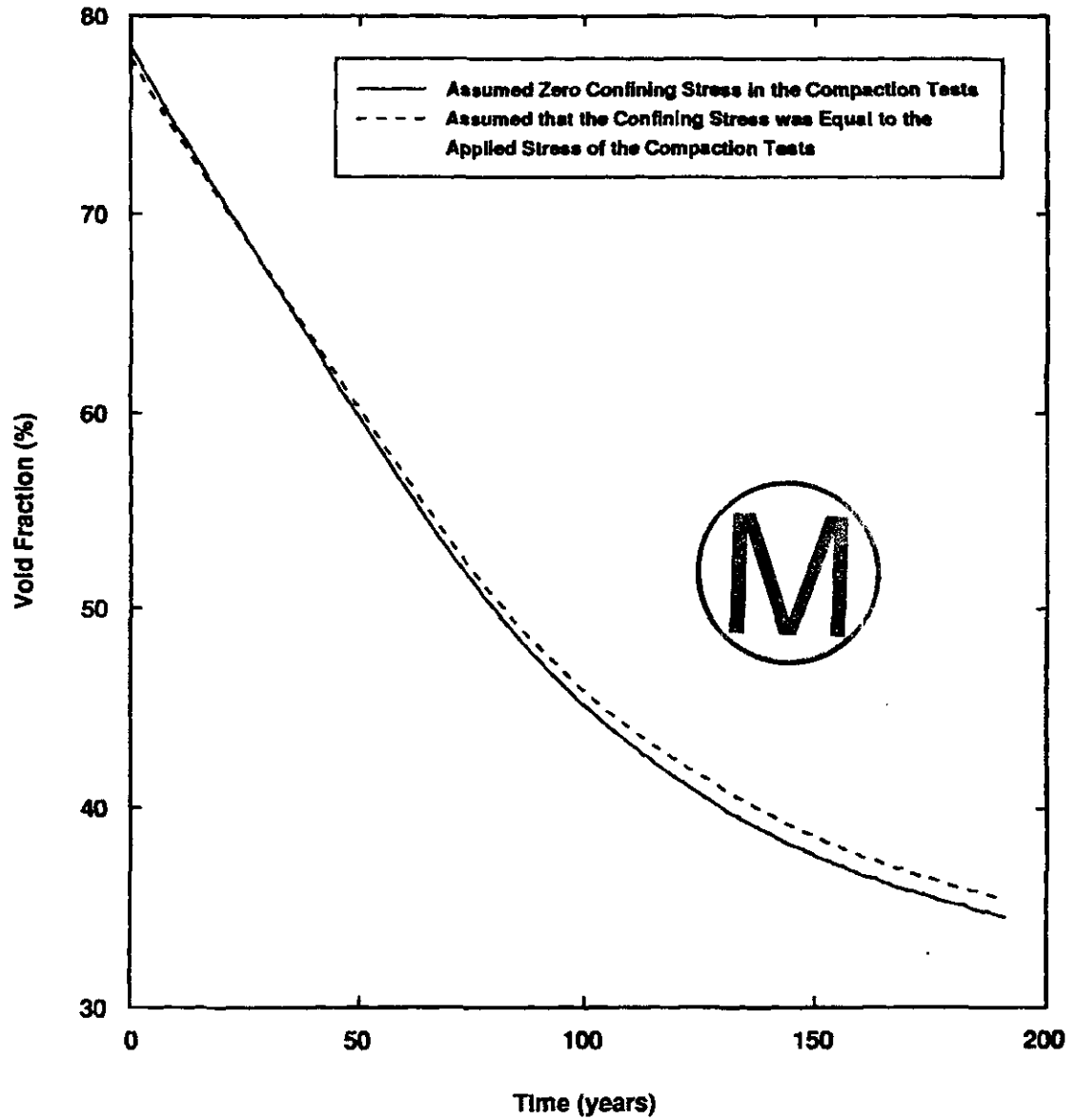
Two compaction models were considered: (1) a model based on the assumption that the confining stress during laboratory compaction tests on the various waste types was zero ( $\sigma_r = 0$ ), and (2) a model based on the assumption that the confining stress in the compaction tests was equal to the applied stress ( $\sigma_r = \sigma_z$ ). These assumptions represent the bounds of waste response as reflected by the magnitudes of the shear stresses that might be generated during consolidation. Assumption (1) represents a material that can support large shearing stresses, and assumption (2) represents a more fluid-like response, with essential no shear stresses developing during consolidation.

The results of the calculations, in Figure 4-3, show little difference between the closure history computed using a maximum possible value for the shear stress in the waste and the history for fluid-like response (the shear stress in this calculation was simply made very small) (Weatherby, personal communication 1991). Void fraction is plotted in this figure because, being equivalent to porosity (as discussed further in Footnote 2) it is the parameter most closely related to the permeability of the room contents. The conclusion from these results is that the closure histories are not very sensitive to the exact value of shear stress selected for the waste; therefore, a precise definition of this parameter is not needed. This observation also supports the original hypothesis of this investigation that a one-dimensional description would prove beneficial in describing waste compaction.

#### 4.4.3 LATERAL COMPACTION OF DRUMS

In reality, lateral compaction curves for the waste are expected to lie somewhere between the limits of  $Y = \sigma_z$ , and  $Y = 0$ , defined in Section 4.4.1. Further, in the sense that (1) axial drum compaction also does not appear to be sensitive to the details of how the drums collapse; and (2) lateral drum collapse is expected to exhibit even less buckling than axial collapse, the exact way that the drums collapse laterally is expected to have little effect on compaction of the waste. Some secondary effects will exist at the ends of the drums because of buckling of the lids, but the creation of collapse rings, such as those observed in the axial drum collapse tests, are considered unlikely. In the absence of information about the magnitude of the shear stresses within the waste, but with the likelihood that they will be small, the recommendation is made that shear stresses be neglected.





TRI-6345-45-0

Figure 4-3. Predicted average void fraction-time history for waste in a room filled with TRU waste and 70% salt/30% bentonite backfill.

## Compliance Certification Application Reference Expansion

---

The reader is cautioned, however, that predictions of how drums collapse laterally within the repository are not nearly as straight forward as for axial collapse. In the axial collapse mode, lateral expansion of the drums is minimal and little or no intrusion into spaces between drums occurs. On the other hand, lateral collapse of the drums is likely to involve considerable alteration of their shapes, depending upon where they are located within the room, and the extent of this shape change will depend upon the nature of the material between them. However, refinement of models to account for this type of detail during consolidation would cause changes in how the waste initially consolidates, but probably not have much effect on the final end point (at lithostatic pressure). Such analyses are presently beyond the capabilities of numerical closure analyses, and it is not clear whether such detail, even if it could be incorporated in the codes, would have much additional impact on performance assessment.



Christian-Frear, G.L., and Webb, S.W. 1996. The Effect of Explicit Representation of the Stratigraphy on Brine and Gas Flow at the Waste Isolation Pilot Plant. SAND94-3173. Sandia National Laboratories, Albuquerque, NM.

**ABSTRACT;**

" Stratigraphic units of the Salado Formation at the Waste Isolation Pilot Plant (WIPP) disposal room horizon includes various layers of halite, polyhalitic halite, argillaceous halite, clay, and anhydrite. Current models, including those used in the WIPP Performance Assessment calculations, employ a "composite stratigraphy" approach in modeling. This study was initiated to evaluate the impact that an explicit representation of detailed stratigraphy around the repository may have on fluid flow compared to the simplified "composite stratigraphy" models currently employed. Sensitivity of model results to intrinsic permeability anisotropy, interbed fracturing, two-phase characteristic curves, and gas-generation rates were studied. The results of this study indicate that explicit representation of the stratigraphy maintains higher pressures and does not allow as much fluid to leave the disposal room as compared to the "composite stratigraphy" approach. However, the differences are relatively small. Gas migration distances are also different between the two approaches. However, for the two cases in which explicit layering results were considerably different than the composite model (anisotropic and vapor-limited), the gas-migration distances for both models were negligible. For the cases in which gas migration distances were considerable, van Genuchten/Parker and interbed fracture, the differences between the two models were fairly significant. Overall, this study suggests that explicit representation of the stratigraphy in the WIPP PA models is not required for the parameter variations modeled if "global quantities" (e.g., disposal room pressures, net brine and gas flux into and out of disposal rooms) are the only concern."



Corbet, T.F. and Knupp, P.M. 1996 The Role of Regional Groundwater Flow in the Hydrogeology of the Culebra Member of the Rustler Formation at the Waste Isolation Pilot Plant (WIPP), Southeastern New Mexico. SAND96-2133. Albuquerque, NM: Sandia National Laboratories.

p. i, para. 1;

1. INTRODUCTION; p. 1, para. 1;

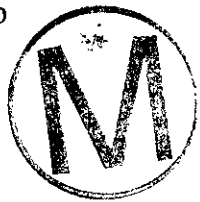
" This report summarizes a study in which numerical simulation is used to enhance conceptual understanding of the hydrogeology of the Culebra Dolomite in the context of groundwater flow on a regional scale in the vicinity of the Waste Isolation Pilot Plant (WIPP). The WIPP is a potential repository for defense-generated transuranic wastes. The Culebra Dolomite is a member of the Permian age Rustler Formation, a sequence of predominantly evaporate deposits that overlie the Salado Formation. The Salado is a thick bedded salt of Permian age that contains the WIPP and provides the primary containment for the repository. The groundwater flow system in the overlying Permian and Triassic deposits forms a secondary barrier to releases from the repository in the even of a breach of the primary containment. Consequently, an important requirement of the performance assessment of the repository is to characterize long-term groundwater flow in the shallow system. We consider the possibility that patterns of groundwater flow in the shallow system change over thousands of years in response to change climate. Although groundwater flow is simulated in all of the strata above the Salado, this report focuses primarily on flow in the Culebra Dolomite because it is thought to be the most likely pathway for lateral migration of radionuclides to the accessible environment."

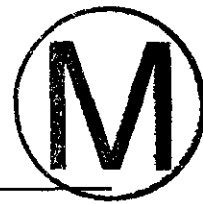
p. 3, para. 2;

" We developed a new numerical code called SECOFL3D, to perform the simulations. The algorithm implements a rigorous treatment of the free-surface and seepage-face boundary conditions (Bear and Verruijt, 1987; Dagan, 1989; de Marsily, 1986) and is designed to be robust even if extremely large contrasts in hydraulic conductivity are present within the model domain. A moving mesh that adaptively deforms so that its upper surface conforms to the moving water table is used to ensure that the entire computational domain remains saturated.

Lateral boundaries of groundwater basins are sub-vertical flow divides that typically coincide with depressions and highs on the land surface. Flow over a region much larger than the WIPP site (Figure 1-1) was simulated in order to have the model boundary coincide with topographic features that are likely to act as groundwater divides over a range of climatic conditions. A series of steady-state simulations was performed to examine the sensitivity of simulation results to assumed values for hydraulic conductivity and recharge rate. Transient simulations provided insight into how patterns of groundwater flow respond to long-term changes in climate. These simulations covered the time period from late in the Pleistocene (14,000 years ago) to 10,000 years in the future.

The simulations results suggest that patterns of groundwater flow in the Culebra in the





Compliance Certification Application Reference Expansion

vicinity of the WIPP are influenced by the hydrology of the entire groundwater basin. Flow rates and directions depend on the position of the water table and heterogeneity in hydraulic conductivity at the basin-scale. Groundwater flow changes with time due to interaction among recharge, movement of the water table, and topography of the land surface."

p. 5, para. 2;

" The simulations also provide information about how flow in the Culebra in the vicinity of the WIPP is coupled with flow in adjacent strata. Vertical leakage across the top of the Culebra is directed downward. The amount of vertical leakage into the Culebra cannot be estimated with confidence because the vertical conductivity of the confining units is not well constrained. Vertical leakage may contribute as little as 5% or more than 50% of the total inflow to the portion of the Culebra that lies within the WIPP-site boundary. All of the outflow from this portion of the Culebra is lateral flow. Therefore, contaminants introduced into the Culebra will travel toward the accessible environment along the Culebra rather than by migrating upward or downward into other units."

p. 103, para. 4;

" We performed mass balances over the reference volumes (defined in the introduction to Section 3) of the more conductive layers. This was accomplished by summing the flow across each face of the reference volumes in order to calculate total flow through each reference volume, as well as the proportions of lateral and vertical inflow and outflow from the reference volumes."

p. 105, para. 1;

" Figures such as 3-46, 3-47, and 3-48 mass balances provide a clear overview of the mass balance but are difficult to interpret quantitatively. To complement these figures, we have included tables in Appendix D that summarize the mass balance data at two simulated times: at the present time (zero years) and at 10,000 years into the future. The total inflow to the Dewey Lake/Triassic rocks, Magenta, and Culebra reference volumes at the simulated present time are 5015, 784, and 2100 cubic meters per year (base case in Table D-1). The inflow rates for these units at 10,000 years are somewhat larger: 16738, 1736, and 3354 cubic meters per year (base case in Table D-4). These numbers show that, in this simulation, most of the flow occurs in the Dewey Lake/Triassic rocks and that more flow occurs in the Culebra than the Magenta."

p. 106, para. 1;

" Table D-2 gives the total flow across the upper surface, lower surface, and sides as a percentage of the total flow through the reference volume at zero years simulation time. For the base-case simulation, 42% of the inflow to the Dewey Lake/Triassic reference volume is from groundwater recharge (i.e., 42% of the inflow to the Dewey Lake/Triassic rocks is across the top). Zero percent of the inflow to the Dewey Lake/Triassic is from upward vertical leakage. In fact, an important aspect of all of the transient simulations performed for

this study is that the vertical flow components are directed downward in all layers within the vicinity of the WIPP site. 98% of the inflow to the Magenta reference volume is vertical leakage from the Dewey Lake/Triassic and 30% of the inflow to the Culebra is leakage from the Magenta. All of the outflow from the Culebra reference volume is by lateral flow. Table D-5 provides the same information at 10,000 years."

p. 139, para. 2;

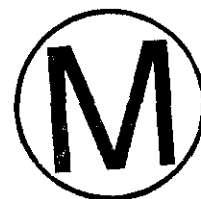
" Within the region of intact strata, the contrast in hydraulic conductivities plays an important role in determining flow patterns. The Dewey Lake and Triassic rocks are more permeable than the anhydrites at the top of the Rustler Formation. Consequently most of the water that recharges the groundwater basin flows only in these rocks above the Rustler. The rest leaks vertically through the upper anhydrites and is available for flow through the rest of the Rustler. Differences in hydraulic head along the base of the Dewey Lake provide the driving force for flow in the Rustler.

Groundwater flow in the Rustler Formation is characterized by very slow vertical leakage through confining units and faster lateral flow in conductive units. Specific discharges (flow rates per unit area) in the Culebra are 2 to 3 orders of magnitude greater than the vertical specific discharges across the top of the Culebra. However, vertical leakage can contribute a significant portion of the total inflow to portions of the Culebra that are extensive enough that the upper surface is very much larger than the area available for lateral flow."

p. 141, para. 4;

" These simulations suggest that, in the vicinity of the WIPP site, vertical flow across the top of the Culebra is directed downward. The amount of vertical leakage into Culebra at this site cannot be estimated with confidence. It contributes a small portion of the total inflow to the Culebra reference volume, perhaps 5% to 10%, if the vertical conductivity of the confining units is  $1 \times 10^{-13}$  m/s or less. However vertical leakage may contribute more than 50% of the total inflow if the conductivity is an order of magnitude larger.

A robust implication of these simulations is that nearly all (greater than 90% in all simulations) outflow from the Culebra reference volume is by lateral flow. Therefore, contaminants introduced into the Culebra will travel toward the accessible environment within the Culebra rather than by leaking upward or downward into other units. This result provides confidence that a flow and transport model that assumes that flow occurs only in the Culebra would include the appropriate release pathways."



Cranwell, R.M., Guzowski, R.V., Campbell, J.E., and Ortiz, N.R. 1990. Risk Methodology for Geologic Disposal of Radioactive Waste, Scenario Selection Procedure. NUREG/CR-1667, SAND80-1429, Sandia National Laboratories, Albuquerque, NM. WPO 26750.

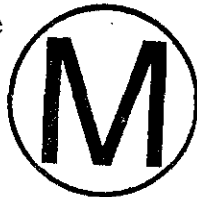
ABSTRACT, p iii;

" This report contains the description of a procedure for identifying and screening those events, features and processes, both natural and human induced, felt to be important to the isolation of radioactive wastes in deep geologic formations. In this report, the term 'scenario' is used to represent a sequence of these events, features and processes. The scenario selection and screening procedure discussed in this report is demonstrated by applying it to the analysis of a hypothetical waste disposal site containing a bedded salt formation as the host medium for the underground facility (repository). A final set of 12 scenarios is selected for this hypothetical site. Detailed risk calculations will be performed on these 12 scenarios in a later report."

PROCEDURE FOR SCENARIO SELECTION, P. 5;

"2.1 Identification of Events and Processes

The first step in any scenario selection procedure should be the identification of a comprehensive set of events and processes, both natural and human-induced, believed to be important to the disruption of the isolation of radioactive waste at the site being considered. This identification would generally be accomplished through discussions among persons knowledgeable in the areas of earth science and waste-management analyses. The use of knowledgeable and experienced individuals helps ensure that potentially important scenarios are not overlooked. For the demonstration of the Performance Assessment Methodology, a panel of knowledgeable earth scientists was convened for the purpose of identifying those events and processes considered to be important to the disruption of the isolation of radioactive waste in bedded salt (see Section 3.3, Table 2).



2.2 Classification of Events and Processes

The classification of events and processes provides a logical aid to help ensure that important scenarios will not be overlooked. The initial list of phenomena (see Table 2) was classified into the categories of natural, human-induced, and waste- and repository-induced. This classification was based on the origin and physical characteristics of these phenomena. A procedure for further classification is presented below. In addition to addressing the question of completeness, this classification also provides the organization needed to begin developing and analyzing scenarios.

Events and processes will also be classified based upon the manner by which they influence the disposal system consisting of the repository and the surrounding geology. Those

phenomena in the near vicinity of the repository, whose major effect is to influence the release and movement of radionuclides from the waste packages and engineered barrier system to a nearby aquifer or directly to the land surface, will be referred to as release phenomena. Similarly, those phenomena in the far field whose major effect is to influence the transport of radionuclides in ground water will be referred to as transport phenomena.

The distinction between those events and processes included as release phenomena and those included as transport phenomena is not always obvious. For example, faulting may be classified as either a release or transport phenomenon, depending on the proximity to the site. If the fault should pass through or very near the repository, its primary effect would be to influence the release and movement of radionuclides from the repository to a nearby aquifer. In this case, the fault would be classified as a release phenomenon. On the other hand, if the fault should occur at some distance away from the repository so that its primary effect is to influence the transport of radionuclides in ground water, then it would be classified as a transport phenomenon. Regardless of its classification, a given event or process may influence both radionuclide release and transport, depending on its effect on the site hydrology. Despite the seemingly arbitrary division of phenomena into release and transport categories, the reasons for this division become more apparent when the one considers the complex thermal, mechanical, geochemical and hydraulic analyses that may be required for near-field (release) phenomena analysis compared to the more straightforward flow and transport analyses required for far-field (transport) phenomena analysis.

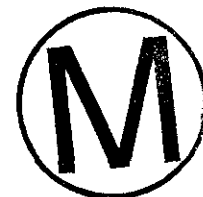
While only two classification schemes are used in this example, additional classifications are helpful in developing a comprehensive list of phenomena.

### 2.3 Screening of Events and Processes

Many of the events and processes from the initial list considered for a potential disposal site can be eliminated based on firm and well-defined screening criteria. A screening of these events and processes is not only desirable but also essential if one considers the thousands of scenarios that could be defined by taking specific combinations of these phenomena.

Initial screening criteria should consist of the following:

1. Physical reasonableness of the events and processes being considered.
2. Probability of significant release of radionuclides from these events and processes.
3. Potential consequences associated with the occurrence of these events and processes.



Physical Reasonableness. Events and processes whose occurrence is impossible due to the physical and chemical characteristics of the waste and characteristics of the engineered

## Compliance Certification Application Reference Expansion

---

facility or geologic site can be eliminated by this screening criterion. Some examples of phenomena that could be eliminated based on the test of physical reasonableness are

- A nuclear explosion in an underground facility designed to prevent criticality.
- Formation of dissolution cavities in crystalline rock.
- Tsunamis for a repository far removed from coastal regions.



Clearly, the elimination of phenomena due to this criterion would be largely site specific. Therefore, this step in the screening process should be repeated for each repository site.

Probability. Events and processes with very "small" probability can generally be rejected. The specification of "small" should be the responsibility of the regulator or the applicant and should be consistent with the appropriate regulations. Once a value has been selected, judgmental decisions will undoubtedly still have to be made as many probabilities associated with various phenomena will have large uncertainties. The value selected in the demonstration analysis of this report was  $10^{-8}/\text{yr}$ .

In several safety studies, numerical probability criteria have been used to reject scenarios. For example, WASH-1400 [U.S. Nuclear Regulatory Commission, 1975] uses a limit of  $10^{-9}/\text{yr}$  to reject accident sequences. Other references [Griesmeyer and Okrent, 1981] suggest larger numbers (e.g.,  $10^{-7}/\text{yr}$ ). The U.S. Environmental Protection Agency (EPA) [U.S. Environmental Protection Agency, 1985] suggests that categories of events and processes with probability of occurrence smaller than  $10^{-8}/\text{yr}$  can be ignored.

Consequence. As used in this report, "consequence" can have different interpretations, depending upon the stage of the screening process. For example, in the earlier stages of the screening process, "consequence" generally refers to the effects that a certain event or process might have on the natural properties of the site (e.g., hydraulic head distribution). Thus, only flow and possibly thermomechanical analyses are needed at this point. In the screening of scenarios, "consequence" generally refers to the amount of radionuclides being discharged to the environment and the health effects associated with these discharges. Thus, radionuclide transport and health effects calculations are needed at this point. The reason for this breakdown is that in the early stages of the screening process, detailed transport and health effects calculations should be avoided because of the higher computer and man-power costs associated with these efforts. The total scenarios should be reduced to a reasonable number before undertaking detailed risk calculations.

At any rate, screening based on consequence can occur in several ways. For example, events and processes having similar consequences (e.g., effects on hydraulic head) could conceivably be grouped together provided the probabilities of these phenomena are

appropriately combined. Also, events and processes with insignificant consequences (e.g., no apparent effect on hydraulic head) could be eliminated. However, before eliminating phenomena based on insignificant consequences, their potential maximum consequence should be considered.

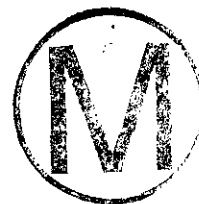
#### 2.4 Scenario Construction

The next step in the scenario selection procedure involves the formation or development of scenarios by taking meaningful combinations of those phenomena remaining after the screening process. Recall that at this point, the events and processes have been classified as to "release" and "transport" phenomena as discussed in Section 2.2. The development of scenarios by taking combinations of the various release and transport phenomena is illustrated by a simple example.

Consider the simple case of two release phenomena (R1, R2) and three transport phenomena (T1, T2, T3). The possible scenarios that can be created by taking combinations of these phenomena are shown in Figure 2. There are 25 - 32 possible combinations in this example. The use of a logic diagram as illustrated in Figure 2 ensures that all possible combinations are identified. The base case scenario represents the initial conceptualization of the disposal system including the repository and emplaced waste. All components of the engineered-barrier system are assumed to perform as designed. The other scenarios are perturbations to these basic conditions.

This organizational method is preferable to the classical event-tree, fault-tree techniques frequently used in the analysis of engineered systems. This statement is made for the following reasons.

1. Many of the so-called "events" associated with geologic environments do not represent immediate or abrupt changes in the system but rather slow, continuous changes over hundreds to thousands of years (e.g., dissolution cavities in bedded-salt formations, shaft or borehole seal degradation, etc.). Hence their occurrence cannot be represented by a simple "yes" or "no" statement
2. Feedback loops frequently appear in the investigation of the processes that could affect the release of radionuclides from the underground facility. Event trees and fault trees do not adequately incorporate interactions between various factors influencing radionuclide movement.
3. For a given set of conditions, many of the processes are basically deterministic. Thus, the question of when and if a certain "barrier" will be breached is answered when a given set of conditions is specified. The real question is, what conditions exist?



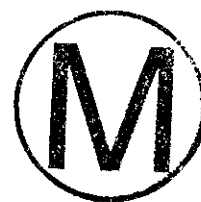
4. Event trees and fault trees force artificial divisions in the representation of processes. The important question is how the entire system behaves.

Other studies [Burkholder, 1981; Koplik et al., 1982] have also concluded that event and fault trees are not useful for analyzing geologic processes or their interactions. They recommend the use of simulation techniques with models to describe the evolution over time of a set of variables representing the scenarios. The latter method is used in this study as described in the next chapter.

### 2.5 Screening of Scenarios

The next step in the scenario selection procedure would be to screen the scenarios developed from taking combinations of the various release and transport phenomena. An initial screening of these scenarios is based on physical reasonableness, probability, and consequence.

Physical Reasonableness. The most readily applicable of these screening criteria is physical reasonableness. Certain combinations of events and processes are incompatible. For example, consider a basaltic dike that intrudes through the repository. The effects of such an intrusion primarily would be on the release of radionuclides. A dike that behaved as a barrier to flow could be designated as R1. If a fracture or rubble zone occurred as a result of the intrusion, a high-conductivity zone could be formed that would enhance ground-water flow. For this example, the presence of a high-conductivity zone is designated R2. The presence of the dike must be considered as either R1 or R2. The combination R1 R2 requires the dike to have incompatible properties. As a result, all scenarios (e.g., Figure 2) that include both R1 and R2 could be dropped from consideration on the basis that the components are not a physically reasonable combination.



Compliance Certification Application Reference Expansion

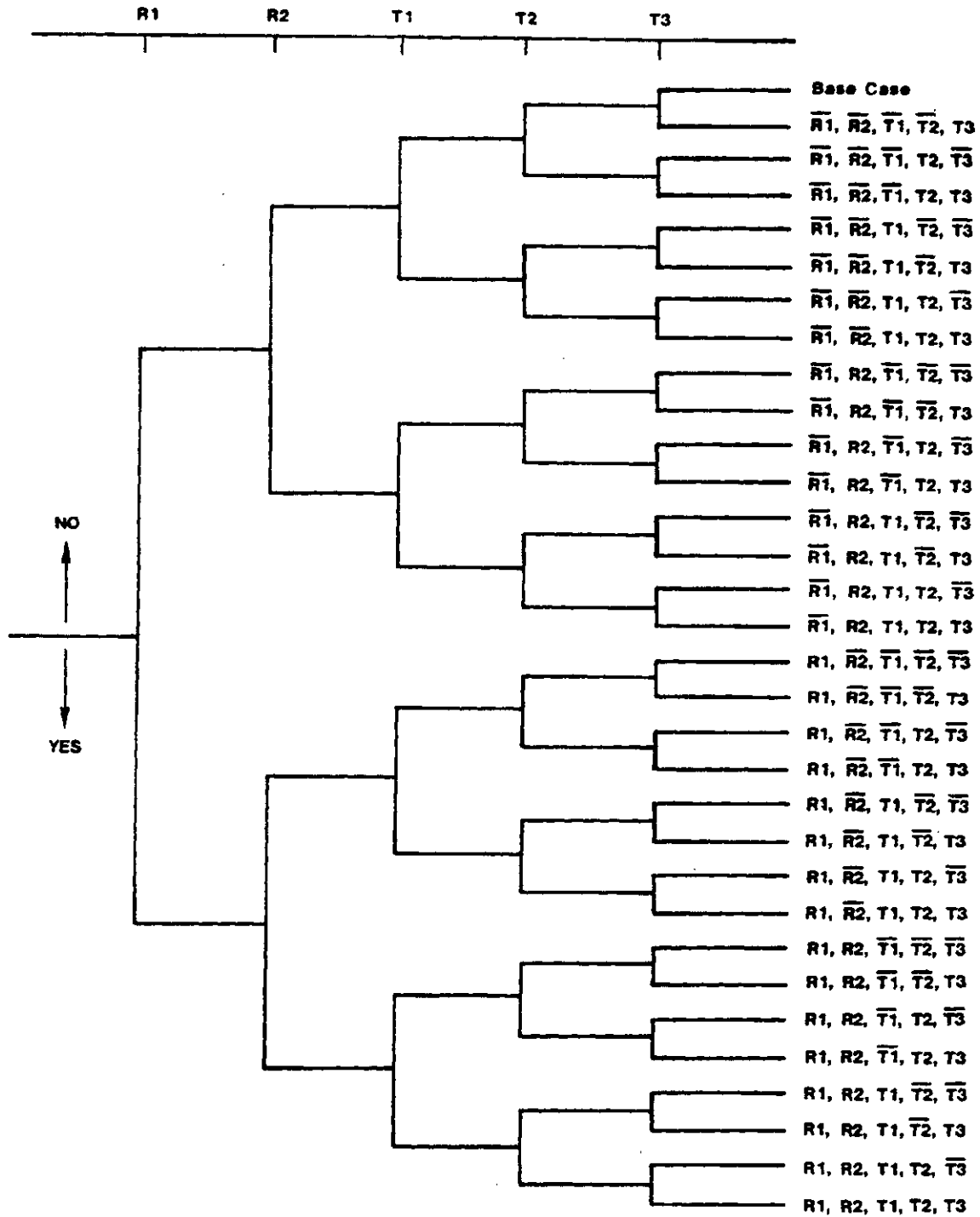


Figure 2. Potential Combinations of Two Release and Three Transport Phenomena

**Compliance Certification Application Reference Expansion**

---

**Probability.** Assuming probabilities have been assigned to the various release and transport phenomena (components) comprising a scenario, a probability of that scenario can be arrived at by simply multiplying the probabilities of each of the components (assuming, of course, independence among the components). If the components of a scenario are not independent, then conditional probabilities can be used to arrive at the probability of the scenario. If this probability falls below the agreed-upon cutoff (e.g.,  $10^{-8}/\text{yr}$ ), and one is relatively confident in the probability estimates for each component comprising the scenario, then this scenario could be eliminated from any further consideration.

**Consequences.** Scenarios can also be screened on the basis of consequence. Here, consequence generally refers to either radionuclide discharges to the environment or the health effects resulting from these discharges. Thus, radionuclide transport and health effects calculations are needed. If, in performing transport calculations for a scenario, no discharges are observed for the period of time used in the analysis, no additional consideration of the scenario is necessary. However, if discharges occur, the scenario must be retained for inclusion in regulatory compliance assessments, such as those specified in the containment requirements, 40 CFR 191.13 [U.S. Environmental Protection Agency, 1985].

A final screening of the scenarios remaining at this point can be accomplished using combined probability and consequence arguments, namely risk. However, unless regulations for disposal are risk-based, the use of risk in screening scenarios is generally not applicable.

TABLE; p. 26, tbl. 2;  
"

Table 2.

**Potentially Disruptive Events and Processes**

---

Natural Events and Process

Celestial Bodies

Meteorite Impacts

Surficial Events and Process

Erosion/Sedimentation

Pluvial Periods

Sea Level Variations

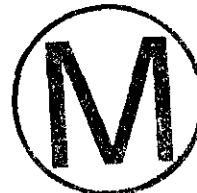
Hurricanes

Seiches

Tsunamis

Regional Subsidence or Uplift

(also applies to subsurface)



Glaciation

Landslides

Subsurface Events and Processes

Seismic Activity  
Volcanic Activity  
Magmatic Activity  
Formation of Dissolution Cavities  
Formation of Interconnected Fracture  
Faulting

Systems

Human-Included Events and Processes

Inadvertent Intrusions  
Explosions  
Drilling  
Mining  
Waste Disposal (Injection Wells)  
Withdrawal Wells

Hydrologic Stresses

Irrigation  
Damming of Rivers

Waste-and Repository-Induced Events and Processes

Subsidence and Caving  
Shaft and Borehole Seal Degradation  
Thermally-Induced Stress/Fracturing in

Host

Rock

Excavation-Induced stress/Fracturing in

Host Site"

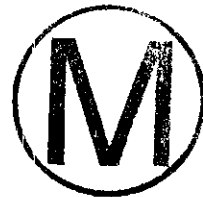


**Compliance Certification Application Reference Expansion**

---

Dale, T. and L.D. Hurtado. 1996. "WIPP Air-Intake Shaft Disturbed-Rock Zone Study," 4th International Conference on the Mechanical Behavior of Salt, Montreal, Quebec, June 17-18, 1996. SAND96-1327C. Albuquerque, NM: Sandia National Laboratories.

NOTE: The above listed document was not available for inclusion in the Reference Expansion as of the printing date. Page changes will be provided as the above document becomes available for inclusion.



Davies, P.B., 1991. Evaluation of the Role of Threshold Pressure in Controlling Flow of Waste-Generated Gas into Bedded Salt at the Waste Isolation Pilot Plant. SAND90-3246. Sandia National Laboratories, Albuquerque, NM, pp. 17-19. WPO 26169.

**ABSTRACT:**

" Anoxic corrosion and microbial degradation of contact-handled transuranic waste may produce sufficient quantities of gas over a long time period to generate high pressure in the disposal rooms at the Waste Isolation Pilot Plant (WIPP) repository. Dissipation of pressure by outward gas flow will be inhibited by the low permeability of the surrounding rock and by capillary forces that resist gas penetration into this water-saturated rock. Threshold pressure is the gas pressure required to overcome capillary resistance to initial gas penetration and to the development of interconnected gas pathways that would allow outward gas flow. The primary objectives of this study are to estimate the magnitude of threshold pressure in the bedded salt that surrounds the WIPP repository and to evaluate the role this parameter plays in controlling the outward flow of waste-generated gas. Estimates of threshold pressure have been made based on an empirical correlation of threshold pressure with intrinsic permeability from other low-permeability rock types and on a capillary tube model. These two approaches yield generally consistent estimates, suggesting that threshold pressure in relatively pure halite is 20 to 50 MPa, or larger; threshold pressure in impure halite is 5 to 25 MPa; and threshold pressure in more permeable nonhalite interbeds is 2 to 1/2 MPa, or less. Because of the compounding effect of low threshold pressure and relatively high permeability, the nonhalite interbeds are likely to be the dominant pathways for flow of waste-generated gas away from a pressurized repository. Near the repository, a number of processes occur that may significantly reduce threshold pressure. Local fracturing and pore dilation in response to excavation-related stresses creates larger pore apertures. Desaturation occurs as a result of drying, dilation, and/or exsolution of gas that is dissolved in Salado brine under natural conditions. All of these processes contribute to the development of a zone surrounding the repository that contains pore space that is readily accessible to waste-generated gas due to significantly decreased threshold pressures. The threshold pressure estimates and analyses presented in this report are based primarily on threshold pressure information from low-permeability, nonsalt rock types and must be confirmed with direct, laboratory, and/or in situ measurements specific to the Salado Formation at the WIPP repository. In particular, such measurements should be directed toward the nonhalite interbeds and impure halite."



**ABSTRACT:**

" Anoxic corrosion and microbial degradation of contact-handled transuranic waste may produce sufficient quantities of gas over a long time period to generate high pressure in the disposal rooms at the Waste Isolation Pilot Plant (WIPP) repository. Dissipation of pressure by outward gas flow will be inhibited by the low permeability of the surrounding rock and by capillary forces that resist gas penetration into this water-saturated rock. Threshold pressure is the gas pressure required to overcome capillary resistance to initial gas penetration and to

the development of interconnected gas pathways that would allow outward gas flow. The primary objectives of this study are to estimate the magnitude of threshold pressure in the bedded salt that surrounds the WIPP repository and to evaluate the role this parameter plays in controlling the outward flow of waste-generated gas. Estimates of threshold pressure have been made based on an empirical correlation of threshold pressure with intrinsic permeability from other low-permeability rock types and on a capillary tube model. These two approaches yield generally consistent estimates, suggesting that threshold pressure in relatively pure halite is 20 to 50 MPa, or larger; threshold pressure in impure halite is 5 to 25 MPa; and threshold pressure in more permeable nonhalite interbeds is 2 to 1/2 MPa, or less. Because of the compounding effect of low threshold pressure and relatively high permeability, the nonhalite interbeds are likely to be the dominant pathways for flow of waste-generated gas away from a pressurized repository. Near the repository, a number of processes occur that may significantly reduce threshold pressure. Local fracturing and pore dilation in response to excavation-related stresses creates larger pore apertures. Desaturation occurs as a result of drying, dilation, and/or exsolution of gas that is dissolved in Salado brine under natural conditions. All of these processes contribute to the development of a zone surrounding the repository that contains pore space that is readily accessible to waste-generated gas due to significantly decreased threshold pressures. The threshold pressure estimates and analyses presented in this report are based primarily on threshold pressure information from low-permeability, nonsalt rock types and must be confirmed with direct, laboratory, and/or in situ measurements specific to the Salado Formation at the WIPP repository. In particular, such measurements should be directed toward the nonhalite interbeds and impure halite."



Section 4.1 Empirical Correlations, p. 17;

"Correlations of threshold pressure with intrinsic permeability have been presented in the soils literature for unconsolidated materials (Stakman, 1968) and in the petroleum literature for consolidated rock (Thomas et al., 1968; Ibrahim et al., 1970). The physical rationale behind this approach is that both threshold pressure and intrinsic permeability are strongly related to pore size and pore interconnections in some fashion. As noted in the previous discussion of the capillary tube model, over the broad spectrum of geologic environments, intrinsic permeability ranges over 13 orders of magnitude (Table 2) and is the dominant factor controlling threshold pressure. The parameter with the second largest range (2-1/2 orders of magnitude) is porosity. Empirical correlations for threshold pressure that incorporate both intrinsic permeability and porosity have also been tested, but show no significant improvement in fit over correlations that use only intrinsic permeability (Ibrahim, 1970).

A detailed literature review has yielded threshold pressure and intrinsic permeability data for a broad range of lithologies with permeabilities ranging from approximately  $1 \times 10^{-9}$  to  $1 \times 10^{-22} \text{ m}^2$  (1000 darcies to 0.1 nanodarcy). Most data at the lower end of this range come from measurements on caprock lithologies associated with underground gas storage research. Data at the high end of this range are primarily from unconsolidated soils and

artificial porous media. Figure 5 is a plot of the threshold pressure versus intrinsic permeability, grouped by lithology. This plot contains only data from research laboratory measurements carried out under carefully controlled conditions. Data from commercial laboratories were not included because of the frequent absence of lithologic information and uncertainty in the range of quality control in the measurements. Data from Cosby et al. (1984) for unconsolidated materials have been presented as a separate curve because these data represent mean values from a large number of samples in groups of different textural classifications rather than individual sample points.

The empirical correlations presented in Figure 5 and summarized in Table 3 reveal a distinct similarity in threshold-pressure versus intrinsic-permeability relationships for the consolidated lithologies, which include sandstone, shale, carbonate, and anhydrite. These data have been fit with a power curve of the form:

$$y = ax^b \tag{7}$$

The best fit power curves for these lithologies are quite similar, with exponents ranging from -0.34 to -0.37 and coefficients ranging from  $3 \times 10^{-7}$  to  $9 \times 10^{-7}$ . On the other hand, the curves for the high permeability lithologies (unconsolidated soils and artificial porous media) are different, with the exponents ranging from -0.46 to -0.71 and coefficients ranging from  $3 \times 10^{-8}$  to  $3 \times 10^{-12}$ . The exponents for the best fit power curves for all lithologies are generally similar to the theoretical -0.50 exponent indicated by the capillary tube model (Equation 5). The Stakman (1968) data for sorted sand are characterized by a close fit ( $R^2$  is equal to 0.97) and by an exponent (-0.46) that is quite similar to the theoretical -0.50 value. Exponents for the consolidated lithologies are all close to -0.35, suggesting that factors other than intrinsic permeability may exert secondary influence on the correlation for consolidated materials."



**Compliance Certification Application Reference Expansion**

---

Dotson, L.J. 1996. Non-Salado Initial Pressure. Sandia National Laboratories, NM. WPO 30713.

NOTE: The above listed document was not available for inclusion in the Reference Expansion as of the printing date. Page changes will be provided as the above document becomes available for inclusion.



Earth Technology Corporation, 1988. Final Report for Time Domain Electromagnetic (TDEM) Surveys at the WIPP Site. SAND87-7144. Albuquerque, NM, Sandia National Laboratories.

EXECUTIVE SUMMARY, p ii;

The Earth Technology Corporation was contracted by Sandia National Laboratories to perform a time domain electromagnetic (TDEM) survey at the WIPP site for the purpose of mapping the depth of occurrence of brine pockets and layers. The impetus for the geophysical survey was that pressurized brine had been encountered in drill holes in the Castile Formation immediately underlying the bedded salts of the Salado Formation in which the waste storage panels are mined. TDEM is a geophysical technique that determines layering in the subsurface from surface resistivity measurements. Because brine layers and pockets have low resistivities compared to the bedded salts of the host rock, they are good targets for electrical exploration.

Most of the measurements (36 out of 38) were located in a 1.5 by 1 km grid directly over the waste storage panels. Two measurements were made next to drill holes WIPP #12 and DOE #1 to validate the interpretation of the geophysical survey. Also, one drill hole (ERDA #9) at the northern boundary of the survey grid was used for calibration.

The results of the survey can be summarized as follows:

- The geoelectric sections derived from the TDEM measurements compare well with geologic and geophysical data of the three drill holes. At WIPP #12 the occurrence of brine at a depth of about 800m (2600 ft.) is clearly seen in the TDEM data.
- The results of the TDEM survey over the waste storage panels show the first occurrence of brine at depths corresponding to the Castile Formation in portions of the area and to the Bell Canyon Formation in the rest of the area, some 400 to 600 m below the mined depth of the waste storage panels in the Salado formation. There is no evidence in the data for brine pockets in the Salado or other formations over the waste storage panels.

Only one sounding was made near drill hole WIPP #12 for the purpose of calibration. Since the center loop TDEM surveys conducted correlate well with drill holes and other geologic data, it is recommended that the areal extent of the brine pocket encountered at WIPP #12 be mapped by surveying a grid centered on WIPP #12."

# Compliance Certification Application Reference Expansion

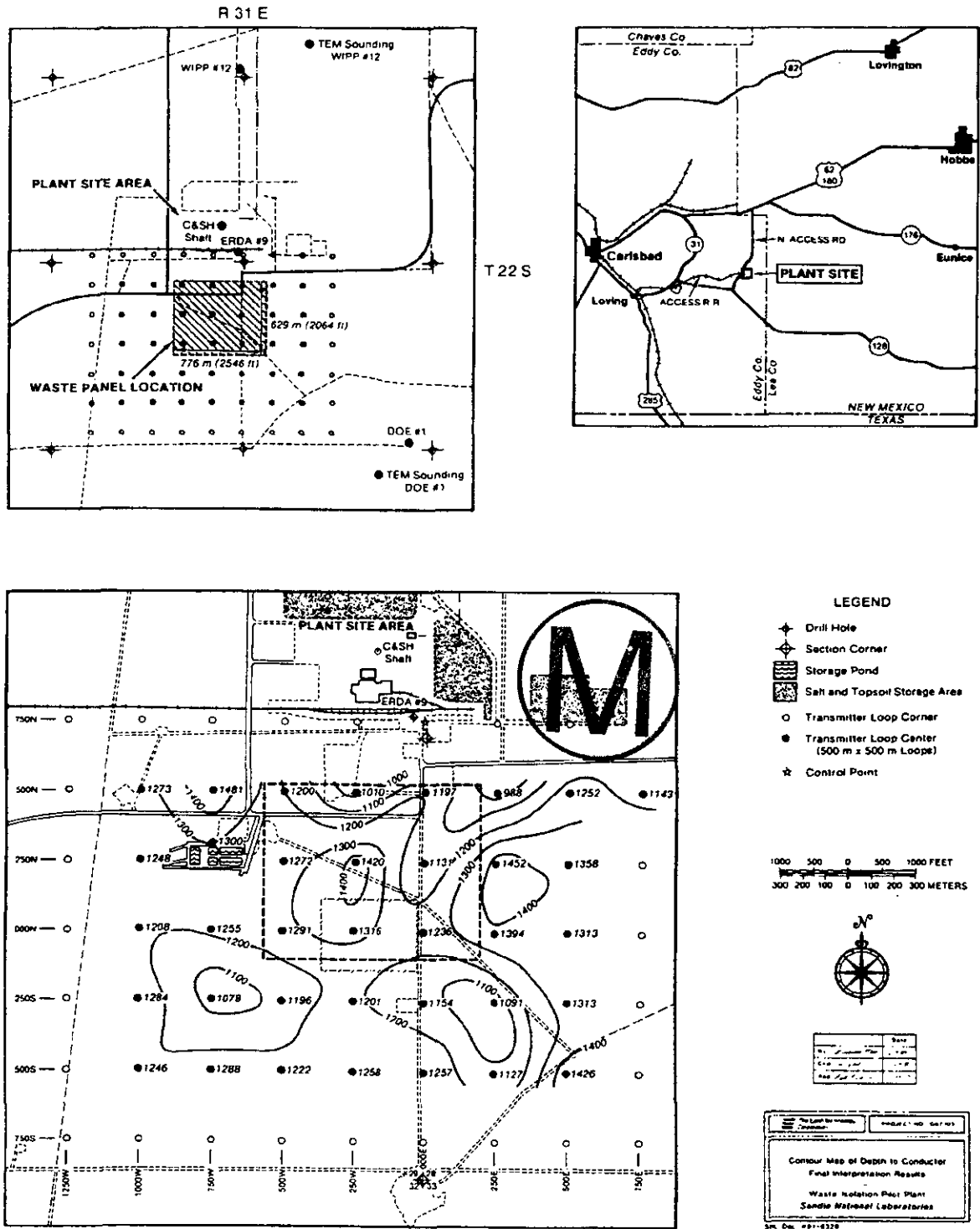


**Figure 1-1. TEM Sounding Locations and Waste Panel Location**

EPA (U.S. Environmental Protection Agency), 1985. "40 CFR Part 191: Environmental Standards for the Management and Disposal of Spent Nuclear Fuel, High-Level and Transuranic Radioactive Wastes; Final Rule." Federal Register, Vol. 50, No. 182, pp.38066-38089, September 19, 1985. Office of Radiation and Air, Washington, D.C. WPO 39132.

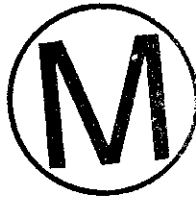
SUMMARY, p. 38066, col. 1;

" The Environmental Protection Agency (EPA) is promulgating generally applicable environmental standards for the management and disposal of spent nuclear fuel and high-level and transuranic wastes. The standards apply to management and disposal of such materials generated by activities regulated by the Nuclear Regulatory Commission (NRC) and to disposal of similar materials generated by atomic energy defense activities under the jurisdiction of the Department of Energy (DOE). These standards have been developed pursuant to the Agency's authorities and responsibilities under the Atomic Energy Act of 1954, as amended; Reorganization Plan No. 3 of 1970; and the Nuclear Waste Policy Act of 1982.

Subpart A of these standards limits the radiation exposure of members of the public from the management and storage of spent fuel or high-level or transuranic wastes prior to disposal at waste management and disposal facilities regulated by the NRC. Subpart A also limits the radiation exposures to members of the public from waste emplacement and storage operations at DOE disposal facilities that are not regulated by the NRC.

Subpart B establishes several different types of requirements for disposal of these materials. The primary standards for disposal are long-term containment requirements that limit projected releases of radioactivity to the accessible environment for 10,000 years after disposal. These release limits should insure that risks to future generations from disposal of these wastes will be no greater than the risks that would have existed if the uranium ore used to create the wastes had not been mined to begin with. A set of six qualitative assurance requirements is an equally important element of Subpart B designed to provide adequate confidence that all containment requirements will be met. The third set of requirements are limitations on exposures to individual members of the public for 1,000 years after disposal. Finally, a set of ground water protection requirements limits radionuclide concentrations for 1,000 years after disposal in water withdrawn from most Class I ground waters to the concentrations allowed by the Agency's interim drinking water standards (unless concentrations in the Class I ground waters already exceed limits in 40 CFR Part 141, in which case this set of requirements would limit the increases in the radionuclide concentrations to those specified in 40 CFR Part 141). Subpart B also contains informational guidance for implementation of the disposal standards to clarify the Agency's intended application of these standards, which address a time frame without precedent in environmental regulations. Although disposal of these materials in mined geologic repositories has received the most attention, the disposal standards apply to disposal by any method, except disposal directly into the oceans or ocean sediments.

This notice describes the final rule that the Agency developed after considering the public comments received on the proposed rule published on December 29, 1982, and the



## Compliance Certification Application Reference Expansion

---

recommendations of a technical review conducted by the Agency's Science Advisory Board (SAB). The major comments received on the proposed standards are summarized together with the Agency's responses to them. Detailed responses to all the comments received are discussed in the Response to Comments Document prepared for this final rule.

DATE: These standards shall be promulgated for purposes of judicial review at 1:00 p.m. eastern time on October 3, 1985. These standards shall become effective on November 18, 1985."

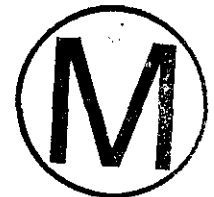
50 FR 38087, col. 2;

"Appendix A--Table for Subpart B . . .

Application of Table 1

Note 1: Units of Waste. The Release Limits in Table 1 apply to the amount of wastes in any one of the following:

- (a) An amount of spent nuclear fuel containing 1,000 metric tons of heavy metal [MTHM] exposed to a burnup between 25,000 megawatt-days per metric ton of heavy metal [MWd/MTHM] and 40,000 MWd/MTHM;
- (b) The high-level radioactive wastes generated from reprocessing each 1,000 MTHM exposed to a burnup between 25,000 MWd/MTHM and 40,000 MWd/MTHM;
- (c) Each 100,000,000 curies of gamma or beta-emitting radionuclides with half-lives greater than 20 years but less than 100 years (for use as discussed in Note 5 or with materials that are identified by the Commission as high-level radioactive waste in accordance with Part B of the definition of high-level waste in NWPA);
- (d) Each 1,000,000 curies of other radionuclides (i.e., gamma or beta-emitters with half-lives greater than 100 years or any alpha-emitters with half-lives greater than 20 years) (for use as discussed in Note 5 or with materials that are identified by the Commission as high-level radioactive waste in accordance with part B of the definition of high-level waste in NWPA); or
- (e) An amount of transuranic (TRU) wastes containing one million curies of alpha-emitting transuranic radionuclides with half-lives greater than 20 years."



EPA (U.S. Environmental Protection Agency), 1993. "40 CFR Part 191: Environmental Radiation Protection Standards for the Management and Disposal of Spent Nuclear Fuel, High-Level and Transuranic Radioactive Wastes; Final Rule." Federal Register, Vol. 48, No. 242, pp. 66398-66416, December 20, 1993. Office of Radiation and Air, Washington, D.C. WPO 39133.

**PREAMBLE: SUMMARY;**

" The U.S. Environmental Protection Agency (EPA) is promulgating amendments to the environmental standards for the disposal of spent nuclear fuel, high-level and transuranic wastes (40 CFR 191.15 and Subpart C).

EPA originally promulgated these standards in 1985 pursuant to the Agency's authorities and responsibilities under the Nuclear Waste Policy Act of 1982, as amended, the Atomic Energy Act of 1954, as amended, and §2(a)(6) of Reorganization Plan No. 3 of 1970 (5 USC app. 1). In 1987, following a legal challenge, the U.S. Court of Appeals for the First Circuit (hereinafter referred to as 'the First Circuit' or 'the court') remanded subpart B of the 1985 standards to the Agency for further consideration. *Natural Resources Defense Council, Inc. v. United States Environmental Protection Agency*, 824 F.2d 1258 (1st Cir. 1987). Recently enacted legislation, (Pub. L. 102-579) known as the Waste Isolation Pilot Plant Land Withdrawal Act (WIPP LWA), however, reinstates the 1985 disposal standards except 'the 3 aspects of §§191.15 and 191.16 of such [standards] that were subject of the remand ordered' by the First Circuit. The WIPP LWA directs EPA to expedite issuance of final disposal standards and specifies that such regulations shall not be applicable to the characterization, licensing, construction, operation, or closure of any site required to be characterized under §113(a) of Public Law 97-425, the Nuclear Waste Policy Act of 1982.

Today's action represents the Agency's response to this legislation and to the issues raised by the court pertaining to individual and ground-water protection requirements. After considering the relevant comments received on the February 10, 1993 proposed rulemaking, the Agency has taken this final action in the form of amendments to parts 191 of title 40 of the Code of Federal Regulations. In so doing, EPA has not revised any of the regulations reinstated by the WIPP LWA.

**DATES:** These amendments will become effective on January 19, 1994. These amendments will be promulgated for purposes of judicial review at 1 p.m. eastern standard time on December 20, 1993."



**STATUTORY AND REGULATORY BACKGROUND;**

" The WIPP Land Withdrawal and Nuclear Waste Policy Acts

As noted above, today's action responds to the directive in section 8 of the WIPP LWA that EPA conduct a rulemaking to issue certain radioactive waste disposal regulations at 40 CFR Part 191, subpart B. The EPA initially promulgated subpart B in 1985 (50 FR 38084 (Sept. 19, 1985)), but those regulations were subsequently vacated in whole as part of a remand order issued by the First Circuit in 1987 (discussed further above and below). See *NRDC v. EPA*, 824 F.2d 1258 (1st Cir. 1987).

**Compliance Certification Application Reference Expansion**

---

Section 8(a)(1) of the WIPP LWA reinstates those portions of subpart B except §§191.15 and 191.16 (which were the bases of remand by the First Circuit). Accordingly, section 8(a)(2)(A) of the WIPP LWA exempts the requirements at 40 CFR 191.15 (individual protection) and 191.16 (ground-water protection) from the statutory reinstatement. Section 8(b)(2) addresses these non-reinstated provisions by directing the EPA promulgate final regulations. Today's action responds to that directive by revising the individual protection requirements in 40 CFR 191.15, discussed above, and by adding new ground-water protection standards as 40 CFR part 191, subpart C (discussed below)."

Federal register, Vol. 58 No. 242, p 66398, dated December 20, 1993

"191.15 Individual protection requirements.

(a) Disposal systems for waste and any associated radioactive material shall be designed to provide a reasonable expectation that, for 10,000 years after disposal, undisturbed performance of the disposal system shall not cause the annual committed effective dose, received through all potential pathways from the disposal system, to any member of the public in the accessible environment, to exceed 15 millirems (150 microsieverts).

(b) Annual committed effective doses shall be calculated in accordance with appendix B of this part.

(c) Compliance assessments need not provide complete assurance that the requirements of paragraph (a) of this section will be met. Because of the long time period involved and the nature of the processes and events of interest, there will inevitably be substantial uncertainties in projecting disposal system performance. Proof of the future performance of a disposal system is not to be had in the ordinary sense of the word in situations that deal with much shorter time frames. Instead, what is required is a reasonable expectation, on the basis of the of the record before the implementing agency, that compliance with paragraph (a) of this section will be achieved.

(d) Compliance with the provisions in this section does not negate the necessity to comply with any other applicable Federal regulations or requirements.

(e) The standards in this section shall be effective on January 19, 1994."

"Subpart C-Environmental Standards for Ground-Water Protection

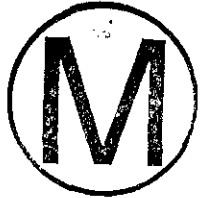
. . .191.23 General provisions.

(a) Determination of compliance with this subpart shall be based upon underground sources of drinking water which have been identified on the date the implementing agency determines compliance with subpart C of this part.

191.24 Disposal standards.

(a) Disposal systems.

(1) General. Disposal systems for waste and any associated radioactive material shall be designed to provide a reasonable expectation that 10,000 years of undisturbed performance after disposal shall not cause the levels of radioactivity in any underground source of drinking water, in the accessible environment, to exceed the limits specified in 40 CFR part 141 as they exist on January 19, 1994.



**Compliance Certification Application Reference Expansion**

---

(2) Disposal systems above or within a formation which within one-quarter ( 1/4) mile contains an underground source of drinking water. [Reserved]

(b) Compliance assessments need not provide complete assurance that the requirements of paragraph (a) of this section will be met. Because of the long time period involved and the nature of the processes and events of interest, there will inevitably be substantial uncertainties in projecting disposal system performance. Proof of the future performance of a disposal system is not to be had in the ordinary sense of the word in situations that deal with much shorter time frames. Instead, what is required is a reasonable expectation, on the basis of the record before the implementing agency, that compliance with paragraph (a) of this section will be achieved. . . ."

§191.27. Effective date: p. 66415, col. 3;

"Appendix A to Part 191--Table for Subpart B

9. Appendix B is redesignated as Appendix C to part 191 and the heading is revised as follows:

Appendix C to Part 191--Guidance for Implementation of Subpart B."

50 FR 38088, p. 38088, col. 2;

" Appendix B--Guidance for Implementation of Subpart B

[Note: The supplemental information in this appendix is not an integral part of 40 CFR Part 191. Therefore, the implementing agencies are not bound to follow this guidance. However, it is included because it describes the Agency's assumptions regarding the implementation of Subpart B. This appendix will appear in the Code of Federal Regulations]"

" Scope of Performance Assessments.

Section 191.13 requires the implementing agencies to evaluate compliance through performance assessments as defined in § 191-12(q). The Agency assumes that such performance assessments need not consider categories of events or processes that are estimated to have less than one chance in 10,000 of occurring over 10,000 years. Furthermore, the performance assessments need not evaluate in detail the releases from all events and processes estimated to have a greater likelihood of occurrence. Some of these events and processes may be omitted from the performance assessments if there is a reasonable expectation that the remaining probability distribution of cumulative releases would not be significantly changes by such omissions."



Compliance Certification Application Reference Expansion

EPA (U.S. Environmental Protection Agency), 1996a. "40 CFR Part 194: Criteria for the Certification and Re-Certification of the Waste Isolation Pilot Plant's Compliance with the 40 CFR Part 191 Disposal Regulations Final Rule." Federal Register, Vol. 61, No. 28, pp. 5224-5245, February 9, 1996. Office of Radiation and Indoor Air, Washington, D.C. In NWM Library as KF70.A35.C751 1996 (Reference).

SUMMARY, p. 5224, col. 1;

" The Environmental Protection Agency (EPA) is promulgating criteria for determining if the Waste Isolation Pilot Plant (WIPP) will comply with EPA's environmental radiation protection standards for the disposal of radioactive waste. If the Administrator of the EPA determines that the WIPP will comply with the standards for disposal, then the Administrator will issue to the Secretary of Energy a certification of compliance which will allow the emplacement of transuranic waste in the WIPP to begin, provided that all other statutory requirements have been met. If a certification is issued, EPA will also use this final rule to determine if the WIPP has remained in compliance with EPA's environmental radiation protection standards, once every five years after the initial receipt of waste for disposal at the WIPP. This rulemaking was mandated by the WIPP Land Withdrawal Act of 1992.

EFFECTIVE DATE: These regulations are effective April 9, 1996."

p. 5238, col. 2;

" §194.14. Content of compliance certification application.

Any compliance application shall include:

(a) A current description of the natural and engineered features that may affect the performance of the disposal system. The description of the disposal system shall include, at a minimum, the following information:

(1) The location of the disposal system and the controlled area;

(2) A description of the geology, geophysics, hydrogeology, hydrology and geochemistry of the disposal system and its vicinity and how these conditions are expected to change and interact over the regulatory time frame. Such description shall include, at a minimum:

(i) Existing fluids and fluid hydraulic potential, including brine pockets, in and near the disposal system; and

(ii) Existing higher permeability anhydrite interbeds located at or near the horizon of the waste.

(3) The presence and characteristics of potential pathways for transport of waste from the disposal system to the accessible environment including, but not limited to: Existing boreholes, solution features, breccia pipes, and other potentially permeable features, such as interbeds.

(4) The projected geophysical, hydrogeologic, and geochemical conditions of the disposal system due to the presence of waste including, but not limited to, the effects of production of heat or gases from the waste."



**Compliance Certification Application Reference Expansion**

---

p. 5240, col. 2;

" §194.24 Waste characterization.

(a) Any compliance application shall describe the chemical, radiological and physical composition of all existing waste proposed for disposal in the disposal system. To the extent practicable, any compliance application shall also describe the chemical, radiological and physical composition of to-be-generated waste proposed for disposal in the disposal system. These descriptions shall include a list of waste components and their approximate quantities in the waste. This list may be derived from process knowledge, current non-destructive examination/assay, or other information and methods."

p. 5243, Assurance Requirements, col. 3;

" §194.44 Engineered barriers.

(a) Disposal systems shall incorporate engineered barrier(s) designed to prevent or substantially delay movement of water or radionuclides toward the accessible environment."



EPA (U.S. Environmental Protection Agency), 1996b. Criteria for the Certification and Re-Certification of the Waste Isolation Pilot Plant's Compliance with the 40 CFR Part 191 Disposal Regulations. Background Information Document for 40 CFR Part 194. EPA 402-R-96-002. Environmental Protection Agency, Office of Radiation and Indoor Air, Washington, D.C.

1. Introduction; p. 1-1, para. 1;

" The Environmental Protection Agency's (EPA) regulation, 40 CFR part 194, sets forth criteria for determining if the Waste Isolation Pilot Plant (WIPP) will comply with EPA's environmental radiation protection standards for the disposal of radioactive waste, found at 40 CFR part 191 subparts B and C. If the Administrator of EPA determines that the WIPP will comply with the standards for disposal, then the Administrator will issue to the Secretary of Energy a certification of compliance which will allow the emplacement of transuranic waste in the WIPP to begin, provided that all other statutory requirements have been met. If a certification is issued, EPA will also use 40 CFR part 194 to determine if the WIPP has remained in compliance with EPA's environmental radiation protection standards, once every five years after the initial receipt of waste for disposal at the WIPP. The final preamble and regulation to 40 CFR part 194, as they appear in the Federal Register, take precedence over any descriptions or interpretations of the final rule that appear in this document.

This document provides much of the necessary background information and technical analyses which the Agency used during the development of 40 CFR part 194. The document explicates fourteen issues considered by EPA in establishing the individual criteria contained in 40 CFR part 194."

p. 8-41, para. 1;

" In 40 CFR part 194, EPA decided that the statistical portion of the determination of compliance with 40 CFR part 191 will be based on the sample mean. The LHS sample sizes should be demonstrated operationally (approximately 300 when 50 variable are considered) to improve (reduce the size of) the confidence interval for the estimated mean. The underlying principle is to show convergence of the mean."

9 Consideration of Human Intrusion

9.4 Intrusion by Mining

9.4.3.2 Other Relevant Studies; p. 9-36, para. 5;

" IT Corporation summarized subsidence observations made at potash mines in southeastern New Mexico (ITC94). Observed angles of draw, measured from vertical edge of the mine workings to the point where surface subsidence ceased, varied from 25 to 58 degrees."

Geologic Column; p. 9-46, para. 4;

" The geologic column used in the analysis was adapted from the ERDA 9 borehole



**Compliance Certification Application Reference Expansion**

near the center of the WIPP site (POW78). Table 9-5 gives the depth, formation, and thickness of the different strata represented in the finite element model."

Table 9-5. Strata Depth and Thickness; p. 9-47, tbl. 9-5;"

Formation	Depth (ft)	Thickness (ft)
1. Dewey Lake	0	550
2. Rustler	550	58
3. Magenta	608	24
4. Rustler	632	82
5. Culebra	714	26
6. Rustler	740	120
7. Upper Salado	860	507
8. McNutt	1,367	176
9. Potash Seam	1,543	10
10. McNutt	1,553	188
11. Lower Salado	1,741	333
12. Storage Zone	2,074	104
13. Lower Salado	2,178	442
14. Storage Zone	2,620	110
15. Lower Salado	2,730	106
16. Castile	2,836	1,664 <sup>11"</sup>



Freeze, G.A., Larson, K.W., and Davies, P.B. 1995. A Summary of Methods for Approximating Salt Creep and Disposal Room Closure in Numerical Models of Multiphase Flow. SAND94-0251. Sandia National Laboratories, Albuquerque, NM. WPO 29557.

**ABSTRACT;**

" Eight alternative methods for approximating salt creep and disposal room closure in a multiphase flow model of the Waste Isolation Pilot Plant (WIPP) were implemented and evaluated; three fixed-room geometries (initial, intermediate, fully consolidated); three porosity functions (moles-time-porosity surface, moles-time-porosity lines, pressure-time-porosity lines); and two fluid-phase-salt methods (boundary backstress, capillary backstress). The pressure-time-porosity line interpolation (pressure lines) method is used in current WIPP Performance Assessment calculations. The room closure approximation methods were calibrated against a series of room closure simulations performed by Stone (1995a) using a creep closure code, SANCHO.

The fixed-room geometries did not incorporate a direct coupling between room void volume and room pressure. The two porosity function methods that utilize moles of gas as an independent parameter for closure coupling were unable to account for the presence of brine in the room and, therefore, could not capture the dynamic relationship between room pressure, brine volume in the room, and room expansion. The capillary backstress method was unable to accurately simulate conditions of re-closure of the room followed room expansion. Only two methods were found to be accurate and robust enough to approximate the effects of room closure under most conditions, the boundary backstress method and pressure-time-porosity line interpolation.

The boundary backstress method is thought to be a more reliable indicator of system behavior due to a theoretical basis for modeling salt deformation as a viscous process. It is a complex method and a detailed calibration process is required. The pressure lines method is thought to be less reliable because the results were skewed towards SANCHO results in simulations where the sequence of gas generation was significantly different from the SANCHO gas-generation rate histories used for closure calibration. This limitation in the pressure lines method is most pronounced at higher gas-generation rates ( $> 0.8$  moles per drum per year) and is relatively insignificant at lower gas-generation rates ( $\leq 0.4$  moles per drum per year). Due to its relative simplicity, the pressure lines method is easier to implement in multiphase flow codes and simulations have a shorter execution time (10 to 20 times faster than boundary backstress). The pressure lines method is suggested for continued use in WIPP Performance Assessment calculations as long as simulated gas-generation rate histories are low or are not significantly different from the SANCHO-simulated rates."



Goodwin, B.W., Stephens, M.E., Davison, C.C., Johnson, L.H., and Zach, R. 1994. Scenario Analysis for the Postclosure Assessment of the Canadian Concept for Nuclear Fuel Waste Disposal. AECL-10969, COG-94-247. Whiteshell Laboratories, Pinawa, Manitoba, Canada.

ABSTRACT; p. 1, para. 1;

" AECL Research has developed and evaluated a concept for disposal of Canada's nuclear fuel waste involving deep underground disposal of the waste in intrusive igneous rock of the Canadian Shield. The postclosure assessment of this concept focusses on the effects on human health and the environment due to potential contaminant releases into the biosphere after the disposal vault is closed. Both radiotoxic and chemically toxic contaminants are considered.

One of the steps in the postclosure assessment process is scenario analysis. Scenario analysis identifies factors that could affect the performance of the disposal system and groups these factors into scenarios that require detailed quantitative evaluation.

This report documents a systematic procedure for scenario analysis that was developed for the postclosure assessment and then applied to the study of a hypothetical disposal system. The application leads to a comprehensive list of factors and a set of scenarios that require further quantitative study. The application also identifies a number of other factors and potential scenarios that would not contribute significantly to environmental and safety impacts for the hypothetical disposal system."



Hodgkinson, D.P. and Sumerling, T.J., 1989. "A Review of Approaches to Scenario Analysis for Repository Safety Assessment." In Proceedings of the IAEA/CEC/NEA (OECD) Symposium on Safety Assessment of Radioactive Waste Repositories (Paris, 1989). OECD/NEA, Paris, France. pp. 333-350.

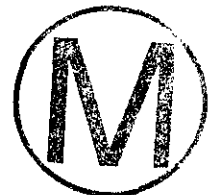
ABSTRACT; p. 333, para. 1;

" This paper surveys approaches to scenario analysis for repository safety assessment which have been under scrutiny by the NEA Scenarios Working Group. Scenario analysis blends information on site and waste characteristics, established understanding of processes, and subjective views of appropriately experienced scientists and others. It is important to follow systematic procedures and to document each step carefully so that it is amenable to scrutiny. There is a wide agreement about the general approach that should be taken to the identification, classification and screening of phenomena that need to be considered. Three general approaches have been identified to the difficult problem of combining these phenomena into scenarios, and consideration has been given to their ranges of applicability."

p. 348, para. 1;

"APPENDIX

EXAMPLE COMPILATION OF EVENTS, FEATURES AND PROCESSES FOR A DEEP REPOSITORY IN HARD ROCK"



Holt, R.M., and Powers, D.W. 1984. Geotechnical Activities in the Waste Handling Shaft Waste Isolation Pilot Plant (WIPP) Project Southeastern New Mexico. WTSD-TME-038. U.S. Department of Energy, Carlsbad, NM.

ABSTRACT, p. v;

" The Waste handling shaft (waste shaft) at the Waste Isolation Pilot Plant (WIPP) site is an enlargement of the drilled, Site and Preliminary Design Validation (SPDV) ventilation shaft. Geotechnical activities in the waste shaft were designed to confirm the SPDV ventilation shaft mapping results and to provide additional information about identified zones of interest. The activities included identification of instrument locations, geologic inspections of the exposed shaft surface during sinking operations, reconnaissance geologic mapping of the waste shaft sump, and detailed geologic mapping in identified zones of interest. These activities were carried out concurrently with construction.

The results of the geologic inspections in the waste shaft and the reconnaissance geologic mapping in the waste shaft sump correlate well with previous characterizations. However, the detailed 360° geologic mapping performed in several zones of interest did not reveal post-depositional dissolution features, thought to occur at several stratigraphic horizons in the Rustler Formation at the WIPP site. At the waste shaft, zones previously identified as dissolution residues in nearby boreholes contained pronounced primary sedimentary features."

4.2.2.4 Culebra Dolomite Member, p. 4-6, para. 4;

" In the waste shaft, the Culebra occurs in the depth interval from 706.5 feet to 728.5 feet (Figure 9). The upper one-half to two feet of the Culebra is a medium brown, microlaminated to thinly laminated carbonate. This unit averages about 0.8 feet in thickness throughout the circumference of the shaft, but thickens up to two feet in the vicinity of mound-like dome structures. In general, the laminations within the carbonate unit are horizontal to subhorizontal. However, the laminae in the mound structures are often crenulated and dip slightly away from the center. It is likely that this unit is of algal origin. A 1/4 to 1-inch thick bed of cohesive, black claystone underlies the carbonate unit. The remainder of the Culebra primarily consists of brown, finely crystalline dolomite containing both empty and gypsum-filled vugs of varying size."

p. 4-9, para. 1;

" From a depth of about 781.0 feet to a depth of about 844.0 feet, the lower member consists of interbedded siltstone, sandstone, mudstone, and claystone with an abundance of primary sedimentary structures. These sedimentary structures include laminated sediments, cross-laminations, trough cross laminations, and channel lag (Plate 4) containing invertebrate fossil hash. The basal contact with the Salado is sharp, and the rock overlying the contact appears to be undisturbed by dissolution. The average depth to the Rustler/Salado contact in the shaft is about 844.0 feet."





Holt, R.M., and Powers, D.W. 1986. Geotechnical Activities in the Exhaust Shaft. DOE/WIPP-86-008. U.S. Department of Energy, Carlsbad, NM.

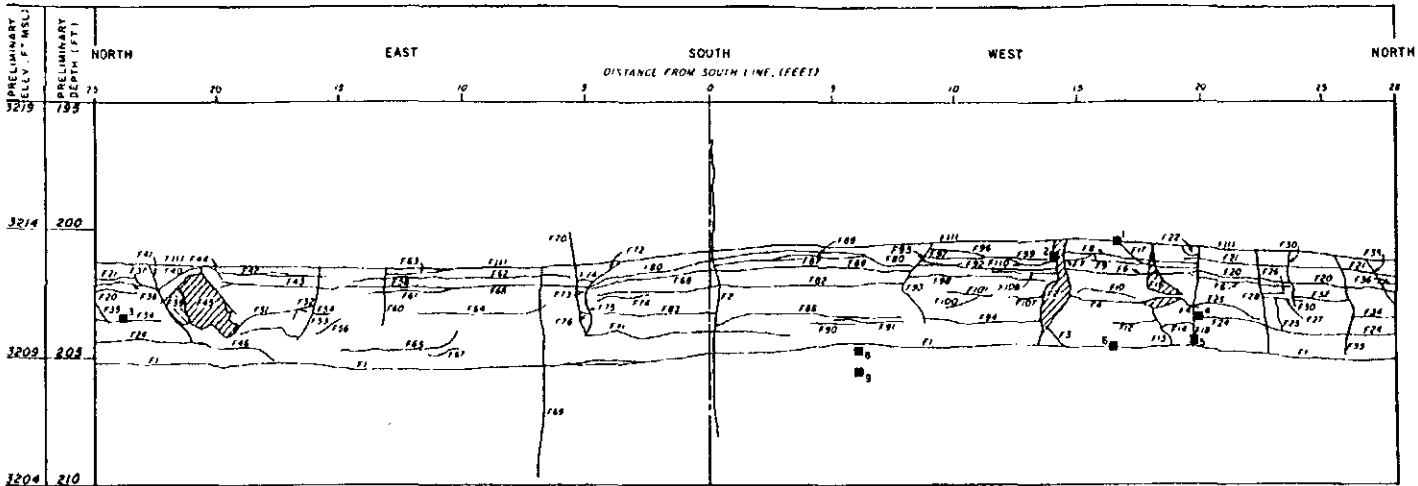
INTRODUCTION, p. 1-1;

" The Waste Isolation Pilot Plant (WIPP) project is a Department of Energy (DOE) research-and-development facility constructed to demonstrate the safe disposal of radioactive wastes derived from the defense activities of the United States. The WIPP project's mission consists of two parts. The first is to demonstrate the safe handling and disposal of transuranic (TRU) waste in bedded salt. The second is to create a research facility for in-situ examination of the technical issues related to the emplacement of defense-related radioactive waste in bedded salt.

The WIPP facility is located approximately 26 miles east of Carlsbad, New Mexico in an area known as Los Medanos (Figure 1). The underground portion of the facility is located at a depth of approximately 2,150 feet in the bedded salt deposits of the Salado Formation (Figure 2). An extensive program of site characterization and validation has been conducted for the past nine years (1976-1985). The results of these studies are summarized in the WIPP 'Geological Characterization Report' (Powers et al., 1978), the WIPP 'Safety Analysis Report' (DOE, 1980), the WIPP 'Preliminary Design Validation Report' (Bechtel, 1983), and the WIPP 'Results of Site Validation Experiments' (Black et al., 1983). Additional site investigations are being conducted as part of an ongoing program to further refine the understanding of the site-specific geology. The geotechnical activities conducted in the exhaust shaft are part of this program.

The exhaust shaft will provide a pathway for the release of exhaust air from the facility to the surface. The shaft is an enlargement of a six-foot diameter, upreamed shaft. The finished diameter is 14 feet in the lined portion of the shaft and 15 feet minimum in the unlined portion. Geotechnical activities consisting of reconnaissance geologic mapping, detailed geologic mapping in specific zones of interest, geologic confirmation of instrument locations, and field adjustment and modification of the key and aquifer seal design were performed concurrently with construction from July 16, 1984 to January 18, 1985. This report presents and discusses the findings from the geologic mapping efforts in the exhaust shaft. Also, the construction history of the exhaust shaft is summarized, and several engineering geology characteristics are discussed."

NOTE: The notes applicable to Figures 6, 7, & 8 (Figure 6 - Sh 2 of 11 through 11 of 11; Figure 7 - Sh 2 of 9 through 9 of 9; and Figure 8 - Sh 2 of 6 through 6 of 6) have not been included in this document to reduce document size.



**NOTES**

- 1) THIS INTERVAL WAS MAPPED ON 10-3-NW.
- 2) THE LITHOLOGY OF THIS INTERVAL IS DESCRIBED IN FIGURE 4.
- 3) DEPTHS AND EVALUATIONS ARE RELATED TO THE REFERENCE ELEVATION OF 3409 FEET ABOVE MSL.
- 4) ONLY FRACTURES THAT WERE DEEMED "MAPPABLE" AT A SCALE OF ONE INCH EQUALS FIVE FEET ARE INCLUDED ON THE MAP. MAPPING EFFORTS WERE CONCENTRATED IN THE DEPTH INTERVAL FROM 195.0 FEET TO 200.0 FEET.

**EXPLANATION**

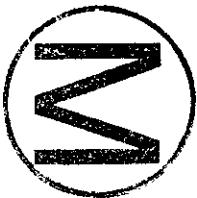
- F20 MAPPED FRACTURE #20, SEE FRACTURE NOTES FOR DESCRIPTION
- 24 SAMPLE LOCATION, EXHAUST SHAFT DETAILED MAPPING SAMPLE
- F29 MAPPED FRACTURE #29, FRACTURE SURFACE EXPOSED

FIGURE 6 - SHEET 3 OF 11  
 FRACTURE LOG IN  
 THE DEWEY LAKE REDBEDS  
 DEPTH 190.0 THROUGH 205.0 FEET  
 EXHAUST SHAFT

WASTE ISOLATION PILOT PLANT  
 CARLSBAD, NEW MEXICO

PREPARED FOR  
 WESTINGHOUSE ELECTRIC CORPORATION  
 CARLSBAD, NEW MEXICO

IT CORPORATION



October 17, 1996

XRE6-78

APPENDIX XRE6

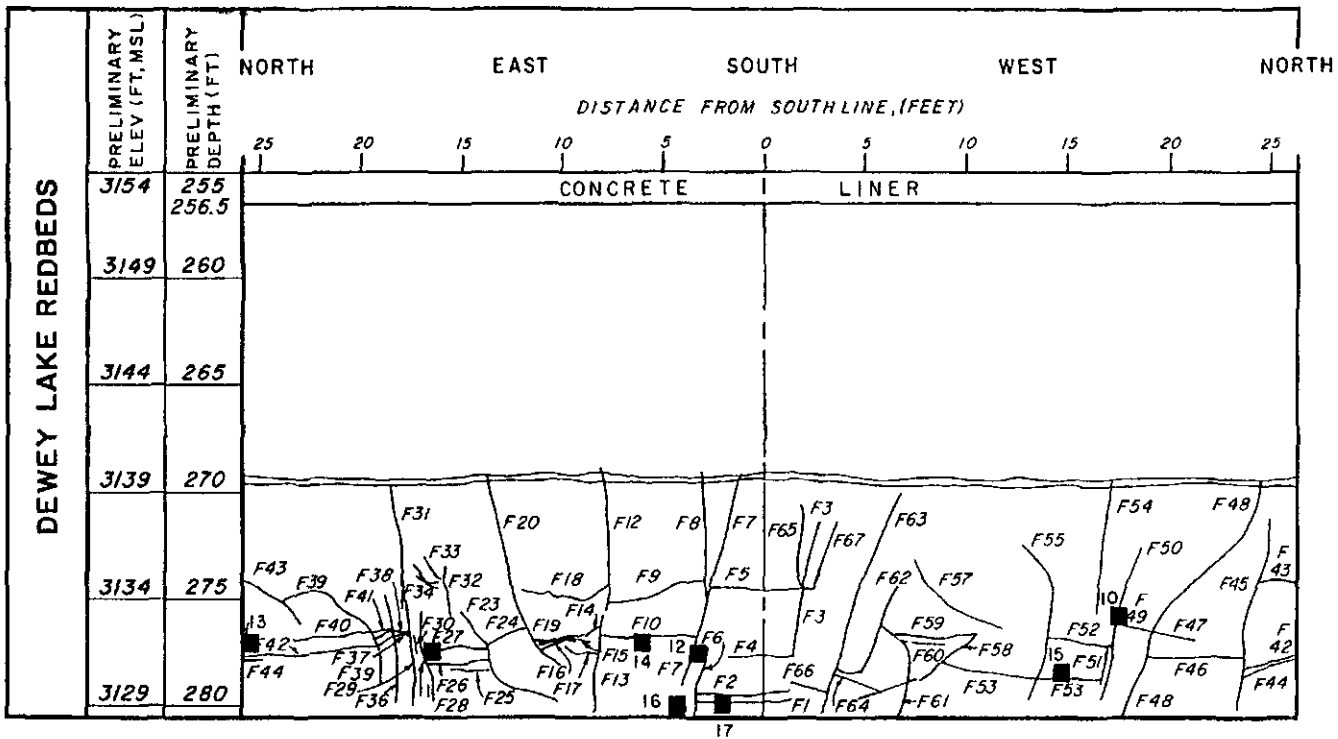


FIGURE 7 - SHEET 1 OF 9  
 FRACTURE LOG IN THE DEWEY LAKE REDBEDS  
 DEPTH 256.5 TO 280.5 FEET, EXHAUST SHAFT

WASTE ISOLATION PILOT PLANT  
 CARLSBAD, NEW MEXICO  
 PREPARED FOR  
 WESTINGHOUSE ELECTRIC CORPORATION  
 CARLSBAD, NEW MEXICO  
 IT CORPORATION



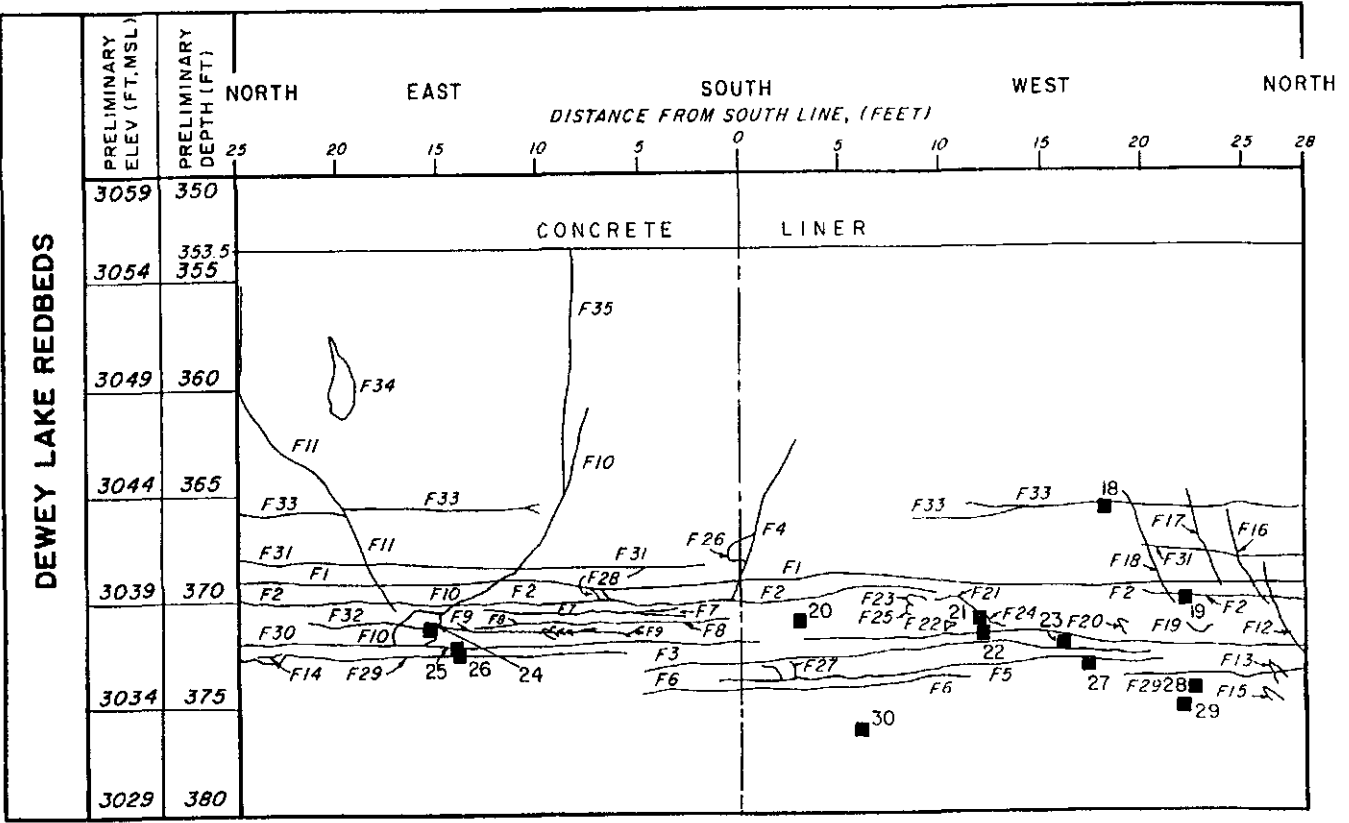


FIGURE 8 - SHEET 1 OF 6  
 FRACTURE LOG IN THE DEWEY LAKE REDBEDS  
 DEPTH 353.5 TO 380.0 FEET, EXHAUST SHAFT  
 WASTE ISOLATION PILOT PLANT  
 CARLSBAD, NEW MEXICO  
 PREPARED FOR  
 WESTINGHOUSE ELECTRIC CORPORATION  
 CARLSBAD, NEW MEXICO  
 IT CORPORATION





## Compliance Certification Application Reference Expansion

Holt, R.M., and D.W. Powers, 1990. Geologic Mapping of the Air Intake Shaft at the Waste Isolation Pilot Plant. DOE/WIPP 90-051. Westinghouse Electric Corporation, Carlsbad, NM.

EXECUTIVE SUMMARY, p ES-1;

" The air intake shaft (AIS) at the Waste Isolation Pilot Plant (WIPP) site was constructed to provide a pathway for fresh air into the underground repository and maintain the desired pressure balances for proper underground ventilation. It was up-reamed to minimize construction-related damage to the rock wall. The upper portion of the shaft was lined with slip-formed concrete, while the lower part of the shaft, from approximately 903 ft below top of concrete at the surface, was unlined. As part of WIPP site characterization activities, the AIS was geologically mapped.

The AIS was geologically mapped during the period from March 11, 1988 to November 14, 1989. The objectives of the geologic mapping were to: 1) provide confirmation and documentation of strata overlying the WIPP facility horizon; 2) provide detailed information of the geologic conditions in strata critical to repository sealing and operations; 3) provide technical basis for field adjustments and modification of key and aquifer seal design, based upon the observed geology; 4) provide geological data for the selection of instrument borehole locations; 5) and characterize the geology at geomechanical instrument locations to assist in data interpretation. All mapping activities were performed from a two deck galloway (work platform) and synchronized with shaft construction activities. The AIS was mapped according to the procedures described in WP 07-503, 'Geologic Mapping of Shafts' (April 25, 1988) (Appendix B).

The entire shaft section including the Mescalero Caliche, Gatuña Formation, Santa Rosa Formation, Dewey Lake Redbeds, Rustler Formation, and Salado Formation to the WIPP facility horizon was geologically described. The shaft construction method, up-reaming, created a nearly ideal surface for geologic description. Small-scale textures usually best seen on slabbed core were easily distinguished on the shaft wall while larger-scale textures not revealed in core were well displayed. Previously undescribed textures were interpreted, and the AIS data were used to further refine depositional and post-depositional models of the units mapped.

The upper part of the Dewey Lake Redbeds displayed features consistent with Schiel's (1988) interpretation of the depositional environments. The geologic mapping data indicated deposition in a fine-grained, ephemeral fluvial system (Schiel, 1988). The lower part of the Dewey Lake, however, was depositionally a continuation of Rustler style sedimentation and accumulated in saline mud flat/mud flat environments. Most gypsum-filled fractures developed incrementally in response to unloading, while some Dewey Lake are syndepositional. Within the Dewey Lake, a cement change between carbonate and, possibly, anhydrite was observed at a depth of 164.5 feet. Perched water tables within the Dewey Lake may rest on this cement change. Above the cement change, the shaft surface was moist and displayed an efflorescent crust consisting of halite. The source of the halitic water is attributed to the muck-piles north and east of the AIS.

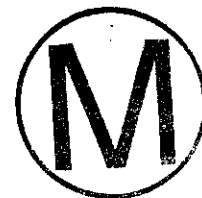
The features observed within the Rustler are consistent with those reported by Holt and Powers (1984, 1986, and 1988). Mudstones within the Rustler created a spalling hazard as several feet of mudstone had spalled out of the units and large slabs to desk-top size had to be scaled from the rib prior to mapping. Liner plate was installed over all Rustler mudstones. The surface of the lower part of the Rustler required extensive washing and scaling prior to mapping as Culebra and construction waters dissolved halite crystals and cements. Extensive vertical fluxing was observed.

The AIS data from the Salado allowed the authors to add considerably to the understanding of the depositional and diagenetic history of the Salado. Unprecedented halite textural and fabric data was collected, characterized, and interpreted from the Salado. An idealized Salado halite sequence was constructed, and all Salado halite observed within the AIS fits partially or wholly into the idealized sequence. Complete Salado halite sequences consist of four lithofacies, in ascending order: 1) stratified mud-poor halite; 2) 'podular' muddy halite; 3) 'dilated' mud-rich halite; and 4) halitic mudstone. These lithofacies developed in four distinct depositional environments: 1) a mud-poor salt pan; 2) a 'hummocky' salt pan; 3) a mud-rich salt pan; and 4) a saline mud flat.

Salado sulfate interbeds (including Markerbeds) displayed abundant previously undescribed textures and fabrics. Textural data from the AIS provided the basis for further interpretation of these interbeds. Salado sulfate interbeds were deposited in shallow saline lagoon environments following eustatically- or meteorically-driven, basin-wide flooding and freshening events (Lowenstein, 1982, 1983, 1988). Different hydrologic conditions produced three distinct types of sulfate interbeds within the Salado. The sulfate interbeds bounding the repository horizon may be laterally variable due to facies changes within the depositional environment. Geologic evidence of naturally occurring late-stage fluid migration or alteration within the halite of the Salado was not found. Mineralized and fluid-filled fractures occur within some sulfate interbeds within the Salado."

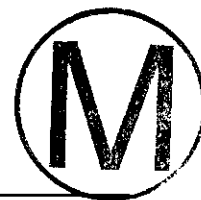
p. 3-3, para. 1;

" At the AIS, the Gatuña is 13 feet thick and consists of very calcareous, very friable, soft sandstone (Figures 4 and 5). The Gatuña is light red and mottled with dark stains. Carbonate occurs as stringers and concretions in probable rhizolithic structures. Clay-sized materials locally appear translocated. Some pebble-sized clasts of sandstone are probably derived from the underlying Santa Rosa Formation. The Gatuña overlies a sharp erosional contact on the Santa Rosa Formation."



p. 3-4, para. 2;

" The Dewey Lake is characterized by its reddish-orange to reddish-brown color and varying sedimentary structure. At the WIPP site (as exposed in the AIS), the Dewey Lake is 476 feet thick and consists of interbedded reddish-brown fine sandstone, siltstone, mudstone and claystone (Figure 5). The Dewey Lake is distinguished from other redbed units by the presence of greenish-gray reduction spots, which are liberally sprinkled throughout the formation, and locally abundant fibrous gypsum-filled fractures. Its upper contact with the



Santa Rosa Formation is sharp and erosional (Figure 6). The lower contact of the Dewey Lake with the Rustler Formation is sharp, with a minor amount of erosional relief (Figure 7 and 8). This contact is locally disconformable, but there is evidence of a regional unconformity (Holt and Powers, 1988)."

3.4.3 Origin and Significance of Gypsum-Filled Fractures, p. 3-8;

" With the exception of the upper portion, the Dewey Lake is characterized by locally abundant gypsum-filled fractures. Most of the fractures are filled with fibrous gypsum, although granular gypsum fracture fillings do occur in the upper portion of the Dewey Lake. In the AIS, gypsum-filled fractures are abundant below 164.5 feet. The fracture filling gypsum is fibrous indicating incremental growth. The fracture pattern and filling morphology is governed by the grain-size of the fractured host material, as discussed below."

3.4.4 Origin of Perched Water Tables in the Dewey Lake, p. 3-10, para. 2;

" At the AIS, the Dewey Lake is cemented with carbonate above 164.5 feet. The coarse-grained units (sandstones and siltstones) are usually moderately hard, though a few are soft. The mudstones and claystones are soft and commonly fissile. Fractures are unfilled or filled with carbonate, and carbonate-filled fractures increase downward. The surface of the AIS wall in the Dewey Lake is moist down to 164.5 feet, and a halitic efflorescence is sometimes present on the shaft wall. ..."

p 3-11, para 2;

" At the WIPP site, meteoric water probably infiltrates through the surface materials (dune sand and construction fill material) to the Mescalero caliche, where it moves downgradient off of the site or evaporites. When the Mescalero caliche and the Pleistocene and Triassic rocks have been disturbed by construction activities, this water can infiltrate along these newly created pathways into the underlying Dewey Lake. The water will infiltrate to the cement change surface and either stop or move down gradient. The impact of this process should be assessed with respect to shaft plugs and seals."

p 3-26, para 3;

" The lower mud-poor section of the sequence is dominated texturally by an overall sense of horizontal to subhorizontal stratification and is named the 'stratified' mud-poor lithofacies (Figure 1, Appendix F). It is subdivided into three zones with small-scale textures. The first zone is dominated by bottom growth halite textures including halite chevron, cornet, and cumulates and clay or sulfate laminae. The second zone shows abundant passive pore-filling halite cements in small dissolution pits and pores. The uppermost zone contains exhibits mostly expansive halite cement textures (displacive halite) mixed with various syndepositional solution textures and fabrics. These textures are consistent with deposition in a mud-poor salt pan.

The 'podular' muddy halite lithofacies is characterized by lenses and pods of fine to medium crystalline halite (Figure 1, Appendix F). Generally, it is more argillaceous than the

**Compliance Certification Application Reference Expansion**

---

'stratified' mud-poor lithofacies. The 'podular' muddy halite lithofacies is subdivided into two zones which laterally and vertically interfinger: 1) a zone dominated by expansive (displacive) halite cements and 2) a zone with few expansive cements. Few textures reflecting subaqueous deposition are preserved, and continuous strata are very rare. Dissolution pits, pipes, and pores are common. Textures within this lithofacies are similar to 'hummocky' salt pan halite in the Devil's Golf Course in Death Valley, California."



Compliance Certification Application Reference Expansion

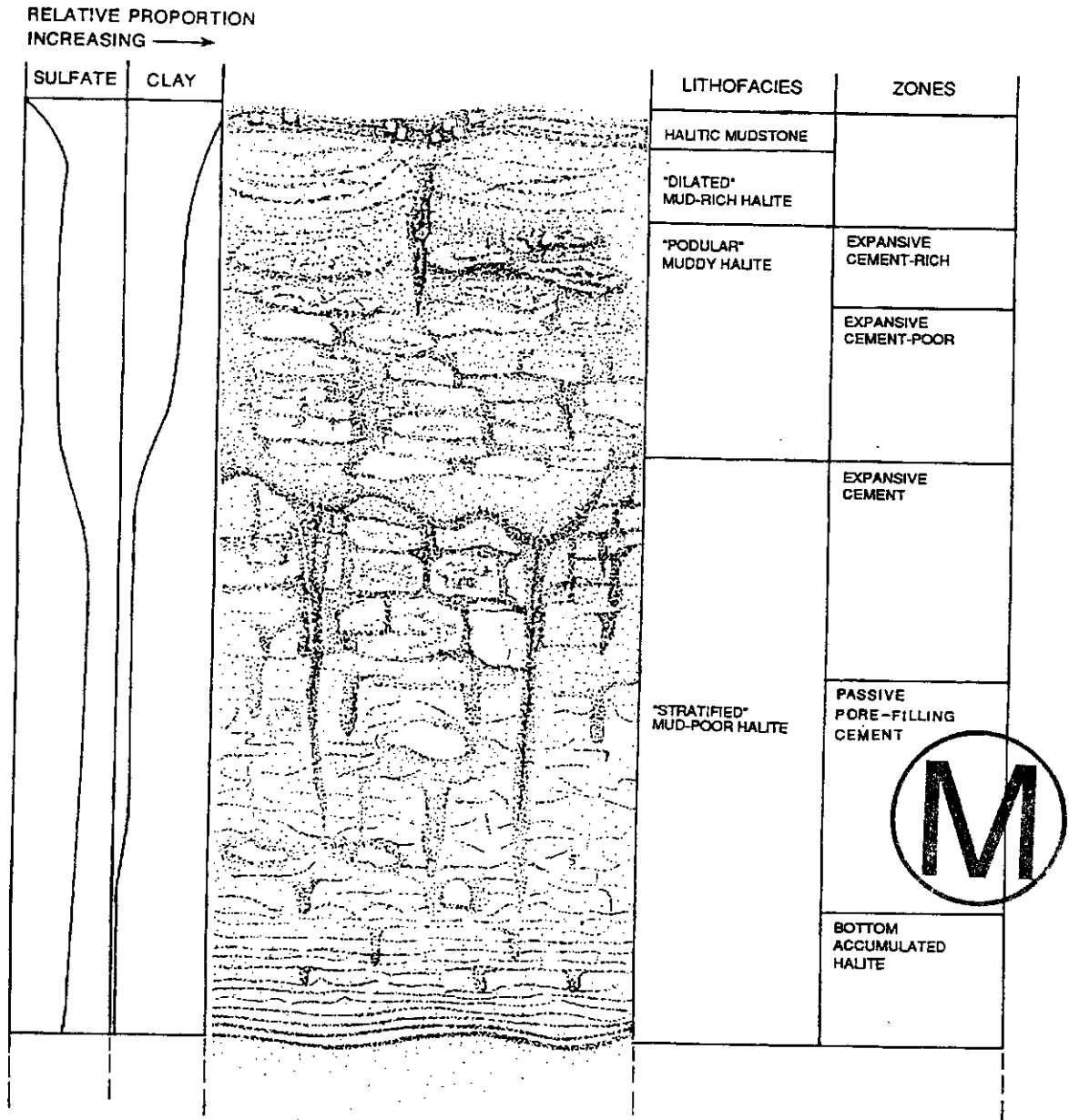
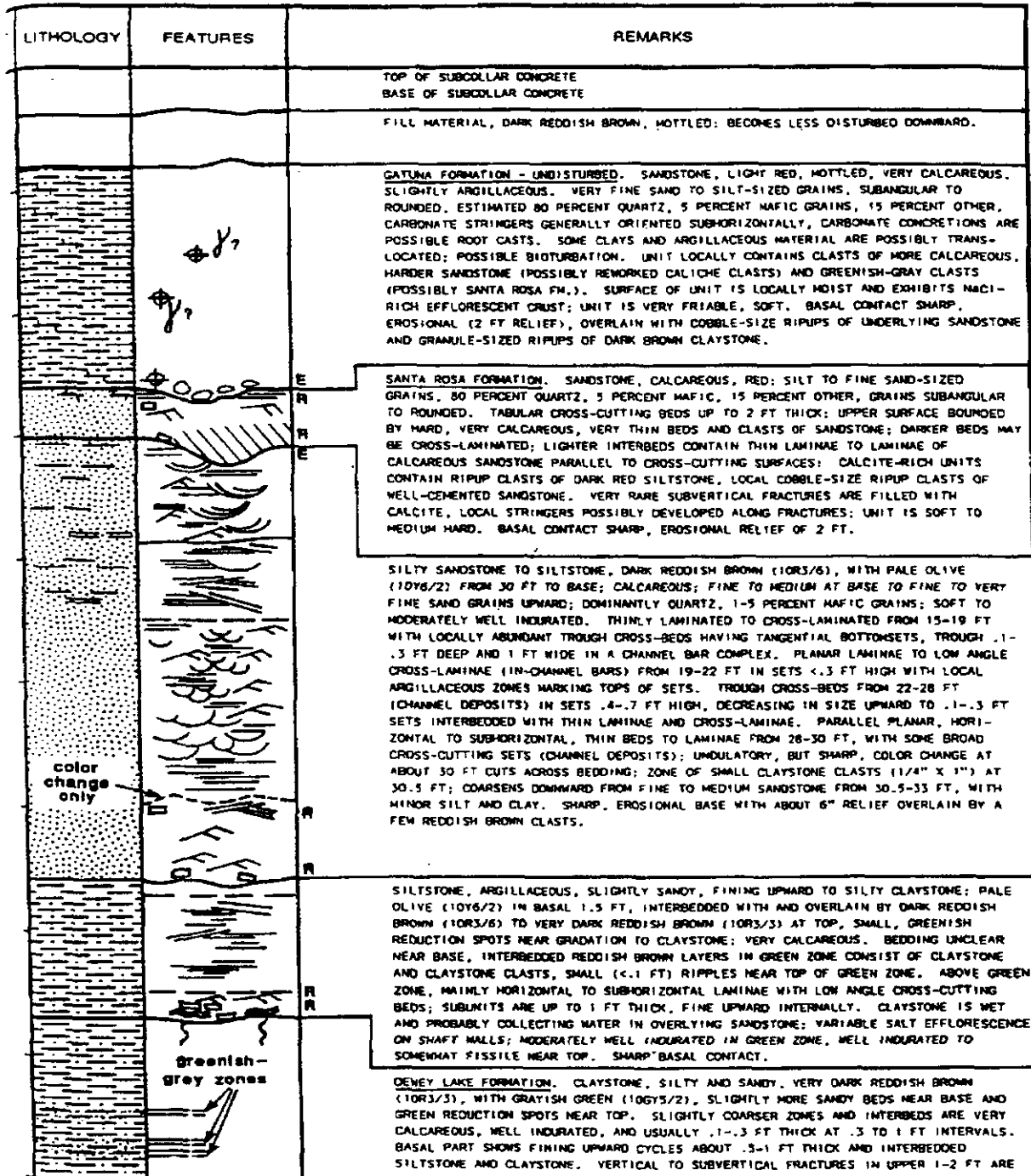


FIGURE 1 IDEALIZED SALADO HALITE SEQUENCE LITHOFACIES AND ZONES.

Compliance Certification Application Reference Expansion

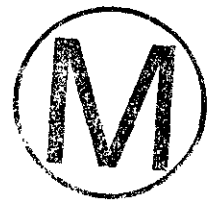


AIR INTAKE SHAFT LITHOLOGIC LOG SHEET 3 OF 22

FIGURE 5

Compliance Certification Application Reference Expansion

NOTE: Figure 16 is a photograph and will not scan in properly, therefore it is not included here.



IAEA (International Atomic Energy Agency). 1981. Safety Assessment for the Underground Disposal of Radioactive Wastes. IAEA Safety Series No. 56, Vienna, Austria.

1. INTRODUCTION; p. 1, para. 1;

" Nuclear energy is playing a continuing and increasing role in electricity generation in many countries. Therefore, these countries are faced with adopting appropriate systems for the management and disposal of the radioactive wastes. These wastes vary greatly in physical/chemical form and isotopic content. While various concepts have been proposed and are being studied, it is generally agreed that disposal underground, with the wastes appropriately immobilized, is an adequate way of providing the necessary protection for humans and the environment.

Underground disposal means the emplacement of radioactive waste materials in the terrestrial subsurface without the intention of retrieval. Accordingly, underground disposal concepts can range from shallow ground burial to emplacement in very deep bore-holes. Most effort is currently focused upon mined repositories in deep (e.g. up to 1000 meters). Continental geologic formations, and this emphasis is reflected in the present document.

Safety assessments are necessary to estimate the expected performance of a system considered for underground disposal of radioactive wastes and to compare it with acceptability criteria, both for the operational and post-operational phases; they are useful also to identify the potential significance of possible improvements of the system. They are important in every phase in system development; system selection; site confirmation; repository design, construction, operation, shutdown and sealing; and licensing processes relevant to these phases. Thus, safety assessments are a tool to predict the probable consequences of creating a waste repository, to compare the consequences with acceptability criteria (as defined in the Glossary), and to present the results for judgement by the appropriate bodies.

Safety assessments proceed from generic to site-specific studies. Generic assessments can be useful for making programmatic decisions regarding the choice of a disposal concept and the appropriate use of available resources. Generic assessments may also be helpful in gaining recognition of the feasibility of a disposal concept. Site-specific assessments are necessary for decisions affecting siting, design, and licensing for construction, operation, shutdown and sealing of a repository.

Safety assessments are performed by:

(a) working backward from acceptability criteria to determine and compare their expected performance with acceptability criteria. working forward

(b) working forward from the characteristics of systems to determine and compare their expected performance with acceptability criteria.

These two approaches are complementary and used in an iterative process. During this process the effects of potential improvements of the overall system of natural barriers



## Compliance Certification Application Reference Expansion

---

and man-made provisions can also be evaluated relative to an 'as low as reasonably achievable' solution for the future consequences of the underground waste disposal, taking present-day economic and social factors into account.

Performance of such safety assessments requires an interdisciplinary team of specialists to cover the many technical aspects, working throughout all phases of repository planning, designing and licensing activities.

The purposes of this document are to introduce:

(a) overall safety assessment approaches that can be useful during all phases of disposal system development, including both generic and site-specific studies;

(b) general methods that can be applied within that overall approach.

Subsequent documents to be published by the IAEA will describe specific safety assessments and present further details on the methodologies used and the status of this rapidly developing technology."



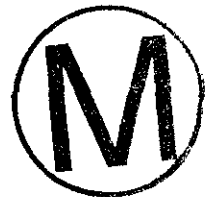
Compliance Certification Application Reference Expansion

---

Iman, R.L. 1982. "Statistical Methods for Including Uncertainties Associated with the Geologic Isolation of Radioactive Waste Which Allow for a Comparison with Licensing Criteria," *Proceedings of the Symposium on Uncertainties Associated with the Regulation of the Geologic Disposal of High Level Radioactive Waste*, Gatlinsburg, Tennessee, March 9-13, 1981, ed. D.C. Kocher. NUREG/CP-0022, CONF810372, Oak Ridge National Laboratory, Oak Ridge, Tennessee, 145-157. Available from NTIS. Order#: DE82008883.

ABSTRACT, p. 145;

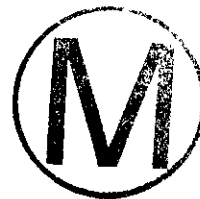
" A project funded at Sandia National Laboratories by the Nuclear Regulatory Commission has as its charter to develop a methodology for evaluating applications for nuclear waste repositories. Since the Sandia methodology has the capability of expressing the output variable (for example integrated discharge rates) as a distribution, this report illustrates how to put uncertainty bounds on the output distribution. Additionally this approach permits a comparison against licensing criteria. The licensing criteria used in this paper while hypothetical in nature did involve guidance from experts."



Iman, R.L., and Conover, W.J. 1982. A Distribution-Free Approach to Inducing Rank Correlation Among Input Variables. *Communications in Statistics: Simulation and Computation*, Vol. B11, No. 3, pp. 311-334.

ABSTRACT, p 311;

" A method for inducing a desired rank correlation matrix on a multivariate input random variable for use in a simulation study is introduced in this paper. This method is simple to use, is distribution free, preserves the exact form of the marginal distributions on the input variables, and may be used with any type of sampling scheme for which correlation of input variables is a meaningful concept. A Monte Carlo study provides an estimate of the bias and variability associated with the method. Input variables used in a model for study of geologic disposal of radioactive waste provide an example of the usefulness of this procedure. A textbook example shows how the output may be affected by the method presented in this paper."



Kaplan, S., and Garrick, B.J. 1981. On the Quantitative Definition of Risk. Risk Analysis, Vol. 1, No. 1, pp. 11-27.

INTRODUCTION, p 11, col 1;

" As readers of this journal are well aware, we are not able in life to avoid risk but only to choose between risks. Rational decision-making requires, therefore, a clear and quantitative way of expressing risk so that it can be properly weighed, along with all other costs and benefits, in the decision process.

The purpose of this paper is to provide some suggestions and contributions toward a uniform conceptual/linguistic framework for quantifying and making precise the notation of risk. The concepts and definitions we shall present in this connection have shown themselves to be sturdy and serviceable in practical application to a wide variety of risk situations. They have demonstrated in the courtroom and elsewhere the ability to improve communication and greatly diminish the confusion and controversy that often swirls around public decision making involving risk. We hope therefore with this paper to widen the understanding and adoption of this framework, and to that end adopt a leisurely and tutorial place.

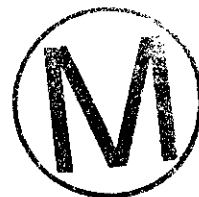
We begin in the next section with a short discussion of several qualitative aspects of the notion of risk. We then proceed to a first-pass or first-level quantitative definition. Since the notion of 'probability' is fundamentally intertwined with the definition of risk, the next section addresses the precise meaning adopted in this paper for the term 'probability.' In particular, at this point, we carefully draw a distinction between 'probability' and 'frequency.' Then, using this distinction, we return to the idea of risk, and give a 'second-level' definition (of risk which generalizes the first-level definition) and is large enough and flexible enough to include at least all the aspects and subtleties of risk that have been encountered in the authors' experience."

3. QUANTITATIVE DEFINITION OF RISK (FIRST LEVEL), p 12, col 2,

3.1 "Set of Triples Idea";

" In analyzing risk we are attempting to envision how the future will turn out if we undertake a certain course of action (or inaction). Fundamentally, therefore, a risk analysis consists of an answer to the following three questions:

- (i) What can happen? (i.e., What can go wrong?)
- (ii) How likely is it that that will happen?
- (iii) If it does happen, what are the consequences?



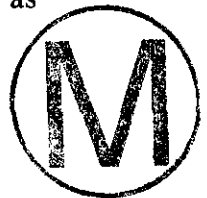
**Compliance Certification Application Reference Expansion**

Table I. Scenario List

Scenario	Likelihood	Consequence
$S_1$	$P_1$	$X_1$
$S_2$	$P_2$	$X_2$
.	.	.
.	.	.
.	.	.
$S_N$	$P_N$	$X_N$

To answer these questions we would make a list of outcomes or 'scenarios' as suggested in Table I. The  $i$ th line in Table I can be thought of as a triplet:

$$(s_i, p_i, x_i)$$



where  $s_i$  is a scenario identification or description;  
 $p_i$  is the probability of that scenario; and  
 $x_i$  is the consequence or evaluation measure of that scenario,  
 i.e., the measure of damage.

If this table contains all the scenarios we can think of, we can then say that it (the table) is the answer to the question and therefore is the risk. More formally, using braces  $\{ \}$ , to denote 'set off' we can say that the risk,  $R$ , 'is' the set of triplets:

$$R = \{(s_i, p_i, x_i)\}, \quad i=1,2,\dots,N.$$

This definition of risk as a set of triplets is our first-level definition. We shall refine and enlarge it later.<sup>3</sup> For now let us show how to give a pictorial representation of risk.

<sup>3</sup>Having defined risk as a set of triplets, we may now, in line with section 2.2, define hazard as a set of doublets thus  $H = \{(s_i, x_i)\}$ ."

5.2. Inclusion of Uncertainty, p 20, col 1;

" Now since we have not yet actually done the thought experiment of the previous section, we have uncertainty about what its outcome would be. The degree of uncertainty depends upon our total state of knowledge as of right now; upon all the evidence, data, and experience with similar courses of action in the past. We seek therefore to express this uncertainty using, naturally, the language of probability.

Since the thing we are uncertain about is a curve,  $\Phi(x)$ , we express the uncertainty by embedding this curve in a space of curves and erecting a probability distribution over this space.

Pictorially, this is represented by a diagram of the form of Fig. 7. This figure is what we call a risk curve in probability of frequency format. It consists of a family of curves  $\Phi_p(x)$ , with the parameter being the cumulative probability. To use this diagram we

## Compliance Certification Application Reference Expansion

---

would, for example, enter with a specific  $x$  value and choose say the curve  $P=0.90$ . The ordinate of this curve  $\Phi_{0.90}(x)$  is then the 90th percentile frequency of  $x$ . That is to say, we are 90% confident that the frequency with which damage level  $x$  or greater occurs, is not larger than  $\Phi_{0.90}(x)$ .

Figure 7 is the pictorial form of our level 2 definition of risk. It is of interest to express this definition also in terms of the set of triplets idea.



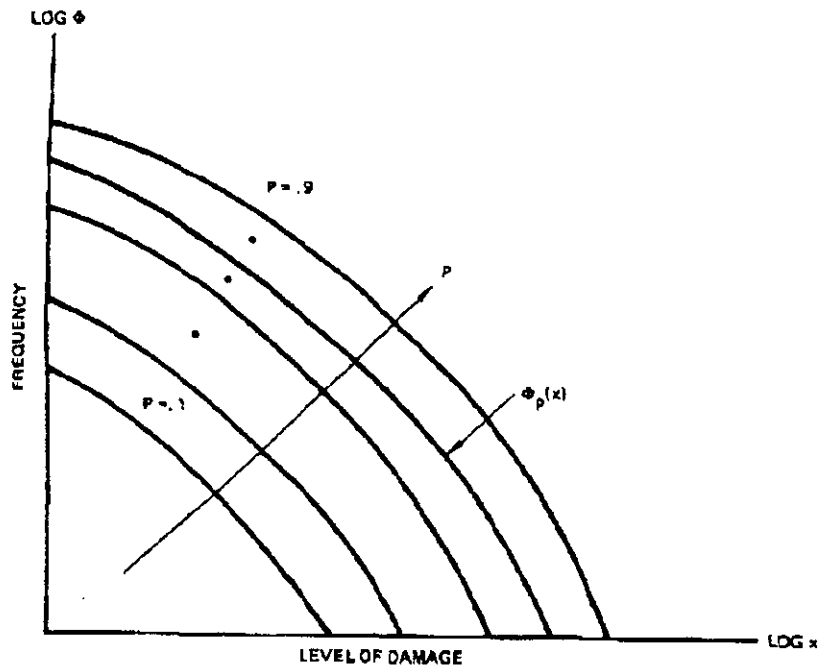


Fig. 7. Risk curve in probability of frequency format.



Lappin, A.R., Hunter, R.L., Garber, D.P., Davies, P.B., Beauheim, R.L., Borns, D.J., Brush, L.H., Butcher, B.M., Cauffman, T., Chu, M.S.Y., Gomez, L.S., Guzowski, R.V., Iuzzolino, H.J., Kelley, V., Lambert, S.J., Marietta, M.G., Mercer, J.W., Nowak, E.J., Pickens, J., Rechard, R.P., Reeves, M., Robinson, K.L., and Siegel, M.D., eds., 1989. Systems Analysis, Long-Term Radionuclide Transport, and Dose Assessments, Waste Isolation Pilot Plant (WIPP), Southeastern New Mexico: March 1989. SAND89-0462. Sandia National Laboratories, Albuquerque, NM. WPO 24125.

EXECUTIVE SUMMARY, p iii;

" This report summarizes the current understanding of the expected long-term behavior of the Waste Isolation Pilot Plant (WIPP) repository and estimates long-term radionuclide doses in a series of six analyses investigating both undisturbed repository performance (Case I) and performance in response to a relatively high-consequence human Intrusion (Case II). It is the result of an intensive effort over a short time. The U. S. Department of Energy (DOE) decided to have Sandia National Laboratories prepare this report as a result of a meeting held January 5, 1989. The conceptual model of the expected long-term behavior of the WIPP repository used in this report was formulated in early to mid January 1989, drawing on information and understanding developed over the past decade. Numerical modeling of ground-water flow, radionuclide transport, and doses to humans began January 20, 1989 and was completed March 20, 1989.

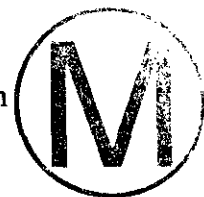
The report has several objectives:

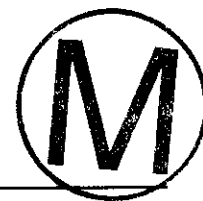
1. To briefly summarize Sandia's current technical understanding of the major components of long-term performance of the WIPP repository. The following areas are specifically addressed:

- .....
- f. radionuclide-transport mechanisms and properties of the Culebra Dolomite, the major pathway for ground-water transport of radionuclides from the WIPP to the biosphere.
- .....

4. To describe, document, and interpret six sets of calculations estimating the potential health effects to individuals resulting from emplacement of CH-TRU wastes in the WIPP, hydrologic saturation of the repository as a result of either natural processes or human intrusion, direct and indirect exposure during and after drilling (where appropriate), and ground-water transport of radionuclides to a hypothetical stock well south of the WIPP site.

The calculations presented here investigate radionuclide transport and resulting health effects both during undisturbed performance of the WIPP repository and in response to a relatively high-consequence human intrusion into the repository. The human intrusion considered is drilling that results in a long-term interconnection of the repository, an underlying brine reservoir in the Castile Fm., and the overlying Culebra Dolomite. The Culebra Dolomite provides a relatively permeable pathway for ground-water transport of radionuclides to the hypothetical stock well."





#### E.1.5.1 Use of a Stream Tube to Calculate Transport, p. E-15;

" To calculate transport, the numerical model assumes that the steady-state flow field and brine-density distribution of LaVenue et al. (1988) is disturbed significantly by the release. To justify this approach, particle travel times in the Culebra Dolomite from the release point to the stock-well location have been calculated for three flow fields, corresponding to steady-state, Case IIA, and Case IIB/IIC/IID conditions. By definition, particle travel times are calculated using the Darcy velocities and a selected porosity. The process of dispersion, matrix diffusion, and sorption are not included. The calculated particle travel times assumed fracture-dominated transport to assess the maximum transport impact of the transient brine-reservoir perturbations to the undisturbed Culebra flow field. The particle travel time for the undisturbed, steady-state flow simulation differs by about 2% from the Case IIA particle travel time and about 7% from the CASE IIB, IIC, and IID travel times. Thus, a release from the breach borehole to the Culebra Dolomite will form a plume, the centerline of which will coincide with the transport pathway illustrated in Figure E-2. The numerical model calculates transport along this centerline using a stream tube. Constructed as described in Appendix B of Reeves et al. (1987), the stream tube yields the same spatial variations in velocity along the transport pathway as the flow model of LaVenue et al. (1988).

Figure E-3 represents an idealized contaminant plume formed as the result of point-source injection at constant rate  $Q$  into a unidirectional flow field, which has Darcy velocity  $u_0$  and aquifer thickness  $b$ . The stream-tube concept, based on undisturbed flow, can be considered with the disturbed flow field (Figure E-3). The latter describes a release of brine-reservoir fluids to the Culebra Dolomite, focusing on the streamlines near the borehole. These streamlines diverge from the point of release  $a_n$ , at a distance, become parallel to the direction of natural ground-water flow.

The streamlines of the injected fluids form a plume of contaminated water of width  $2w$  from flow divide to flow divide, as illustrated in Figure E-3 and defined by the relation

$$2w = Q/bu_0 \quad (\text{E-27})$$

Asymptotically, the flux within the plume equals that of the natural ground-water  $u_0$ . The distance  $s$  that separates the points of release and stagnation is defined by the relation

$$s = Q/2\pi bu_0 \quad (\text{E-28})$$

This distance also provides a measure of the spatial extent of the region in which fluid velocities differ significantly from  $u_0$ . The maximum rate of fluid release  $Q_{\max}$  calculated for the borehole and the natural ground-water velocity  $u_0$  calculated by LaVenue et al. (1988) at the point of release (i.e., the borehole) yield stagnation-point distances (Table E-3) for Cases IIA, IIB, IIC, and IID. A comparison of the 7.8 to 69.6-m range of stagnation-point distance at 75 years with the 4840-m distance from the point of release to the stock well indicates that the region of disturbed velocities is small relative to the overall scale for solute

**Compliance Certification Application Reference Expansion**

---

transport, thus supporting the assumption of a negligibly disturbed steady-state flow field."





## Compliance Certification Application Reference Expansion

---

Luker, R.S., Thompson, T.W., and Butcher, B.M. 1991. "Compaction and Permeability of Simulated Waste." In *Rock Mechanics as a Multidisciplinary Science: Proceedings of the 32nd U.S. Symposium, University of Oklahoma, Norman, OK, July 10-12, 1991*. J.C. Roegiers, ed.. SAND90-2368C, pp. 694-702. A. A. Balkema, Brookfield, VT. WPO 38847.

### ABSTRACT:

" This paper focuses on the mechanical and hydraulic properties of simulated contact handled transuranic radioactive waste that are associated with the Waste Isolation Pilot Plant (WIPP). In particular, the mechanical behavior of the simulated (nonradioactive) waste and its permeability after substantial time dependent compaction are being measured to give input data for modeling contaminated brine flow in a geologic repository stratum.

A number of deformation and permeability tests have been performed on materials comprising this waste. A variety of material mixtures were used, including cloth, wood, metals (various geometries), plastics, and minerals (various grain size distributions). Prior to the permeability tests, specimens were loaded under a constant stress (2000 psi) from 1 to 50 days and allowed to achieve a stable density state. Specimens, four inches in diameter with various lengths, were loaded axially via a piston and confined radially by the pressure vessel cylinder wall. Axial deformation was measured for production of stress-density and density-time curves. Subsequent to the deformation stage, which was terminated after evidence of density stabilization, brine was passed through the specimen for permeability measurements.

Deformation and permeability measurements of the simulated waste material are presented. Permeability values ranged through several orders of magnitude."

## 1. 0 INTRODUCTION

### .1 Project Overview

The Waste Isolation Pilot Project (WIPP) facility, near Carlsbad, New Mexico, is currently being evaluated for the purpose of storing contact handled and remotely handled transuranic radioactive waste.

Characterization of the mechanical and hydrological properties of the waste is important for predicting the repository behavior with time. More specifically, the potential for migration of groundwater through the storage areas and the dispersal of radioactive materials must be established. The radioactive waste to be stored in the WIPP facility consists of a variety of materials, including metals, combustibles (plastics and fibers) and "sludge". A large portion of these materials will be contained in 55 gallon drums and stored in rooms that will be backfilled. Because most of the materials initially have high porosities, they will be highly permeable. However over time the drums may be expected to collapse due to volume decreases in the rooms because of creep closure. Under these conditions the waste will compact leading to a reduction in porosity and permeability (Butcher 1989).

## Compliance Certification Application Reference Expansion

---

This paper summarizes the results of a series of experiments performed to investigate the time dependent compaction and permeability of simulated waste materials. The experiments were limited to ambient laboratory conditions. Permeability measurements were only performed on compacted specimens. Procedures, equipment, and data from these studies are presented and the results are discussed.

### 2 0 PROGRAM PLANNING

Butcher (1989) identified five major waste components: plastics, fibers (cellulosics: paper, cloth, wood, etc.) sorbents, metals, and sludge. The results from earlier 55-gallon drum testing (Butcher et al., in preparation) together with information on the anticipated waste inventories, were used to select mixtures of some of the waste components for the tests discussed here. Certain additional materials were also tested. These included granular limonite and magnetite, which were chosen to represent metal materials after decomposition, a mixture of granular magnetite and steel, representing an intermediate corrosion state, and a mixture of shredded metal and crushed salt, which is being considered as an engineered alternative to untreated wastes. These mixtures are described by their respective weight percentages in Table 2 1.

Table 2 1 Specimen Summary

MATERIAL NUMBER	MATERIAL DESCRIPTION
1	39% Intact and sectioned bottles, 42% PVC Conduit, 19% Surgeons Gloves
2	40% Rags, 60% Pine wood cubes (1" dimension)
3	60% 1" dimension steel, 40% crushed salt
4	45% Material 1, 37% Material 2, 9% 1" dimension metals, 9% Dry Portland Cement
5	Magnetite granules (coarse, well graded)
6	Limonite granules (coarse, well graded)
7	50% Magnetite particles, 50% 1" dimension steel
8	80% crushed salt, 20% shredded metals





### 3.0 EXPERIMENTATION

Two uniaxial strain compaction and brine permeability tests were run on each of the materials in an oedometer to a maximum axial stress of approximately 2000 psi, the estimated lithostatic pressure at the repository horizon.

Because the mechanical and hydrological properties of the simulated contact handled transuranic waste were thought to be variable through a broad range, a laboratory measurement system had to be assembled that accommodated acceptable precision and accuracy at extreme levels of strain and permeability. System reliability was another concern due to the lengthy nature of most tests (weeks to months), specimen transience (i.e., destructive testing), corrosive properties of the saturating brine, and rigid quality assurance requirements.

To alleviate some of these concerns, a redundancy in data collection was assured by incorporating several transducers into the measurement system. For example, three pressure transducers and two flowmeters were put in the permeability flow circuit; thermocouples were placed in the fluid reservoir enclosure and on the pressure vessels. In this manner, back-ups were available in case the primary transducer failed, and additionally, a larger range of measurement was realized by using two or more transducers with different ranges, without sacrificing significant precision or accuracy.

#### 3.1 Specimen Preparation

All specimens were assembled according to weight percent specifications, photographed, and mixed together in the pressure vessel. A 'random' yet well mixed blend was attempted for most of the specimens (e.g., particulate matter and small components), while other specimens were packed in specific configurations due to the specimen component size and composition (e.g., metal blocks and particulate matter). After specimen insertion brine was introduced into the pressure vessel chamber to saturate the specimen. The brine consisted of a prototypical chemistry, designed to simulate in situ water chemistry after several thousand years of waste emplacement.

#### 3.2 Compaction System

Apparatus for these tests consisted of an oedometer (pressure vessel) used as the sample holder, a load control system for maintaining constant axial stress, a flow control system for permeability testing, and instrumentation to monitor loads, deformations, and brine flow.

Samples were contained in a 4" ID, 6" OD steel pressure vessel fitted with an integral axial piston to provide axial stress (Figure 3.1). The axial piston assembly attached to the bottom of the sample holder, and extended to the hydraulic pressure system through a standard dog-bone strain gaged load cell. Both the top end-piece and the bottom piston were pierced to allow flow of brine through the sample; mesh screens were used at either end of the sample to allow brine flow without extrusion of any sample material.

Hydraulic pressure to the axial position system was provided by a gas control system consisting of an a gas/hydraulic bladder accumulator backed by a nitrogen bottle. Both the accumulator and the nitrogen bottle were in an insulated enclosure, with temperature

controlled at 24 to 26 °C. Load on the sample was monitored using a strain-gaged load cell, with backup provided by a pressure transducer in the hydraulic pressure line.

Axial deformation was monitored with a 4" stroke LVDT attached to the lower loading piston. Temperature of the vessel during the tests was monitored using a thermocouple.

Load was applied to the axial piston by pressurizing the bladder accumulator to the required gas pressure, then slowly opening the valve to the piston assembly until the required hydraulic pressure and axial load were achieved. Axial load, line pressure, temperature, and sample deformation were monitored during specimen loading. On achieving full load the gas and hydraulic fluid pressure were maintained for the duration of the test while monitoring compaction. In the longer term tests load was held constant until a density/time slope of approximately  $10^{-5}$  gm/cm<sup>3</sup>/hr was obtained, or until the specified test duration was reached. Final density/time slopes ranged from  $1.2 \times 10^{-8}$  to  $3.9 \times 10^{-4}$  kg/m<sup>3</sup>/hr. The duration of the tests varied from 1 to 59 days.

### 3.3 Permeability System

Brine permeability was determined at the end of the constant stress compaction portion of the tests. Brine flow was initiated by pressurizing an accumulator using a nitrogen bottle and controlled via a metering valve. Flow rate and pressure drop were monitored, and upstream pressure adjusted until a constant flow was established within the range of the flow meter and pressure transducer. In several tests different flow rates were used. Good agreement was obtained between the two flow measuring devices. Pressure difference between the upstream and downstream sides was monitored using one of three available upstream pressure transducers, with ranges of 25, 100 and 1000 psi.

### 3.4 Data Acquisition System

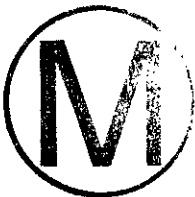
All instrumentation outputs were monitored using an IBM compatible 8086 computer with an internal clock, and a 16-bit analog-to-digital converter. Data were stored on hard disc, and backed up periodically onto a floppy disc.

Prior to testing, all instrumentation, including the load cells, LVDTs, pressure transducers, and flowmeters, were calibrated. Additional system calibrations were performed on the permeability measurements system, including a flow rate-pressure calibration for the flow lines.

Data were acquired at different frequencies during the tests. During the initial portion of the compaction test when specimen loading was relatively rapid, the automated DAS acquired data every 20 seconds the decremented the rate to a minimum of one scan every hour during the latter stages of compaction, a total of four scanning rates were used through each test.

### 3.5 Equipment Limitations

The equipment had limitations imposed by the resolution of the instruments, which determined the lower bound of measurable permeability, and by the friction in the lines which imposed an effective upper bound on the permeabilities. The flowmeter has a resolution of 0.0036 cc/s, based on the resolution of the voltmeter and the calibration constant for the instrument. The accuracy of the LVDT float system, including electronic



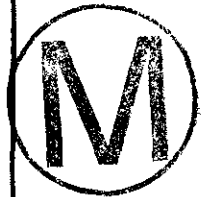
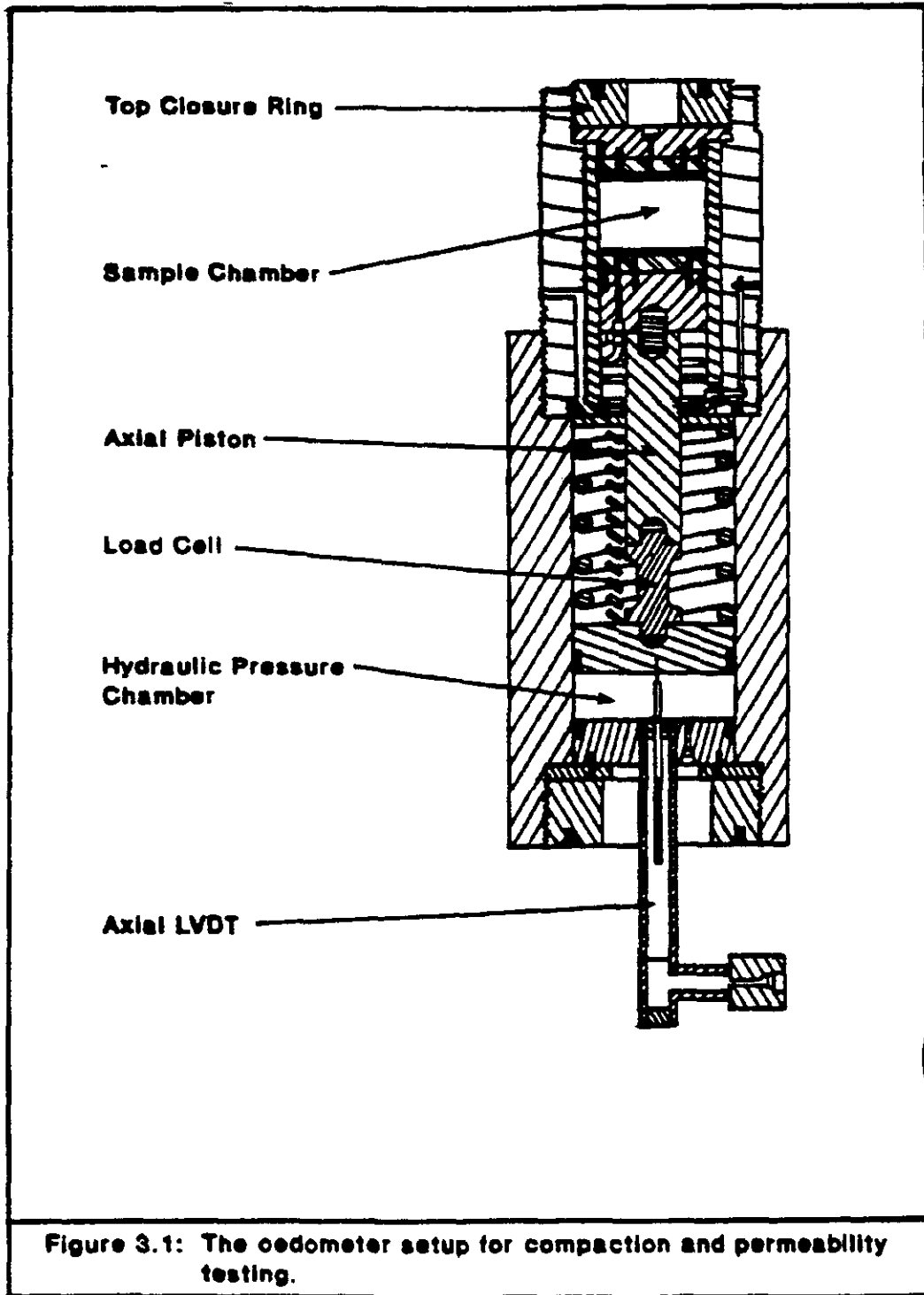
## Compliance Certification Application Reference Expansion

---

noise, is +/- 0.005 liters: this translates to an accuracy of the order of 0.083 cc/s over a 60 second reading, or 0.0083 cc/s over 600 seconds.

A practical upper limit for permeability is reached when the pressure drop through the specimen is not significantly different than the pressure drop through the tubing. This is true because, as the pressure drop becomes dominated by the tubing, the correction for tubing flow resistance (some delta pressure value) involves the subtraction of two similar values and approaches zero. The upper limit is seen as an increase in uncertainty as the conductivity of the sample approaches that of the tubing, the actual limit depending on the relative values of these specimen conductivities and their individual uncertainties. Related to tubing (flow) friction was an upstream filter to remove particulates from the brine; early in the test series this filter was positioned downstream of the pressure transducers. Since this added additional line pressure loss, the filter was moved upstream of the pressure transducers for later tests of high permeability materials.





## 4 0 RESULTS

### 4 1 Time Dependent Compaction Results

The compaction results for the various tests are presented in Table 4.1. Stress/density and density/time plots are given for the two plastics specimens that exhibited the most extreme changes in density values (Figures 4.1 and 4.2). Data in the tables are presented in terms of the densities and porosities of the materials at various times during the tests.

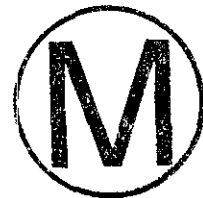
The compaction curves for the earlier tests show a periodic variation in density. This is not temperature related but is a function of the early load control system. In the earliest tests the bladder accumulator used for pressure control was isolated from the back up nitrogen bottle. Due to the small volume of fluid in the system early compaction and small system leaks, reductions occurred in hydraulic pressure which were adjusted manually on a daily basis and are seen as density fluctuations in the plots. Despite these periodic variations the overall curves follow a regular trend and can be smoothed to give needed time dependent compaction parameters such as those discussed by Butcher (1989). In later tests the control system was modified to give continuous back up to the nitrogen bottles. Smoother time dependent compaction curves were observed with this system. In some of the compaction curves especially for the magnetite and limonite irregular curves are seen. This is believed to be a true effect

which is exaggerated in the plots because of the small density changes involved.

### 4.2 Permeability Results

Permeability results are given in Table 4.1. Typical data acquired by the automated DAS for permeability testing are shown in Figures 4.3 and 4.4. Brine permeabilities were determined on all examples at the end of the time dependent compaction phase by flowing brine through the samples and recording flow rate and pressure.

Slopes of the permeability calibration curves (flow rate versus pressure drop exemplified in Figure 4.4) designated here as  $K_1$  were used to correct the measured permeabilities. The correction is applied by treating the lines ( $K_1$ ) and sample ( $K_s$ ) as two elements in series so that:



October 17, 1996

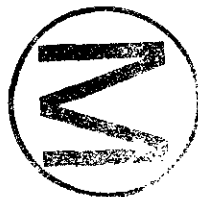
XRE6-106

APPENDIX XRE6

TABLE 4.1

MATERIAL DESCRIPTION	SPECIMEN TYPE #	TEST #	TEST DURATION (hours)	Initial Final		Initial Final		DENSITY/TIME SLOPE (kg/m <sup>3</sup> /hr) <sup>3</sup>	PERMEABILITY (mD)
				-----DENSITIES----- (kg/m <sup>3</sup> )		-POROSITY <sup>2</sup> - (%)			
Wood/Rags	2	1	243	184.3	933.8	83.3	15.4	3.2x10 <sup>-6</sup>	17
	2	6	330	200.6	808.0	81.8	26.7	5.4x10 <sup>-6</sup>	>71
Plastics	1	2	325	290.3	1042.0	71.0	-4.2	1.4x10 <sup>-8</sup>	No Flow
	1	11	643	309.7	970.7	69.0	2.9	1.2x10 <sup>-8</sup>	99
SPEC. 1, 2, metals, cement	4	3	430	343.1	1092.0	71.6	9.6	3.6x10 <sup>-7</sup>	63
	4	10	973	378.3	979.4	77.1	4.1	3.3x10 <sup>-8</sup>	45
Steel cubes/ crushed salt	3	5	383	1181.0	2003.0	69.0	47.4	6.8x10 <sup>-8</sup>	27
Magnetite granules	5	7	26	2429.0	3134.0	53.3	39.7	3.5x10 <sup>-7</sup>	109
	5	12	24	2540.0	3121.0	51.2	40.0	3.9x10 <sup>-6</sup>	1096
Limonite granules	6	8	28	1454.0	2046.0	46.1	24.2	6.8x10 <sup>-8</sup>	93
	6	13	24	1430.0	1996.0	47.0	26.1	3.1x10 <sup>-8</sup>	1136
Magnetite gran./ steel cubes	7	9	24	1883.0	2696.0	69.9	56.9	7.2x10 <sup>-7</sup>	88
	7	14	24	1808.0	2728.0	71.1	56.4	2.0x10 <sup>-7</sup>	8
Shredded metal/ crushed salt	8	15	1414	1168.0	1917.0	53.4	23.4	1.6x10 <sup>-8</sup>	100-5000 <sup>2</sup>
	8	16	1414	1165.0	2260.0	53.5	9.8	1.6x10 <sup>-8</sup>	151

NOTES: <sup>1</sup> Porosities were calculated using assumed values for solid densities. Uncertainties in these assumed values result in large uncertainties at low calculated porosity, leading to calculated small (or negative) values.  
<sup>2</sup> A range of permeability values indicates that steady-state conditions were poorly defined during the test.  
<sup>3</sup> Taken from latter (time) stage of density/time curve.



Compliance Certification Application Reference Expansion

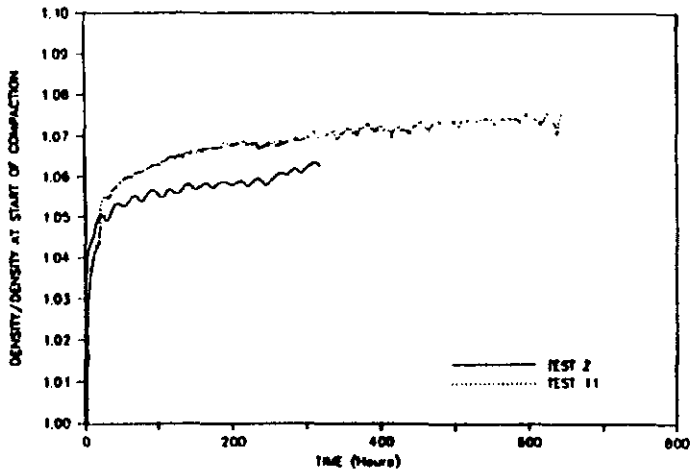


Figure 4.1. Change in density with time of simulated plastics waste at a constant stress of 2000 psi.

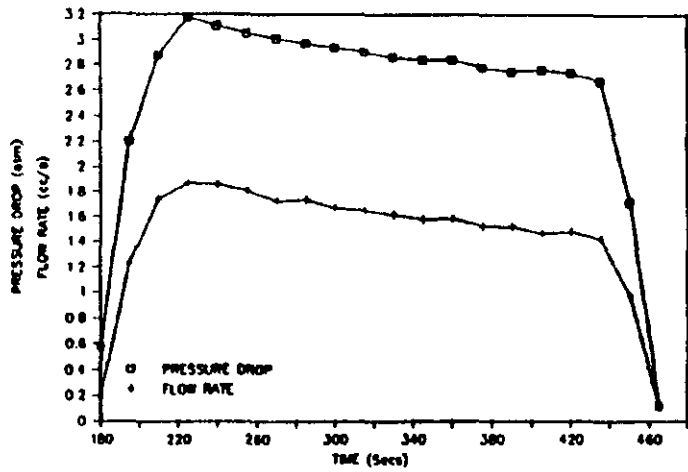


Figure 4.3. Permeability test history for simulated plastics waste.

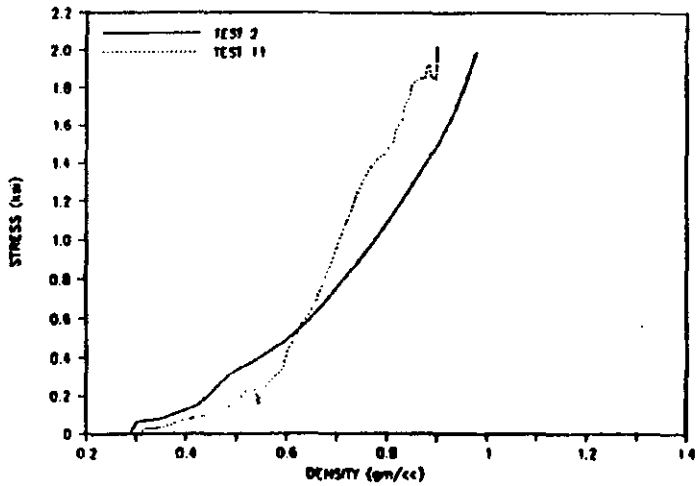


Figure 4.2. Change in density with applied axial stress of simulated plastics waste.

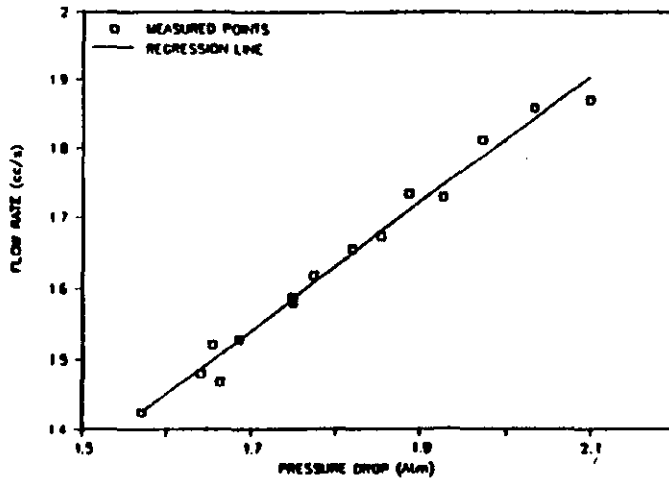


Figure 4.4. Flow rate - pressure drop relationship for simulated plastics waste.

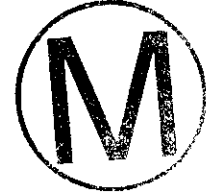


$$(1) 1/K_s = 1/K' - 1/K_1,$$

where  $K'$  is the slope of the  $Q$  (flow rate) vs  $dP$  (pressure difference) plot. Sample permeability  $k_s$ , is then calculated from Darcy's Law:

$$(2) k_s = (Q/dP) \cdot v \cdot L_s A_s, \text{ and}$$

$$(3) k_s = K_s \cdot v \cdot L_s / A_s,$$



where

$A_s$  is the sample area (internal area of the sample holder) = 81.073 cm<sup>2</sup>

$L_s$  is the sample length (determined from the original sample height and the axial deformation determined during the load up and time dependent compaction tests)

$v$  is the viscosity of brine (assumed to be 1.2 cp at 25 °C).

Permeabilities for the various tests have in general been calculated from the slopes of the pressure difference ( $dP$ ) - flow rate ( $Q$ ) curves, this method having the advantages of allowing a check on the linearity of the results and of removing the effects of small offsets in the pressure or flowrate data. In one test, magnetite and steel cubes, the flow rate was too small for this method to be used. Here an average of the flow rate/pressure drop ( $Q/dP$ ) values over the stable portion of the test was used to determine permeabilities. In another test, shredded metal and crushed salt, the permeability of the sample varied by large amounts during the flow test, and point by point permeabilities were calculated.

#### 5.0 CONCLUSIONS

A series of uniaxial strain time dependent compaction and brine permeability tests was performed on materials simulating wastes to be stored at the WIPP site. Some of the materials were designed to simulate the long term corrosion products of metal waste and steel drums. One specimen was made up of crushed salt mixed with shredded metals to simulate an alternate form of metallic waste.

All of the materials tested show increasing density and decreasing porosity when loaded in an oedometer to an axial stress of 2000 psi. All of the materials showed some time dependent compaction under constant stress. Final porosities were low for the plastics (less than 5%) but remained quite high for the limonite and magnetite samples (25% to 57%). Final time dependent compaction density/time slopes of the order of  $10^{-6}$  to  $10^{-8}$  kg/m<sup>3</sup>/s were reached in 24 to 1400 hours.

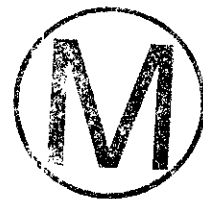
Brine permeabilities determined at the end of the compaction stage while still under an axial stress of 2000 psi, varied with materials and were quite variable between different samples of the same materials. Most of the waste materials had permeabilities of the order of 10 to 100 millidarcies. Granular magnetite and limonite had permeabilities of the order of 100 to 1000 millidarcies, while the values for crushed salt and metals varied from less than 100 to over 1000 millidarcies. It should be noted that the various granular materials had large grain sizes to intentionally represent worst case scenarios with respect to permeability.

REFERENCES

Butcher, B. M., 1989 "Waste Isolation Pilot Plant Simulated Waste Compositions and Mechanical Properties," Sandia National Laboratories, SAND89-0372.

Butcher, B. M., Thompson, T. W., van Buskirk, R. and N. C. Patti (in preparation) "Mechanical Compaction of WIPP Simulated Waste," Sandia National Laboratories.

Thompson, T. W., von Buskirk, R. and N. C. Patti, 1989. " ~ Material Compaction and Drum Collapse Test Results," Report by Science Applications International Corporation for Sandia National Laboratories."



Mercer, J.W., and Orr, B.R. 1979. Interim Data Report on Geohydrology of the Proposed Waste Isolation Pilot Plant Site, Southeast New Mexico. Water Resources Investigations 79-98. U.S. Geological Survey, Albuquerque, NM.

ABSTRACT, p. 1;

" Data were collected during hydrologic investigations at the Waste Isolation Pilot Plant site in southeast New Mexico through September 1977. These data will be considered as part of a site characterization study evaluating the feasibility of nuclear-waste storage within bedded salt of the Salado Formation of Permian age.

Liquids in the rocks overlying the Salado Formation are found at the contact between the Permian-Rustler and Salado Formations, and in the Culebra and Magenta Dolomite Members of the Rustler Formation.

Calculations of hydraulic gradient and direction of flow of water moving along the Rustler-Salado contact have been hindered because heads are stabilizing very slowly. Preliminary calculations of transmissivity range from  $10^{-1}$  feet squared per day on the western margin of the site to  $10^{-4}$  feet squared per day on the eastern margin. Liquids from the Rustler-Salado contact contain from 311,000 to 325,800 milligrams per liter total dissolved solids. Liquid chemistry suggests long residence times and extensive liquid-rock interaction, increasing with decreasing permeability.

Liquids in the Culebra Dolomite Member move southeast at gradients ranging from 7 to 120 feet per mile. Preliminary transmissivity calculations range from 140 feet squared per day on the western margin to  $10^{-4}$  feet squared per day to the east. Total dissolved solids range from 23,721 milligrams per liter along the western margin of the site to 118,292 milligrams per liter to the east. Liquid chemistry within the Culebra varies from well to well probably as a function of fracture distribution.

Liquids in the Magenta Dolomite Member move southwest at a gradient of about 50 feet per mile. Preliminary transmissivity estimates range from less than 1 foot squared per day to 40 feet squared per day. Total dissolved solids range from 10,347 milligrams per liter to 29,683 milligrams per liter.

The extremely low vertical hydraulic conductivity within the Rustler Formation restricts liquid migration between the Magenta and Culebra Dolomite Members, and between the Culebra and the Rustler-Salado contact. Heads are highest in the Magenta and lowest at the Rustler-Salado contact.

Liquid levels in wells tapping the Permian Bell Canyon Formation near the site are lower than levels in wells tapping the Rustler Formation. Liquids from the Bell Canyon Formation contain 189,000 milligrams per liter total dissolved solids. Liquid density and chemistry indicate long residence times and extensive liquid-rock interaction."



Shallow-zone hydrology, p. 173, para. 2;

" Hydrologic tests of liquid-bearing zones in the Rustler Formation indicate that heads decrease with depth; consequently, potential liquid movement would be downward in rocks above the salt. The degree to which ground water can move toward the Salado, however, is

controlled by the very low vertical hydraulic conductivity of the Rustler.

Minor solution of salt has occurred along the western margin of the site at the top of the Salado Formation. Solution of salt in the Rustler ranges from complete removal in the west to little or no removal in the east.

High concentrations of dissolved solids, particularly sodium chloride, occur in liquids above the salt, and chemical composition of these liquids is dependent upon extensive interaction with the evaporite host rocks resulting from long residence times.

Rustler-Salado contact.--Brines are found along the Rustler-Salado contact, but extremely low yields require long-term testing to establish reliable heads. Preliminary values of transmissivity of the Rustler-Salado contact range from  $10^{-1}$ ft<sup>2</sup>/day in P-14 to  $10^{-4}$ ft<sup>2</sup>/day in P-18. Water from the Rustler-Salado contact contains from 31,000 mg/L to 327,000 mg/L dissolved solids. Sodium Chloride ranges from 266,000 mg/L to 300,000 mg/L.

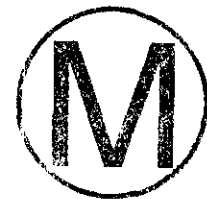
Culebra Dolomite Member of the Rustler Formation.--Head distribution determined for the Culebra Dolomite Member indicates liquid movement to the southeast beneath the site. Gradients range from 7 to 120 ft/mi and vary as a function of hydraulic conductivity.

Salt dissolution in the Rustler and Salado Formations, with accompanying subsidence of the Rustler, causes an increase in fracture porosity of the Culebra and contributes to variabilities in transmissivities.

Preliminary values of transmissivity for the Culebra range from 140 ft<sup>2</sup>/day in P-14 on the flanks of Nash Draw, to  $10^{-1}$ ft<sup>2</sup>/day in H-1 near the site center, to  $10^{-4}$  ft<sup>2</sup>/day in P-18 to the east. Culebra liquids range from 8,890 mg/L to 118,000 mg/L dissolved solids. Sodium chloride ranges from 4,900 mg/L to 89,200 mg/L.

Magenta Dolomite Member of the Rustler Formation.--Head distribution within the Magenta Dolomite Member has only been determined in three holes (H-1, H-2a, and H-3) and suggests fluid movement to the southwest. The hydraulic gradient in the vicinity of these three holes is 50 ft/mi.

Preliminary values of transmissivity for the Magenta range from 2 ft<sup>2</sup>/day in H-3 to less than 1 ft<sup>2</sup>/day in H-1. Magenta liquids range from 10,300 mg/L to 29,700 mg/L dissolved solids. Sodium chloride ranges from 6,800 mg/L to 24,300 mg/L."



Miller, W.M., and Chapman, N.A., Ed., 1992. Identification of Relevant Processes, System Concept Group Report, UKDOE/HMIP Report TR-ZI-11, London, England.

Summary; p. iii, para. 1;

" The System Concept Group (SCG) consisted of a group of eight experts in various aspects of deep disposal of radioactive wastes and was conceived as a means of providing a preliminary but comprehensive overview of processes and factors which could be important in the post-closure safety assessment of the proposed repository at Sellafield. Part of the Dry Run 3 exercise involved the elicitation of a list of processes relevant to the Harwell site considered in Dry Run 3. For the current assessment it was considered appropriate to use the Dry Run 3 Process List as the starting point for the SCG.

In general the Dry Run 3 Process List was found to be comprehensive and a few additional processes were added. A number of processes were removed or substituted where they were obviously specific to the Harwell site environment. In addition the list was restructured to take into account, (a) the necessary re-ordering of the biosphere component processes which were generally thought to be far too complex, given the inherent uncertainties in the earlier parts of the release chain (near and far-fields), and (b) to bring to prominence the following processes which the SCG felt were critical to the behaviour of a repository at the Sellafield site.

- Stability of the repository-The backfill used in the ILW vaults is seen as having no structural function. There will be no backfill in the LLW vaults and, possibly, no backfill above the ILW concrete cells. Vault roof stability, therefore, becomes an issue. Progressive collapse of the roof onto the degrading wastes and upwards migration of the collapse-damage rock is anticipated producing an extensive zone of increased porosity and permeability in the host rock.

- ILW near-field chemical environment-The long-term maintenance of low-flow, stable flux, highly alkaline, reducing conditions in the ILW vaults are central to the Nirex disposal concept and safety case. Consequently, this aspect requires close scrutiny to determine that chemical homogeneity will develop rapidly, persist and behave as predicted.



- Hydrology at repository depth-Groundwater fluxes at depth will require careful evaluation given the proximity of the repository to the Ravenglass sub-basin and other features. It must be determined whether the system can be evaluated exclusively in terms of steady-state topographically related head differences, or if other driving forces need to be taken into consideration.

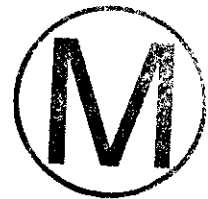
- Groundwater flow and radionuclide transport modeling-It is likely that models used to date to represent groundwater flow and radionuclide transport are based on overly simplistic assumptions and do not adequately characterize the

**Compliance Certification Application Reference Expansion**

---

system. Alternative concepts should be considered to model planar and fracture flow.

- Consequences of glaciation-It is likely that climatic cycling will continue for the whole period covered in the quantitative assessment and that significant climate changes will be apparent within 5,000 years from present. Evidence exists to suggest that there is potential for deep incision to occur as a consequence of glaciation and that the effect on deep groundwater flows may be significant."



NAGRA, 1985. Nuclear Waste Management in Switzerland: Feasibility Studies and Safety Analyses (Project Gewähr, 1985). NAGRA Project Report NGB 85-09 (English Summary), Wettingen, Switzerland.

SUMMARY; p. v, para. 1;

" The validity of the operational licences of the existing Swiss nuclear power plants (NPP) Beznau I and II, Mühlberg, GÖsgen and Leibstadt after 31st December 1985 is, because of official requirements, dependent on the demonstration of permanent, safe management and final disposal of radioactive waste. Accordingly, the NPP companies have been required to prepare a so-called "guarantee project" (Project Gewähr) and to present this to the Swiss Federal Government (Bundesrat) for review.

The appropriate investigations and research have been carried out by Nagra (National Cooperative for the Storage of Radioactive Waste). The 1985 Project Gewähr is described in an eight volume report NGB 85-01 to 85-08 and individual research projects are documented in separate NTB-series reference reports.

The main tasks of Project Gewähr 1985, as determined by official requirements, can be defined by three points:

- Sufficiently detailed projects based on present-day knowledge and technology must illustrate the technical feasibility of repository construction in Switzerland.
- By means of safety analyses it must be shown quantitatively that final disposal of all categories of radioactive waste is currently feasible without exposing the population to unreasonable radiation risks (demonstration of long-term safety).
- The data used in the safety analyses must be derived from appropriate investigations in Switzerland or abroad or must, in some other way, correspond to the present technical and scientific state of knowledge. The data include geological, hydrogeological and material-specific parameters and also a quantitative description of the behaviour of radionuclides in the geo-and biosphere as determined by their physical and chemical properties."

p. 4-13;

" Table 4-1 gives a list of processes and events for a type C repository location in the geological formations of northern Switzerland which can potentially have an effect on the repository system."



OECD Nuclear Energy Agency. 1992. Systematic Approaches to Scenario Development. Organisation for Economic Co-Operation and Development, Paris, France. NWM Library, NNA.920610.0027.

ABSTRACT, p. 4;

" This report describes and discusses the current approaches to the identification and selection of scenarios for the safety assessment of radioactive waste disposal systems. The scenario development process blends information on site and waste characteristics, and the understanding of various processes at work within the disposal system, with the judgement of appropriately experienced scientists and others. In this process, it is important to follow systematic procedures and to carefully document each step so that it is amenable to scrutiny. There is wide agreement on the general approach that should be taken for the identification, classification, and screening of phenomena that need to be considered. Several approaches have been identified to meet the challenge of combining these phenomena into scenarios, and consideration has been given to their range of applicability. Although several different approaches can be applied to form scenarios, experience to date indicates that the scenarios selected for detailed assessment will be very similar.

The approach adopted in a particular case will be determined by a range of factors, including the purpose of the assessment, regulatory requirements, available resources, experience, and confidence in the methods used. Scenario development is an interactive and iterative process within the overall safety assessment procedure. Different approaches to scenario development may be used at different stages of a safety assessment programme depending on the level of information and resources available and the immediate goal, e.g., direction of site investigation, determining research priorities. However, for safety assessments in support of licensing applications, a consistent and systematic scenario development procedure must be followed, which should fulfill the need to be both transparent and to provide a high level of confidence that all important safety aspects of the disposal system will be covered by the assessment."



Popielak, R.S., Beauheim, R.L., Black, S.R., Coons, W.E., Ellingson, C.T., and Olsen, R.L. 1983. Brine Reservoirs in the Castile Formation Waste Isolation Pilot Plant (WIPP) Project, Southeastern New Mexico. TME-3153, Vols. 1 and 2. Westinghouse Electric Corp., Carlsbad, NM.

EXECUTIVE SUMMARY, p 1;

" The Waste Isolation Pilot Plant (WIPP) project is a U. S. Department of Energy (DOE) research and development facility to demonstrate the safe disposal of radioactive wastes resulting from the defense activities and programs of the United States. This demonstration consists of two parts. First, about six million cubic feet of TRU waste will be emplaced in the thick bedded-salt deposits of the Salado Formation in southeastern New Mexico at a depth of about 2150 feet. Second, the WIPP will provide for research relative to the interactions of defense high-level waste with bedded salt, though all high-level waste will be removed prior to facility decommissioning.

A potential location was selected for the WIPP in the northern Delaware Basin of New Mexico, and three exploratory core holes were drilled (AEC-7, AEC-8, and ERDA-6; Figure 1). While drilling the third such hole (ERDA-6), substantial geologic structural deformation was noted, and brine and gas sufficiently pressurized to flow to the surface were encountered. The unpredictability of the geology led to relocation of the site to its present location in 1974 (Figure 1). Since relocation, an extensive site characterization program has been conducted, and the adequacy of the site has generally been demonstrated.

In 1981, an agreement was signed between the State of New Mexico, the DOE, and others which included several studies intended to address the State's concerns relative to the suitability of the proposed WIPP site. Some of these studies addressed an area of geologic interest north of the proposed site, and pressurized brine reservoirs in the Delaware Basin. The work was begun in October 1981 and included the reopening and testing of ERDA-6, and the deepening and testing of WIPP-12, an exploration borehole which also encountered pressurized brine and gas. This report provides an account of these studies.

These studies and preparation of the brine reservoir report were performed by the WIPP Technical Support Contractor (TSC), primarily by D'Appolonia Consulting Engineers, Inc. (a member of the WIPP-TSC) under subcontract to the Westinghouse Electric Corporation (the TSC prime contractor). Sandia National Laboratories, Albuquerque, N.M., provided critical review of the studies and report; the U. S. Geological Survey also made comments.

The occurrence of pressurized brine reservoirs in the Castile Formation (underlying the Salado Formation) of the Delaware Basin has been documented over the past 40 years by reports of reservoir encounters by hydrocarbon exploration drilling. In general, these reservoirs were known to be contained in fractured anhydrite with associated hydrogen sulfide gas and were thought to be related to antiforms in the Castile.

Various theories were advanced to explain the origin of reservoirs, which include dissolution of evaporites by recent ground waters, dehydration of gypsum to form anhydrite, entrapment of ancient seawater during evaporite deposition, and ancient dissolution and





reprecipitation of evaporite minerals. Should certain of these theories be correct, the suitability of the WIPP site could be in question. Thus, the purpose of this study was to determine the characteristics and origin of these reservoirs and evaluate their potential impact on the integrity and stability of the WIPP site.

Data used in the performance of this study were obtained from drilling and hydrological testing in boreholes ERDA-6" and WIPP-12 and from chemical analyses of samples of reservoir brine and gas collected at these two wells. Information was also obtained from a review of published and unpublished literature on the geology and hydrology of the basin. The principle data reviewed and analyzed in this report are contained in "Data File report - ERDA-6 and WIPP-12 Testing" (D'Appolonia, 1982, 1983)."

SUMMARY OF FINDINGS, p2, col 2, para 2;

" The analyses and interpretations by three disciplines -- geology, hydrology, and chemistry -- have been integrated to form a model of brine reservoir genesis, and to assess the current and future status of brine reservoirs as they relate to the WIPP site. The development of the brine reservoirs began in the Permian Period about 235 million years before present. The Castile evaporites, consisting primarily of anhydrite and halite as shown in Figure 2, were deposited at that time. During the initial chemical sedimentation (or precipitation) period, the solids were poorly consolidated and highly porous. Much or all of this pore space was filled with Permian seawater that had been enriched in dissolved solids, oxygen-18, and probably deuterium by evaporation. As sedimentation in the basin continued, the seawater became trapped as an interstitial fluid between individual grains of anhydrite and halite. As compaction increased, grain boundary accretion of halite probably surrounded some of the pore fluids and gave rise to fluid inclusions in halite crystals. Examination of ratios of major and minor element concentrations in the brines leads to the conclusion that the reservoir brines originated from ancient seawater with no evidence for fluid contribution from present meteoric waters."

p. 4, col. 2, para. 2;

" The ERDA-6 and WIPP-12 brine reservoirs, which are located in fractured anhydrites above thickened halite (Figure 2), may be modeled as fractured heterogeneous systems. The volumes of the ERDA-6 and WIPP-12 brine reservoirs are estimated, within an order of magnitude, to be about 630,000 barrels and 17,000,000 barrels, respectively. The vast majority of brine is stored in low-permeability microfractures, and therefore is not readily released in the event the reservoirs are intercepted. In fact, less than three percent of the reservoir fluids would flow unassisted to the surface if encountered during exploration drilling. About five percent of the overall brine volume in each reservoir is stored in large, open fractures.

SUMMARY OF FINDINGS, p 5, col 1, para 2;

" At present, the Castile brine reservoirs appear to be isolated. There is no evidence to suggest hydraulic or chemical connection between reservoirs, or between reservoirs and other

ground-water systems, either at the present or in the past. The persistence of high and different hydraulic heads in Castile brine reservoirs for at least one million years (the age of the most recent tectonic activity) is the principle hydrologic evidence for their isolation. The four Castile brine reservoirs for which accurate data are available show differences in hydraulic head ranging from 280 to 871 feet of water. Similarly, measured heads in the brine reservoirs are at least 1330 feet higher than heads in aquifers in the subjacent Delaware Mountain Group, and at least 1530 feet higher than heads in the overlying Rustler Formation (Figure 4). Hence, there is no physical mechanism for the brine reservoirs to receive recharge from these underlying and overlying units."

p 5, col 1, para 3;

" As regards chemical mechanisms, the gas and brine chemistries of the two reservoirs are distinctly different from each other and from local ground waters. For example, large differences in the reservoir gas compositions exist between WIPP-12 and ERDA-6. The gas in WIPP-12 is composed mostly of methane and has little or no carbon dioxide. The ERDA-6 reservoir contains substantial quantities of carbon dioxide, and more hydrogen sulfide than WIPP-12. Differences observed in the brine composition include boron, bromide, magnesium, potassium, and lithium concentrations. Connection between reservoirs would eliminate or mitigate these differences, especially with respect to the highly mobile gases. Accordingly, if connected in the past, the current brine (and associated gas) compositions of the two reservoirs would be more similar.

In addition to being isolated, the brines appear to be in chemical equilibrium with their surroundings, and they are stagnant. For example, the brines are chemically saturated with the primary phases of the reservoir host rock (anhydrite and calcite). WIPP-12 brine also appears to be saturated with halite, the principle phase of the confining strata. Furthermore, calculations indicate bulk system equilibrium among solid, liquid, and gas.

In summary, the brine reservoirs appear to be local, isolated features that have reached equilibrium with their environment. Evidence for long-term hydraulic and chemical isolation includes:

- Hydraulic heads that are substantially different from reservoir to reservoir and higher than the heads of local ground waters.
- The containment of gas by the reservoirs.
- Brine and associated gas chemistries that differ from reservoir to reservoir.
- Geographic separation and non-uniform distribution of reservoirs, i.e., extensive drilling has taken place in this area, but only a few wells have intercepted pressurized brines. There is no evidence for a continuous, extensive aquifer in the Castile.
- Bulk chemical equilibrium between the brine, gas, and reservoir rock in the ERDA-6 and WIPP-12 reservoirs."



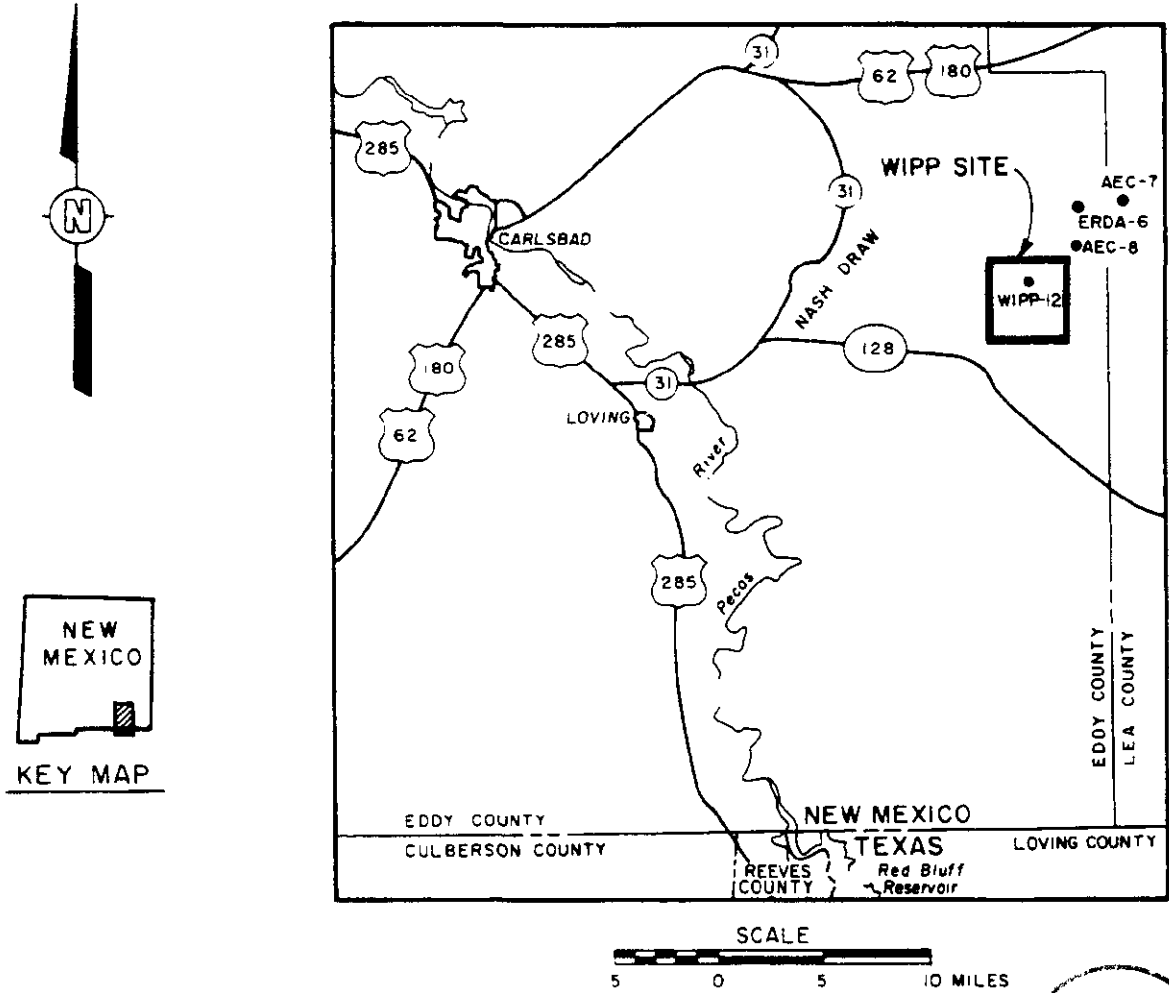


Figure 1 — Location of WIPP Site and Boreholes AEC-7, AEC-8, WIPP-12 and ERDA-6

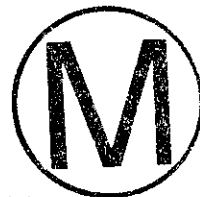


1.0 INTRODUCTION AND SUMMARY, p. G-1, para. 3;

" At WIPP-12 the Castile Formation is comprised of five members (in ascending order): Anhydrite I, Halite I, Anhydrite II, Halite II, and Anhydrite III. Halite I is somewhat thicker than the typical section in the basin. The anhydrite rock is microcrystalline and dense, with thin bedding laminae made up of carbonates, organic material, and clays. Fractures are present in Anhydrite III, Anhydrite II, and an anhydrite stringer within Halite II, which dip between 70° and vertical. The fracture at 3016 feet depth produced brine. No fractures were detected in the halite members. At ERDA-6, the Anhydrite III member is apparently missing, based on previous geologic interpretation (Jones, 1981a). High-angle fractures are located in Anhydrite II which contain pressurized brine. Information on other brine occurrences was analyzed and compared with WIPP-12 and ERDA-6 data to determine any basic patterns. Brine occurrences are associated with a belt of deformation in the Castile that parallels the Capitan reef subcrop and underlies the WIPP site. The brines appear to be located in the uppermost Castile anhydrite unit present at each location. At WIPP-12, Anhydrite III produced brine; at ERDA-6 the brine is thought to be located in Anhydrite II. Brine occurrences are associated in every known case with anticlinal structures of varying size within the belt of deformation."

p. G-33, para. 5;

" The acoustic log, which measures compressional wave travel time through the rock, uses a correlation between the wave velocity and elastic rock properties to estimate the bulk modules of the rock (Dresser Atlas, 1981b). The computed values of bulk modules range from 8 to 11 x 10<sup>6</sup> psi. Laboratory compression tests on anhydrite from other WIPP locations indicate similar results (Teufel, 1981; Pfieffe and Senseny, 1981). This value is representative of the bulk modules of relatively intact, unfractured rock, because the laboratory tests are performed on unbroken rock and the acoustic logging tool measures velocities over a relatively short distance with few if any fractures included."



p. H-45, Reservoir Pressure;

" The maximum pressure measured for the Erda-6 brine reservoir at the wellhead is 604 psig. Extrapolated to a reservoir depth of 2711 feet below ground surface with a fluid pressure gradient of 0.5326 psi/ft of brine, this corresponds to a reservoir pressure of 2048 psig. As shown in Figure H-12, this pressure corresponds to a potentiometric surface at 5551 feet above mean sea level when calculated for the specific gravity of pure water. This is the highest hydraulic head of any ground-water body known in the Delaware Basin.

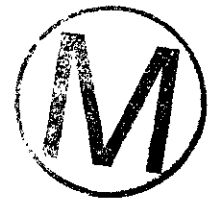
Following the end of testing in November 1981 and a BOP change in February 1982, the wellhead shut-in pressure at ERDA-6 rose steadily as a result of both reservoir recovery and gas cap formation in the wellbore. A series of apparent gauge-related malfunctions have left the pressure data collected before and after the gas cap release on March 8, 1983 of uncertain validity. The highest pressure measured before the gas cap release was 558 psig on March 5, 1983. Because of a possible fluid leak from a diaphragm assembly attached to the gauge, this value may be too low. The first fully reliable pressure measurement made

after the gas cap release was 552 psig on March 19, 1983."

p. H-52, Reservoir Pressure;

" The maximum pressure for the WIPP-12 reservoir at the wellhead is 208 psig. Extrapolated to a reservoir depth of 3017 feet below ground surface with a fluid pressure gradient of 0.5378 psi/ft of brine, this corresponds to a reservoir pressure of 1831 psig. As shown in Figure H-12, this corresponds to a potentiometric surface at 4680 feet above mean sea level calculated for the specific gravity of pure water. Section 3.4.1 contains a detailed discussion of hydraulic heads throughout the Delaware Basin.

Following the end of testing in June 1982, the wellhead shut-in pressure at WIPP-12 rose steadily as a result of both reservoir recovery and gas cap formation in the wellbore. Just prior to releasing the gas cap on March 7, 1983, the wellhead pressure was about 175 psig. On March 7, 1983, approximately 173 ft<sup>3</sup> of gas (at STP) were released from the well (D'Appolonia, 1983). Under the pressure (175.2 psig) and temperature (58°F) conditions then existing in the wellbore, this gas would have occupied a volume of about 14 ft<sup>3</sup>, corresponding to maximum gas cap thickness of about 33 feet. Some minor fraction of the gas released probably came from gas exsolution from the brine during the release, however, and is not representative of gas cap volume in the wellbore. From March 8 through at least March 20, 1983, the wellhead pressure at WIPP-12 remained steady at about 162 psig. After more than nine months of recovery, the WIPP-12 reservoir should be near equilibrium. Future increases in wellhead pressure will be predominantly the result of renewed gas cap formation."



Sandia National Laboratories. 1991. Preliminary Comparison with 40 CFR Part 191, Subpart B for the Waste Isolation Pilot Plant, December 1991. Volume 1: Methodology and Results. SAND91-0893/1. Sandia National Laboratories, WIPP Performance Assessment Division, Albuquerque, NM. wpo 26404.

ABSTRACT, p i;

" Before disposing of transuranic wastes at the Waste Isolation Pilot Plant (WIPP), the United States Department of Energy must have a reasonable expectation that the WIPP will comply with the quantitative requirements of Subpart B of the United States Environmental Protection Agency's (EPA) Standard, *Environmental Radiation Protection Standards for Management and Disposal of Spent Nuclear Fuel, High-Level and Transuranic Radioactive Wastes*. Sandia National Laboratories, through iterative performance assessments of the WIPP disposal system, is conducting an evaluation of the long-term performance of the WIPP that includes analyses for the Containment Requirements and the Individual Protection Requirements of Subpart B of the Standard. Recognizing that unequivocal proof of compliance with the Standard is not possible because of the substantial uncertainties in predicting future human actions or natural events, the EPA expects compliance to be determined on the basis of specified quantitative analyses and informed, qualitative judgment. Performance assessments of the WIPP will provide as detailed and thorough a basis as practical for the quantitative aspects of that decision.

The 1991 preliminary performance assessment is a snapshot of a system that will continue to evolve until a final compliance evaluation can be made. Results of the 1991 iteration of performance assessment are preliminary and are not suitable for final compliance evaluations because portions of the modeling system and data base are incomplete, conceptual model uncertainties are not fully included, final scenario probabilities remain to be determined, and the level of confidence in the results remains to be established. In addition, the final version of the EPA Standard, parts of which were remanded to the EPA in 1987 for further consideration, has not been promulgated. Results of the 1991 preliminary performance assessment do not indicate potential violations of Subpart B of the Standard and support the conclusion based on previous analyses, including the 1990 preliminary performance assessment, that reasonable confidence exists that compliance with Subpart B of the Standard can be achieved."

Volume 1, Section 3. PERFORMANCE-ASSESSMENT OVERVIEW, p 3-1;

" The design and implementation of a performance assessment is greatly facilitated by a clear conceptual model for the performance assessment itself. The purpose of this chapter is to present such a model and then to indicate how the individual parts of the WIPP performance assessment fit into this model. The WIPP performance assessment is, in effect, a risk assessment, for nuclear power plants and other complex systems is also appropriate for the WIPP performance assessment."

Volume 1, Section 3.1.3 CHARACTERIZATION OF UNCERTAINTY IN RISK, p 3-8;



" If the inputs to a performance assessment as represented by the vector  $\mathbf{x}$  in Equation 3-3 are uncertain, then so are the results of the assessment. Characterization of the uncertainty in the results of a performance assessment requires characterization of the uncertainty in  $\mathbf{x}$ . Once the uncertainty in  $\mathbf{x}$  has been characterized, then Monte Carlo techniques can be used to characterize the uncertainty in the risk results.

The outcome of characterizing the uncertainty in  $\mathbf{x}$  is a sequence of probability distributions

$$D_1, D_2, \dots, D_{nV}, \tag{3-5}$$

where  $D_j$  is the distribution developed for the variable  $x_j$ ,  $j=1,2 \dots,nV$ , contained in  $\mathbf{x}$ . The definition of these distributions may also be accompanied by the specification of correlations and various restrictions that further define the possible relations among the  $x_j$ . These distributions and other restrictions probabilistically characterize where the appropriate input to use in the performance assessment might fall, given that the analysis is structured so that only one value can be used for each variable under consideration. In most cases, each  $D_j$  will be a subjective distribution that is developed from available information through a suitable review process and serves to assemble information from many sources into a form appropriate for use in an integrated analysis. However, it is possible that the  $D_j$  may be obtained by classical statistical techniques for some variables.

Once the distributions in Equation 3-5 have been developed, Monte Carlo techniques can be used to determine the uncertainty in  $R(\mathbf{x})$  from the uncertainty in  $\mathbf{x}$ . First, a sample

$$\mathbf{x}_k = [x_{k1}, x_{k2}, \dots, x_{knV}], k=1, \dots, nK \tag{3-6}$$



is generated according to the specified distributions and restrictions, where  $nK$  is the size of the sample. Performance-assessment calculations are then performed for each sample element  $\mathbf{x}_k$ , which yields a sequence of risk results of the form

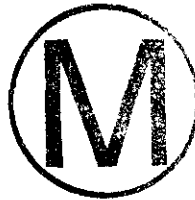
$$R(\mathbf{x}_k) = \{(S_i(\mathbf{x}_k), cS_i(\mathbf{x}_k), i=1, \dots, nS(\mathbf{x}_k)\}, \tag{3-7}$$

for  $k=1, \dots, nK$ . Each set  $R(\mathbf{x}_k)$  is the result of one complete performance assessment performed with a set of inputs (i.e.,  $\mathbf{x}_k$ ) that the review process producing the distributions in Equation 3-5 concluded was possible. Further, associated with each risk result  $R(\mathbf{x}_k)$  in Equation 3-7 is a probability or weight<sup>1</sup> that can be used in making probabilistic statements about the distribution of  $R(\mathbf{x})$ .

In most performance assessments, CCDFs are the results of greatest interest. For a particular consequence result, a CCDF will be produced for each set  $R(\mathbf{x}_k)$  of results shown

in Equation 3-5. This yields a distribution of CCDFs of the form shown in Figure 3-4.

Although Figure 3-4 provides a complete summary of the distribution of CCDFs obtained for a particular consequence result by propagating the sample shown in Figure 3-6 through a performance assessment, the figure is hard to read. A less crowded summary can be obtained by plotting the mean value and selected percentile values of the exceedance probabilities shown on the ordinate for each consequence value on the abscissa. For example, the mean plus the 5th, 50th (i.e., median), and 95th percentile values might be used. The mean and percentile values can be obtained from the exceedance probabilities associated with the individual consequence values and the weight or 'probabilities' associated with the individual sample elements.<sup>1</sup> The determination of the mean and percentile values for  $cS = 1$  is illustrated in Figure 3-5. If the mean and percentile values associated with individual consequence values are connected, a summary plot of the form shown in Figure 3-6 is obtained. Due to their construction, the percentile bounds for the distribution of  $R(x)$ , which is a distribution of functions. However, the mean curve is an estimate for the expected value of this distribution of functions. . . ."



Volume 1, Section 3.2 Definition of Scenarios, p 3-32;

" As indicated in Equation 3-1, the outcome of a performance assessment for WIPP can be represented by a set of ordered triples. The first element of each triple, denoted  $S_i$ , is a set of similar occurrences or, equivalently, a scenario. As a result, an important part of the WIPP performance assessment is the development of scenarios.

Volume 1, p 4-64, line 15 thru p 4-66, line 34

" Radionuclide migration depends on the degree of saturation within the repository. Gas pressure resulting from microbial activity and corrosion may prevent brine inflow and desaturate the nearby Solado Formation, MB139, and anhydrite layers A and B. These conditions, in addition to the consumption of water by anoxic corrosion and possibly microbial activity, also would result in a decrease in the amount of water in the waste and backfill and a lower potential for radionuclide transport.

Two pathways for groundwater flow and radionuclide transport dominate the disposal system (Figure 4-6). In the first path, brine and radionuclides enter MB139, either through fractures in salt or directly as a result of rooms and drifts intersecting the marker bed during construction or room closure. Following repository decommissioning, waste-generated gas will begin to pressurize the waste panels (Weatherby et. al., 1989). Brine will drain by gravity to the lower half of the panels. Gas will saturate the DRZ above the panel and open flow paths to anhydrite layers A and B above the panel. MB139 beneath the panel will remain brine saturated, but gas will open flow paths into the MB139 beyond the panels. The more-mobile gas phase will flow outward over the less-mobile brine phase. After gas generation ceases, pressure and phase distribution will gradually equilibrate throughout the entire region. Gas will continue to expand outward, but brine flow reverses, flowing inward primarily along the lower portions of anhydrite layers A and B and MB139. Gas saturation near the waste panels will diminish. The anhydrite layers above the waste panels will be a

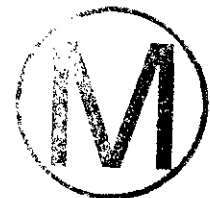
major flow path for gas. In contrast, brine will inhibit gas inflow in the MB139 beneath the waste panels.

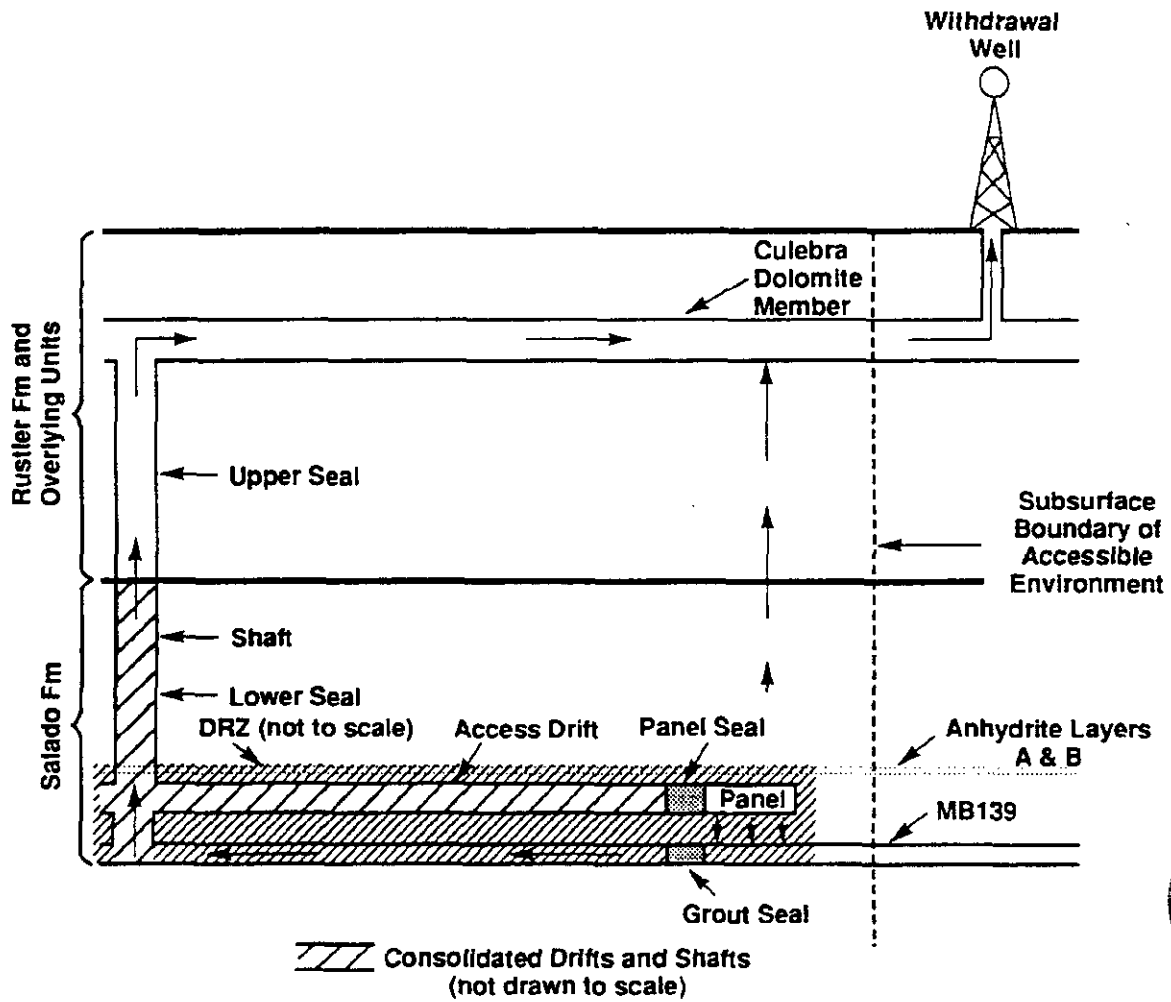
Because material in the upper shaft is expected to be poorly consolidated, the hydraulic pressure at the junction of the upper and lower parts of the shaft seals is assumed to approximate the pressure head of the Culebra Dolomite member. As a result, the pressure gradient resulting from waste-generated gas (approximately 15 MPa+) and hydrostatic pressure at the Culebra (1 MPa) tends to force radionuclide-bearing brine from MB139 beneath the panel through the seal in the marker bed, along the fractures in MB139 to the base of the shaft. Concurrently, gas flows through the upper portion of the drifts and the anhydrite layers A and B to the shaft. Gas saturation in the shaft seals will inhibit brine migration up the shaft to the Culebra Dolomite Member. Brine and radionuclides will eventually reach the Culebra and Migrate downgradient to the accessible environment.

Relative motion during salt creep and gas generation prevents MB139 from returning to its original position, and the salt-creep-induced fractures do not completely close. Flow is through MB139 instead of through the overlaying access drift because of the substantially higher hydraulic conductivity in MB139. Flow in MB139 is to the north through the seal rather than to the south down the pre-excavation hydraulic gradient within MB139, because the pressure drop to the north is greater after excavation, and the flow to the south would be impeded by extremely low permeability of the intact marker bed. Therefore, the horizontal path directly through MB139 to the accessible environment is not included for this assessment, but this path is considered for other analyses (see Volume 2 of this report).

The other dominant path is assumed to be from the repository vertically through the intact Solado Formation toward the Culebra Dolomite Member (Figure 4-6) (Lappin et. al., 1989). This path has the largest pressure decline over the shortest distance of any path. In addition, large potential exists for radionuclides to leave the repository along this path because of the large horizontal cross-sectional area of the waste-bearing rooms and drifts in the repository.

The methodology can determine pathways to individuals and calculate doses to humans if a release pathway is added. The pathway used in an earlier analysis (Lappin et. al., 1989) is described in the next section. Because undisturbed performance releases no radionuclides in 1,000 years, these calculations are not necessary for this scenario (Marietta et. al., 1989)"





TRI-6342-200.5

Figure 4-6. Conceptual Model Used in Simulating Undisturbed Performance.

Volume 1, p 5-47, lines 3 through 5:

"5.2 The Engineered Barrier System

5.2.2 Repository and Seal Design . . .

Seals in the lower portion of the shafts must provide a long-term, low-permeability barrier that will prevent Salado Formation brine from migrating up the shaft."

Volume 2, Section 3. CONSTRUCTION OF COMPLEMENTARY CUMULATIVE DISTRIBUTION FUNCTIONS, p 3-1;

" Sandia National Laboratories is conducting an ongoing performance assessment for the Waste Isolation Pilot Plant (WIPP) in southeastern New Mexico (Bertram-Howery and Hunter, 1989; Lappin et. al., 1989). At present, a performance assessment is performed each year to summarize what is known about the WIPP and to provide guidance for future work (Marietta et. al., 1989; Bertram-Howery et. al., 1990). It is anticipated that these iterative performance assessments will continue until the WIPP is either licensed for the disposal of transuranic wastes or found to be unsuitable for such disposal.

The results of greatest interest obtained in these performance assessments is a complimentary cumulative distribution function (CCDF) that is used for comparison with the U. S. Environmental Protection Agency (EPA) release limits for radioactive waste disposal (U.S.EPA, 1985). As discussed in the preceding chapter (Chapter 2 of this volume), the EPA standard requires that the normalized releases to the accessible environment be expressed as a single CCDF and that this CCDF fall under certain specified bounds. At present, drilling intrusions are believed to be the most severe potential disruptions that need be considered at the WIPP (Guzowski, 1990 and 1991). Thus, the construction of this CCDF for the WIPP is based on summary scenarios that result from drilling intrusions.

This presentation will describe how a CCDF can be constructed for comparison against the EPA release limits when the disruptions to the waste disposal site under consideration result from drilling intrusions. For the results presented here, the drilling intrusions are assumed to follow a Poisson process (i.e., occur randomly in time and space)(Cox and Lewis, 1966; Haight, 1967; Cox and Isham, 1980) with a fixed rate constant. However, the described approach would work with any probability model for drilling intrusions.

With regard to the risk representation

$$\mathbb{R} = \{(S_i, pS_i, cS_i), i=1, \dots, nS\} \tag{3-1}$$



described in the preceding chapter and elsewhere (Kaplan and Garrick, 1981; Helton et. al., 1991).  $S_i$  is a set of similar time histories defined on the basis of drilling intrusions,  $pS_i$  is the probability for  $S_i$ , and  $cS_i$  contains the EPA normalized release for  $S_i$ . The  $S_i$  appearing in (3-1) are obtained by discretizing a suitable sample space. For comparisons with the EPA release limits, this sample space is

$S = \{x: x \text{ a single 10,000-year time history beginning at decommissioning of the facility under consideration}\}$ . (3-2)

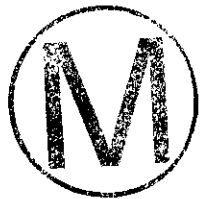
In what follows, an approach will be described for defining the  $S_i$ , assigning probabilities  $pS_i$ , and consequences  $cS_i$ , to these  $S_i$ , and then constructing the resultant CCDF."

Volume 2, Section 5.2.3 SPATIAL AND TEMPORAL GRIDS, p 5-22;

" The geometry used in the two-phase disturbed conditions modeling is similar to that used in the undisturbed calculations. It represent as axisymmetric approximation to an equivalent panel. Cylindrical geometry was necessary for two reasons. First, the actual geometry of the WIPP repository is too complex for PA modeling; a mesh having all the detail of the repository, or even of a single panel, would be prohibitively large and would require more computation time than is available for a single year's PA calculation. Second, BRAGFLO is currently a two-dimensional model; cylindrical geometry allows the most important aspects of flow over a large areal extent to be simulated in only two dimensions. Specifically, the convergence of flow radially toward a point sink can be modeled more accurately in cylindrical geometry than in rectangular geometry. This is important because on a large scale the flow radial toward the intrusion borehole, which is located along the axis of symmetry. Even within a panel, because of the relatively high permeability of the waste, flow will be essentially radial, though constrained by the pillars to be more rectilinear. For flow into a panel from the far field, the most important features of a panel are its perimeter, both the length and the distance of the perimeter from the center where an intrusion well is assumed located, and the enclosed volume. How these parameters are averaged into a cylinder is somewhat arbitrary, and compromises are necessary.

In modeling a panel for PA purposes, the panel is treated as a cylinder having the same enclosed floor area as an actual panel, including the area occupied by the pillars. This results in a cylinder having a radius of 96.78 m. To account for the inclusion of pillars, which have a very low porosity, the porosity of the panel is adjusted from the final porosity of the waste alone. The initial brine saturation is also adjusted for the presence of pillars that are fully saturated with brine. These calculations are discussed in Section 3.4.8 of Volume 3.

The region modeled includes the cylindrical equivalent panel and the surrounding Salado formation with anhydrite layers above and below (see Figure 4-1). The borehole is coincident with the axis of symmetry. The region extends upward to the top of the Culebra, downward to the bottom of the Castile brine reservoir, and outward approximately 22.3 km. By including the Castile and Culebra, the major sources and sinks for brine flow to and from the repository are represented in a single model. The far-field boundary is intended to be far enough away to justify the use of a no-flow boundary, which is required in BRAGFLO, without the boundary effecting the behavior of the repository. While a further removed boundary might be desirable for greater accuracy with this model, the formations being modeled actually extend only about 10 km north of the repository (see Figure 1.5-2, Volume 3). Anhydrite layers a and b immediately above the repository have been consolidated into a



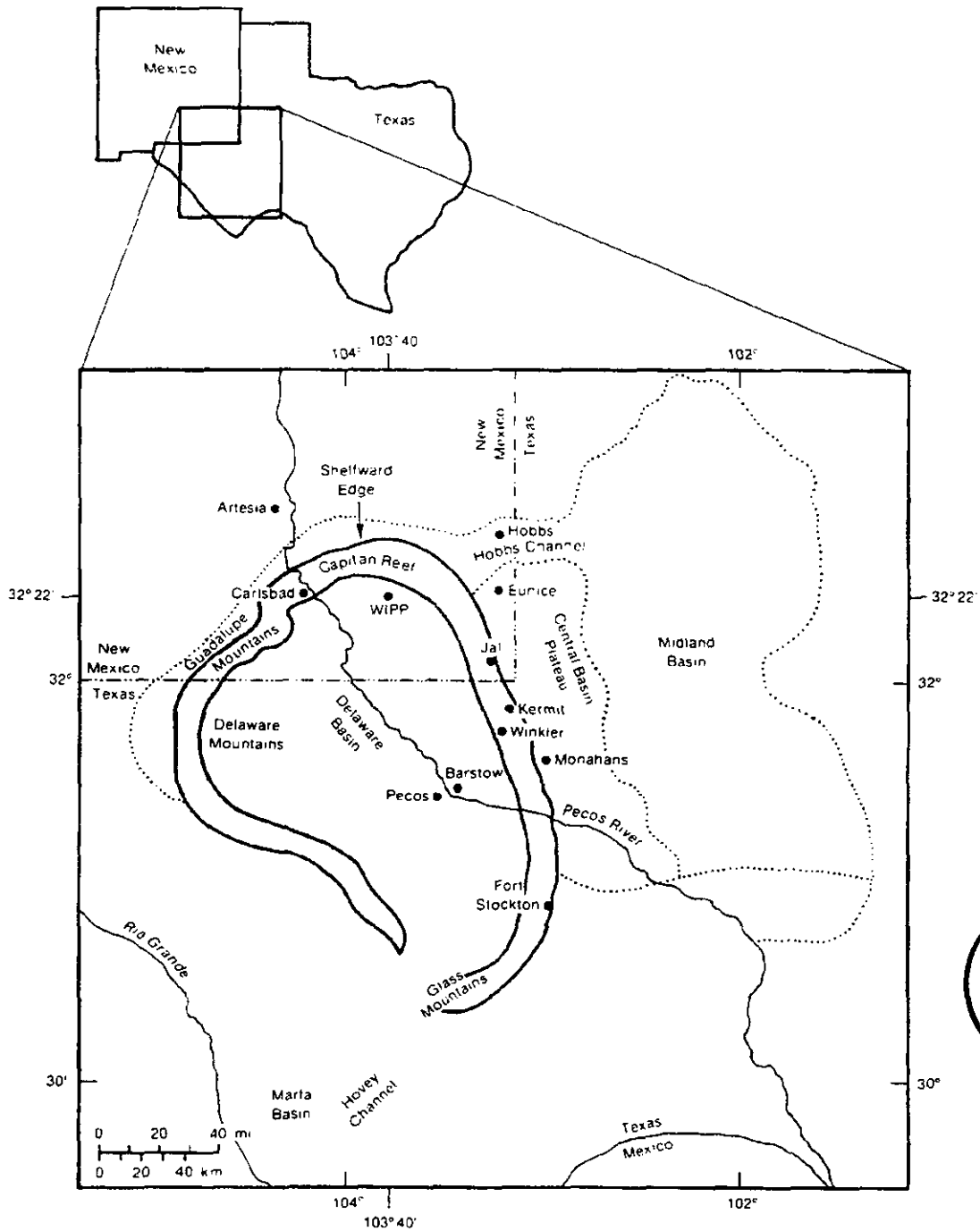
## Compliance Certification Application Reference Expansion

---

single layer with a thickness equal to the combined thicknesses of a and b and located at the elevation of layer b, the one closer to the repository. The panel thickness was varied, depending on the final porosity of the waste, which in turn depends on the composition of the waste and the total gas generation potential. The procedure for calculating the panel height and porosity, and the assumptions used, are described in Section 3.4.8 of Volume 3. The DRZ extends vertically upward through the anhydrite layer and downward through MB139. Beyond the outer radius of the panel, both the anhydrite layers and the Salado are intact. The center of the intrusion borehole is located at the axis of symmetry."



Compliance Certification Application Reference Expansion



TRI-6342-251-2

Figure 1.5-2. Location of the WIPP in the Delaware Basin (modified from Richey et al., 1985 and Lappin, 1988, Figure 1.4).



Volume 2, Section 6.2 Generation of Transmissivity Fields by Geostatistics, p 6-5;

" Previous WIPP Performance Assessments used a simple zonal approach for including uncertainty in the transmissivity ( $T$ ) field within the Culebra Dolomite Member of the Rustler Formation. The zonal method divides the regional and local computational domains into geographic regions; 8, 13, and 15 regions have been used for different analyses reported in Marietta et. al. (1989) and Bertram-Howery et. al. (1990). In each region, a distribution was constructed using transmissivity measurements from available wells. This empirical distribution was sampled and one constant value used for the transmissivity in each zone. Each zone was sampled independently, so a single simulation used 8 (or 13 or 15) transmissivity values to represent the regional  $T$  field. Some simulations used distributions constructed from pilot point values (LaVenue et. al., 1990) at locations assigned during calibration in addition to actual measurements at well locations.

This approach can be improved in two ways:

- The reason for varying transmissivity over geographic zones is to include spatial variability in the  $T$  field. Correlations exist in the  $T$  field over distances greater than five kilometers; however, assuming that the 8 (or 13 or 15) zones are independent during sampling is only a first approximation. Spatial dependence should be included over the whole model domain.
- The  $T$  fields generated by the simple zonal approach directly used transmissivity measurements whereas other information was included indirectly through pilot point values. Many other data are available, and it would be better to incorporate these data directly, e.g. hydraulic head measurements and geologic information.

Several methods have been proposed in the scientific literature to resolve these two issues. Most suggestions have relied on geostatistical techniques combined with inverse methods (de Marsily, 1986; Yeh, 1986). To obtain fast guidance on development of a package for WIPP PA to use in the final compliance assessment, a Geostatistical eXpert Group (GXG) was convened. The GXG was asked to provide advice given the modeling work completed, calibrated transmissivity field, data collected, and the above two objectives listed for improvement of the earlier zonal approach. The group's recommendations were organized into three categories:

- Proposing methods for generating conditional random fields to be used in the present assessment.
- Proposing methods for including conceptual model uncertainty.
- Proposing methods for including geological information.

These recommendations are summarized in the following discussion. . . ."

Volume 2, Section 6.4.2.2 Changing Climate Models, p 6-35;

" The climate model was planned to utilize the user-modifiable climate factor routines to input a modified sinusoidal variability of flux, including an LHS-sampled, uniformly distributed factor. This climatic variability was entered as a boundary recharge along 15 kilometers of the north and west regional boundaries. Difficulties arose from trying to apply

a single average flux value along the entire recharge boundary. The variability of sampled transmissivities changed this property by six orders of magnitude along this boundary, requiring a similar range of head values. This required us to look at other ways to incorporate climatic change in the model. For preliminary analysis a steady-state simulation with heads along the same recharge boundary set to the land surface elevation was used to represent the effects on climatic change.

Section 6.4.2.3 Climate Factors and Climatic Variability Calculations; p 6-35;

" For the 1991 preliminary comparison, climate variability was modeled by varying head along the recharge boundary. The amplitude of the climate function was bounded between present values and the land surface elevation, multiplied by a uniformly sampled value, *ClimtIdx*, ranging from zero to one. The user-modifiable climate function routine was utilized to model an equation with three peaks in ten thousand years (see Volume 3). This does not match the data base definition of five peaks in ten thousand years because it was written before the data base was defined. However, the integrated effect will be the same and the historical data show three minor climate peaks in the last ten thousand years. This model with its peaks occurring at exactly four thousand year intervals is not intended to predict the exact climatic change but only to model its effect."



Volume 2, Section 6.5.2 LOCAL TRANSPORT MODELING OF STAFF2D, p 6-47;

" The local transport modeling was performed with the STAFF2D finite element program. STAFF2D calculates either Darcy fluid flow or radionuclide transport. The flow fields used in the transport calculations were also calculated with STAFF2D as discussed above. Transport was calculated using the dual-porosity conceptual model. The flow and transport are assumed to take place in the fractures with a solute exchange between the fractures and matrix controlled by a one-dimensional diffusion equation. Single porosity fracture transport was calculated using a fracture field derived from the specific discharge by scaling the fracture porosity. Dual porosity transport used the fracture flow field but included diffusion into the matrix. Transport was also calculated using single-porosity fracture transport with no diffusion into the matrix."

Volume 3, Section 1.3.4 Elicitation of distributions from Experts, 1-20;

" This section discusses formal elicitation of probability distributions for model parameters that are uncertain and are considered significant in the performance assessment (e.g., estimate of radionuclide concentration in the disposal region [Trauth et. al., 1991]). Formal elicitation is also being used in the performance assessment of the WIPP to hypothesize about possible futures of society and the effects of appropriate markers to warn future societies about the WIPP; these elicitation efforts are discussed elsewhere (Hora et. al., 1991).

In all aspects of data gathering, professional judgement (i.e., opinion) must bridge the gaps in knowledge that invariably exist in scientific explanations. For example, the selection of methods to collect data (characterizing a site), interpretation of data, development of

conceptual models, and selection of model parameters all require professional judgement by the investigator. This volume summarizes these judgements.

When data are lacking, either because of the complexity of the processes or the time and resources it would take to collect data or when data have a major impact on the performance assessment, a formal elicitation of expert judgement is pursued. The procedure has the following advantages. First, formal elicitation offers a structured procedure for gathering opinion. Second, it encourages diversity in opinions and thus guards against understating the uncertainty. Finally, it promotes clear and thorough documentation of how the results were achieved (Hora and Iman, 1989).

The judgements that result from formal elicitation are a snapshot of the current state of knowledge. As new observations are made, the state of knowledge is refined. Even though the compilation of information through formal elicitation is often enlightening and helps to prevent bias, it does not create information. An important aspect of elicitation, which occurs either during or following the procedure, is to examine how new data collected may improve understanding."

Section 3.4.7 Permeability, p 3-130;

<b>Parameter:</b>	<b>Permeability (k), combustibles</b>	
<b>Median:</b>	1.7 x 10 <sup>-14</sup>	
<b>Range:</b>	2 x 10 <sup>-15</sup> 2 x 10 <sup>-13</sup>	
<b>Units:</b>	m <sup>2</sup>	
<b>Distribution:</b>	Cumulative	
<b>Source(s)</b>	Butcher, B. M., T. W. Thompson, R. G. Van Buskirk, and N. C. Patti. 1991. <i>Mechanical Compaction of WIPP Simulated Waste</i> . SAND90-1206. Albuquerque, NM: Sandia National Laboratories	
<b>Parameter:</b>	<b>Permeability (k), metals/glass</b>	
<b>Median:</b>	5 x 10 <sup>-13</sup>	
<b>Range:</b>	4 x 10 <sup>-14</sup> 1.2 x 10 <sup>-12</sup>	
<b>Units:</b>	m <sup>2</sup>	
<b>Distribution:</b>	Cumulative	
<b>Source(s)</b>	Butcher, B. M., T. W. Thompson, R. G. Van Buskirk, and N. C. Patti. 1991. <i>Mechanical Compaction of WIPP Simulated Waste</i> . SAND90-1206. Albuquerque, NM: Sandia National Laboratories	

<b>Parameter:</b>	<b>Permeability (k), sludge</b>
<b>Median:</b>	1.2 x 10 <sup>-16</sup>
<b>Range:</b>	1.1 x 10 <sup>-17</sup> 1.7 x 10 <sup>-16</sup>
<b>Units:</b>	m <sup>2</sup>
<b>Distribution:</b>	Cumulative
<b>Source(s)</b>	Butcher, B. M., T. W. Thompson, R. G. Van Buskirk, and N. C. Patti. 1991. <i>Mechanical Compaction of WIPP Simulated Waste</i> . SAND90-1206. Albuquerque, NM: Sandia National Laboratories

Mean Permeability of Drum, p 3-131, para 3;

" For computational ease, the PA Division assumed that the permeabilities of each component were uniformly distributed from the minimum to the maximum values given above in evaluating the permeability of an average drum. Consequently,, the distribution of local permeability (i.e., the effective permeability of a collapsed drum) was the weighted sum of uniform distributions, the weights being percent by volume of each component."



(Swift, P.N., 1991. Appendix A: Volume 3)

Introduction, p A-110;

" Ideally, it could be possible to describe variability in recharge within a single conceptual model for flow in the Culebra using a single parameter--future recharge as a function of present recharge. I recommend, however, separating recharge into two component functions: variability in mean annual precipitation and variability in the amount of precipitation that reaches our Culebra model domain as recharge. This distinction allows examining model sensitivity to climatic change independently of the uncertainty in the physical recharge process. The distinction is meaningful because we can assess climatic variability relatively confidently, whereas uncertainty about the recharge process is high. Sampling on separate parameters will permit us to perform sensitivity analyses (to be reported by Swift et. al., [in prep.], separately from the 1991 *Preliminary Comparison*) on both climate variability and the assumed recharge function.

This memo defines climate and recharge functions and the associated parameters to be sampled. The memo does not address conceptual model uncertainty about the location or amount of present recharge to the model domain, or about the location of the future recharge. These model uncertainties will be addressed in 1992 or later, as results become available from the geostatistics project addressing uncertainty in the Culebra flow model. The assumption is made here that future model recharge will be expressed as a function of nominal present flux into a calibrated steady-state flow model.

For the 1991 PA calculations, there appears to be little need to sample on a distribution of climate parameter values. As explained below, we can select 'best estimate' values for climate variability for the full-system simulations, and wait for the separate sensitivity analysis report to examine the impact of the assumptions. This does not mean that



the 1991 calculations will not include climate variability. Climate variability will be incorporated, and the results will reflect the knowledge that some future climates will be wetter than that of the present. The function and values I am recommending will give us an 'average' future precipitation roughly 1.3 times present, with peaks of just over 2 times present.

I do recommend sampling on the recharge function parameter. As defined here, this parameter is a simple multiplier that is applied to the nominal increase in precipitation, yielding the change in model recharge. The multiplier represents uncertainty in numerous parameters, including (i) the location and extent of the surface recharge area, (ii) groundwater flow between the surface recharge area and the boundary of the model domain, and (iii) the relationship between precipitation and infiltration in the surface recharge area, which in turn is dependent on factors such as vegetation, temperature, local topography, and soil characteristics. There is no particular reason to assume a 1-to-1 correlation between increases in precipitation and increases in model recharge, and limited evidence for water-table conditions in semi-arid climates suggests that increases in precipitation may result in substantially larger increases in infiltration. I recommend that we incorporate recharge uncertainty in the 1991 calculations by sampling a uniformly distributed recharge parameter (defined below) over a range that permits the relationship between mean annual precipitation and model recharge to vary between 1-to-1 and 10-to-1. This would mean that with precipitation at a maximum of 2x present, model recharge could range from 2x to 20x present. Both the range and the distribution are preliminary, and should be adjusted as new data or interpretations warrant."

Volume 4, ABSTRACT, p i;

" The most appropriate conceptual model for performance assessment at the Waste Isolation Pilot Plant (WIPP) is believed to include gas generation due to corrosion and microbial action in the repository and a dual-porosity (matrix and fracture porosity) representation for solute transport in the Culebra Dolomite Member of the Rustler Formation. Under these assumptions, complementary cumulative distribution functions (CCDFs) summarizing radionuclide releases to the accessible environment due to both cuttings removal and groundwater transport fall substantially below the release limits promulgated by the Environmental Protection Agency (EPA). This is the case even when the current estimates of the uncertainty in analysis inputs are incorporated into the performance assessment. The best-estimate performance-assessment results are dominated by cuttings removal. The releases to the accessible environment due to groundwater transport make very small contributions of CCDFs that must be considered in comparisons with the EPA release limits is dominated by the variable LAMBDA (rate constant in Poisson model for drilling intrusions). The variability in releases to the accessible environment due to individual drilling intrusions is dominated by DBDIAM (drill bit diameter). Most of the imprecisely known variables considered in the 1991 WIPP performance assessment relate to radionuclide releases to the accessible environment due to groundwater transport. For a single borehole (i.e., an E2-type scenario), whether or not a release from the repository to the Culebra even

occurs is controlled by the variable SALPERM (Salado permeability), with no releases for small values (i.e.,  $< 5 \times 10^{-21} \text{m}^2$ ) of this variable. When SALPERM is small, the repository never fills with brine and so there is no flow up an intruding borehole that can transport radionuclides to the Culebra. Further, releases that do reach the Culebra for larger values of SALPERM are small and usually do not reach the accessible environment. A potentially important scenario for the WIPP involves two or more boreholes through the same waste panel, of which at least one penetrates a pressurized brine pocket and at least one does not (i.e., an E1E2-type scenario). For these scenarios, the uncertainty in release to the Culebra is dominated by the variables BHPERM (borehole permeability), BPPRES (brine pocket pressure), and the solubilities for the individual elements (i.e., Am, Np, Pu, Th, U) in the projected radionuclide inventory for the WIPP. Once a release reaches the Culebra, the matrix distribution coefficients for the individual elements are important, with releases to the Culebra often failing to reach the accessible environment over the 10,000-yr period specified in the EPA regulations. To provide additional perspective, the following variants of the 1991 WIPP performance assessment have also been considered: (1) no gas generation in the repository and a dual-porosity transport model in the Culebra; (2) gas generation in the repository and a single-porosity (fracture porosity) transport model in the Culebra; (3) no gas generation in the repository and a single-porosity transport model in the Culebra; (4) gas generation in the repository and a dual-porosity transport model in the Culebra without chemical retardation; and (5) gas generation in the repository, a dual-porosity transport model in the Culebra, and extremes of climatic variation. All of these variations relate to groundwater transport and thus do not affect releases due to cuttings removal, which were found to dominate the results of the 1991 WIPP performance assessment. However, these variations do have the potential to increase the importance of releases due to groundwater transport relative to releases due to cuttings removal."

Volume 4, 2.1 Conceptual Model, p 2-3, para 4;

" Once the distributions in Eq. 2.1-4 have been developed, Monte Carlo techniques can be used to determine the uncertainty in  $R(x)$  that results from the uncertainty in  $x$ . First, a sample

$$x_k = [x_{k1}, x_{k2}, \dots, x_{k,nV}], k=1, \dots, nK, \quad (2.1-5)$$



is generated according to the specified distributions and restrictions, where  $nK$  is the size of the sample. The performance assessment is then performed for each sample element  $x_k$ , which yields a sequence of risk results of the form

$$R(x_k) = [S_i(x_k), pS_i(x_k), cS_i(x_k)], i=1, \dots, nS(x_k) \quad (2.1-6)$$

for  $k = 1, \dots, nK$ . Each set  $R(x_k)$  is the result of one complete performance assessment performed with a set of inputs (i.e.,  $x_k$ ) that the review process producing the distributions in Eq. 2.1-4 concluded was possible. Further, associated with each risk result  $R(x_k)$  in Eq. 2.1-6 is a probability or weight that can be used in making probabilistic statements about the distribution of  $R(x)$ . When random or Latin hypercube sampling is used, this weight is the reciprocal of the sample size (i.e.,  $1/nK$ )."

Volume 4, Section 3. UNCERTAIN VARIABLES, p 3-7, para 4;

" In addition to the variation between the cases shown in Table 3-2, the sampling-based approach to the treatment of subjective uncertainty also produces uncertainty and sensitivity results for the individual cases. In the following two chapters, box plots and distributions of CCDFs will be used to display the effect of subjective uncertainty on the cases listed in Table 3-2, and the impact of individual variables will be investigated with sensitivity analysis techniques based on scatterplots, regression analysis and partial correlation analysis. Scatterplots will also be used to compare results obtained with the different analysis cases listed in Table 3-2."



Sandia National Laboratories. 1992-1993. Preliminary Performance Assessment for the Waste Isolation Pilot Plant, December 1992. SAND92-0700, Vols. 1-5. Sandia National Laboratories, WIPP Performance Assessment Division, Albuquerque, NM. Vol. 1-WPO 20762, Vol. 2-WPO 20805, Vol. 3-WPO 23529, Vol. 4-WPO 20958, Vol. 5-WPO 20929.

Volume 1:

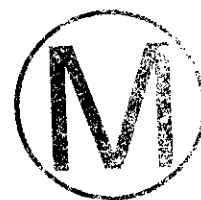
ABSTRACT, p i;

" Before disposing of transuranic wastes in the Waste Isolation Pilot Plant (WIPP), the United States Department of energy (DOE) must evaluate compliance with applicable long-term regulations of the United States Environmental Protection Agency (EPA). Sandia National Laboratories is conducting iterative performance assessments of the WIPP for the DOE to provide interim guidance while preparing for final compliance evaluations.

This volume contains an overview of WIPP performance assessment and a preliminary comparison with the long-term requirements of the *Environmental Radiation Protection Standards for Management and Disposal of Spent Nuclear Fuel, High-Level and Transuranic Radioactive Wastes (40 CFR 191, Subpart B)*. Detailed information about the technical basis for the preliminary comparison is contained in Volume 2. The reference data base and values for input parameters used in the modeling system are contained in Volume 3. Uncertainty and sensitivity analyses related to 40 CFR 191B are contained in Volume 4. Volume 5 contains uncertainty and sensitivity analyses of gas and brine migration for undisturbed performance. Finally, guidance derived from the entire 1992 performance assessment is presented in Volume 6.

Results of the 1992 performance assessment are preliminary, and are not suitable for final comparison with 40 CFR 191, Subpart B. Portions of the modeling system and the data base remain incomplete, and the level of confidence in the performance estimates is not sufficient for a defensible compliance evaluation. Results are, however, suitable for providing guidance to the WIPP Project.

All results are conditional on the models and data used, and are presented for preliminary comparison to the Containment Requirements of 40 CFR 191, Subpart B as mean complimentary cumulative distribution functions (CCDFs) displaying estimated probabilistic releases of radionuclides to the accessible environment. Results compare three conceptual models for radionuclide transport in the Culebra Dolomite Member of the Rustler Formation and two approaches to estimating the probability of inadvertent human intrusion into the WIPP by exploratory drilling. The representation for disposal-system performance believed to be most realistic includes intrusion probabilities based on expert-panel judgement and dual-porosity transport with chemical retardation. For intrusions occurring 1000 years after decommissioning, the mean CCDF for this representation lies more than one order of magnitude below the EPA limits. Using the same approach to intrusion probabilities used in the 1991 performance assessment (i.e., not taking expert judgement into account and basing the probability model on the maximum intrusion probability indicated in Appendix B of 40 CFR 191, Subpart B) significantly increases the probability of releases, regardless of the model used for subsurface transport. Assuming the higher intrusion probabilities and dual-



porosity transport without chemical retardation, the mean CCDF is approximately one order of magnitude below the EPA limits. For the higher intrusion probabilities and single-porosity, fracture-only transport, the mean CCDF is less than one order of magnitude below the EPA limits."

4. PERFORMANCE-ASSESSMENT METHODOLOGY; p. 4-1, para. 1;

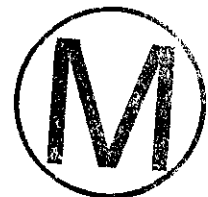
" This chapter contains a brief and simplified overview of the methodology used in WIPP performance assessment. A more complete discussion is presented in Volume 2 of this report and in references cited therein.

The WIPP performance assessment represents risk as a triplet consisting of the answers to the following three questions (Kaplan and Garrick, 1981):

- (1) What can happen? (scenarios)
- (2) How likely are things to happen? (probabilities of scenarios)
- (3) What are the consequences of these things (scenarios) happening?

The first question is answered by a systematic scenario construction procedure that results in a set of comprehensive and mutually exclusive scenarios for consequence analysis (Guzowski, 1990; Cranwell et al., 1990; NEA, 1992b). Answering the second question requires that probability estimates be made for the scenarios retained for analysis. A formal elicitation procedure using expert panels has been recommended by other programs (Hora and Iman, 1989; Andersson et al., 1989; Stephens and Goodwin, 1989; Bonano et al., 1990) and employed by WIPP performance assessment. Answering the third question requires a modeling system to estimate consequences, expressed in terms of the performance measures of interest. The WIPP performance assessment uses a Monte Carlo technique to examine uncertainty in performance estimates and to perform sensitivity analyses that provide guidance to the Project.

The WIPP performance assessment is iterative, and answers to each of these three questions will be reexamined as the Project moves toward a final regulatory compliance evaluation. Thus, the set of scenarios selected for consequence analysis may change as new information dictates (although the scenarios examined in 1992 are essentially unchanged from 1991). Scenario probabilities have changed as expert judgement is incorporated, and the modeling system continues to change as new models and data become available."



**Compliance Certification Application Reference Expansion**

---

State of New Mexico, Oil Conservation Division, Energy, Minerals, and Natural Resources Department. 1988. "Application of the Oil Conservation Division Upon It's Own Motion to Revise Order R-111. As Amended. Pertaining to the Potash Areas of Eddy and Lea Counties, New Mexico." Case 9316, Revision to Order R-111-P, April 21, 1988. Santa Fe, NM. On file in the NWM Library as KFN2581.

**F. PLUGGING AND ABANDONMENT OF WELLS;**

" (1) All wells heretofore and hereafter drilled within the Potash Area shall be plugged in a manner and in accordance with the general rules or field rules established by the Division that will provide a solid cement plug through the salt section and any water-bearing horizon and prevent liquids or gases from entering the hole above or below the salt section.

(2) The fluid used to mix the cement shall be saturated with the salts common to the salt section penetrated and with suitable proportions but not more than three (3) percent of calcium chloride by weight of cement being considered the desired mixture whenever possible."



## Compliance Certification Application Reference Expansion

---

Stenhouse, M.J., Chapman, N.A., and Sumerling, T.J. 1993. SITE-94 Scenario Development FEP Audit List Preparation: Methodology and Presentation. SKI Technical Report 93:27. Swedish Nuclear Power Inspectorate, Stockholm. Available from NTIS as DE 94621513.

### PREFACE;

" This report concerns a study which is part of the SKI performance assessment project SITE-94. SITE-94 is a performance assessment of a hypothetical repository at a real site. The main objective of the project is to determine how site specific data should be assimilated into the performance assessment process and to evaluate how uncertainties inherent in site characterization will influence performance assessment results. Other important elements of SITE-94 are the development of a practical and defensible methodology for defining, constructing and analyzing scenarios, the development of approaches for treatment of uncertainties, evaluation of canister integrity, and the development and application of an appropriate Quality Assurance plan for Performance Assessments."



Thorne, M.C. 1992. Dry Run 3 - A Trial Assessment of Underground Disposal of Radioactive Wastes Based on Probabilistic Risk Analysis - Volume 8: Uncertainty and Bias Audit. United Kingdom Department of Environment Report DOE/HMIP/RR/92.040, London, England.

Preface to Volume 8, p. ii, para. 3;

" This volume-Uncertainty and Bias Audit-describes a possible procedure for carrying out a post-closure radiological safety assessment incorporating an audit of uncertainties and biases. This procedure has not been applied in Dry Run 3 since the methodology was under development in parallel with Dry Run 3. However, Dry Run 3 has provided a convenient opportunity to test certain aspects of the methodology. In particular:

- an Expert Group has been utilised to advise on factors/phenomena that should be included in a comprehensive assessment and to determine priorities for modelling;

- scoping calculations have been carried out to provide illustrative results, which have been used to demonstrate the potential biases inherent in the trial assessment;

- expert judgements have been used to assess the status of Dry Run 3 relative to a minimal assessment, as defined below.

Following a brief introduction (Chapter 1), Chapter 2 of the report summarises the over-all procedure for a post-closure radiological assessment incorporating an uncertainty and bias audit which was developed prior to the start of Dry Run 3. This procedure relies to a significant extent on the use of expert judgements. Such judgements have to be elicited in an appropriately structured manner, so that the judgements made, their bases, and their applications in the assessment, can be suitably documented. The use of expert judgements in the quantification of uncertainty, by the elicitation of parameter value distribution, is the subject of Volume 4. Expert judgement in relation to factors/phenomena that should be included in an assessment is the topic of Chapter 3 of this volume. This includes discussion of a formal procedure selecting the expert group (often the least well-documented part of the process), a description of the various phases of work involved in deriving groups of factors/phenomena for modelling, and assignment of levels of confidence in the results that would be obtained from assessments of different degrees of complexity.

Overall, it proved possible for the expert group to define a minimal assessment that they estimated would not exhibit gross bias because of excluded factors/phenomena. Small deletions from this minimal assessment could be tolerated with only a limited to moderate (less than a factor of 10) estimated effect on peak individual risks. More extensive deletions resulted in the expert group judging that too much of substance had been deleted and that the degree of bias would be unquantifiable without modeling studies, which effectively

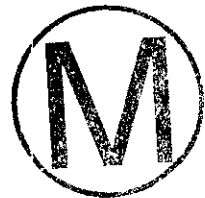


corresponds to reintroducing the factors/phenomena into the assessment.

The material included in Chapter 3 provides a justification for the various modelling studies described in Chapter 4. These include both scoping calculations and deterministic calculations related to the pra studies undertaken as part of the main Dry Run 3 exercise and reported in Volume 6. In this section, reference is also made to the component model investigations reported in Volume 5.

The deliberations of the expert group, and the various calculations undertaken, lead to a variety of results. The individual results are summarised in Chapter 5, where approaches to their presentation and aggregation are explored, in so far as the limited material available allows.

Chapter 6 provides a discussion of the work undertaken. In particular, the Dry Run 3 experienced is used to estimate resource requirements for those parts of the uncertainty and bias component of a comprehensive post-closure radiological assessment of a site, which have been exercised. Limitations and deficiencies of the methodology are also discussed and areas requiring further development are highlighted."



**Compliance Certification Application Reference Expansion**

---

Van Pelt, R.S. 1995. "Permeability Estimates of MGFT08 and MGFT09." SNL Technical Memorandum to M.K. Knowles. Contained in SWCF Record Package, "Small-Scale Seals Performance Test: Series A Post-Mortem," WPO 39631.

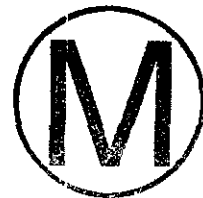
NOTE: The above listed document was not available for inclusion in the Reference Expansion as of the printing date. Page changes will be provided as the above document becomes available for inclusion.

**Compliance Certification Application Reference Expansion**

---

Vaughn, P., Bean, J., Garner, J., Lord, M., MacKinnon, R., McArthur, D., Schreiber, J., and Shinta, A. 1995. FEPs Screening Analysis DR2, DR3, DR6, DR7, and S6. Record Package submitted to SWCF-A:1.1.6.3:PA:QA:TSK:DR2, DR3, DR6, DR7, and S6. Sandia National Laboratories, Albuquerque, NM. WPO 38152.

NOTE: The above listed document was not available for inclusion in the Reference Expansion as of the printing date. Page changes will be provided as the above document becomes available for inclusion.



Compliance Certification Application Reference Expansion

---

Wallace, M.G., Beauheim, R., Stockman, C., Martell, M.A., Brinster, K., Wilmot, R., and Corbet, T. 1995. FEPs Screening Analysis, NS-1: Dewey Lake Data Collection and Compilation. Record Package submitted to SWCF-A:1.1.6.3:PA:QA:TSK:NS1. Sandia National Laboratories, Albuquerque, NM WPO 30650.

NOTE: The above listed document was not available for inclusion in the Reference Expansion as of the printing date. Page changes will be provided as the above document becomes available for inclusion.



Wang, Y., and Brush, L.H. January 26, 1996. "Estimates of Gas Generation Parameters for the Long-Term WIPP Performance Assessment." WPO 31943.

Introduction, p. 1, para. 1;

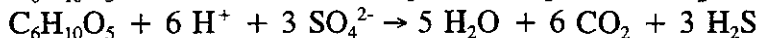
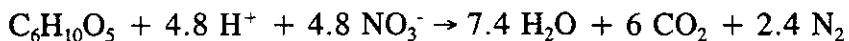
" Steel corrosion and organic-material biodegradation have been identified as major gas-generation processes in the WIPP repository (Brush, 1995). Gas production will affect room closure and chemistry (Butcher, 1990; Brush, 1990). This memorandum provides the current estimates of gas-generation parameters for the long-term WIPP performance assessment. The parameters provided here include the rates of gas generation under inundated and humid conditions, the stoichiometric factors of gas generation reactions, and the probability of the occurrence of organic material biodegradation (Table 1). To satisfy the quality assurance (QA) requirement (QAP 9-5), we summarize all hand calculations for estimating these parameters in Appendices I and II.

### Biodegradation of Organic Materials

Cellulosics, plastics, and rubbers have been identified as the major organic materials to be emplaced in the WIPP repository (DOE/CAO, 1996) and could be degraded by microbes in 10,000 years. Cellulosics has been demonstrated experimentally to be the most biodegradable among these materials (Franci et al., 1995). The occurrence of significant microbial gas generation in the repository will depend on: (1) whether microbes capable of consuming the emplaced organic materials will be present and active; (2) whether sufficient electron acceptors will be present and available; (3) whether enough nutrients will be present and available. Considering uncertainties in evaluation of these factors and also in order to bracket all possible effect of gas generation on the WIPP performance assessment, we assign a 50% probability to the occurrence of significant microbial gas generation.

#### ●Microbial Reactions

Microorganism will consume cellulosics mainly via the following reaction pathways in the repository (Brush, 1995):



We assume that Reactions 1 to 3 will proceed sequentially according to the energy yield of each reaction. Here we ignore the reaction pathways of aerobic respiration, Mn(IV) and Fe(III) dissimilatory reduction, since the quantities of O<sub>2</sub>, Mn(IV) and Fe(III) initially present in the repository will be negligible relative to the other electron acceptors. In Reactions 1 to 3, biomass accumulation is also taken into account. This is because significant biomass accumulation seems unlikely in the WIPP repository and the accumulated

biomass, if any, will be recycled by microbes after all biodegradable cellulose is consumed.

In addition to Reaction (3), methanogenesis may proceed via:



However, this reaction will be ignored in our calculations, because (1) no experimental data are available to evaluate the rate of this reaction and (2) the net effect of this reaction is to reduce the total gas generation and the amount of CO<sub>2</sub> in the repository and, therefore, it is conservative to ignore this reaction in respect of repository pressurization and actinide solubility."

Anoxic Steel Corrosion, p. 4, para. 2;

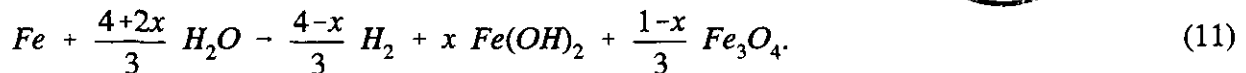
" According to current waste inventory estimates, a large amount of steels will be emplaced in the WIPP repository (DOE/CAO, 1996). Those steels will be capable of reacting with the repository brine to form H<sub>2</sub> gas. Both thermodynamic calculations and experimental observations indicate that the H<sub>2</sub> gas can be generated to pressures exceeding the lithostatic pressure at the WIPP horizon, if enough brine enters the repository (Brush, 1990; Telander & Westerman, 1993, 1995). Since the repository will become anoxic shortly after waste emplacement and sealing, we here focus only on anoxic steel corrosion."

Stoichiometric Factors in the Average-Stoichiometry Model, p. 6, para. 3;

" In the Average-Stoichiometry Model, which is currently implemented in BRAGFLO, microbial gas generation is represented by the overall reaction:



and H<sub>2</sub> production due to steel corrosion is described by:



The stoichiometric factors *x* and *y* in Reaction 10 and 11 are estimated as follows.

● Average-Stoichiometric Factor *y* in Microbial Reaction

The stoichiometric factor *y* depends on the extent of the progress of each individual reaction pathway (Reactions 1 through 3). It can be estimated based on the inventory estimates of the transuranic waste to be emplaced in the Waste Isolation Pilot Plant

(DOE/CAO, 1996; Drez, 1996).

First, we estimate the maximum quantities (in moles) of cellulose and steel that will be potentially consumed in 10,000 years:

$$M'_{cel} = \min \left\{ \frac{6000M_{cel}}{162}, 10000R'_c M_{cel} \right\} \quad (12)$$

$$M'_{Fe} = \min \left\{ \frac{1000M_{Fe}}{56}, 1410R_{c,i} A \right\} \quad (13)$$



with

$$R'_c = \max \{ R_{m,i}, R_{m,h} \} \quad (14)$$

where  $M_{cel}$  and  $M_{Fe}$  are the quantities (in kg) of cellulose and steel initially present in the repository;  $R_{c,i}$  is the inundated steel-corrosion rate ( $\mu\text{m}/\text{year}$ );  $R_{m,i}$  and  $R_{m,h}$  are the sampled rates of cellulose biodegradation under inundated and humid conditions respectively (mole/kg/year). In Equation (13), we use the factor of 0.141 mole/ $\mu\text{m}/\text{m}^2$  to convert steel-corrosion-rate unit from  $\mu\text{m}/\text{year}$  to mole/ $\text{m}^2/\text{year}$  (Telander and Westerman, 1995). Here, we assume that cellulose biodegradation and steel corrosion both follow zero order reaction kinetics. Next, we calculate the average stoichiometric factor  $y$  by distributing  $M'_{cel}$  into individual biodegradation pathways. Consider two extreme cases, corresponding to the maximum and minimum values of  $y$ : (1) no reaction of microbially produced  $\text{CO}_2$  and  $\text{H}_2\text{S}$  with steel and steel-corrosion products.

If no  $\text{CO}_2$  or  $\text{H}_2\text{S}$  is consumed by reactions with steel and steel-corrosion products, we would expect the maximum quantity of microbial gas production in the repository and therefore the maximum value for  $y$ . We assume that Reactions 1 to 3 will proceed sequentially. The maximum value of  $y$  can be estimated by averaging the gas-yields for all reaction pathways:

$$y_{max} = \frac{\frac{8.4M_{NO_3}}{4.8} + \frac{9M_{SO_4}}{3} + \left( M'_{cel} - \frac{6M_{NO_3}}{4.8} - \frac{6M_{SO_4}}{3} \right)}{M'_{cel}} \quad (15)$$

where  $M_{NO_3}$  and  $M_{SO_4}$  are the quantities of  $NO_3^-$  and  $SO_4^{2-}$  (in moles) initially present in the repository.

If  $CO_2$  or  $H_2S$  reacts with steel and steel-corrosion products, we expect that a significant quantity or, perhaps, all of these microbially produced gases would be consumed, thus forming  $FeCO_3$  and  $FeS$ . This would result in the minimum value of  $y$ . The total gas consumed by those reactions ( $G$ ) is:

$$G = \min \left\{ \frac{6M_{NO_3}}{4.8} + \frac{9M_{SO_4}}{3} + \frac{3}{6} \left( M'_{cel} - \frac{6M_{NO_3}}{4.8} - \frac{6M_{SO_4}}{3} \right), M'_{Fe} \right\} \quad (16)$$

The minimum value of  $y$  can then be estimated by:

$$y_{min} = \frac{\frac{8.4M_{NO_3}}{4.8} + \frac{9M_{SO_4}}{3} + \left( M'_{cel} - \frac{6M_{NO_3}}{4.8} - \frac{6M_{SO_4}}{3} \right) - G}{M'_{cel}} = y_{max} - \frac{G}{M'_{cel}} \quad (17)$$

For each BRAGFLO simulation,  $y$  will be uniformly sampled over  $[y_{min}, y_{max}]$ :

$$y = y_{min} + \beta(y_{max} - y_{min}) \quad (18)$$

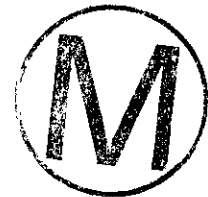
with  $0 \leq \beta \leq 1.0$ . The calculational scheme proposed here automatically correlates  $y$  with waste inventory estimates as well as with reaction rates.

The above calculational scheme does not take into account the  $SO_4^{2-}$  that will be brought into repository by brine inflow. Based the previous BRAGFLO simulations for undisturbed cases, the total volume of the brine entering the repository in 10000 years is unlikely to be larger than  $2.2 \times 10^7$  liters, the value corresponding to the case with unrealistically low gas generation and therefore the worst repository flooding. With a typical  $SO_4^{2-}$  concentration of 200mM in WIPP brines (Brush, 1990), we estimate that the amount of  $SO_4^{2-}$  brought into the repository by brine inflow would be less than  $0.4 \times 10^7$  moles. This amount of  $SO_4^{2-}$  will increase the fraction of sulfate reduction pathway in total cellulose

biodegradation only by less than 1%. Therefore, neglecting the sulfate brought by brine inflow would introduce an error of no more than a few percents in y values.

● Average-Stoichiometric Factor X in Steel Corrosion Reaction

While magnetite ( $\text{Fe}_3\text{O}_4$ ) has been observed to form on steel as a corrosion product in low-Mg anoxic brines at elevated temperatures (Telander & Westerman, 1995) and in oxic brine (Haberman & Frydrych, 1988), there is no evidence that it will form at WIPP repository temperatures. If  $\text{Fe}_3\text{O}_4$  were to form, it would be expected that  $\text{H}_2$  would be produced (on a molar basis) in excess of Fe consumed. But, the anoxic corrosion experiments did not show the production of  $\text{H}_2$  in excess of Fe reacted. Therefore, we set the stoichiometric factor x to 1.0 in Reaction 11."



**BIBLIOGRAPHY DOCUMENTS**



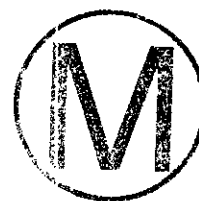
Compliance Certification Application Reference Expansion

---

Adams, J.E. 1944. Upper Permian Ochoa Series of the Delaware Basin, West Texas and Southeastern New Mexico. American Association of Petroleum Geologists Bulletin, Vol. 28, No. 11, pp. 1596-1625. WPO 37940.

ABSTRACT, p 1596;

" The Ochoa series includes the uppermost Permian deposits of the southwestern United States. Most of the rocks included in the series are poorly exposed unfossiliferous evaporites. The well known subsurface section in and around the Delaware basin is described and illustrated by cross sections. A short chapter discusses theories on the origin and distribution of the characteristic evaporites."



Anderson, R. Y., 1978. Deep Dissolution of Salt, Northern Delaware Basin, New Mexico. Sandia National Laboratories, Albuquerque, NM. WPO 29527 - WPO 29530.

Abstract, p v:

" Deep-seated dissolution in the Delaware basin has developed in association with the Capitan (reef) and the underlying Bell Canyon (Delaware) aquifers and at a more permeable horizon between the Castile and Salado formations. The uplift, erosion, and exposure of the reef in the Guadalupe and Glass mountains has channeled meteoric waters through the reef aquifer. These waters gained access to the salt through fractures around the reef margin, and dissolved overlying and superjacent salt by means of brine density flow. This type of deep dissolution moved into the salt beds laterally at a horizon of increased permeability between the Castile and Salado formations and dissolved a wedge that undercut the overlying evaporites. The deep-seated dissolution also produced a number of large-scale collapse structures along the basin margin and along the western edge of salt. This wedge-like effect, combined with surface dissolution, has removed 50 percent of the original salt from the basin and removed 70 percent of the original salt at the lower Salado horizon.

The water in the aquifers, by gaining access to overlying chambers through fractures, have also dissolved smaller scale localized chambers in overlying salt beds that subsequently collapse to form breccia pipes, deep-seated sinks, and other collapse structures. These features have been exhumed to different stratigraphic levels in the tilted and eroded basin, resulting in surface expression as limestone buttes (Castiles), collapsed outliers, domal structures with collapsed centers (breccia pipes), and deep-seated sinks. Many of the deep-seated sinks are associated with salt anticlines which probably formed as a result of differential stress from unloading related to dissolution. Localized collapse, as well as regional dissolution, is an ongoing process.

The W.I.P.P. site lies in a corner of the Delaware basin that has been relatively protected from regional but not localized effects of deep dissolution. Deep seated, wedge-like dissolution, however, has progressed from north to south in the basin and salt in the northern part of the Delaware basin will eventually be dissolved at the lower Salado horizons before overlying salt has been removed from the basin by processes of near-surface dissolution (suberosion)."



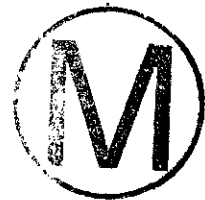
Compliance Certification Application Reference Expansion

---

Anderson, R. Y., and Kirkland, D.W. 1980. Dissolution of Salt Deposits by Brine Density Flow. *Geology*, Vol. 8, No. 2, pp. 66-69.

ABSTRACT, P 66;

" The origin of collapse structures and breccias that vertically penetrate or occur within impermeable evaporites has never really been understood. The density of the brine that develops as salt deposits are dissolved can generate continuous gravitational brine movement. If the source of the dissolving water is artesian, or continuous, a flow cycle is developed in which the salt itself supplies the density gradient that becomes the vehicle of its own dissolution. The Delaware Basin in western Texas and southeastern New Mexico provides a particularly good example of how brine density flow can produce dissolution chambers that collapse to form breccias. The potential for dissolution by brine flow is an inherent property of partly exhumed evaporites and may constitute a risk factor in the storage of radioactive waste in evaporite deposits."



Anderson, R.Y., Dean, W.E., Kirkland, D.W., and Snider, H. I. 1972. Permian Castile Varved Evaporite Sequence, West Texas and New Mexico. Geological Society of America Bulletin, Vol. 83, No. 1, pp. 59-85.

ABSTRACT; p 59, col 1;

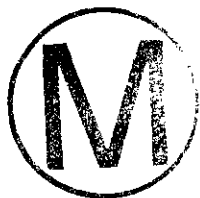
" Laminations in the Upper Permian evaporite sequence in the Delaware Basin appear in the preevaporite phase of the uppermost Bell Canyon Formation as alternation of siltstone and organic layers. The laminations then change character and composition upward to organically laminated claystone, organically laminated calcite, the calcite-laminated anhydrite typical of the Castile Formation, and finally to the anhydrite-laminated halite of the Castile and Salado.

Laminae are correlative for distances up to 111 km (70.2 mi) and probably throughout most of the basin. Each laminae is synchronous, and each couplet of two laminated components is interpreted as representing an annual layer of sedimentation--a varve.

The thickness of each couplet in the 260,000-varve sequence (a total thickness of 447.2 m, (1465 ft) has been measured individually and recorded and provides the basis for subdividing and correlating major stratigraphic units within the basin. The uppermost 9.2 m (30.3 ft) of the Bell Canyon Formation contains about 50,850 varve couplets; the Basal Limestone Member of the Castile about 600; the lowermost anhydrite member of the Castile (Anhydrite I) contains 38,397; Halite I, 1,063; Anhydrite II, ??,414; Halite II, 1,758; Anhydrite III, 46,592; Halite III, 17,879; and Anhydrite IV, 54,187. The part of the Salado collected (126.6 m) contains 35,422 varve couplets. The Bell Canyon-Castile sequence in the cores studies is apparently continuous, with no recognizable unconformities.

The dominant petrologic oscillation in the Castile and Salado, other than the laminations, is a change from thinner undisturbed anhydrite laminae to thicker anhydrite laminae that generally show a secondary or penecontemporaneous nodular character, with about 1,000 to 3,000 units between major oscillations or nodular beds. These nodular zones are correlative throughout the area of study and underly halite when it is present. The halite layers alternate with anhydrite laminae, are generally recrystallized, and have an average thickness of about 3 cm. The halite beds were once west of their present occurrence in the basin but were dissolved, leaving beds of anhydrite breccia. The onset and cessation of halite deposition in the basin was nearly synchronous.

The Anhydrite I and II Members thicken gradually across the basin from west to east, whereas the Halite I, II, and III Members are thickest in the eastern and northeastern part of the basin and thicken from southeast to northwest. This distribution and the synchronicity indicate a departure from the classical model of evaporite zonation."



**Compliance Certification Application Reference Expansion**

---

Argüello, J.G., Molecke, M.A., and Beraun, R., 1989. "3D Thermal Stress Analysis of WIPP T RH TRU Experiments." Rock Mechanics as a Guide for Efficient Utilization of Natural Resources, Proceedings of the 30th U.S. Rock Mechanics Symposium, West Virginia University, Morgantown, WV, June 19-22, 1989, A.W. Khair, Ed. SAND88-2734C, pp. 681-688. A. A. Balkema, Brookfield, VT. WPO 25724.

NOTE: The above listed document was not available for inclusion in the Reference Expansion as of the printing date. Page changes will be provided as the above document becomes available for inclusion.



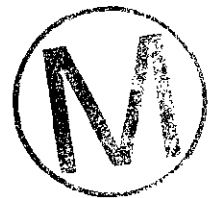
Compliance Certification Application Reference Expansion

---

Bachman, G.O. 1973. Surficial Features and Late Cenozoic History in Southeastern New Mexico. Open-File Report 4339-8. U.S. Geological Survey, Reston, VA.

ABSTRACT, p. 1;

" Since deposition of the Ogallala Formation during Pliocene time, southeastern New Mexico has been subjected to erosion, solution, subsidence, and widespread eolian activity. These processes have combined to influence the formation and morphology of major drainage systems. Aligned drainage patterns resulted from solution of caliche localized by longitudinal sand dunes. San Simon Swale appears to have formed by processes of erosion and solution-subsidence of Permian evaporites, and was formerly an important tributary to the Pecos River. The combination of processes that formed San Simon Swale was similar to the combination of erosion and coalescing sinks that formed the lower Pecos Valley in southern New Mexico.



Compliance Certification Application Reference Expansion

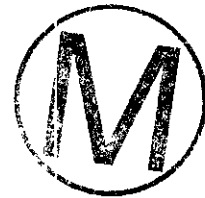
---

Bachman, G.O. 1974. Geologic Processes and Cenozoic History Related to Salt Dissolution in Southeastern New Mexico. Open-File Report 74-194, U.S. Geological Survey, Denver, CO.

ABSTRACT, P 1;

" Salt of Permian age in the subsurface of an area near The Divide, east of Carlsbad, N. Mex., is being considered for a nuclear waste repository. The geologic history of the region indicates that dissolution of salt has occurred in the past during at least three distinct epochs: (1) after Triassic but before middle Pleistocene time; (2) during middle Pleistocene; and (3) during late Pleistocene. Thus, destructive geologic processes have been intermittent through more than 100 million years.

Nash Draw, near The Divide, formed during late Pleistocene time by the coalescing of collapse sinks. The rate of its subsidence is estimated to have been about 10 cm (0.33 ft) per thousand years. The immediate area of the Divide adjacent to Nash Draw has not undergone stress by geologic processes during Pleistocene time and there are no present indications that this geologic environment will change drastically within the period of concern for the repository."



Compliance Certification Application Reference Expansion

---

Bachman, G.O., 1976. Cenozoic Deposits of Southeastern New Mexico and an Outline of the History of Evaporite Dissolution. Journal of Research, Vol. 4, No. 2, pp. 135-149. US Geological Survey, Denver, CO.

ABSTRACT, p 135;

" Sedimentary records of Cenozoic history in Southeastern New Mexico begin with the Ogallala Formation , Miocene and Pliocene age. Later records include the Gatuna Formation of early or middle Pleistocene age, Mescalero caliche, an informal term, of middle Pleistocene age, and fluvial deposits of late Pleistocene age but there are many gaps in some record. The modern landscape is the result of erosion and deposition in climates that have ranged from semihumid to semiarid as well as dissolution of soluble rocks in Permian Formations in the subsurface. This dissolution may have been as early as Jurassic time and has continued intermittently to the present.



Bachman, G.O., 1980. Regional Geology and Cenozoic History of Pecos Region, Southeastern New Mexico. Open-File Report 80-1099. U.S. Geological Survey, Denver, CO.

ABSTRACT, p 1;

" This report summarizes the Cenozoic history of the Pecos drainage in the Delaware basin, southeastern New Mexico, and incorporates an outline of the dissolution and karst development in Permian evaporites in the region.

Evaporites include anhydrite, gypsum, halite and related minerals. They are included in the Castile, Salado and Rustler Formations of Late Permian (ochoan) age. These formations have been transgressed by strata of the Dockum Group of Late Triassic age and unnamed formations of early Cretaceous age.

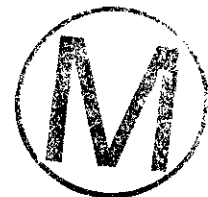
Complex karst features include collapse sinks, karst mounds (new term), karst domes (new term) and caves. Karst mounds are erosional remnants of regional breccia. Karst domes are structural features which have formed on a very irregular dissolution surface. They are analogous to towers, kegelkarst or mogotes in tropical regions except that karst domes are almost buried by their own dissolution residue.

Breccia chimneys are collapse sinks which have formed over the Capitan aquifer system. They appear to be the result of unsaturated water rising under a strong hydraulic head through fractures and dissolving upward into the evaporite sequence.

Breccia chimneys, karst mounds and karst domes studied during this work were formed during middle Pleistocene time.

Dissolution has been an active process in the Delaware basin at least since Triassic time and it is impractical to attempt to calculate a rate of dissolution for the basin. Earlier estimates of the rate of dissolution are considered to be conservative. Subsurface evidence does not suggest that deep dissolution is presently an active process in the Castile Formation beneath the thick beds of Salado salt.

Pleistocene glaciation in the northern and central United States was probably accompanied by 'pluvial' periods in southeastern New Mexico. Pluvials are characterized by less extreme temperatures, less evaporation and more effective moisture than at present."



Compliance Certification Application Reference Expansion

---

Bachman, G.O. 1981. Geology of Nash Draw, Eddy County, New Mexico. Open-File Report 81-31. U.S. Geological Survey, Denver, CO.

ABSTRACT, p. 1;

" Nash Draw is a partially closed depression about 29 km (17 mi) east of Carlsbad, Eddy County, New Mexico. It has been mapped geologically in conjunction with detailed studies to evaluate the proposed nuclear Waste Isolation Pilot Plant (WIPP). Maps at scales of 1:24,000 accompany this report.

The stratigraphic section exposed in Nash Draw includes the Rustler Formation and Dewey Lake Red Beds of Late Permian (Ochoan) age, the Dockum Group of Late Triassic age, and the Pleistocene Gatuna Formation. Other deposits of Middle to late Quaternary age include the Mescalero caliche, spring deposits, and windblown sand.

Dissolution of evaporites has been a major process in the formation of Nash Draw. Nash Draw formed before, and during, Gatuna time about 600,000 years ago. Near-surface dissolution of gypsum in the Rustler Formation is presently active and is responsible for numerous collapse sinks and related karst features."



Compliance Certification Application Reference Expansion

---

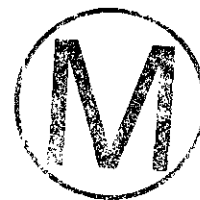
Bachman, G.O., 1984. Regional Geology of Ochoan Evaporites, Northern Part of Delaware Basin. Circular 184, pp. 1-22. New Mexico Bureau of Mines and Mineral Resources Socorro, NM.

ABSTRACT, p 5;

" The Ochoan Series (Permian) in the northern part of the Delaware Basin, southeastern New Mexico, includes in ascending order the Castile, Salado, and Rustler Formations, and the Dewey Lake Red Beds. The Castile and Salado Formations comprise a sequence of evaporites which include anhydrite, gypsum, halite, and associated potash salts. The Rustler Formation contains some halite and minor amounts of potash minerals. These evaporites were deposited within the basin formed by the Capitan barrier reef, as well as across the reef. The evaporites, as well as the Capitan reef, are all subject to dissolution with resulting karst features analogous to those formed in limestone regions.

An Ancestral Pecos River was the major drainage system in the western part of the Delaware Basin, New Mexico, during the Cenozoic time. That ancient river system was responsible for the formation of an extensive karst terrain along the east side of the present Pecos River in New Mexico and southward into Texas. During late Cenozoic time extensive dissolution occurred in the Salado Formation within the karst area as a result of the ground-water regime. The dissolution front was perched on the upper anhydrite member of the Castile Formation.

On the eastern side of the Delaware Basin in New Mexico, a large collapse sink--San Simon sink--overlies the Capitan reef which is a prominent aquifer system in that area. So-called 'breccia pipes' are ancient sinks which collapsed into the caverns in the reef on the northern margin of the basin. These have since been partially exhumed. The San Simon sink is presumed to be a modern analog of these breccia pipes."



Bachman, G.O., 1985. Assessment of Near-Surface Dissolution at and Near the Waste Isolation Pilot Plant (WIPP), Southeastern New Mexico. SAND84-7178. Sandia National Laboratories, Albuquerque, NM. WPO 24609.

ABSTRACT, p. 3;

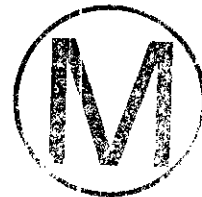
" The area at and near the WIPP site was examined for evidence of karst development on the geomorphic surface encompassing the site. Certain surficial depressions of initial concern were identified as blowouts in sand dune fields (shallow features unrelated to karstification). An ancient stream system active more than 500,000 years ago contained more water than any system since. During that time (Gatuña, Middle Pleistocene), many karst features such as Clayton Basin and Nash Draw began to form in the region. Halite was probably dissolved from parts of the Rustler Formation at that time. Dissolution of halite and gypsum from intervals encountered in Borehole WIPP-33 west of the WIPP site occurred during later Pleistocene time (i.e., <450,000 yr ago). However, there is no evidence of active near-surface dissolution within a belt to the east of WIPP-33 in the vicinity of the WIPP shaft."



Bachman, G.O., 1987. Karst in Evaporites in Southeastern New Mexico. SAND86-7078. Sandia National Laboratories, Albuquerque, NM. WPO 24006.

ABSTRACT;

" Permian evaporites in southeastern New Mexico include gypsum, anhydrite, and salt, which are subject to both blanket and local, selective dissolution. Dissolution has produced many hundreds of individual karst features including collapse sinks, karst valleys, blind valleys, karst plains, caves, and breccia pipes. Dissolution began within some formations during Permian time and has been intermittent but continual ever since. Karst features other than blanket deposits of breccia are not preserved from the early episodes of dissolution, but some karst features preserved today--such as breccia pipes--are remnants of karst activity that was active at least as early as mid-Pleistocene time. Rainfall was much more abundant during Late Pleistocene time, and many features visible today may have been formed then. The drainage history of the Pecos River is related to extensive karstification of the Pecos Valley during mid-Pleistocene time. Large-scale stream piracy and dissolution of salt in the subsurface resulted in major shifts and excavations in the channel. In spite of intensive groundwater studies that have been carried out in the region, major problems in groundwater in near-surface evaporite karst remain to be solved. Among these are determination of recharge areas and time of recharge."



Bachman, G.O., Johnson, R.B., and Swenson, F.A. 1973. Stability of Salt in the Permian Salt Basin of Kansas, Oklahoma, Texas, and New Mexico, Open-File Report 4339-4. U.S. Geological Survey, Denver, CO.

ABSTRACT, p 1;

" The Permian salt basin in the Western Interior of the United States is defined as that region comprising a series of sedimentary basins in which halite and associated salts accumulated during Permian time. The region includes the western part of Kansas, Oklahoma, and Texas, and eastern parts of Colorado and New Mexico.

Following a long period of general tectonic stability throughout the region during most of early Paleozoic time, there was much tectonic activity in the area of the Permian salt basin during Late Pennsylvanian and early Permian time just before bedded salt was deposited. The Early Permian tectonism was followed by stabilization of the basins in which the salt was deposited. These salt basins were neither contemporaneous nor continuous throughout the region so that many salt beds are also discontinuous. In general, beds in the northern part of the basin (Kansas and northern Oklahoma) are older, and the salt is progressively younger towards the south.

Since Permian time, the Permian salt basin has been relatively stable tectonically. Regionally, the area of the salt basin has been tilted and warped, has undergone periods of erosion, and has been subject to a major incursion of the sea; but deep-seated faults or igneous intrusions that postdate Permian salt are rare. In areas of the salt basin where salt is near the surface, such as southern New Mexico and central Kansas, there are no indications of younger deep-seated faulting and only a few isolated igneous intrusives of post-Permian age.

On the other hand, subsidence or collapse of the land surface resulting from dissolution has been commonplace in the Permian salt basin. Some dissolution of salt deposits has probably been taking place ever since deposition of the salt more than 230 million years ago. Nevertheless, the subsurface dissolution fronts of the thick bedded-salt deposits of the Permian basin have retreated at a very slow average rate during that 230 million years.

The preservation of bedded salt from subsurface dissolution depends chiefly on the isolation of the salt from moving groundwater that is not completely saturated with salt. Karst topography is a major criterion for recognizing areas where subsurface dissolution has been active in the past; therefore, the age of the karst development is needed to provide the most accurate

estimate of the dissolution rate. The Ogallala Formation of Pliocene age is probably the most widespread deposit in the Permian salt basin that can be used as a point of reference for dating the development of recent topography. It is estimated that salt has been dissolved laterally in the vicinity of Carlsbad, New Mexico, at an average rate of about 6-8 miles per million years.

Estimates of future rates of salt dissolution and the resulting lateral retreat of the underground dissolution front can be projected with reasonable confidence for southeastern



**Compliance Certification Application Reference Expansion**

---

New Mexico of the assumption that the climatic changes there in the past 4 million years are representative of climatic changes that may be expected in the near future of geologic time.

Large amounts of salt are carried by present-day rivers in the Permian salt basin; some of the salt is derived from subsurface salt beds, but dissolution is relatively slow. Ground-water movement through the Permian salt basin is also relatively slow."



## Compliance Certification Application Reference Expansion

---

Baes, C.F., and Mesmer, R.E. 1976. The Hydrolysis of Cations. John Wiley & Sons, New York, NY.

1. Introduction, p 1;

" The word *hydrolysis* is applied to chemical reactions in which a substance is split or decomposed by water. In organic chemistry, the products of the reaction are usually molecular, being formed by combination with H and OH groups, as in hydrolysis of an ester to an alcohol and a carboxylic acid. In inorganic chemistry, the word most often has been applied to solutions of salts and the reactions by which they are converted to new ionic species or to precipitates--oxides, hydroxides, or basic salts. The hydrolysis of salts can involve either the cation, the anion, or both. We shall be concerned primarily with the hydrolysis of cations to form soluble hydroxide or oxide complexes and, to a lesser extent, with the formation of hydroxide and oxide precipitates."



Barker, D.S. 1977. Northern Trans-Pecos Magmatic Province: Introduction and Comparison with the Kenya Rift. Geological Society of America Bulletin. Vol. 88, no. 10, pp. 1421-1427.

ABSTRACT, p 1421, col 1;

" The Trans-Pecos magmatic province of West Texas and southern New Mexico is a more eroded analogue of the Kenya (Gregory) rift in East Africa. Trans-Pecos alkalic-rocks are similar to the basalt-phonolite-trachyte-rhyolite assemblage from fissure and multicenter eruptions, and from some central volcanoes, in the Kenya rift. In both provinces, quartz-normative and nepheline-normative mafic rocks occur, providing likely parents for the entire observed range of silica saturation. Thus, no special mechanism is needed for deriving silica-undersaturated and silica-oversaturated rocks from one another, because both groups evolved independently. The Kenya rocks tend to be more mafic and, at the silicic end of their compositional range, more peralkalic than the Trans-Pecos rocks.

Similarities in tectonic style, extent and duration of magnetism, and igneous rock compositions in the two provinces suggest that the alkalic rocks in both regions were generated by differentiation from quartz- and nepheline-normative parents in the upper parts of elongate mafic or ultramafic intrusions, probably diapiric welts that caused doming and normal faulting."



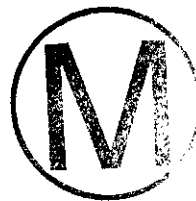
Bear, J. 1988. *Dynamics of Fluids in Porous Media*. Dover Publications, Inc., New York, NY. NNA. 911127.0046.

PREFACE, p xvii;

" This book is an attempt to present, in an ordered manner, the theory of dynamics (actually, also of statics) of fluids in porous media, as applicable to many disciplines of science and engineering. For some years I have taught courses on flow through porous media, and have treated this subject as a part of other courses, such as ground water hydrology, while at the Technion--Israel Institute of Technology, at M.I.T., while I spent my sabbatical leave (1966-7), and at several other institutions. I have felt the lack of a suitable textbook on this subject. Ideally, such a text should start from first principles of fluid mechanics and mechanics of continua, should show the passage from the microscopic to the macroscopic level of treatment, should emphasize the special features of porous media, establish the macroscopic theory and then show how it is applied to cases of practical interest.

It is rather surprising that in spite of its performance in many fields of practical interest, such as petroleum engineering, ground water hydrology, agricultural engineering and soil mechanics, so small number of treatises is available on fluids in porous media. This circumstance is even more surprising in view of the vast amount of literature published on the subject in a number of scientific and engineering journals. Although dynamics of fluids in porous media could become an interesting interdisciplinary course serving several departments, I believe that the relatively small number of courses offered by universities on the subject is due in part to lack of a suitable textbook. To overcome this lack I prepared notes for my own classes, which I present here in the form of a book, hoping that it will serve others in a similar situation.

The book is designed primarily for advanced undergraduate students and for graduates in fields such as ground water hydrology, soil mechanics, soil physics, drainage and irrigation engineering, sanitary engineering, petroleum engineering and chemical engineering, where flow through porous media plays a fundamental role. The book, I hope, will also serve the needs of scientists and engineers already active in these fields, who require a sound theoretical basis for their work. The emphasis in this book is on understanding the microscopic phenomena occurring in porous media and on their macroscopic description. The reader is led to grasp the meanings of the various parameters and coefficients appearing in the macroscopic descriptions of problems of flow through porous media, and their actual determination, as well as the limitations and approximations inherent in their description. In each case, the objective is to achieve a clear formulation of the flow problem considered and a complete mathematical statement of it in terms of partial differential equations and a set of initial and boundary conditions. Once a flow problem is stated properly in mathematical terms, three methods of solution are possible in principle: analytic solution, numerical solution aided by high speed digital computers and solution by means of laboratory models and analogs. All three tools are described in this book. Typical examples of analytic solutions are scattered throughout the book, but no attempt is made to present a collection of



a large number of solved problems. The principles of the numerical method of solution are presented, and a detailed description is given of laboratory models and analogs, their scaling and applications.

Mathematics is employed extensively and the reader is expected to have a good background in advanced engineering mathematics, including such subjects as vector analysis, Cartesian tensor analysis, partial differential equations and elements of the theory of functions.

Obviously, a single book, even of this size, cannot include everything related to the subject treated. Although we consider porous media in general, the discussion is limited to media with relatively large pores, thus excluding clays and media with micropores or colloidal-size particles. Similarly, chemical and electrochemical surface phenomena are excluded. The discussion is restricted to Newtonian fluids.

With these objectives and limitations in mind, the book starts with examples of two important porous media: the ground water aquifer and the oil reservoir. An attempt is made to define porous media, and the continuum approach is introduced as a tool for treating phenomena in porous media. This requires the definition of a 'representative elementary volume' based on the definition of porosity. Chapter 2 includes a summary of some important fluid and porous media properties. In chapter 3, the concepts of pressure and piezometric head are introduced. Chapter 4 starts with the definition of velocities and fluxes in a fluid continuum. Then the equations of conservation of mass, momentum and energy in a fluid continuum are presented, and using a porous medium conceptual model these equations are averaged to obtain the basic equations that describe flow through porous media: the equations of volume and mass conservation, including the equation of mass conservation of a species in solution (also called the equation of hydrodynamic dispersion), and the motion equation for the general case of an anisotropic medium and inhomogeneous fluid. Although the basic equations of motion and of mass conservation are developed from first principles in chapter 4, chapters 5 and 6 return to these topics, discussing them from a different point of view, perhaps more suitable for the reader who is less versed in fluid mechanics. Chapter 5 presents the equations of motion, starting from its original one-dimensional form (as suggested by Darcy on the basis of experiments), and extending it to three-dimensional flow, compressible fluids and anisotropic media. This chapter also contains a review of theoretical derivations of Darcy's law. My objectives in presenting this and similar reviews is to indicate research methods, such as the use of conceptual and statistical models. A section on the motion equation at high Reynolds numbers is also included.

In chapter 6, the control volume approach is introduced as a general tool for developing mass conservation equations. Special attention is devoted to deformable media. Also included in this chapter is the stream function and its relationship to the piezometric head. Once the continuity or mass conservation equations have been established, the next natural step is to consider the initial and boundary conditions. These are discussed in detail in chapter 7. Special attention is given to the phreatic surface boundary condition and to its description in the hodograph plane. The second part of this chapter contains a discussion on various analytic and numerical solution techniques.



Upon reaching this point, the reader should be able to state a problem of flow through porous media in terms of an appropriate partial differential equation and a set of initial and boundary conditions. He should also know the major methods of solution (analog solutions are discussed in chapter 11).

Chapter 8 deals with the problem of flow in unconfined aquifers. This is a problem often encountered in ground water hydrology and in drainage. The Dupuit assumptions are explained and employed to derive the continuity equations for unconfined flow. The hodograph method, as a tool for solving two-dimensional, steady phreatic flow problems, is discussed in detail with many examples. Several linearization techniques and solutions of the nonlinear equation of unconfined flow are also presented in this chapter.

In chapter 9 the discussion, hitherto confined to single-phase flow, is extended to polyphase flow in porous media, a topic of special interest in petroleum engineering. Starting from the fundamental concepts of saturation, capillary pressure and relative permeability, the motion and continuity equations are established. The case of unsaturated flow as treated by soil physicists is presented as a special case of flow of immiscible fluids, where one of the fluids--the air--is stationary and at constant pressure. Special cases of interest, dealing with infiltration into soils, are considered in more detail. A new concept is introduced: that of an abrupt interface as an approximation replacing the actual transition zone that occurs between two fluids, whether miscible or immiscible. A detailed discussion is presented on the coastal interface, of great interest to ground water hydrologists.

Chapter 10 deals with hydrodynamic dispersion. Again, although the fundamental equation is developed from first principles in chapter 4, a review of several other theories leading to this equation is presented. Special attention is given to the coefficient of dispersion and its relationship to matrix and flow characteristics. A section on heat and mass transfer completes the discussion on hydrodynamic dispersion.

Chapter 11 presents the use of models and analogs, both as research tools and as tools for solving boundary value problems. Following the presentation of a general method for deriving analog scales, a detailed description is given of the sand box model, the electric analogs of various types, the Hele-Shaw analogs and the membrane analog. Recommendations for application are indicated in each case.

In brief, this is the subject matter I have chosen to cover in this book. I have made an effort to present the information in such a way as to require a minimum of supplementary material, except for those who wish to dig more deeply into the subject. A large number of problems and exercises is included in this book.

I should like to express my appreciation to the many individuals who, through their comments and criticism, have contributed to the completion of this book. Special thanks . . .

I realize that an attempt to represent a systematic account of a theory, such as I have made here, is bound to have defects. I will accept with gratitude all readers' suggestions directed toward the improvement of this book."



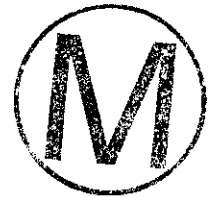
Bear, J., and Verruijt, A. 1987. Modeling Groundwater Flow and Pollution. D. Reidel Publishing Company, Boston, MA. NNA. 900212.0003.

PREFACE, p. xi;

" Groundwater constitutes an important component of many water resource systems, supplying water for domestic use, for industry, and for agriculture. Management of a groundwater system, an aquifer, or a system of aquifers, means making such decisions as to the total quantity of water to be withdrawn annually, the location of wells for pumping and for artificial recharge and their rates, and control conditions at aquifer boundaries. Not less important are decisions related to groundwater quality. IN fact, the quantity and quality problems cannot be separated. In many parts of the world, with the increased withdrawal of groundwater, often beyond permissible limits, the quality of groundwater has been continuously deteriorating, causing much concern to both suppliers and users. In recent years, in addition to general groundwater quality aspects, public attention has been focused on groundwater contamination by hazardous industrial wastes, by leachate from landfills, by oil spills, and by agricultural activities such as the use of fertilizers, pesticides, and herbicides, and by radioactive waste in repositories located in deep geologic formations, to mention some of the most acute contamination sources.

In all these cases, management means making decisions to achieve goals without violating specified constraints. In order to enable the planner, or the decision maker, to compare alternative modes of action and to ensure that the constraints are not violated, a tool is needed that will provide information about the response of the system (the aquifer) to various alternatives. Good management requires the ability to forecast the aquifer's response to planned operations, such as pumping and recharging. The response may take the form of changes in water levels, changes in water quality, or land subsidence. Any planning of mitigation, clean-up operations, or control measures, once contamination has been detected in the saturated or unsaturated zones, requires the prediction of the path and the fate of the contaminants in response to the planned activities. Any monitoring or observation network must be based on the anticipated behavior of the system.

The necessary information about the response of a system is . . . "



Bear, J., Tsang, C.F., and de Marsily, G. 1993. Flow and Contaminant Transport in Fractured Rock. Academic Press, Inc., San Diego, CA.

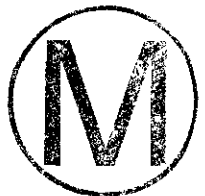
PREFACE, p xi;

" The question of how to deal with fractured rock domains has always been on the agenda of geohydrologists. Are Darcy's law and the theory of flow through porous media applicable to fractured rock aquifers, at least when the flow is assumed to be in the laminar flow range? And is the continuum approach applicable? The subject has always been investigated by reservoir engineers, this time in connection with multiphase flow, because many important petroleum reservoirs are in fractured rock formations. Of special interest are reservoirs composed of fractured porous rocks, in which the blocks surrounded by the network of fractures are porous. The permeability of such blocks is often rather low; but the porosity, and hence the storage capacity for fluids, is very high. This 'double porosity' model for fractured porous rock domains was first introduced in the field of reservoir engineering.

In the past two or three decades, fractured rock domains have received increasing attention not only in reservoir engineering and hydrology but also in connection with geological isolation of radioactive waste. Locations in both the saturated and unsaturated zones have been under consideration. Such repositories are sources of heat and potential sources of ground water contamination. Thus, in addition to the transport of mass of fluid phases in single or multiphase flow, the issues of heat transport and mass transport of components have to be addressed.

A large number of articles on these subjects exist in the scientific and professional literature of a number of disciplines, including geology, hydrology, reservoir engineering, and environmental engineering. We feel that the time is ripe to put together the main ideas and methodologies found in the literature on flow and tracer transport in fractured rock domains, in the form of an edited book written by experts from various disciplines, for the benefit of researchers and practitioners. We have decided not to excessively edit or unify the chapters. This has the advantage that each chapter is relatively self-contained and can be studied independently of the others. Also, the reader may find it interesting to sample the varying styles of different authors in different disciplines.

The editors hope that the book will serve its purposes: to present the state of the art on flow and tracer transport in fractured rock domains as viewed by scientists working in different disciplines, to encourage practical field engineers and scientists to use the various methods suggested in this book, and to stimulate researchers to further advance the state of the art of this fruitful research area."



Beauheim, R.L., 1986. Hydraulic-Test Interpretations for Well DOE-2 at the Waste Isolation Pilot Plant (WIPP) Site. SAND86-1364. Sandia National Laboratories, Albuquerque, NM. WPO 27656.

ABSTRACT, p 3;

" Eleven different zones were tested in Well DOE-2 in five phases of testing between 1984 and 1986. Testing techniques included a constant-head, borehole-infiltration test, drill-stem tests, slug tests, pressure-pulse tests, and multiwell pumping tests. Four of the zones tested--the lower Dewey Lake Red Beds, the Tamarisk Member of the Rustler Formation, the lower unnamed member of the Rustler Formation and the Rustler/Salado contact, and the entire Salado Formation--had permeabilities too low to measure with the equipment and test techniques used. The other zones had permeabilities ranging over six orders of magnitude. No saturated strata were encountered above the Rustler Formation, although parts of the middle Dewey Lake Red Beds appear to have appreciable permeability.

In the Rustler Formation, the Culebra Dolomite Member is the most permeable unit, having a transmissivity of  $\sim 90 \text{ ft}^2/\text{day}$ . The Culebra behaves hydraulically as a double-porosity system, with the major permeability provided by fractures and the major storage provided by matrix porosity. The Culebra at DOE-2 is well connected hydraulically to the Culebra at Wells H-6b and WIPP-13 to the west, probably by interconnected fractures. Response times between these wells are very short ( $< 1 \text{ day}/10,000 \text{ ft}$ ). The Culebra does not appear to be as fractured to the south at Wells WIPP-12 and 18, or to the east at Well H-5b, as indicated by delayed, low-magnitude (or nonexistent) responses to DOE-2 pumping, and by low permeabilities interpreted from other tests conducted at those wells. The other Rustler members at DOE-2, which are not known to be fractured and do not display hydraulic responses typical . . ."



Beauheim, R.L., 1987. Interpretation of the WIPP-13 Multipad Pumping Test of the Culebra Dolomite at the Waste Isolation Pilot Plant (WIPP) Site. SAND87-2456. Sandia National Laboratories, Albuquerque, NM. WPO 28512.

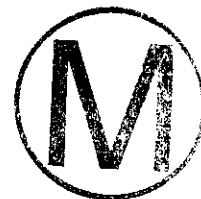
ABSTRACT, p 3;

" A large-scale pumping test of the Culebra Dolomite Member of the Rustler Formation was performed in early 1987 at the Waste Isolation Pilot Plant (WIPP) site in southeastern New Mexico. This test (the WIPP-13 or northern) multipad test, complemented the H-3 (or southern) multipad test (conducted in late 1985 and early 1986) by creating a hydraulic stress that could be measured over the northern portion of the WIPP site. The test consisted of pumping well WIPP-13 at a rate of 30 gpm for 36 days and monitoring drawdown and recovery responses in 17 observation wells and one WIPP shaft. Responses were observed in 14 of these wells, including one well 20 550 ft from WIPP-13 and in the WIPP exhaust shaft. Several of these wells had also responded during the H-3 multipad test.

Individual well tests at locations around the WIPP site have demonstrated that the Culebra is a heterogeneous, water-bearing unit. The responses measured at observation wells to pumping tests in heterogeneous systems cannot be rigorously interpreted using standard analytical (as opposed to numerical) techniques developed for tests in homogeneous, porous media. Application of analytical techniques to data from heterogeneous media results in evaluations of average hydraulic properties between pumping and observation wells that are nonunique in the sense that they are representative only of the responses observed when a hydraulic stress is imposed at a certain location. These 'apparent' hydraulic properties do, however, provide a qualitative understanding of the nature and distribution of both hydraulic properties and heterogeneities or boundaries within the tested area.

The interpretations of the responses at the pumping and observation wells are consistent with the following conceptualization: The Culebra is a fractured, double-porosity system around WIPP-12, H-6, and DOE-2, with relatively high transmissivity ( $\sim 70$  ft<sup>2</sup>/day) and relatively low storativity ( $5 \times 10^{-6}$  to  $8 \times 10^{-6}$ ). This system appears to extend further to the north toward WIPP-30, although WIPP-30 itself lies in a lower transmissivity zone. The apparent transmissivity between WIPP-13 and observation wells toward the center of the WIPP site to the south and east, where fracturing in the Culebra decreases, decreases to 16 to 28 ft<sup>2</sup>/day, and apparent storativity increases to  $3.6 \times 10^{-5}$  to  $5.5 \times 10^{-5}$ . To the west toward Nash Draw, the apparent transmissivity increases to 265 to 650 ft<sup>2</sup>/day, reflecting increased fracturing in that direction, while the apparent storativity increases to  $5.2 \times 10^{-5}$  to  $6.4 \times 10^{-5}$ .

The analyses of the responses measured at observation wells to the WIPP-13 multipad pumping test provide a qualitative conceptualization of three distinct domains within a heterogeneous portion of the Culebra north of the center of the WIPP site. This conceptualization is being refined by using numerical-modeling techniques to simulate the WIPP-13 multipad test and other tests at the WIPP site in an attempt to define the distribution of hydraulic properties that will reproduce the responses observed."



Beauheim, R.L. 1987. Analysis of Pumping Tests of the Culebra Dolomite Conducted at the H-3 Hydropad at the Waste Isolation Pilot Plant (WIPP) Site. SAND86-2311. Sandia National Laboratories, Albuquerque, NM. WPO 28468.



**ABSTRACT;**

" Two pumping tests were conducted in the Culebra Dolomite Member of the Rustler Formation at the H-3 hydropad at the Waste Isolation Pilot Plant (WIPP) site. The first test was in 1984, with well H-3b3 pumped for 14 days at an average rate of 4 gpm. The second test, the H-3 multipad test, was in late 1985 and early 1986, with well H-3b2 pumped for 62 days at an average rate of 4.8 gpm. Both tests provided information on the hydraulic properties of the Culebra at the H-3 hydropad. The second test provided information on average Culebra hydraulic properties on a much larger scale; responses were observed up to 8000 ft from the pumping well.

The interpretation of these tests had three principle objectives. The first was to determine the most appropriate conceptualization of the nature of the Culebra flow system around the H-3 hydropad. The pumping well responses during the H-3 tests appear to be those of wells completed in a double-porosity medium with unrestricted interporosity flow. In such a system, fractures provide the bulk of the permeability, while matrix pores provide the majority of the storage capacity. The importance of fracture flow is indicated by the speed with which the observation wells on the H-3 hydropad respond to pumping and the nearly identical behaviors of these wells and the pumping well. The similarity between pumping- and observation-well behavior on the H-3 hydropad is so pronounced that the responses of all three wells on the hydropad can be interpreted only by using pumping-well analytical techniques, not observation-well analytical techniques. H-3b1 and H-3b3, in particular, appear to be very well connected by fractures.

The second objective was to quantify the hydraulic properties of the Culebra in the vicinity of the H-3 hydropad. The total-system (fractures plus matrix) transmissivity of the Culebra derived from the first test is 2.9 ft<sup>2</sup>/day; that from the second test is 1.7 ft<sup>2</sup>/day. The lower value derived from the second test probably represents lower transmissivity (lower fracture connectivity) at H-3b2 than at H-3b3, and/or lower average transmissivity of the volume of Culebra stressed in the multipad test as opposed to the smaller volume stressed in the first test. The fracture-to-total-system storativity ratios derived from the various analyses range from 0.03 to 0.25, indicating a relatively high degree of storage within the fractures. The highest storativity ratios were consistently found at H-3b1. Wellbore skin values are highly negative, indicating direct wellbore connection with fractures.

The third objective was to quantify the average hydraulic properties of the Culebra between the H-3 hydropad and more-distant observations wells. Meeting this objective . . ."

Compliance Certification Application Reference Expansion

---

Beauheim, R.L., and Holt, R.M. 1990. "Hydrogeology of the WIPP Site." Geological and Hydrological Studies of Evaporites in the Northern Delaware Basin for the Waste Isolation Pilot Plant (WIPP), New Mexico. Field Trip #14 Guidebook, Geological Society of America 1990 Annual Meeting, Dallas, TX, October 19-November 1, 1990. pp. 131-179. D.W. Powers, R.M. Holt, R.L. Beauheim, and N. Rempe, leaders. SAND90-2035J. Dallas Geological Society, Dallas, TX. WPO 29377.

Introduction, p 2, col. 1;

" The field trip provides an on site introduction to the geology and hydrology of the Waste Isolation Pilot Plant (WIPP) site in southeastern New Mexico. The mission of the WIPP is to dispose of transuranic (TRU) waste generated since 1970 by the U. S. defense programs. After 18 years of study and the publication of hundreds of documents, these studies remain unknown to many geologists. Although many of the studies are unique, they lack recognition. This field trip and guidebook begin to redress this imbalance."



Beauheim, R.L., Hassinger, B.W. and Klaiber, J.A. 1983. Basic Data Report for Borehole Cabin Baby-1 Deepening and Hydrologic Testing, WTSD-TME-020, Albuquerque, NM, U.S. DOE.

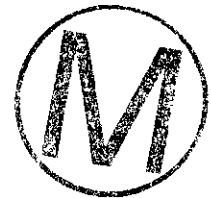
Section 1.0 ABSTRACT, p 1-1;

" Borehole Cabin Baby-1 was originally drilled to a depth of 4159.0 feet below kelly bushing (8.0 feet above ground surface) in 1974 and 1975 as a 'wildcat' hydrocarbon exploratory well. Control of the borehole was given to the U. S. Department of Energy (DOE) after it was found to be a 'dry hole'. Cabin Baby-1 was reentered, deepened, and hydrologically tested in August and September, 1983. The well is located in Section 5, T23S, R31E, just outside the limit of WIPP Zone III, approximately 2.5 miles south of the WIPP exploratory shaft.

The deepening and testing of Cabin Baby-1 was undertaken for several reasons:

- To provide data on the hydrologic properties, including hydrostatic head potential of selected permeable zones in the Bell Canyon Formation.
- To provide representative fluid samples from selected permeable zones in the Bell Canyon Formation for determination of fluid composition and density.
- To define further the stratigraphy of the upper Bell Canyon Formation at the Cabin Baby-1 location.

The borehole was deepened from the previous total depth to a new depth of 4298.6 feet below kelly bushing by continuous coring. Field operations related to deepening and logging of the borehole began August 12, 1983 and were completed August 30, 1983. Hydrologic testing activities began August 30, 1983 and were completed September 29, 1983. Drill-stem tests were conducted in four zones in the Bell Canyon Formation, and one test of the Salado Formation was performed. Fluid samples were collected from the Hays and Olds sandstones of the Bell Canyon Formation."



Compliance Certification Application Reference Expansion

---

Beauheim, R.L., Dale, T.F., and Pickens, J.F. 1991. Interpretations of Single-Well Hydraulic Tests of the Rustler Formation Conducted in the Vicinity of the Waste Isolation Pilot Plant (WIPP) Site, 1988-1989. SAND89-0869. Sandia National Laboratories, Albuquerque, NM.

ABSTRACT, p i;

" In 1988 and 1989, hydraulic tests were conducted in seven wells to provide data on the transmissivities of four members of the Rustler Formation. These data will be used in modeling of groundwater flow through the Rustler Formation. Pressure-pulse, slug, and pumping tests were performed. The pressure-pulse and slug tests were simulated using the computer code GTFM to obtain estimates of transmissivity and the radius of influence of the testing. The pressure-pulse tests proved difficult to interpret because no measurements of test-zone compressibility were made. Slug tests at two of the wells were also interpreted using type curves based on an analytical solution for slug tests. The type-curve results differed by 35 percent or less from the transmissivities determined using GTFM. The pumping test was interpreted using the computer code Interpret/2. The slug-test interpretations provided estimates of transmissivity as follows:  $2.1 \times 10^{-4}$  to  $3.0 \times 10^{-4}$  ft<sup>2</sup>/day for the siltstone within the unnamed lower member of the Rustler at well H-16; 0.16 to 0.20 ft<sup>2</sup>/day and 1.9 to 2.5 ft<sup>2</sup>/day for the Culebra dolomite at wells AEC-7 and D-268, respectively;  $2.1 \times 10^{-3}$  to  $2.7 \times 10^{-3}$  ft<sup>2</sup>/day and 0.14 to 0.18 ft<sup>2</sup>/day for the Magenta dolomite at wells H-2b1 and H-3b1, respectively; and  $3.5 \times 10^{-3}$  to  $4.5 \times 10^{-3}$  ft<sup>2</sup>/day for the Forty-niner claystone at well H-3d. The calculated radii of influence of the tests ranged from about 50 to 300 ft. Interpretations of the pumping test of the Culebra dolomite at well H-18 are ambiguous in that the test responses are equally representative of a single-porosity medium having a transmissivity of 2.0 ft<sup>2</sup>/day and a no-flow boundary 58 ft from H-18, and of a double-porosity medium with a transmissivity of 1.0 ft<sup>2</sup>/day and no apparent boundaries."



Beauheim, R.L., Saulnier, Jr., G.J., and Avis, J.D. 1991. Interpretation of Brine-Permeability Tests of the Salado Formation at the Waste Isolation Pilot Plant Site: First Interim Report, SAND90-0083, Albuquerque, NM, Sandia National Laboratories.

ABSTRACT, p i;

" Pressure-pulse tests have been performed in bedded evaporites of the Salado Formation at the Waste Isolation Pilot Plant (WIPP) site to evaluate the hydraulic properties controlling brine flow through the Salado. Hydraulic conductivities ranging from about  $10^{-14}$  to  $10^{-11}$  m/s (permeabilities of about  $10^{-21}$  to  $10^{-18}$  m<sup>2</sup>) have been interpreted from nine tests conducted on five stratigraphic intervals within eleven meters of the WIPP underground excavations. Tests of a pure halite layer showed no measurable permeability. Pore pressures in the stratigraphic intervals range from about 0.5 to 9.3 MPa. An anhydrite interbed (Marker Bed 139) appears to be one or more orders of magnitude more permeable than the surrounding halite. Hydraulic conductivities appear to increase, and pore pressures decrease, with increasing proximity to the excavations. These effects are particularly evident within two or three meters of the excavations. Two tests indicated the presence of apparent zero-flow boundaries about two to three meters from the boreholes. The other tests revealed no apparent boundaries within the radii of influence of the tests, which were calculated to range from about four to thirty-five meters from the test holes. The data are sufficient to determine if brine flow through evaporites results from Darcy-like flow driven by pressure gradients within naturally interconnected porosity or from shear deformation around excavations connecting previously isolated pores, thereby providing pathways for fluids at or near lithostatic pressure to be driven towards the low-pressure excavations. Future testing will be performed at greater distances from the excavations to evaluate hydraulic properties and processes beyond the range of excavation effects.



**Compliance Certification Application Reference Expansion**

---

Bechtel National. 1986. Quarterly Geotechnical Field Data Report. DOE/WIPP-221. U.S. Department of Energy, Carlsbad, NM.

FOREWORD, p iii;

" The purpose of the Quarterly Geotechnical Field Data Reports is to meet the U.S. Department of Energy intent to provide geotechnical and related information from WIPP underground activities to interested persons or groups in a timely manner. This Quarterly Geotechnical Field Data Report (GFDR) presents information obtained from the geotechnical studies at the WIPP site underground facilities from April 1 through June 30, 1985, as well as all previous data collected from the geomechanical instruments. During this period, the geotechnical activities at the site included maintaining and repairing instruments and monitoring previously installed geomechanical instruments in shafts, underground drifts, and test rooms. The data presented in this GFDR reflect the update of continuing measurements and monitoring. Also continuing and included in this report are preliminary geotechnical and structural analyses and interpretations of the data.

The GFDR is organized into two principle parts. The first part, Geotechnical Field Data, . . ."



Compliance Certification Application Reference Expansion

---

Bell, J.T., Coleman, C.F., Costanzo, D.A., and Biggers, R.E. 1973. "Plutonium polymerization--III. The nitrate precipitation of Pu(IV) polymer." Journal of Inorganic and Nuclear Chemistry. Vol. 35: 629-632.

ABSTRACT, p 629;

" The precipitation of aged Pu(IV) polymer by  $\text{HNO}_3$ ,  $\text{LiNO}_3$ ,  $\text{Al}(\text{NO}_3)_3$  and  $\text{NaNO}_3$  has been observed. With the exception of  $\text{LiNO}_3$ , the precipitation of 0.00678M Pu(IV) polymer was independent of the source of  $\text{NO}_2^-$  and the maximum amount of precipitated polymer occurred at 1.0  $\text{NO}_2^-$ . Further addition of  $\text{NO}_2^-$  redissolved the polymer. The nitrate precipitation of Pu(IV) polymer has been analyzed according to the solubility product principle and has been found to closely resemble a solubility product mechanism."



Bell, J.T., Costanzo, D.A. and Biggers, R.E. 1973. "Plutonium polymerization--II. Kinetics of the plutonium polymerization." *Journal of Inorganic and Nuclear Chemistry*. Vol. 35: 623-628.

ABSTRACT, p 623;

" Experimental data for the distribution of Pu(III), Pu(IV), Pu(V), Pu(VI) and Pu(IV) polymer have been used to calculate the rates of polymerization of Pu(IV). The rate of formation of Pu(IV) polymer is proportional to the first power of the Pu(IV) concentration and to the inverse square of the acidity as long as the solution contains a detectable amount of Pu(IV). When the concentration of Pu(IV) is not detectable, the rate of polymerization is proportional to the product of the square roots of the Pu(V) and (III) concentrations. When the concentrations of both the Pu(IV) and (III) are not detectable, the rate of polymerization is proportional to the product of the squares of the Pu(V) and the acid concentrations and to the inverse first power of the Pu(VI) concentration."



Bellin, A., Salandin, P., and Rinaldo, A. 1992. Simulation of Dispersion in Heterogeneous Porous Formations: Statistics, First-Order Theories, Convergence of Computations. *Water Resources Research*, Vol. No. 9, pp. 2211-2228.

ABSTRACT, p. 2211;

" This paper discusses the results of numerical analysis of dispersion of passive solutes in two-dimensional heterogeneous porous formations. Statistics of flow and transport variables, the accuracy and the role of approximations implicit in existing first-order theories, and the convergence of computational results are investigated. The results suggest that quite different rates of convergence with Monte Carlo runs hold for different spatial moments and that over 1000 realizations are required to stabilize second moments even for relatively mild heterogeneity ( $\sigma_Y^2 < 1.6$ ). This has implications for the extent of the spatial domain for single-realization numerical studies of the same type. A comparison of the variance of plumes with the results of linear theories ( $0.05 < \sigma_Y^2 < 1.6$ ) shows an unexpectedly broad validity field for the theoretical solution obtained from a suitable linearization of flow and transport. Reformulation of the same problem linearizing in turn the flow or the transport equation shows opposite deviations from the linear theory. The interesting consequence is that the errors induced by linearizations in the flow or the transport equations have different signs, and their effects on the moments of dispersing plumes are compensating, thereby yielding consistent formulations. Unexpected features of the statistics of probability distributions of longitudinal and transverse velocities and travel times are also computed and discussed."



Berger, A. 1988. "Milankovitch Theory and Climate," *Reviews of Geophysics*. Vol. 26, no. 4, 624-657.

ABSTRACT, p 624, col 1;

" Among the longest astrophysical and astronomical cycles that might influence climate (and even among all forcing mechanisms external to the climatic system itself), only those involving variations in the elements of the Earth's orbit have been found to be significantly related to the long-term climatic data deduced from the geological record. The aim of the astronomical theory of paleoclimates, a particular version of which being due to Milankovitch, is to study this relationship between insolation and climate at the global scale. It comprises four different parts: the orbital elements, the insolation, the climate model, and the geological data. In the nineteenth century, Croll and Pilgrim stressed the importance of severe winters as a cause of ice ages. Later, mainly during the first half of the twentieth century, Köppen, Spitaler, and Milankovitch regarded mild winters and cool summers as favoring glaciation. After Köppen and Wagerer related the Milankovitch new radiation curve to Penck and Brückner's subdivision of the Quaternary, there was a long-lasting debate on whether or not such changes in the insolation can explain the Quaternary glacial-interglacial cycles. In the 1970s, with the improvements in dating, in acquiring, and in interpreting the geological data, with the advent of computers, and with the development of astronomical and climate models, the Milankovitch theory revived. Over the last 5 years it overcame most of the geological, astronomical, and climatological difficulties. The accuracy of the long-term variations of the astronomical elements and of the insolation values and the stability of their spectra have been analyzed by comparing seven different astronomical solutions and four different time spans (0-0.8 million years before present (Myr B.P.), 0.8-1.6 Myr B.P., 1.6-2.4 Myr B.P., and 2.4-3.2 Myr B.P.). For accuracy in the time domain, improvements are necessary for periods earlier than 2 Myr B.P. As for the stability of the frequencies, the fundamental periods (around 40, 23, and 19 kyr) do not deteriorate with time over the last 5 Myr, but their relative importance for insolation and each astronomical parameter is a function of the period considered. Spectral analysis of paleoclimatic records has provided substantial evidence that, at least near the obliquity and precession frequencies, a considerable fraction of the climatic variance is driven in some way by insolation changes forced by changes in the Earth's orbit. Not only are the fundamental astronomical and climatic frequencies alike, but also the climatic series are phase-locked and strongly coherent with orbital variations. Provided that monthly insolation (i.e., a detailed seasonal cycle) is considered for the different latitudes, their long-term deviations can be as large as 13% of the long-term average, and sometimes considerable changes between extreme values can occur in less than 10,000 years. Models of different categories of complexity, from conceptual ones to three-dimensional atmospheric general circulation models and two-dimensional time-dependent models of the whole climate system, have now been astronomically forced in order to test the physical reality of the astronomical theory. The output of most recent modeling efforts compares favorably with data of the past 400,000 years. Accordingly, the model predictions for the next 100,000 years are used as a basis for



**Compliance Certification Application Reference Expansion**

---

forecasting how climate would evolve when forced by orbital variations in the absence of anthropogenic disturbance. The long-term cooling trend which began some 6,000 years ago will continue for the next 5,000 years; this first temperature minimum will be followed by an amelioration at around 15 kyr A.P. (after present), by a cold interval centered at 23 kyr A.P., and by a major glaciation at around 60 kyr A.P."



Bertram-Howery, S.G., and R. L. Hunter, eds. 1989. Preliminary Plan for Disposal-System Characterization and Long-term Performance Evaluation of the Waste Isolation Pilot Plant. SAND89-0178. Albuquerque, NM: Sandia National Laboratories.

ABSTRACT;

" The U. S. Department of Energy is planning to dispose of transuranic wastes at the Waste Isolation Pilot Plant (WIPP) near Carlsbad, New Mexico. Sandia National Laboratories is responsible for evaluating the compliance of the WIPP with the Environmental Protection Agency's Environmental Standards for the Management and Disposal of Spent Nuclear Fuel, High-Level and Transuranic Radioactive Wastes (40 CFR 191, Subpart B). This plan has been developed to present the issues that will be addressed before compliance can be evaluated. These issues examine the procedural requirements for evaluating compliance, which follow from the procedural nature of the Standard, and the technical requirements for further characterizing the behavior of the disposal system, including uncertainties, to support the compliance assessment. The plan briefly describes the activities that will be conducted prior to 1993 by Sandia to characterize the WIPP disposal system's behavior and predict its performance."





Bertram-Howery, S.G., M.G. Marietta, R.P. Rechard, P.N. Swift, D.R. Anderson, B.L. Baker, J.E. Bean, Jr., W. Beyeler, K.F. Brinster, R.V. Guzowski, J.C. Helton, R.D. McCurley, D.K. Rudeen, J.D. Schreiber, and P. Vaughn, 1990. Preliminary Comparison with 40 CFR Part 191, Subpart B for the Waste Isolation Pilot Plant, December 1990, SAND90-2347, Albuquerque, NM, Sandia National Laboratories.

ABSTRACT, p i;

" The Waste Isolation Pilot Plant (WIPP) is planned as the first mined geologic repository for transuranic (TRU) wastes generated by defense programs of the United States Department of Energy (DOE). Before disposing of waste at the WIPP, the DOE must evaluate compliance with the United States Environmental Protection Agency's (EPA) Standard, *Environmental Radiation Protection Standards for Management and Disposal of Spent Nuclear Fuel, High-Level and Transuranic Radioactive Wastes* (40 CFR Part 1919, U. S. EPA, 1985). Sandia National Laboratories (SNL) is evaluating long-term performance against criteria in Subpart B of the Standard. 'Performance assessment' as used in this report includes analyses for the Containment Requirements (§ 191.13(a)) and the Individual Protection Requirements (§ 191.15). Because proving predictions about future human actions or natural events is not possible, the EPA expects compliance to be determined on the basis of specified quantitative analyses and informed, qualitative judgment. The goal of the WIPP performance-assessment team at SNL is to provide as detailed and thorough a basis as practical for the quantitative aspect of that decision.

This report summarizes SNL's late-1990 understanding of the WIPP Project's ability to evaluate compliance with Subpart B. This preliminary assessment cannot be defensibly compared to the requirements of the Standard to interpret whether the WIPP disposal system complies with Subpart B. Defensibility of the compliance evaluation ultimately will be determined primarily by qualitative judgment regarding 'reasonable expectations of compliance,' assuming that concept is retained by the EPA in promulgating the vacated Subpart B. Other considerations such as completeness and adequacy of the numerical simulations will also be factors in determining defensibility. Performance assessment must determine the events that can occur, the likelihood of these events, and the consequences of these events. The impacts of uncertainties must be characterized and displayed; however, no single summary measure can adequately display all the information produced in a performance assessment. Adequate documentation is an essential part of a performance assessment.

In lieu of results suitable for comparison with the Standard, this report presents results of sensitivity analyses that address specific uncertainties in the modeling system. All results are preliminary, and are conditional on assumed conceptual models and parameter value distributions. The results show the degree to which some uncertainties in the conceptual models that describe aspects of disposal-system behavior may affect predicted performance. The results also demonstrate the methodology used to assess performance. The reported complementary cumulative distribution functions (CCDF's) are statistical means of families of CCDFs. The modeling system is sensitive to changes in scenario probabilities,

## Compliance Certification Application Reference Expansion

---

and reductions in the probability of intrusion significantly reduce predicted probabilistic cumulative releases. Comparison of clay-lined-fracture and dual-porosity transport models for the dominant water-bearing unit above the repository indicate a significant increase in radionuclide retardation and a consequent reduction in predicted releases with the dual-porosity model. Simulations of a variable number of intrusions show that, for the selected probability model, multiple intrusions do not increase the largest cumulative releases. Simulations of a hypothetical waste modification suggest that for modifications to be effective, waste permeability must be reduced more than four orders of magnitude below the estimated unmodified value to restrict brine flow to an intruding borehole. Simulations of gas generation and the effects gas will have on brine flow and radionuclide transport are not sufficiently advanced to be incorporated in this year's CCDF curves, but preliminary results of one-dimensional simulations are included. Preliminary analyses for the Individual Protection Requirements suggest that no releases will occur; therefore, dose predictions are not likely to be required.

Although disposal-system characterization work has been underway for about 15 years, and much is known about the WIPP, all work necessary to support the performance assessment has not been completed. Most work currently in progress to support the performance assessment is not advanced enough to support a defensible comparison to the Standard because many important modules are in preliminary or intermediate stages of understanding or readiness. The compliance assessment system can be used for sensitivity and uncertainty analyses, and is adequate for preliminary performance studies."



Bird, R.B., Stewart, W.E., and Lightfoot, E.N. 1960. Transport Phenomena. Wiley & Sons, New York, NY. NNA. 900919.0195.

Chapter 16, p 513;

"§16.5 THEORIES OF ORDINARY DIFFUSION IN LIQUIDS

In the absence of rigorous theory for diffusion in liquids, there are two rough theories that have been useful in making order of magnitude of calculations: the *hydrodynamical theory* and *Eyring theory*. (We have already given some results of the theories of Eyring and co-workers in connection with the calculation of viscosity and thermal conductivity of liquids.)

The *hydrodynamical theory* takes as its starting point the Nernst-Einstein equation,<sup>1</sup> which states that the diffusivity of a single particle or solute molecule of *A* through a stationary medium *B* is

$$D_{AB} = \kappa T \frac{u_A}{F_A} \tag{16.5-1}$$

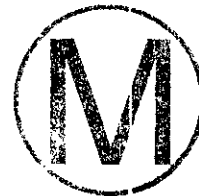
in which  $u_A/F_A$  is the 'mobility' of the particle *A* (that is, the steady-state velocity attained by the particle under the action of a unit force). A relation between force and velocity for a rigid sphere moving in 'creeping flow' (that is,  $Re \ll 1$ ) may be obtained from hydrodynamics. If the possibility of 'slip' at the sphere-fluid interface is taken into account, then<sup>2</sup>

$$F_A = 6\pi \mu_B \mu_A R_A \left( \frac{2\mu_B + R_A \beta_{AB}}{3\mu_B + R_A \beta_{AB}} \right) \tag{16.5-2}$$

in which  $\mu_B$  is the viscosity of the pure solvent,  $R_A$  is the radius of the diffusing particle, and  $\beta_{AB}$  is the *coefficient of sliding friction*. It has been pointed out<sup>3</sup> that there are two limiting cases of interest:

a. If there is no tendency for the fluid to slip at the surface of the diffusing particle ( $\beta_{AB} = \infty$ ), then Eq. 16.5-2 becomes Stoke's law. (See §2.6).

$$F_A = 6\pi \mu_B \mu_A R_A$$



(16.5-3)

and substitution into Eq. 16.5-1 gives

$$\frac{D_{AB}\mu_B}{\kappa T} = \frac{1}{6\pi R_A} \quad (16.5-4)$$

which is usually called the *Stokes-Einstein equation*. Equation 16.5-4 has been shown to be fairly good for describing the diffusion of *large spherical particles* or *large spherical molecules*, under which conditions the solvent appears to the diffusing species as a continuum.<sup>4</sup>

b. If there is no tendency for the fluid to stick at the surface of the diffusing particle ( $\beta_{AB} = 0$ ), Eq 16.5-2 becomes

$$F_A = 4\pi\mu_B\mu_A R_A \quad (16.5-5)$$

and substitution into Eq. 16.5-1 gives

$$\frac{D_{AB}\mu_B}{\kappa T} = \frac{1}{4\pi R_A} \quad (16.5-6)$$

If the molecules are all alike (that is, *self-diffusion*) and if they can be assumed to be arranged in a cubic lattice with all molecules just touching, the  $2R_A$  may be set equal to

$$(\tilde{V}_A/\tilde{N})^{1/2} \quad \text{and}$$

$$\frac{D_{AA}\mu_A}{\kappa T} = \frac{1}{2\pi} \left( \frac{\tilde{N}}{\tilde{V}_A} \right)^{1/2} \quad (16.5-7)$$



It has been shown<sup>5</sup> that Eq. 16.5-7 predicts the self-diffusion data for a number of liquids within about  $\pm 12$  per cent; that comparison includes polar substances, associated substances, liquid metals, and molten sulfur.

It is thus seen that the simple hydrodynamical approach gives expressions for the diffusion coefficient for spherical molecules in dilute solution and also for the coefficient of self-diffusion. The theory further predicts that there should be a variation of  $D_{AB}$  with the size of the diffusing species. The hydrodynamical theory suggests that the shape of the

Compliance Certification Application Reference Expansion

---

diffusing species may well be important, since the friction factor increases by a factor of about 2 as the length-to-width ratio of a body goes from 1 to 10.

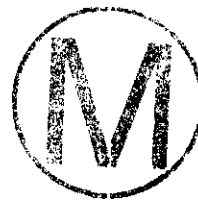
<sup>1</sup>F. Daniels and R. A. Alberty, *Physical Chemistry*, Wiley, New York (1955), p. 650. See also Eq. 18.4-14a.

<sup>2</sup>H. Lamb, *Hydrodynamics*, Dover, New York, §337.

<sup>3</sup>R. Fürth, in *Handbuch der physikalischen und technischen Mechanik*, Barth, Leipzig (1931), Vol. 7, p. 635.

<sup>4</sup>W. Sutherland, *Phil. Mag.*, **9**, 781-785 (1905).

<sup>5</sup>J.C.M. Li and P. Chang, *J. Chem. Phys.*, **23**, 518-520 (1955)."



Compliance Certification Application Reference Expansion

---

Borns, D.J., 1985. Marker Bed 139: A Study of Drillcore From A Systematic Array, SAND85-0023, Sandia National Laboratories, Albuquerque, NM.

ABSTRACT, p 3;

" In southeastern New Mexico, Marker Bed 139 (referred to in this report as MB139) is one of 45 numbered siliceous or sulfatic units within the Salado Formation of the northern Delaware Basin. MB139 is divided into five zones. Zones I and V are the upper and lower contact zones, respectively. Zone II is a syndepositionally deformed subunit of polyhalitic anhydrite. Zone III is mixed anhydrite and polyhalitic anhydrite, a distinctive pale-green and pink, with subhorizontal fractures. Zone IV consists of interlayered halite and anhydrite without the overprint of polyhalite.

This sequence was transitional between submarine and subaerial. The anhydritic units of MB139 formed in salt-pan or mudflat environments or both. Undulations observed along the upper contact of MB139 are interpreted to result from traction deposits or from reworking of the upper portion of the marker bed during the transition from anhydrite to halite deposition. Zones II and III exhibit soft-sediment deformation and later traces of dewatering; e.g., formation of stylolites. Such deformation is not observed in the halite above MB139 or in Zone V and the halite units below MB139.

A distinctive set of subhorizontal fractures occurs in MB139 in mid-Zone III and, to some extent, in Zone IV. These fractures are partially infilled with halite and polyhalite. Brine occurrences at the mined facility horizon at the Waste Isolation Pilot Plant may be related to these fractures. The fractures formed either in response to stress cycles that were functions of sedimentation and erosion, or in response to deformation in the underlying Castile Formation. The subhorizontal orientation, dominant in the sampling to date, is more consistent with the interplay between stress and sedimentation cycles."



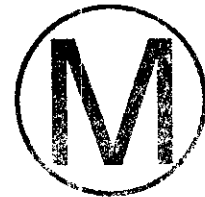
Compliance Certification Application Reference Expansion

---

Borns, D.J. and S.E. Shaffer. 1985. Regional Well-Log Correlation in the New Mexico Portion of the Delaware Basin. SAND83-1798. Sandia National Laboratories, Albuquerque, NM. WPO 24511.

ABSTRACT, p 3;

" Although well logs provide the most complete record of stratigraphy and structure in the northern Delaware Basin, regional interpretations of these logs generate problems of ambiguous lithologic signatures and one-hole anomalies. Interpretation must therefore be based on log-to-log correlation rather than on inferences from single logs. In this report, logs from 276 wells were used to make stratigraphic picks of Ochoan horizons (the Rustler, Salado, and Castile Formations) in the New Mexico portion of the Delaware Basin. Current log correlation suggests that: (1) the Castile is characterized by lateral thickening and thinning; (2) some Castile thinnings are of Permian age; (3) irregular topography in the Guadalupian Bell Canyon Formation may produce apparent structures in the overlying Ochoan units; and (4) extensive dissolution of the Salado is not apparent in the area of the Waste Isolation Pilot Plant (WIPP) site."



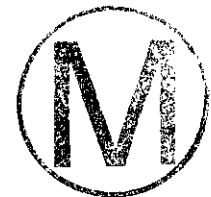
## Compliance Certification Application Reference Expansion

---

Borns, D.J., and Stormont, J.C. 1988. An Interim Report on Excavation Effect Studies at the Waste Isolation Pilot Plant: The Delineation of the Disturbed Rock Zone, SAND87-1375, Sandia National Laboratories, Albuquerque, NM. WPO 24694.

ABSTRACT, p i;

" For nuclear waste repositories with both long operational periods (50 yr) and long performance assessment periods (10 000 yr), the Disturbed Rock Zone (the zone of rock in which the mechanical and hydrologic properties have changed in response to excavation; abbreviated as DRZ) is important to both operational (e.g., slab or fracture failure of the excavation) and long term performance (e.g., seal system performance and fluid transport). At the Waste Isolation Pilot Plant (WIPP), the DRZ has been characterized with three approaches: visual observation; geophysical methods; and permeability measurements. Visual observations in drillholes indicate that fluids and fractures are common in the host rock of the underground facility. Geophysical studies have utilized radar, electromagnetic (EM), and direct current (DC) electromagnetic methods. Radar has been useful, but the penetration is limited by the water content and the bedded nature of the host rock. The EM method was able to detect a fourfold increase in resistivity from 1 to 5 m into the rock. This trend reflects a fourfold increase in the moisture content from near the excavation (0.5 to 1% by weight) to 5 m into the host rock (2 to 3% by weight). The DC method has been able to detect zones of moisture around the excavation. Numerous gas permeability measurements indicate that beyond 2 m from an excavation halite and interbeds (anhydrite and clay) allow very low gas flow (calculated permeabilities < 1 microdarcy for gas flow tests and < 0.01 microdarcy for brine-based permeability tests). Within 2 m of the excavation, very high flow rates ( $10^4$  SCCM) were measured. All three approaches have defined a DRZ at the WIPP extending laterally throughout the excavation and varying in depth from 1 to 5 m, according to the size and age of the opening."



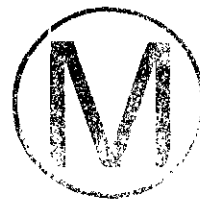
## Compliance Certification Application Reference Expansion

---

Borns, D.J., and Stormont, J.C. 1989. "The Delineation of the Disturbed Rock Zone Surrounding Excavations in Salt," Rock Mechanics as a Guide for Efficient Utilization of Natural Resources, Proceedings of the 30th U.S. Symposium, Morgantown, WV, June 19-22, 1989, A.W. Khair, ed., pp. 353-360. SAND88-2230C. A.A. Balkema, Brookfield, VT. WPO 29974.

ABSTRACT, p 353;

" At the Waste Isolation Pilot Plant (WIPP) in southeastern New Mexico, the Disturbed Rock Zone (DRZ, the zone of rock in which the mechanical and hydrologic properties have changed in response to excavation) has been characterized with visual observations, geophysical methods, and gas-flow measurements. The visual observations, geophysics, and gas-flow tests have defined a DRZ at the WIPP extending laterally throughout the excavation and varying in depth from 1 to 5 m. Desaturation and microfracturing has occurred to some degree within the zone. The dilation that results from the microfracturing in the DRZ provides a component of the observed closure."



Borns, D.J., Pfeifer, M.C., Andersen, H.T., and Skokan, C.K. 1990. "Electrical Methods to Delineate Fluid Flow In Situ in Bedded Salt." In Society of Exploration Geophysicists Workshop on Permeability, Fluid Pressure and Pressure Seals in the Crust, Denver, CO, August 5-8, 1990. SAND90-1685A. Sandia National Laboratories, Albuquerque, NM. WPO 28590.

" Seepage into excavations and the observation of brine infilling boreholes suggest that brine flows at a depth of 650 m in the bedded salts at the Waste Isolation Pilot Plant near Carlsbad, NM. Due to the very low permeability ( $\leq 10^{-19} \text{m}^2/\text{sec}$ ) and the deformation around excavations and boreholes, traditional borehole hydrologic methods are problematic. Since there are large contrasts in resistivity between salt, unsaturated fractures and the brine that fills pores, geophysical methods, especially electrical, provide alternate techniques to characterize flow systems in bedded salt.

At the WIPP site, we have conducted charged-body (mise-a-la-mase), modified direct current (DC), and permanent DC-Resistivity array surveys. Each method shows that the geoelectric structure varies markedly in the seemingly homogeneous salt. Our assumption is that these differences mirror variations in the hydrologic flow system. The modified DC-Method and mise-a-la-mase methods suggest that the electrical structure and the fluid flow reflect a network of fractures in an anhydrite interbed. These fractures form in response to burial/denudation cycles and stress redistribution around underground excavations. Such fractures can remain propped for extended periods. The presence of stiff inclusions, such as the anhydrite interbeds, are important in the development flow systems and localized reservoirs.

Spontaneous potential surveys using the DC-Resistivity array show different current flow in each distinct interbed (approx. 1 m thick) that the underground excavation intersects. We map these units based on clay (generally  $\approx 5\%$ ) and secondary mineral content. We believe that the spontaneous potential reflects electrokinetic (pore fluid motion) currents and not chemoelectric currents. The different spontaneous potentials may indicate that fluid flow is highly stratified. This stratification may reflect the effects of intergranular impurities such as clays, polyhalite, and hematite. The DC-Resistivity arrays show that the excavation induced flow system rapidly dominates the natural flow system. The growth of a disturbed rock zone in part by dilatancy around the excavation affects fluid flow within a depth of several meters. Resistivity increases in some interbeds and decreases in other interbeds reflecting changes in saturation and permeability adjacent to the excavation."





Bredehoeft, J.D., Riley, F.S., and Roeloffs, E.A. 1987 Earthquakes and Groundwater. Earthquakes and Volcanoes, Vol 19, no. 4, pp. 138-146.

Dynamic Response, p 139;

" Certain seismic waves, especially Rayleigh waves, cause a volume change in the rock. A volume change in an aquifer produces a pressure change in the fluid. A Rayleigh wave produces a fluctuating fluid pressure in an aquifer, or fluid reservoir rock. The fluid level in an open observation well will try to go up and down in an attempt to balance pressure fluctuations in the aquifer. The dynamics of the oscillation in the well involve further complications.

As frequencies approach those of the Rayleigh waves (period from 8 to 30 seconds) the open water well behaves as a simple harmonic oscillator. In elementary physics the classic simple harmonic oscillator is a spring with a suspended mass. When disturbed, the mass will tend to oscillate up and down with the motion gradually decaying away. Some water wells behave in a similar manner. An experiment was performed in the Florida well in which the water level fluctuated 17 feet during the Alaskan earthquake. What is interesting is the free oscillation. The forcing, which was near the natural frequency of the well, built the oscillation; the oscillation then died away following the forcing.

If you remember back to freshman physics, you may recall that simple harmonic oscillators could be overdamped or underdamped. When disturbed, underdamped ones oscillate; overdamped ones do not oscillate but simply return with an exponential motion to their original resting place. Hilton Cooper and some colleagues at the USGS in the mid-60's developed the theory for the water well as a simple harmonic oscillator. The mass is provided by the height of the water column in the well; the damping depends on the ease with which water can move in and out of the well. In a highly permeable aquifer, water moves readily in and out of the well; if the permeability is sufficiently high, the well behaves as an underdamped oscillator. If the permeability is low, water can not move in and out of the well readily; the well is overdamped and the oscillation at the well is smaller than the pressure-head fluctuation in the aquifer. In particularly 'tight' (less permeable) formations, the well may not respond at all to seismic-pressure fluctuations in the aquifer.

The Florida well, which fluctuated so dramatically during the Alaskan earthquake, was excited by a Rayleigh wave-pressure change very close to the natural resonant frequency of the well. A 'sympathetic' response occurred; because of the inertia of the fluid column, the actual fluctuation of the water well was larger than the pressure-head change in the aquifer."

Static Response, p 141;

" The static response of a well to an earthquake is much less complicated than the dynamic response. The simplest geophysical model of an earthquake is a displacement along a finite rupture plane in an elastic material.

Using this simple elastic conceptual model, a dislocation along a finite rupture in an elastic space requires that the elastic material strain accommodate the displacement along the

## Compliance Certification Application Reference Expansion

---

rupture plane. Frank Press showed, following the Alaskan earthquake, that the simple model predicted measurable strains to large distances, perhaps to several thousand kilometers or more, for great earthquakes. The size of larger earthquakes is more or less correlated with the length of the fault which ruptures during the earthquake. The measurable strain field also depends upon the size of the rupture plane."



Brush, L.H., and Anderson, D.R. 1989. "Appendix E: Estimates of Gas Production Rates, Potentials, and Periods, and Dissolved Radionuclide Concentrations for the WIPP Supplemental Environmental Impact Statment." In Performance Assessment Methodology Demonstration: Methodology development for Evaluating Compliance With EPA 40 CFR Part 191, Subpart B, for the Waste Isolation Pilot Plant. M.G. Marietta, S.G. Bertram-Howery, D.R. Anderson, K.F. Brinster, R.V. Guzowski, H. Iuzzolino, and R.P. Rechard, eds. SAND89-2027. Sandia National Laboratories, Albuquerque, NM. pp. E-1 through E-14. In Appendix E of WPO 25952.

ABSTRACT;

" This report describes a demonstration of the performance assessment methodology for the Waste Isolation Pilot Plant (WIPP) to be used in assessing compliance with the Environmental Protection Agency's Standard, *Environmental Radiation Protection Standards for the Management and Disposal of Spent Nuclear Fuel, High-Level and Transuranic Radioactive Wastes* (40 CFR Part 191, Subpart B). This demonstration incorporates development and screening of potentially disruptive scenarios. A preliminary analysis of the WIPP disposal system's response to human intrusion scenarios produces preliminary complementary cumulative distribution functions (CCDFs) similar to those that will ultimately be used to assess the compliance of the WIPP with the Containment Requirements of the Standard. Preliminary estimates of scenario probabilities are used to construct two demonstration CCDFs. The conceptual model of the disposal system consists of geologic,, hydrologic, and disposal system subsystems along with the physical and chemical processes associated with these subsystems. Parameter values defining the systems contain uncertainties and modeling approximations of such a disposal system contributes to those uncertainties. The WIPP compliance assessment methodology consists of a system of techniques and computer codes that estimate releases of radionuclides from the disposal system, incorporating analysis of the parameter uncertainties in the estimates. Demonstration CCDFs are presented, but are not yet credible enough to judge the probability of compliance of the WIPP with the EPA Standard. One CCDF, based primarily on conservative reference data and conservative conceptual models, exceeds EPA limits, and another CCDF that represents effects of possible engineered alternatives does not exceed EPA limits."

Compliance Certification Application Reference Expansion

---

Buddemeier, R.W., and Hunt, J.R. 1988. "Transport of Colloidal Contaminants in Groundwater: Radionuclide Migration at the Nevada Test Site," Applied Geochemistry. Vol. 3, no. 5, 535-548.

ABSTRACT, p 535;

" Large-volume groundwater samples were collected at the Nevada Test Site from within a nuclear detonation cavity and from approximately 300 m outside the cavity. The samples were filtered and ultrafiltered, and the filtrates and various particle size fractions were analyzed for chemical composition and radionuclide activity. In samples from both locations, approximately 100% of the transition element (Mn,Co) and lanthanide (Ce,Eu) radionuclides were associated with colloids. Their presence outside the cavity indicates transport in the colloidal form. Distribution coefficients calculated for Ru, Sb, and Cs nuclides from both field sample locations indicate equilibrium partitioning on the 0.05-0.003  $\mu\text{m}$  colloids. Calculation of transport efficiencies relative to colloid mass concentrations and dissolved neutral or anionic nuclides indicates that both the cations and the radiolabelled colloids appear to experience capture by or exchange with immobile aquifer surfaces."



Compliance Certification Application Reference Expansion

---

Burton, P.L., Adams, J.W., and Engwall, C. 1993. "History of the Washington Ranch, Eddy County, New Mexico." In Carlsbad Region, New Mexico and West Texas. D.W. Love, J.W. Hawley, B.S. Kues, J.W. Adams, G.W. Austin, and J. M. Barker, eds., Forty-Fourth Annual Conference, October 6-9, 1993, pp 65-67. New Mexico Geological Society, Roswell, NM.

p 66, col 1, para 1;

" By today's standards, W. E. Washington, aka, Bill Washington, aka 'Uncle Bill' would be called 'a colorful character.' He *was* an unusual individual. With his intermarriage into the Chickasaw tribe, he was able to start what would become a small empire. The father of his bride was a wealthy man in his own right in Mississippi until he was forced into exile and marched over the terrible Trail of Tears to Indian Territory (now Oklahoma).

By marriage to May Ellen, Bill was . . ."



## Compliance Certification Application Reference Expansion

---

Cauffman, T.L., LaVenue, A.M., and McCord, J.P. 1990. Ground-Water Flow Modeling of the Culebra Dolomite. Volume II: Data Base, SAND89-7068/2, Sandia National Laboratories, Albuquerque, NM. WPO 10551.

PREFACE, p ii;

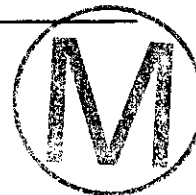
" The objective of this report is to present and discuss the hydrogeologic data base for the Culebra dolomite at the WIPP site. The data base includes:

- coordinates of the WIPP-area boreholes,
- Culebra elevations,
- Culebra transmissivities,
- Culebra storativities,
- Culebra formation-fluid densities,
- borehole fluid-density histories for the WIPP-site boreholes,
- estimates of the uncertainty in the borehole-fluid densities and the uncertainty in the related equivalent-freshwater heads,
- transient freshwater heads,
- estimates of an undisturbed freshwater head, and the uncertainty in this value for the WIPP-site boreholes, and
- shaft construction, grouting, and inflow histories.

This report documents the hydrogeologic data base subsequently used in a study which modeled ground-water flow in the Culebra dolomite. The modeling study is given in a companion report 'Ground-Water Flow Modeling of the culebra Dolomite: Volume I - Model Calibration', SAND89-7068/1, by A.M. LaVenue, T.L. Cauffman, and J.F. Pickens."



Chapman, J.B., 1986. Stable Isotopes in Southeastern New Mexico Groundwater: Implications for Dating Recharge in the WIPP Area, EEG-35, DOE/AL/10752-35. Environmental Evaluation Group, Santa Fe, NM.



EXECUTIVE SUMMARY, p iv;

" The first geologic repository for nuclear waste in the United States, the Waste Isolation Pilot Plant (WIPP), is being excavated at a depth of 2150 ft below ground surface in the Salado Formation in southeastern New Mexico. If a breach of the repository occurs, the water-bearing zones of the Rustler Formation, overlying the Salado, are considered to be the most likely pathways for the transport of radionuclides to the biosphere. A thorough characterization of the hydrology of the Rustler Formation is crucial to the evaluation of the consequences of a breach of the WIPP repository.

The Department of Energy is currently conducting studies of the Rustler Formation (many at the request of the State of New Mexico) that should significantly improve knowledge about the radionuclide contaminant transport ability of the Rustler. One recently completed study examined stable isotope data from Rustler groundwater and concluded that Rustler groundwater in the vicinity of the WIPP Site is not receiving significant modern meteoric recharge (Lambert, 1986). In addition, Lambert (1986) concludes that the stable isotope data reveal an hydraulic isolation of two possible discharge areas (well WIPP-29 and Surprise Spring) from the Rustler Formation elsewhere in Nash Draw and near the site. The conclusion of Lambert's (1986) stable isotope study allow longer residence time of water in the Rustler Formation and reduce the calculated consequences of a breach of the WIPP repository.

The present study compiles stable isotope data from throughout southeastern New Mexico and compares them to data from the WIPP area. The stable isotopic compositions of most samples of groundwater from the Rustler Formation are similar to the composition of other, verifiable young, groundwater in the area. Though the stable-isotope data cannot indicate ages for water in the various aquifers, neither do the data show any distinction between most Rustler groundwater and verifiable young groundwater.

A small number of samples, primarily from the Rustler/Salado contact east of Nash Draw, have isotopic compositions that are not characteristic of recently recharged meteoric water. These waters' enrichment in heavy isotopes may be due to mixing with deeper groundwater (supported by the stable isotopic composition of Salado fluid inclusions and Castile brine) or to exchange between the groundwater and hydrous minerals.

A comparison of the heavy isotope enrichment observed in evaporating waters and the composition of the water at WIPP-29 and Surprise Spring shows that the isotopic composition of these Nash Draw waters could be derived by evaporating Rustler groundwater. Based on stable isotopes, both WIPP-29 and Surprise Spring could be discharge areas for Rustler groundwater moving from elsewhere in Nash Draw and the east.

The enrichment in heavy isotopes found in water from pools in Carlsbad Caverns was used by Lambert (1986) as evidence that the relatively depleted Rustler water was recharged during a past, more pluvial, time. However, the uniqueness of the isotopic composition of

**Compliance Certification Application Reference Expansion**

---

water in the Caverns' pools suggest that rather than representing the composition of recent recharge, the heavy isotopes are enriched by evaporation and equilibrium isotope exchange in the humid cave environment. Recharge in the extreme karst environment near the cavern may also favor isotopically heavy precipitation."



Compliance Certification Application Reference Expansion

---

Chappell, J., and Shackelton, N.J. 1986. "Oxygen Isotopes and Sea Level," Nature. Vol. 324, No. 6093, 137-140.

p 137, para 1;

" From the time that detailed oxygen isotope records derived from foraminifera living in the constant-temperature environment of the abyssal ocean became available, there has been a discrepancy between the ice volume record that these records imply, and that derived from the altitude of dated coral terraces around the world. Here, we re-examine the data and conclude that the temperatures of the abyssal ocean has been an actively varying component of the climate system."



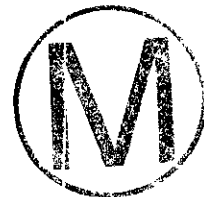
Compliance Certification Application Reference Expansion

---

Chaturvedi, L. 1993. "WIPP-Related Geological Issues." In Carlsbad Region, New Mexico and West Texas. D.W. Love, J.W. Hawley, B.S. Kues, J.W. Adams, G.S. Austin, and J. M. Barker, eds., Forty-Fourth Annual Field Conference, October 6-9, 1993, pp 331-338. New Mexico Geological Society, Roswell, NM.

ABSTRACT, p 331;

" The Waste Isolation Pilot Plant (WIPP) is a proposed repository for disposal of defense transuranic (TRU) radioactive waste. Located in southeastern New Mexico, 25 mi (40 km) east of Carlsbad, the repository has been excavated in the Salado Formation bedded salt at a depth of 2150 ft (655 m) below the surface. The concept of geologic isolation of radioactive waste, with the half-life of the radionuclides measured in tens of thousands of years, is to primarily rely on the geologic barriers to keep the radionuclides from leaking to the biosphere. Several geologic features and processes have been identified during the site characterization of the WIPP site that could impact the performance of the repository for the 10,000 year regulatory period. These include salt dissolution, breccia chimneys, brine reservoirs, Salado Formation hydrology, hydrology of the overlying Rustler Formation water-bearing units, disturbed rock behavior and natural resources. These geologic factors are being considered in the analysis of breach scenarios from the WIPP repository for the next 10,000 year period."

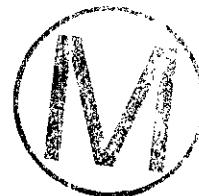


Choppin, G.R. 1988. "Humics and Radionuclide Migration." *Radiochimica Acta*. Vol 44/45: 23-28.

ABSTRACT, p. 23;

" Humic materials occur throughout the ecosphere in soils and waters, even in deep anoxic underground systems. The spectrum of molecular weights, the nature of the carbon skeleton and the types, positions and relative numbers of functional groups vary widely, in part depending on the origin and age of the humic material. Acid-base titration, C-13 CP/MAS solid-state nuclear magnetic resonance and ultrafiltration serve to define major operational characteristics of these materials. Humic materials sorb to surfaces and particulate matter in waters and can form colloids themselves. The structures and other general properties of humic substances are discussed briefly.

Of importance in the migration of radionuclides in geological media is the strong complexing and redox interactions of humic materials to metal ions. The polyelectrolyte nature of humic molecules leads to very strong complexing which increases in strength with the increasing degree of ionization of the carboxylate groups. In addition, metal ions can be reduced to lower states; e.g., Pu(VI) to Pu(IV). Some unique problems are encountered in measuring the metal binding and/or redox by humic materials. However, such data is important as humic material can have significant effects on metal ion speciation and behavior in geologic systems even at 0.1 ppm levels. Measurements of actinide-humate interactions and their possible consequences on actinide migration are reviewed. "



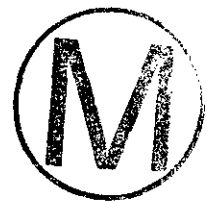
Compliance Certification Application Reference Expansion

---

Chugg, J.C., Anderson, G.W., King, D.L., and Jones, L.H. 1952. Soil Survey of Eddy Area, New Mexico. U.S. Department of Agriculture, Washington, D.C.

"Major fieldwork for this soil survey was done in the period 1960-1965. Soil names and descriptions were approved in 1966. Unless otherwise indicated, statements in this publication refer to conditions in the Area in 1965. This survey was made cooperatively by the Soil Conservation Service and the New Mexico Agricultural Experiment Station. It is part of the technical assistance furnished to the Carlsbad, Central Valley, and Penasco Soil and Water Conservation Districts.

Either enlarged or reduced copies of the soil map in this publication can be made by commercial photographers, or they can be purchased on individual order from the Cartographic Division, Soil Conservation Service, USDA, Washington, D.C. 20250."



Coats, K.H. 1989. "Implicit Compositional Simulation of Single-Porosity and Dual-Porosity Reservoirs." In Proceedings, Tenth SPE Symposium on Reservoir Simulation, Houston, TX. February 6-8, 1989. SPE 18427, pp. 239-275. Society of Petroleum Engineers, Richardson, TX.

ABSTRACT, p 239;

" This paper describes an implicit numerical model for compositional simulation of single-porosity and dual-porosity oil or gas condensate reservoirs. A 3-component equation-of-state compositional approach is proposed as a desirable alternative to extended black oil modeling, requiring little more computing time than the latter. The approach is illustrated for an actual near-critical volatile oil reservoir. A simple method for reducing implicit formulation time truncation error is described and illustrated. A new bottomhole constraint function is described for better preservation of production well target rates in compositional models. A new matrix-fracture transfer formulation including matrix-fracture diffusion is presented for the dual-porosity description; its accuracy is examined in connection with several test problems where correct results are available from single-porosity simulation. Results are discussed for a 3D 600-block simulation of a highly fractured near-critical volatile oil reservoir."



Cooper, J.B., and Glanzman, V.M. 1971. Geohydrology of Project Gnome Site, Eddy County, New Mexico. United States Geological Survey Professional Paper 712-A. U.S. Geological Survey, Washington, D.C.

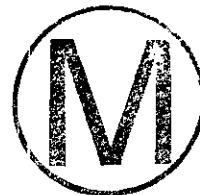
ABSTRACT, p A1;

" On December 10, 1961, a nuclear device was detonated 1,200 feet underground in the massive salt of the Salado Formation in southeastern Eddy County, N. Mex. In support of the public safety program of the U. S. Atomic Energy Commission, the water regimen of about 1,200 square miles, mostly east of the Pecos River and within 15 miles of the project site, was investigated before, at the time of, and after the explosion. Preliminary investigations determined that about 70 wells were in use in the area around the Project Gnome site. The wells range in depth from a few tens of feet to nearly 800 feet and tap water in rocks of Permian, Triassic, Tertiary, and Quaternary ages. Most ground water in the area is saline; however, it is a valuable resource utilized for stock water. Seven test holes drilled at the project site penetrated similar sequences of rocks overlying the massive salt.

All aquifers in the Project Gnome area lie above the massive salt of the Salado Formation. The only water at the project site is contained in the Culebra Dolomite Member of the Rustler Formation, a confined aquifer about 30 feet thick. The aquifer is about 500 feet beneath the surface and about 200 feet above the top of the salt. The potentiometric surface for the confined water is 75 feet above the top of the aquifer and slopes 0.2 to 1.0 foot per mile westward. Fluctuations of water levels observed in wells are small. Data from a pumping test on the aquifer at the Project Gnome site indicate that 100 gallons per minute could be pumped continuously from a well for as long as 1 year without lowering pumping levels below the top of the aquifer. Pressure changes in the aquifer due to the release of water through drill holes and removal by bailing were easily detected by a recording gage.

Water levels in four observation wells at the site were being recorded at the time of the nuclear explosion. The estimated maximum rise of water level immediately following the explosion was about 4 feet at a distance of 2,000 feet from ground zero. About 3,200 feet from ground zero, the water level rose about 2.2 feet, then gradually returned to normal level within a period of about 11 hours. Water in the four test holes returned to preexplosion levels 2 days after the explosion.

Continued observations of water level in those holes and three additional observation wells indicated no anomalous water-level fluctuations after the nuclear explosion, suggesting that the aquifer probably was not significantly ruptured by the explosion."



Corbet, T.F., and Wallace, M.G. 1993. "Post-Pleistocene Patterns of Shallow Groundwater Flow in the Delaware Basin, Southeastern New Mexico and West Texas," In Carlsbad Region, New Mexico and West Texas, D.W. Love, J.W. Hawley, B.S. Kues, J.W. Adams, G.S. Austin, and J.M. Barker, eds. Forty-Fourth Annual Field Conference, October 6-9, 1993, SAND93-1318J, pp. 321-351. New Mexico Geological Society, Roswell, NM. WPO 28643.

ABSTRACT, p 321;

" We used a numerical model to evaluate factors potentially affecting ground water flow in the Rustler and Dewey Lake Formations within a northern portion of the Delaware basin. The model, which is based on the concept of the ground water basin, suggests that flow patterns respond significantly to changes in climate. We include the effects of climate change in the model by varying the amount of moisture that infiltrates to the saturated zone. Calculated hydraulic heads in confined units, such as the Culebra Dolomite Member of the Rustler formation, change by as much as tens of meters in response to long-term changes in the infiltration rate. Results support the concept that patterns of ground water flow in confined units are strongly influenced by the relief of the overlying water table. A substantial portion of the water flowing in the confined units is derived from slow vertical leakage through underlying and overlying aquitards. Flow rates and directions at depth can apparently be affected by changes of only a few tenths of a millimeter per year in the rate of infiltration to the saturated zone. During the simulated period of time, reversals in the direction of vertical flow through the aquitards occur over extensive areas of the model domain. There is great uncertainty in many of the parameters used in our calculations. We do not, therefore, claim that these results are quantitatively correct. Instead, these results improve our intuitive understanding of regional ground water flow in the shallow portion of the Delaware Basin."



Compliance Certification Application Reference Expansion

---

Cranwell, R.M., Campbell, J.E., Helton, J.C., Iman, R.L., Longsine, D.E., Ortiz, N.R., Runkle, G.E., and Shortencarier, M.J. 1987. Risk Methodology for Geologic Disposal of Radioactive Waste: Final Report. NUREG/CR-2452, SAND81-2573. Sandia National Laboratories, Albuquerque, NM. WPO 28296.

ABSTRACT, p 5;

" This report contains the description of a risk assessment methodology developed for the US Nuclear Regulatory Commission for use in assessing the risk from the disposal of radioactive wastes in deep geologic formations. This methodology consists of (1) techniques for selecting and screening scenarios, (2) models for use in simulating the physical processes and estimating the consequences associated with the occurrence of these scenarios, (3) probabilistic and statistical techniques for use in risk estimates and sensitivity and uncertainty analyses, and (4) a procedure for utilizing these models and techniques to assess compliance with regulatory standards. The use of this methodology is demonstrated in this report by applying it in the analysis of a hypothetical disposal site containing a bedded-salt formation as the host medium for the waste."



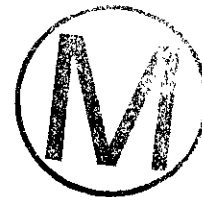
Davies, P.B. 1983 "Assessing the Potential for Deep-Seated Salt Dissolution and the Subsidence at the Waste Isolation Pilot Plant (WIPP)." In State of New Mexico Environmental Evaluation Group Conference, WIPP Site Suitability for Radioactive Waste Disposal, Carlsbad, NM, May 12-13, 1983. (Copy on file at the Nuclear Waste Management Library, Sandia National Laboratories, Albuquerque, NM as WPO 29533.)

INTRODUCTION, p 1;

" The following discussion of technical questions concerning deep-seated salt dissolution and the Waste Isolation Pilot Plant (WIPP) has been prepared for the Environmental Evaluation Group conference on "WIPP Site Suitability for Radioactive Waste Disposal" (May 12-13, 1983, Carlsbad, New Mexico). The discussion focuses on recently released WIPP studies of the geologic and hydrologic evidence for and against the occurrence of deep-seated salt dissolution within the Delaware Basin (as opposed to dissolution associated with the Capitan Reef around the margin of the basin) (Figures 1-1 and 1-2). This paper assumes that the reader has a working knowledge of the geology and hydrology of the Delaware Basin, as well as familiarity with the WIPP project.

The central question of concern is whether or not deep-seated salt dissolution and the associated development of breccia chimneys (breccia pipes) or other subsidence structures pose a significant threat to the long term integrity of the WIPP repository. This question can be broken down into the following geotechnical problems:

- Are the hydrogeologic conditions at WIPP capable of producing deep-seated salt dissolution?
- If deep-seated salt dissolution occurs, what type of subsidence would be produced, and how would this subsidence affect the hydrologic integrity of the repository? . . ."



Davies, P.B., 1989. Variable-Density Ground-Water Flow and Paleohydrology in the Waste Isolation Pilot Plant (WIPP) Region, Southeastern New Mexico, Open-File Report 88-490. U.S. Geological Survey. Albuquerque, NM. WPO 38854.

ABSTRACT, p 1;

" A series of analyses, including variable-density flow simulations, was used to examine groundwater flow in the vicinity of the Waste Isolation Pilot Plant (WIPP) in the context of the regional flow system. WIPP is an underground repository mined from a thick bedded-salt unit to provide a facility for the disposal of radioactive waste. WIPP is located in southeastern New Mexico. The analyses primarily examined the Culebra Dolomite Member of the Rustler Formation, which is a potential pathway for the transport of radionuclides to the biosphere in the event of a breach of the WIPP repository.

An analysis of the relative magnitude of pressure-related and density-related flow-driving forces indicates that density-related forces are not significant at the WIPP Site and to the west but are significant in areas to the north, northeast, and south of the site. The area to the south is important because it lies along potential transport pathways from the site. In this area, groundwater flow simulations based on equivalent-freshwater head produce very misleading information on predicted flow directions and velocity magnitudes.

A regional-scale, variable-density model of ground-water flow in the Culebra Dolomite Member was developed in which a baseline, approximate steady-state simulation was calibrated to the distribution of equivalent-freshwater heads. The flow field from the baseline simulation, along with long-term brine transport patterns, indicates that flow velocities are relatively fast west of the site and extremely slow east and northeast of the site. In the transition zone between these two extremes, which includes the WIPP Site, velocities are highly variable.

A series of sensitivity simulations was used to analyze boundary effects and vertical flux. These simulations indicate that if the Culebra is as impermeable to the east and northeast of the WIPP Site as geologic conditions indicate, the central and western parts of the region, including the WIPP Site, are fairly well insulated from the eastern and northeastern boundaries and are insensitive to whatever conditions are assumed to be present along these boundaries. A simulation of a 5-meter head increase along the Pecos River boundary indicates that if the Culebra were tightly confined throughout the entire region, approximately 50 percent of any change in river elevation would eventually reach the WIPP Site. Uncertainty in the regional distribution of storage characteristics in the Culebra makes it difficult to accurately predict how long it would take for Pecos-related stresses to propagate through the WIPP region. A series of vertical-flux simulations indicates that as much as 25 percent of total inflow to the Culebra could be entering as vertical flux. These simulations also indicate that if significant volumes of water enter the Culebra vertically, most of the influx must be occurring in the westernmost part of the transition zone adjacent to Nash Draw.

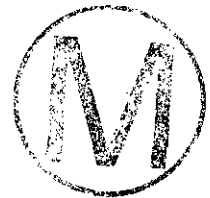
Motivated by recent isotopic and geochemical analyses, a simple cross-sectional model was developed to provide a physically based analysis of the flow system as it may



Compliance Certification Application Reference Expansion

---

have drained through time following recharge during a past glacial pluvial. Drainage for 20,000 years was simulated using a variety of hydraulic-conductivity distributions for rock units overlying the Culebra. These simulations indicate that the system as a whole drains very slowly and that it apparently could sustain flow from a purely transient drainage following recharge of the system during the Pleistocene. Although these simulation do not prove that this has been the case, they do show that such long-term transient drainage is physically possible. The simulations also indicate that the observed underpressuring of the Culebra in the vicinity of the WIPP site is most likely the hydrodynamic result of the Culebra having a relatively high hydraulic conductivity and being well connected to its discharge area but poorly connected to sources of recharge."



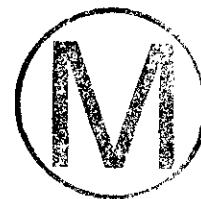
## Compliance Certification Application Reference Expansion

---

Dearlove, J.P.L., Longworth, G., Ivanovich, M., Kim, J.I., Delakowit, B. and Zeh, P. 1990. "Organic Colloid Transport of Radionuclides at Gorleben, West Germany." In Proceedings of the Symposium on Waste Management, Tucson, AZ, February 25-March 1, 1990. R.G. Post, ed., Vol. 2, pp. 565-569. University of Arizona, Tucson, AZ.

### ABSTRACT, p 565;

" A study has been carried out on the Gorleben glacial sand/silt aquifer system, West Germany, to determine both the nature and actinide loading of the organic colloids present at the site and their transport characteristics. Six boreholes were sampled and two distinct groundwaters were identified, an organic-rich groundwater containing humic colloids and a saline groundwater which appears to contain mainly fulvic acid. A mixed organic-rich/saline groundwater has also been identified. There is unequivocal evidence for the association of uranium and thorium isotopes with the humic colloids in the organic-rich groundwaters. The values of the  $^{234}\text{U}/^{238}\text{U}$  activity ratio for the colloid fraction in all the boreholes sampled are different from the corresponding values for the solution phase. Uranium isotopes in the colloid fraction are therefore not in chemical equilibrium with those in solution. Other elements strongly bound to the humic colloids in the organic-rich groundwaters include lanthanides and trivalent/tetravalent metals such as Fe, Mn and Ti. Divalent alkaline earths and monovalent metals are less strongly bound."



Doctor, P.G. Liebtrau, A.M., Eslinger, P.W., Reimus, P.W., Elwood, D.M., Strenge, D.L., Engel, D.W., Tanner, J.E., and Freshley, M.D. 1992. An Example Postclosure Risk Assessment Using the Potential Yucca Mountain Site. PNL-8081. Pacific Northwest Laboratory, Richland, WA. NNA. 930414.0031.

PREFACE, p iii;

" The risk analysis described in this document was performed for the U.S. Department of Energy's (DOE) Office of Civilian Radioactive Waste management (OCRWM) over a 2-year time period ending in June 1988. The objective of Pacific Northwest Laboratory's (PNL) task was to demonstrate an integrated, though preliminary, modeling approach for estimating the postclosure risk associated with a geologic repository for the disposal of high-level nuclear waste. The modeling study used published characterization data for the proposed candidate site at Yucca Mountain, Nevada, along with existing models and computer codes available at that time. Some of the site data and conceptual models reported in the Site Characterization Plan published in december 1988, however, were not yet available at the time that PNL conducted the modeling studies.

The final report describing PNL's study was subsequently reviewed by OCRWM and its contractors, with the comment period extending to August 1989. At that time, DOE decided, based on the reviewer's concerns, not to proceed with comment resolution and publication of the document. Even though PNL's study was conducted as a demonstration of performance assessment methodology, reviewers were concerned that the results would be perceived as an actual risk assessment for the Yucca Mountain site at a time when most detailed site characterization studies had not even been initiated.

In April 1991, OCRWM requested PNL to continue publication of the document, after addressing the review comments, but without performing significant new calculations. This report provides not only a citable reference for work completed in 1988, but documentation for some of the early performance assessment studies that contribute to OCRWM's eventual approach to the risk analyses needed for the license application. New Models have been developed, more site data have been collected, and new risk calculations have been initiated since this work was completed. The results contained here should be interpreted as only a demonstration of an initial stage of study for determining the risk of the proposed repository, rather than a definitive statement of risk based on comprehensive models and the most recent data."



## Compliance Certification Application Reference Expansion

---

DOE (U.S. Department of Energy), 1980. Final Environmental Impact Statement, Waste Isolation Pilot Plant, DOE/EIS-0026, Vols. 1 and 2, U.S. Department of Energy, Washington, D.C. WPO 38835, WPO 38838 - WPO 38839.

p 1-2, Section 1.2.1 1980 WIPP FEIS

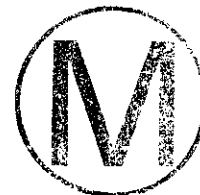
" The 1980 WIPP Final Environmental Impact statement (FEIS) and the associated public review and comment period provided environmental input for the DOE's initial decision to proceed with the WIPP (DOE, 1980). The significance of impacts associated with the various alternatives was assessed. For the selected alternative, a two-phased approach to development was proposed: 1) a site and preliminary design validation (SPDV) program, as discussed in Subsection 8.2.1 of the FEIS, and 2) full construction, as discussed in FEIS Subsection 8.2.2. The durations of key WIPP activities are shown in Figure 1.1.

The 1980 FEIS presented an analysis of the environmental impacts of a number of alternatives for demonstrating the safe disposal of TRU waste. The alternatives considered include:

- Alternative 1. No action. A research and development facility to demonstrate safe disposal of TRU waste would not be developed and post-1970 TRU waste would continue to be retrievably stored.
- Alternative 2. Developing the WIPP at the Los Medanos site in southeastern New Mexico.
- Alternative 3. Disposing of stored TRU waste in the first available repository for high-level radioactive waste.
- Alternative 4. Delaying a decision on the site for a WIPP until at least 1984 to allow for investigation of alternative sites.

Alternative methods and geologic media for TRU waste disposal were also considered but rejected in the FEIS. The alternative methods included burial in deep ocean sediments, emplacement in deep drillholes, transmutation, and ejection into space. The alternative geologic media included igneous, volcanic, and argillaceous rocks.

The DOE's Record of Decision, published January 28, 1981 (46 FR 9162), announced the DOE's selection of Alternative 2: to proceed with the phased development of the WIPP at the Los Medanos site in southeastern New Mexico. . . ."





Compliance Certification Application Reference Expansion

DOE (U.S. Department of Energy), 1990. Final Safety Analysis Report. WP02-9, Rev. 0, May 1990. Westinghouse Electric Corporation, Waste Isolation Division, Carlsbad, NM.

PREFACE

**Background**

This Final Safety Analysis Report (FSAR) has been prepared for the Waste Isolation Pilot Plant (WIPP) in order to satisfy the commitments made in the Working Agreement for Consultation and Cooperation (Article III, Section C and Article IV, Section K, known as the Working Agreement) between the State of New Mexico and the U.S. department of energy (DOE) and the requirements of Order DOE 5481.1B, Safety Analysis and Review System.

The objectives of the Safety Analysis Preparation and Review process, as specified in Order DOE 5481.1B, ensure that:

1. Potential hazards are systematically identified;
2. Potential consequences are analyzed;
3. Reasonable measures to eliminate, control or mitigate the hazards have been taken, including, where applicable, compliance with commitments made in environmental assessments and impact statements;
4. There is documented management authorization of the DOE operation based upon an objective assessment of the safety analysis.

Specific hazards that are analyzed include credible natural hazards such as flood, weather (tornado, wind, etc.) and earthquake; and credible man made hazards such as fire, explosion, radiation, and mining hazards. Mitigating measures include facility design and construction, operational controls, and administrative limits.

This FSAR represents a statement and commitment by the DOE that the WIPP facility can be operated safely and at minimum risk, if operated in accordance with this FSAR. Consequently, this FSAR has been prepared to document that a systematic analysis of the potential hazards associated with operating the WIPP facility has been performed (objective 1 of Order DOE 5481.1B); that potential consequences have been analyzed (objective 2 of Order DOE 5481.1B); and that reasonable measures have been taken to eliminate, control, or mitigate the hazards (objective 3 of Order DOE 5481.1B). In addition, this FSAR documents the implementation of commitments made in the environmental impact statement regarding the mitigation of adverse impacts to the environment (objective 3 of Order DOE 5481.1B)."

DOE (U.S. Department of Energy). 1990. WIPP Test Phase Plan: Performance Assessment. DOE/WIPP-89-011, Rev. 0. U.S. Department of Energy, Waste Isolation Pilot Plant, Carlsbad, NM.

EXECUTIVE SUMMARY, p ES-1;

" The U. S. Department of Energy (DOE) is responsible for managing the disposition of transuranic (TRU) waste resulting from nuclear weapons production activities of the United States. These wastes are currently stored nationwide at several of the DOE's waste generating/storage sites. The goal is to eliminate interim waste storage and achieve environmentally and institutionally acceptable permanent disposal of these TRU wastes, much of which is mixed waste, that is, waste that is also contaminated with hazardous substances. The Waste Isolation Pilot Plant (WIPP) in southeastern New Mexico is being considered as a disposal facility for these TRU wastes.

The mission of WIPP as established by Congress in 1979 (Public Law 96-164) is to provide '...a research and development facility to demonstrate the safe disposal of radioactive wastes resulting from the defense activities and programs of the United States exempted from regulation by the Nuclear Regulatory Commission.' The fundamental responsibility of WIPP's mission, to demonstrate safe disposal of TRU wastes, is being fulfilled in a phased stepwise approach, leading up to the decision whether to designate WIPP a disposal facility. With the Construction Phase nearing completion, WIPP is ready to initiate the next major phase in its development, the Test Phase. The Test Phase period is proposed to collect additional technical data to improve confidence in the prediction of the long-term performance of the repository as required by the applicable environmental regulations (40 CFR 191 and 268). . . ."





DOE (U.S. Department of Energy), 1991. Evaluation of the Effectiveness and Feasibility of the Waste Isolation Pilot Plant Engineered Alternatives: Final Report of the Engineered Alternatives Task Force, DOE/WIPP 91-007, Rev. 0, Vols. 1 and 2. Waste Isolation Pilot Plant, Carlsbad, NM.

EXECUTIVE SUMMARY, p ES-i;

" The Engineered Alternatives Task Force (EATF) was established by the United States Department of Energy (DOE) WIPP Project Office (WPO) in September, 1989 (Hunt, A., 1990), to evaluate the relative effectiveness and feasibility of implementation of selected design enhancements (referred to as 'engineered alternatives') for the Waste Isolation Pilot Plant (WIPP). These enhancements consist of modifications of existing waste forms and/or the WIPP facility, and other design variations such as passive marker systems. The purpose of this report is to summarize the methodologies and results of evaluation of the effectiveness of selected engineered alternatives relative to the existing repository design, and to discuss the feasibility of implementing these alternatives with respect to availability of technology, cost, schedule, and regulatory concerns.

Preliminary analyses of the long-term performance of the WIPP disposal system performed by Sandia National Laboratories (SNL) (referred to as 'performance assessment') have identified two potential problems in demonstrating compliance with the applicable regulation 40 CFR Part 191 (EPA, 1985) that governs the disposal of transuranic radioactive waste. The first potential problem relates to gas generation. Lappin et al. (1989) discuss the possibility that up to 1,500 moles of gas can be generated per drum (or drum equivalent) of waste from anoxic corrosion, microbial degradation, and radiolysis, at rates that may be as high as 2.55 moles/drum/year. Although processes exist to dissipate excess gas pressure, these processes are currently believed to be slow relative to the current estimates of gas generation rates, resulting in gas pressures in storage rooms that may temporarily exceed lithostatic pressure. The consequences of exceeding lithostatic pressure are currently being evaluated by SNL (Lappin et al., 1989). Unless these evaluations demonstrate that either excess pressures will not occur, or that excess pressures will not degrade the performance of the disposal system, some type of waste form or facility modification may be required to either eliminate gas generation or reduce the rate of gas generation. For example, if the organics in the waste are incinerated and vitrified, then microbial gas generation can be eliminated.

A second potential problem in demonstrating compliance with 40 CFR Part 191 relates to the consequences predicted from future inadvertent human intrusion events. Preliminary evaluations of compliance with the containment requirement of 40 CFR Part 191 performed by SNL suggest that some of the current waste forms (under current interpretations of human intrusion provisions) may eventually be found to be unacceptable for disposal at the WIPP (Marietta et al., 1989). This may be due to uncertainties in key performance parameters of the waste forms. Key parameters that control the release of radionuclides during human intrusion scenarios are permeability of the waste storage rooms, radionuclide solubilities, and the availability of brine. Permeability of the storage rooms can

**Compliance Certification Application Reference Expansion**

---

be effectively reduced by the use of a grout backfill and/or shredding and cementation of the waste. Solubilities can be reduced by the use of grout backfill or the addition of lime to raise the pH of any brine that may come in contact with the waste."



DOE (U.S. Department of Energy), 1991. Integrated Data Base for 1991: U.S. Spent Fuel and Radioactive Waste Inventories, Projections, and Characteristics, DOE/RW-0006, Revision 7, Oak Ridge National Laboratory, Oak Ridge, TN. HQX. 910711.0004.

ABSTRACT; P 1;

" The Integrated Data Base (IDB) Program has compiled current data on inventories and characteristics of commercial spent fuel and both commercial and U. S. government-owned radioactive wastes through December 31,1990. These data are based on the most reliable information available from government sources, the open literature, technical reports, and direct contacts. The current projections of future waste and spent fuel to be generated generally through the year 2020 and characteristics of these materials are also presented. The information forecasted is consistent with the latest U.S. Department of Energy/Energy Information Administration (DOE/EIA) projections of U.S. commercial nuclear power growth and the expected DOE-related and private industrial and institutional (I/I) activities.

The radioactive materials considered, on a chapter-by-chapter basis, are spent fuel, high-level waste, transuranic waste, low-level waste, commercial uranium mill tailings, environmental restoration wastes, commercial reactor and fuel cycle facility decommissioning wastes, and mixed (hazardous and radioactive) low-level waste. For most of these categories, current and projected inventories are given through the year 2020, and the radioactivity and thermal power are calculated based on reported or estimated isotopic compositions. In addition, characteristics and current inventories are reported for miscellaneous radioactive materials that may require geologic disposal."



## Compliance Certification Application Reference Expansion

---

DOE (U.S. Department of Energy). 1994. Compliance Status Report for the Waste Isolation Pilot Plant. DOE/WIPP 94-019, Rev. 0. U.S. Department of Energy, Carlsbad Area Office, Carlsbad, NM.

1.0 Introduction, p 1-1;

" The U.S. Department of Energy (DOE) is responsible for the disposition of transuranic (TRU) waste generated through national defense-related activities. Approximately 53,700 m<sup>2</sup> of these wastes have been generated and are currently stored at government defense installations across the country. The Waste Isolation Pilot Plant (WIPP), located in southeastern New Mexico, has been sited and constructed to meet the criteria established by the scientific and regulatory community for the safe, long-term disposal of TRU and TRU-mixed wastes. This Compliance Status Report (CSR) provides an assessment of the progress of the WIPP Program toward compliance with long-term disposal regulations, set forth in Title 40 CFR 191 (EPA, 1993a), Subparts B and C, and Title 40 CFR §268.6 (EPA, 1993b), in order to focus on-going and future experimental and engineering activities. The CSR attempts to identify issues associated with the performance of the WIPP as a long-term repository and to focus on the resolution of these issues. This report will serve as a tool to focus project resources on the areas necessary to ensure complete, accurate, and timely submittal of the compliance application. This document is not intended to constitute a statement of compliance or a demonstration of compliance."



**Compliance Certification Application Reference Expansion**

---

DOE (U.S. Department of Energy). 1994. Experimental Program Plan for the Waste Isolation Pilot Plant. DOE/WIPP 94-008, Rev. 0. U.S. Department of Energy, Carlsbad Area Office, Carlsbad, NM.

EXECUTIVE SUMMARY, p ES-2, para 3;

" This Plan describes DOE plans for demonstrating compliance with both long- and short-term regulations that apply to the WIPP. For the demonstrations of compliance for the long-term as required by 40 CFR Part 191 and 40 CFR 268.6, the DOE will use performance assessment to predict the behavior of the WIPP over thousands of years. Performance assessment is an analytical process that begins by using available information to characterize the waste and the disposal system. This assessment evaluates the natural barriers provided by the host rock and the surrounding formations and the design of the repository and the engineered barriers. The assessment identifies the processes (i.e., phenomena that might develop slowly, over long periods of time) and events that might affect the system. It examines the effects of these processes and events on the performance of the overall system. Release estimates of radionuclides and hazardous chemical constituents can then be developed, considering associated uncertainties, and sensitivity analyses can be performed to determine which characteristics of the disposal system or which processes or events exert the greatest effect on system performance.



DOE (U.S. Department of Energy) 1994. U.S. Department of Energy Waste Isolation Pilot Plant Transuranic Waste Baseline Inventory Report, DOE/CAO-94-1005, Rev. 1, Vols. 1-2. WIPP Technical Assistance Contractor for U.S. Department of Energy, Carlsbad, NM.

EXECUTIVE SUMMARY, p ES-1;

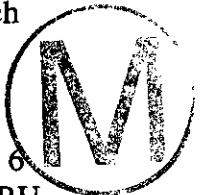
" The Waste Isolation Pilot Plant (WIPP) Transuranic Waste Baseline Inventory Report (WTWBIR) establishes a methodology for grouping wastes of similar physical and chemical properties, from across the U.S. Department of Energy (DOE) transuranic (TRU) waste system, into a series of 'waste profiles' that can be used as the basis for waste form discussions with regulatory agencies.

The WIPP baseline inventory is estimated using waste streams identified in the recent information released in the Mixed Waste Inventory Report (MWIR), supplemented by information from the Nonradionuclide Inventory Database (NID) and the 1993 Integrated Data Base (IDB). Each waste stream is defined in a waste stream profile and has been assigned a waste matrix code (WMC) by a DOE TRU waste generator/storage site. Waste stream profiles with WMCs that have similar physical and chemical properties can be combined into a waste matrix code group (WMCG), which is then documented in a site-specific waste profile for each TRU waste generator/storage site that contains waste streams in that particular WMCG.

Based on methodology presented here in the WTWBIR, a maximum of 11 site-specific waste profiles have been identified for contact-handled (CH) TRU waste and a maximum of 11 have been identified for remote-handled (RH) TRU waste. Based on analyses of existing inventories, no site has more than 10 site-specific CH-TRU waste profiles, nor more than 5 site-specific RH-TRU waste profiles. Each of these site-specific waste profiles have unique WMCG criteria and they are developed, if appropriate, for each of the TRU waste generator/storage sites. A particular site-specific waste profile, with a specific WMCG, can be combined with other site-specific waste profiles having identical WMCGs from the TRU waste generator/storage sites to derive a WIPP waste profile. Therefore, a maximum of 11 WIPP waste profiles for CH-TRU waste and a maximum of 6 WIPP waste profiles for RH-TRU waste have been identified that describe the different TRU wastes across the DOE system.

The anticipated inventory of TRU waste is defined as the sum of retrievably stored waste plus currently projected TRU waste volumes. The anticipated inventory is not sufficient to fill the allowed capacity of WIPP (calculated:  $6.2 \times 10^6 \text{ ft}^3$  [ $\sim 1.76 \times 10^5 \text{ m}^3$ ]), and scaling has been developed as a means of examining the impacts of the full repository. Additionally, there is a high uncertainty in and a current lack of data on wastes produced from decontamination and decommissioning (D&D) and environmental restoration (ER) activities. Therefore, the anticipated inventory has been 'scaled' to the WIPP capacity. The scaling of the inventory in future revisions of the WTWBIR will be derived from the best available data and assumptions.

An example of five waste streams at two sites (Idaho National Engineering Laboratory and Rocky Flats Plant) has been used to illustrate the waste profile methodology.



Preliminary total WIPP inventory volumes for the 11 CH-TRU and 6 RH-TRU WIPP waste profiles are provided; final volumes will be provided in Revision 1 of this document after the DOE TRU waste generator/storage sites have reviewed the data and after quality checks of the data have been completed.

Using the same waste profile methodology, the WTWBIR also estimates the WIPP disposal inventory (anticipated inventory that has been scaled to WIPP design capacity) in terms of 10 waste material parameters and packaging materials that have been identified as inputs needed for the system prioritization (SP) and performance assessment (PA) calculations. The 10 waste material parameters and packaging materials are waste constituents that occur in TRU waste and are input parameters for one or more SP and PA models or are required to adequately describe the waste form. These parameters may change as a result of SP and PA efforts.

The 10 waste material parameters and packaging materials that are identified and included in the WTWBIR are:

- Inorganics
  - Iron-based metals/alloys
  - Aluminum-based metals/alloys
  - Other metals
  - Other inorganic materials
- Organics
  - Cellulosics
  - Rubber
  - Plastics
- Solidified Materials
  - Inorganic matrix
  - Organic matrix
- Soils
- Packaging Materials
  - Steel
  - Plastic or lead



The waste material parameter information is reported in kilograms per cubic meters ( $\text{kg}/\text{m}^3$ ) and estimates of the uncertainty in the waste material parameters have been calculated, based on data derived from the NID (i.e., average, minimum, and maximum estimates of waste material parameters on a per-waste-stream basis). The maximum values for waste material parameters in the waste stream, site-specific, and WIPP waste profiles are expressed on a weight/volume basis. However, the occurrence of more than one waste material parameter at the maximum value within a waste stream is highly unlikely. During SP and PA calculations, the sampling statistics must be controlled so that several waste material parameters do not get sampled all at their maximum value (weight/volume), lest the maximum weight/volume is exceeded. A five-waste-stream/two-site example is used to illustrate the methodology for estimating quantities of waste material parameters. The preliminary total WIPP inventory for the waste material parameters is provided and should

## Compliance Certification Application Reference Expansion

---

be used in any SP and PA calculations until Rev. 1 of the WTWBIR is published, pending completion of quality checks of the data used. The nonradionuclide and radionuclide inventory presented in this report replaces any previously used information in SP and PA calculations.

Although the initial purpose of this report is to provide data to be included in the Sandia National Laboratories/New Mexico SP and PA processes, all data are presented and explained in such a way that they can be adapted as needed for other applications. The WTWBIR, Revision 0, is presented in two parts: Book 1 contains this Executive Summary through Chapter 7, References; Book 2 contains Appendix A, Glossary, through Appendix M, MWIR Code Designations and Descriptions."



Dowding, C.H., and Rozen, A. 1978. Damage to Rock Tunnels for Earthquake Shaking. Journal of the Geotechnical Engineering Division, American Society of Civil Engineers, Vol. 104, No. GT2, pp. 175-191.

INTRODUCTION, p. 175;

" Observations of rock tunnel response to earthquake motions is compared with calculated peak ground motions for 71 cases to determine damage modes. Damage, ranging from cracking to closure, is recorded in 42 of the observations. These tunnels, located in California, Alaska, and Japan, served as railway and water links and were 10 ft-20 ft (3 m-6 m) in diameter. This comparison of peak motion with observed damage can serve as a framework both for development of analytical models and for estimation of expected losses resulting from earthquake shaking failure of tunnels in rock. This is the first such correlation besides a consulting report by Cooke (2).

The potential damage to tunnels from earthquakes is a factor to be considered in the siting of any subsurface project whose failure would result in severance of life-line supply. This paper focuses upon the evaluation of rock tunnel damage caused by shaking, but treats damage from other causes. There are three reasons for the more restricted focus: (1) Damage from other sources, such as ground failure or displacement from fault movement, is location specific, and potential damage may be minimized through careful siting; (2) shaking can result from movement of a number of faults (i.e., is not location specific) and therefore potentially affects long lengths of tunnel; and (3) it is useful for project planning to compare damage to tunnels with that to above-ground structures at the same intensity of shaking."



Compliance Certification Application Reference Expansion

---

Eager, G.P. 1983. Core from the Lower Dewey Lake, Rustler, and Upper Salado Formation, Culberson County, Texas. Permian Basin Cores. R.L. Shaw and B.J. Pollan, eds. P.B.S.-S.E.P.M. Core Workshop No. 2, pp. 273-283. Permian Basin Section, Society of Economic Paleontologists and Mineralogists, Midland, TX.

INTRODUCTION, p 273;

" Seven hundred and twenty feet of continuous Upper Permian core is displayed by Texasgulf, Inc. The formations cored include the lower portion of the Dewey Lake, the Rustler, and the upper portion of the Salado. This core was obtained by Texasgulf, Inc., as part of a sulphur exploration program. The depth of the core is from 37 feet to 757 feet. It is located in the SE $\frac{1}{4}$ , Section 5, PSL, Block 45 (12 miles southwest of Orla) Culberson County, Texas (Fig. 1). Gamma ray and neutron logs are included (Fig. 2) so that the lithology can be compared to the geophysical response. All depths are reported in feet.

The core is presented to give Delaware Basin geologists a 'hands-on' look at the strata that comprise the 'overburden' and troublesome drilling zones through which they must drill to reach the deeper oil-bearing horizons. The Rustler Formation may have reservoir potential."

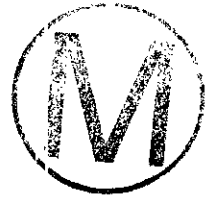


**Compliance Certification Application Reference Expansion**

---

EPA (U.S. Environmental Protection Agency), 1996. Criteria for the Certification and Re-Certification of the Waste Isolation Pilot Plant's Compliance with the 40 CFR Part 191 Disposal Regulations Final Rule. Response to Comments Document for 40 CFR Part 194. EPA 402-R-96-001. Environmental Protection Agency, Office of Radiation and Indoor Air, Washington, D.C.

NOTE: The above listed document was not available for inclusion in the Reference Expansion as of the printing date. Page changes will be provided as the above document becomes available for inclusion.



Francis, A.J., and Gillow, J.B. 1994. Effects of Microbial Processes on Gas Generation Under Expected Waste Isolation Pilot Plant Repository Conditions. SAND93-7036. Sandia National Laboratories, Albuquerque, NM. WPO 26555.

ABSTRACT, p i;

" Microbial processes involved in gas generation from degradation of the organic constituents of transuranic waste under conditions expected at the Waste Isolation Pilot Plant (WIPP) repository are being investigated at Brookhaven National Laboratory. These laboratory studies are part of the Sandia National Laboratories - WIPP Gas Generation Program. Gas generation due to microbial degradation of representative cellulosic waste was investigated in short-term (< 6 months) and long-term (> 6 months) experiments by incubating representative paper (filter paper, paper towels, and tissue) in WIPP brine under initially aerobic (air) and anaerobic (nitrogen) conditions. Samples from the WIPP surficial environment and underground workings harbor gas-producing halophilic microorganisms, the activities of which were studied in short-term experiments. The microorganisms metabolized a variety of organic compounds including cellulose under aerobic, anaerobic, and denitrifying conditions. In long-term experiments, the effects of added nutrients (trace amounts of ammonium nitrate, phosphate, and yeast extract), nutrients plus excess nitrate, and no nutrients on gas production from cellulose degradation were investigated. Results to date (up to 200 days of incubation) show that: (i) gas production was not detected in abiotic control samples; (ii) cellulose incubated without nutrients showed limited but sustained gas production; (iii) the addition of nutrients enhanced the biodegradation of cellulose as evidenced by an increase in the production of total gas, carbon dioxide, and nitrous oxide; (iv) in the presence of excess nitrate, gas production was the highest and nitrous oxide accumulated to varying amounts; (v) the addition of bentonite increased the background carbon-dioxide concentration and stimulated microbial activity specifically in aerobic samples; and (vi) in addition to total gas and carbon dioxide production, cellulose degradation in nutrient-amended samples was evidenced by the gradual bleaching of brown paper towel, the formation of gas bubbles, the formation of paper pulp, and the appearance of a red color at the bottom of the sample bottles, indicating the growth of halophilic microorganisms. Estimates of the total gas production on the basis of initial results ranged from 0.001 to 0.039 mL g<sup>-1</sup> cellulose day<sup>-1</sup>."



Freeland, M.H. 1982, "Basic Data Report for Borehole DOE-1, Waste Isolation Pilot Plant (WIPP) Project, Southeastern New Mexico," TME 3159, U.S. Department of Energy, Waste Isolation Pilot Plant, Albuquerque, NM.

ABSTRACT, p 1-1;

" Borehole DOE-1 is one of several exploratory boreholes drilled at the Waste Isolation Pilot Plant (WIPP) site for the purpose of gathering stratigraphic, hydrologic and structural data. DOE-1 is located in Section 28, T22S, R31E in Eddy County, New Mexico. Within the WIPP site proper, DOE-1 is located in Zone III about 1.25 miles to the southeast of the exploratory shaft location.

This project was undertaken for several reasons:

- To investigate the presence of an anticlinal structure in the Castile Formation indicated by seismic reflection surveys in the area.
- To gather data on the stratigraphy, structure and lithology of the rocks which comprise the facility horizon in an area immediately southeast of the facility itself.
- To test for the presence of gas or fluids in the rocks associated with the anticlinal structure, if present, or in the flat-lying rocks.
- To determine the nature of the Castile Formation near the site, but outside the 'disturbed zone'.

Field operations were initiated July 12, 1982 and completed July 30, 1982. The borehole was drilled to a depth of 4065.3 feet below kelly bushing, with approximately 420 feet of that interval cored. Where no core was taken, cutting samples were collected and described at ten-foot intervals, largely for stratigraphic control and estimation of coring points.

Data collected and observations made during drilling indicate that the lithology, stratigraphy and structure penetrated in DOE-1 are similar to that observed elsewhere in the WIPP vicinity. No brine or gas was noted, either by sensors at the wellhead or in trace amounts in the mud. Cored sections showed no structural disruption in the halite and anhydrite units of the Castile, other than minor, commonly observed folding and tilting of laminae in the anhydrites.

This Basic Data Report includes lithologic and geophysical information collected during the field operations. With minor exceptions, no analytical interpretive work was performed on the data for inclusion in this report. Slight adjustments were made on drilling depths to achieve correlation with the geophysical logs and some lithologic assumptions were made for a few sample intervals where unrepresentative cuttings samples resulted from inadequate brine saturation."



Freeze, R.A., and Cherry, J.A. 1979. Groundwater. Prentice-Hall, Englewood Cliffs, NJ. NNA. 870406.0444.

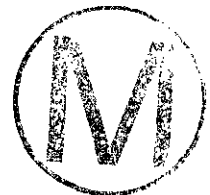
PREFACE, p xv;

" We perceive a trend in the study and practice of groundwater hydrology. We see a science that is emerging from its geological roots and its early hydraulic applications into a full-fledged environmental science. We see a science that is becoming more interdisciplinary in nature and of greater importance in the affairs of man.

This book is our response to these perceived trends. We have tried to provide a text that is suited to the study of groundwater during this period of emergence. We have made a conscious attempt to integrate geology and hydrology, physics and chemistry, and science and engineering to a greater degree than has been done in the past.

This book is designed for use as a text in introductory groundwater courses of the type normally taught in the junior or senior year of undergraduate geology, geological engineering, or civil engineering curricula. It has considerably more material than can be covered in a course of one-semester duration. Our intention is to provide a broad coverage of groundwater topics in a manner that will enable course instructors to use selected chapters or chapter segments as a framework for a semester-length treatment. The remaining material can serve as a basis for a follow-up undergraduate course with more specialization or as source material for an introductory course at the graduate level. We recognize that the interdisciplinary approach may create some difficulties for students grounded only in the earth sciences, but we are convinced that the benefits of the approach far outweigh the cost of the additional effort that is required.

The study of groundwater at the introductory level . . ."



Compliance Certification Application Reference Expansion

---

Galson, D.A., Hicks, T.W., Wilmot, R.W., and Swift, P.N. 1995. Systems Prioritization Method--Iteration 2 Baseline Position Paper: Scenario Development for Long-Term Performance Assessments of the WIPP. Sandia National Laboratories, Albuquerque, NM. WPO 28726

NOTE: The above listed document was not available for inclusion in the Reference Expansion as of the printing date. Page changes will be provided as the above document becomes available for inclusion.



## Compliance Certification Application Reference Expansion

---

Gonzales, M.M. 1989. Compilation and Comparison of Test-Hole Location Surveys in the Vicinity of the Waste Isolation Pilot Plant Site. SAND88-1065. Sandia National Laboratories, Albuquerque, NM. WPO 24121.

### ABSTRACT;

" Between 1976 and 1988, many surveys were performed related to the Waste Isolation Pilot Plant and its geologic and hydrologic test holes, which are part of the hydrogeologic-characterization program. Among these surveys were two First-Order, Class I vertical surveys, a satellite survey, and a number of township-range surveys. An overview of the basic function, history, and methodology of each survey type is provided in this report along with a review and comparison of the two major test-hole surveys. Elevation and location data for 96 test holes and 4 shafts are also included. The comparison of the satellite survey to the township-range surveys showed that the latter have the following advantages: their data are more complete; their elevation data are more accurate; and their techniques can be used for surveying new wells, keeping the data set consistent. Therefore, the final township-range surveys were selected as the best source of elevation and location data to use in the WIPP hydrology program."



Griswold, G.B., 1977. Site Selection and Evaluation Studies of the Waste Isolation Pilot Plant (WIPP), Los Medaños, Eddy County, NM. SAND77-0946. Sandia National Laboratories, Albuquerque, NM. WPO 28125.

ABSTRACT, p. 3;

" Bedded-salt deposits of the Salado Formation have been selected for evaluation for a proposed Waste Isolation Pilot Plant (WIPP) to be located in Eddy County, NM, ~26 mi east of Carlsbad. Site selection and evaluation studies that included geologic mapping, geophysical surveys, drilling, and resource appraisal were conducted over and under the prospective location. The lower portion of the Salado meets essential criteria for waste isolation. Beds chosen for waste storage lie 2074-2730 ft below the surface. High-purity salt exists at these depths, and the geologic structure revealed by geophysical surveys indicates that these beds are essentially flat. Additional geophysical surveys are now under way. The initial interpretation of the new data indicates that more structure may exist in the salt beds in the northern portion of the site area. Full evaluation of potentially commercial deposits of potash and natural gas within the WIPP site will be reported by separate studies, as will be the hydrologic details of the region."

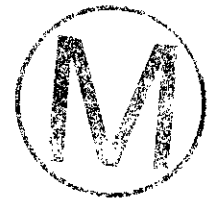


Hays, J.D., Imbrie, J. and Shackleton, N.J. 1976. Variations in the Earth's Orbit: Pacemaker of the Ice Ages," Science. Vol. 194, No. 4270, pp. 1121-1132.  
HQS.880517.2140.

p 1121, col 1;

" For more than a century the cause of fluctuations in the Pleistocene ice sheets has remained an intriguing and unsolved scientific mystery. Interest in this problem has generated a number of possible explanations (1,2). One group of theories invokes factors external to the climate system, including variations in the output of the sun, or the amount of solar energy reaching the earth caused by changing concentrations of interstellar dust (3); the seasonal and latitudinal distribution of incoming radiation caused by changes in the earth's orbital geometry (4); the volcanic dust content of the atmosphere (5); and the earth's magnetic field (6). Other theories are based on internal elements of the system believed to have response times sufficiently long to yield fluctuations in the range  $10^4$  to  $10^6$  years. Such features include the growth and decay of ice sheets (7); the surging of the Antarctic ice sheet (8); the ice cover of the Arctic ocean (9); the distribution of carbon dioxide between atmosphere and ocean (10); and the deep circulation of the ocean (11). Additionally, it has been argued that as an almost intransitive system, climate could alternate between different states on an appropriate time scale without the intervention of any external stimulus or internal time constant (12).

Among these ideas, only the orbital hypothesis has been formulated so as to predict the frequencies of major Pleistocene glacial fluctuations. Thus it is the only explanation that can be tested geologically by determining what these frequencies are. Our main purpose here is to make such a test. . . ."





Helton, J.C., Garner, J.W., McCurley, R.D., and Rudeen, D.K. 1991. Sensitivity Analysis Techniques and Results for Performance Assessment at the Waste Isolation Pilot Plant. SAND90-7103. Sandia National Laboratories, Albuquerque, NM. WPO 23803.

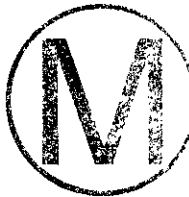
ABSTRACT, p i;

" The purposes of this report are to (1) review available techniques for the performance of uncertainty and sensitivity analyses for computer models, (2) discuss the approach to uncertainty and sensitivity analysis selected for use in performance assessment for the Waste Isolation Pilot Plant (WIPP), (3) present the results of uncertainty and sensitivity analyses performed in support of the 1990 preliminary performance assessment for the WIPP, and (4) discuss the U. S. Environmental Protection Agency (EPA) release limits to the accessible environment (40 CFR 191) in the context of a formal representation for risk. The following approaches to uncertainty and sensitivity analysis are reviewed: differential analysis, Monte carlo analysis, response surface methodology, and Fourier amplitude sensitivity test. Of these approaches, Monte Carlo analysis is felt to be the most widely applicable to the problems that arise in performance assessment for radioactive waste disposal. Monte Carlo analysis is based on performing multiple model evaluations with probabilistically selected model input, and then using the results of these evaluations to determine both the uncertainty in model predictions and the independent variables that give rise to this uncertainty. A Monte Carlo analysis involves five steps: (1) selection of a range and distribution for each independent variable, (2) generation of a sample from the ranges and distributions assigned to then independent variables, (3) evaluation of the model for each element of the sample, (4) assessment of the uncertainty in model predictions through the use of estimated means, variances and distribution functions, and (5) determination of the sensitivity of model predictions to model input on the basis of scatterplots, regression analysis and correlation analysis. The preceding steps are discussed and then applied in uncertainty/sensitivity analyses for scenarios involving drilling intrusions that arose in the 1990 preliminary performance assessment for the WIPP. These analyses used Latin hypercube sampling to select model input and made extensive use of stepwise regression analysis with rank-transformed data to assess the impact of individual variables on model predictions. Releases to the accessible environment due to groundwater transport were dominated by solubility limit and retardation; releases to the surface environment due to the removal of cuttings from boreholes were dominated by borehole cross-sectional area, time of intrusion, and number of boreholes. Overall, the releases were small, usually much smaller than the EPA release limits for the WIPP. Calculation of the EPA release limits involves a Monte carlo calculation of the complementary cumulative distribution function (CCDF). The calculation of this CCDF is discussed and shown to fit into a formal representation for risk based on scenarios, scenario probabilities, and scenario consequences. The relationship between the Monte carlo procedures used in the WIPP performance assessment and this formal representation for risk are developed."

Helton, J.C., Garner, J.W., Rechard, R.P., Rudeen, D.K., and Swift, P.N. 1992 Preliminary Comparison with 40 CFR Part 191, Subpart B for the Waste Isolation Pilot Plant, December 1991. Volume 4: Uncertainty and Sensitivity Analysis Results. SAND91-0893/4, Sandia National Laboratories, Albuquerque, New Mexico, WPO 26423.

Volume 4, ABSTRACT, p i;

" The most appropriate conceptual model for performance assessment at the Waste Isolation Pilot Plant (WIPP) is believed to include gas generation due to corrosion and microbial action in the repository and a dual-porosity (matrix and fracture porosity) representation for solute transport in the Culebra Dolomite Member of the Rustler Formation. Under these assumptions, complementary cumulative distribution functions (CCDFs) summarizing radionuclide releases to the accessible environment due to both cuttings removal and groundwater transport fall substantially below the release limits promulgated by the Environmental Protection Agency (EPA). This is the case even when the current estimates of the uncertainty in analysis inputs are incorporated into the performance assessment. The best-estimate performance-assessment results are dominated by cuttings removal. The releases to the accessible environment due to groundwater transport make very small contributions of CCDFs that must be considered in comparisons with the EPA release limits is dominated by the variable LAMBDA (rate constant in Poisson model for drilling intrusions). The variability in releases to the accessible environment due to individual drilling intrusions is dominated by DBDIAM (drill bit diameter). Most of the imprecisely known variables considered in the 1991 WIPP performance assessment relate to radionuclide releases to the accessible environment due to groundwater transport. For a single borehole (i.e., an E2-type scenario), whether or not a release from the repository to the Culebra even occurs is controlled by the variable SALPERM (Salado permeability), with no releases for small values (i.e.,  $<5 \times 10^{-21} \text{m}^2$ ) of this variable. When SALPERM is small, the repository never fills with brine and so there is no flow up an intruding borehole that can transport radionuclides to the Culebra. Further, releases that do reach the Culebra for larger values of SALPERM are small and usually do not reach the accessible environment. A potentially important scenario for the WIPP involves two or more boreholes through the same waste panel, of which at least one penetrates a pressurized brine pocket and at least one does not (i.e., an E1E2-type scenario). For these scenarios, the uncertainty in release to the Culebra is dominated by the variables BHPERM (borehole permeability), BPPRES (brine pocket pressure), and the solubilities for the individual elements (i.e., Am, Np, Pu, Th, U) in the projected radionuclide inventory for the WIPP. Once a release reaches the Culebra, the *matrix distribution coefficients for the individual elements are important, with releases to the Culebra often failing to reach the accessible environment over the 10,000-yr period specified in the EPA regulations.* To provide additional perspective, the following variants of the 1991 WIPP performance assessment have also been considered: (1) no gas generation in the repository and a dual-porosity transport model in the Culebra; (2) gas generation in the repository and a single-porosity (fracture porosity) transport model in the Culebra; (3) no gas generation in the repository and a single-porosity transport model in the Culebra; (4) gas



## Compliance Certification Application Reference Expansion

---

generation in the repository and a dual-porosity transport model in the Culebra without chemical retardation; and (5) gas generation in the repository, a dual-porosity transport model in the Culebra, and extremes of climatic variation. All of these variations relate to groundwater transport and thus do not affect releases due to cuttings removal, which were found to dominate the results of the 1991 WIPP performance assessment. However, these variations do have the potential to increase the importance of releases due to groundwater transport relative to releases due to cuttings removal."



## Compliance Certification Application Reference Expansion

---

Helton, J.C., Marietta, M.G., and Rechar, R.P. 1993. Conceptual Structure of Performance Assessments Conducted for the Waste Isolation Pilot Plant. SAND92-2285. Sandia National Laboratories, Albuquerque, NM. WPO 27834.

ABSTRACT, p i;

" The Waste Isolation Pilot Plant (WIPP) in southeastern New Mexico is being developed by the U. S. Department of Energy as a disposal facility for transuranic waste. In support of this project, Sandia National Laboratories is conducting an ongoing performance assessment (PA) for the WIPP. The ordered triple representation for risk proposed by Kaplan and Garrick is used to provide a clear conceptual structure for this PA. This presentation describes how the preceding representation provides a basis in the WIPP PA for (1) the definition of scenarios and the calculation of scenario probabilities and consequences, (2) the separation of subjective and stochastic uncertainties, (3) the construction of the complementary cumulative distribution functions required in comparisons with the U. S. Environmental Protection Agency's standard for the geologic disposal of radioactive waste (i.e., 40 CFR Part 191, Subpart B), and (4) the performance of uncertainty and sensitivity studies. Results obtained in a preliminary PA for the WIPP completed in December of 1991 are used for illustration.



Hiemenz, P.C., 1986. Principles of Colloid and Surface Chemistry. 2nd ed. Marcel Dekker, Inc., New York, NY.

PREFACE TO THE SECOND EDITION, p iii;

" In the preface to the first edition, I stated that this is 'primarily a textbook, written with student backgrounds, needs, and objectives in mind.' This continues to be true of the second edition, and many of the revisions I have made are attempts to make the book even more useful than its predecessor to student readers. In addition, colloid and surface science continue to flourish. In preparing the second edition I have also attempted to 'open up' the coverage to include some of the newer topics from an ever-broadening field.

A number of differences between the first and second editions can be cited which are readily traceable to either one or both of the foregoing considerations.

Two new chapters have been added which explore--via micelles and related structures and metal surfaces under ultra-high vacuum--both 'wet' and 'dry' facets of colloids and surfaces. Although neither of these areas is new, both are experiencing an upsurge of activity as new instrumentation is developed and new applications are found.

A number of chapters have been overhauled so thoroughly that they bear only minor resemblance to their counterparts in the first edition. The thermodynamics of polymer solutions is introduced in connection with osmometry and the drainage and spatial extension of polymer coils is discussed in connection with viscosity. The treatment of contact angle is expanded so that it is presented on a more equal footing with surface tension in the presentation of liquid surfaces. Steric stabilization as a protective mechanism against flocculation is discussed along with the classical DLVO theory.

Solved problems have been scattered throughout the text. I am convinced that students must work problems to gain mastery of the topics we discuss. Including examples helps bridge the gap between the textbook presentation of theory and student labors over the analysis and mechanics of problem solving.

SI units have been used fairly consistently throughout the book. Since the problems. . ."



Hill, A.C., and Thomas, G.W. 1985. "A New Approach for Simulating Complex Fractured Reservoirs." In Proceedings, Eighth SPE Symposium on Reservoir Simulation, Dallas, TX, February 10-13, 1985, L.C. Young, ed. SPE 13537. pp. 429-440. Society of Petroleum Engineers of AIME, Richardson, TX.

ABSTRACT, p 429;

" This paper treats a dual porosity and dual permeability system in which two grids - one each for the fractures and matrix occupy the same volume. We employ 5 pseudo components in the formulation which extends the capability beyond normal black-oil applications. The formulation also permits inert gas injection (i.e. nonhydrocarbon -  $N_2$ ,  $CO_2$ , etc.) which can diffuse into the liquid phases. Moreover, the oil properties can be optionally treated as functions of pressure and API gravity.

We briefly review the mathematical description of the system. We also describe a memory management scheme whereby one can study large reservoir problems (in excess of 20,000 cells) on computers offering modest core capability. Finally, we present example applications for an isolated fracture system, the effect of cyclic water injection, and the effect of variable API gravity."



Hills, J.M., and Kottowski, F.E. 1983. Southwest/Southwest Mid-Continent Region: Correlation of Stratigraphic Units of North America (COSUNA) Project. Correlation Chart Series 1983. AAPG Bookstore, Tulsa, OK.

EDITOR'S NOTE;

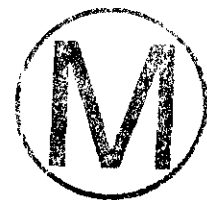
" The COSUNA Correlation Charts are intended to show stratigraphic columns which provide fairly complete coverage of the geology of the United States. In most cases, these columns are generalizations of the geology of an area and do not represent single surface or subsurface locations. The locations of the columns on the index map are intended to show the areas in which the stratigraphy is uniform enough to be shown in a single column. Since the columns are generalized they often show a range of thicknesses for each of the units and their dominant lithology within the map area.

Because the COSUNA Charts are correlation charts and not cross-sections their vertical scale is time, not thickness. Due to this difference, a number of features which may be shown on cross-sections cannot be shown on correlation charts.

The positional relationships of units separated by angular unconformities are not necessarily shown properly in each of the columns. Tilted contact lines show a time transgressive relationship the geographic directionality of which is not necessarily implied by the tilt of the line in the column. Units involved in faulting and especially those involved in thrust sheets are shown at a time at which they were deposited, not in the position into which they were thrust.

Igneous intrusives are shown at the time that they were intruded, not necessarily in the strata in which they intrude. Questioned contacts were placed for convenience in the vertical position near where they are most likely to occur. The amount of question in their positioning may vary from contact to contact.

Detailed information regarding the contacts, lithology, paleontology, references, and other significant information on each of the units on this chart is available by accessing the computerized COSU data file on the Petroleum Data System of the University of Oklahoma, Norman, Oklahoma."



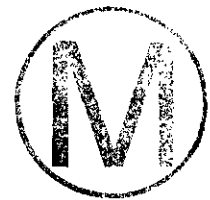
Compliance Certification Application Reference Expansion

---

Holcomb, D.J. 1988. "Cross-Hole Measurements of Velocity and Attenuation to Detect a Disturbed Zone in Salt at the Waste Isolation Pilot Plant." In Key Questions in Rock Mechanics: Proceedings of the 29th U.S. Symposium, University of Minnesota, Minneapolis, MN, June 13-15, 1988, P.A. Cundall, R.L. Sterling, and A.M. Starfield, eds. SAND87-3016C, pp. 633-640. A.A. Balkema, Brookfield, VT. WPO 29992.

ABSTRACT, p. 633;

" Cross-hole ultrasonic measurements were made at the Waste Isolation Pilot Plant (near Carlsbad, New Mexico) to delineate the disturbed zone around drifts and rooms. Using compressional mode waves it was found that there was a small decrease in velocity and a large increase in attenuation immediately after the test room was mined. Disturbances extended at least 3 metres from a room with a width of 5.5 metres. The results are interpreted as resulting from the introduction of about 0.5% crack-like, pore space."



Compliance Certification Application Reference Expansion

---

Hora, S.C. 1992. Appendix A: Probabilities of Human Intrusion into the WIPP, Methodology for the 1992 Preliminary Comparison. In Preliminary Performance Assessment for the Waste Isolation Pilot Plant, December 1992, Volume 3: Model Parameters. SAND92-0700/3, Sandia National Laboratories, Albuquerque, NM. In Appendix A of WPO 23529, pp. A-69 through A-99.

(vol 3)Page A-71, line 6;

" . . . The second group, after considering the findings of the first group, studied how markers might be used to warn future societies about the presence and danger of the buried waste. Both groups provided probabilities and probability distributions for critical aspects of the human intrusion problem."

(vol 3)Page A-71, para 4;

"The Markers Group

A second group of thirteen experts was organized into two teams to study markers for the WIPP site. These markers are to serve as warnings to future societies about the presence of nuclear waste. Such warnings, hopefully, will deter inadvertent intrusions. Each team was asked to consider the findings of the futures teams, to suggest design characteristics for a marker system, and to assess the efficacy of such a system of markers. The ability of a marker system to deter intrusions rests on the survival of the marker system over an extended period of time, and the ability of potential intruders to detect the markers and to understand the message that they carry. The markers team members where (sic) asked to provide probabilities for several events. The first of these is the event that a marker and its message(s) remain intact at various times in the future. Second, for several types of intrusion, the team members were asked to provide probabilities that, given the marker and its messages are intact, the potential intruders are able to understand the message and thus become forewarned of the inherent dangers of intrusion. These assessments were made under various assumptions about the state of technology in the future."



Hora, S.C., von Winterfeldt, D., and Trauth, K.M. 1991. Expert Judgment on Inadvertent Human Intrusion into the Waste Isolation Pilot Plant. SAND90-3063. Sandia National Laboratories, Albuquerque, NM. WPO 26161.

ABSTRACT, p i;

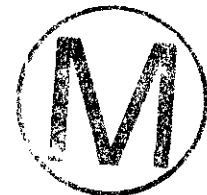
" Four expert-judgement teams have developed analyses delineating possible future societies in the next 10,000 years in the vicinity of the Waste Isolation Pilot Plant (WIPP). Expert-judgement analysis was used to address the question of future societies because neither experimentation, observation, nor modeling can resolve such uncertainties. Each of the four, four-member teams, comprised of individuals with expertise in the physical, social, or political sciences, developed detailed qualitative assessments of possible future societies. These assessments include detailed discussions of the underlying physical and societal factors that would influence society and the likely modes of human-intrusion at the WIPP, as well as the probabilities of intrusion. Technological development, population growth, economic development, conservation of information, persistence of government control, and mitigation of danger from nuclear waste were the factors the teams believed to be most important. Likely modes of human-intrusion were categorized as excavation, disposal/storage, tunneling, drilling, and offsite activities. Each team also developed quantitative assessments by providing probabilities of various alternative futures, of inadvertent human intrusion, and in some cases, of particular modes of intrusion. The information created throughout this study will be used in conjunction with other types of information, including experimental data, calculations from physical principles and computer models, and perhaps other judgements, as input to a 'performance assessment.' The more qualitative results of this study will be used as input to another expert panel considering markers to deter inadvertent human intrusion at the WIPP."



Houghton, J.T., Jenkins, G.J., and Ephraums, J.J. 1990. Climate Change: The IPCC Scientific Assessment. Cambridge University Press, New York, NY.

**ABSTRACT;**

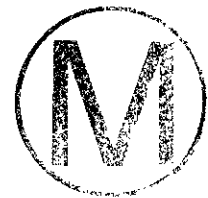
" This is the final Report of Working Group 1 of the Intergovernmental Panel on Climate Change, which is sponsored jointly by the World Meteorological Organization and the United Nations Environment Programme. This report considers the scientific assessment of climate change. Several hundred working scientists from 25 countries have participated in the preparation and review of the scientific data. The result is the most authoritative and strongly supported statement on climate change that has ever been made by the international scientific community. The issues confronted with full rigour include: global warming, greenhouse gases, the greenhouse effect, sea level changes, forcing of climate, and the history of the Earth's changing climate. The information presented here is of the highest quality. It will inform the necessary scientific, political and economic debates and negotiations that can be expected in the immediate future. Appropriate strategies in response to the issue of climate change can now be firmly based on the scientific foundation that the Report provides. The Report is, therefore, an essential reference for all who are concerned with climate change and its consequences."



Howard, C.L., Jensen, A.L., Jones, R.L., and Peterson, T.P. 1993. Room Q Data Report: Test Borehole Data From April 1989 Through November 1991. SAND92-1172. Sandia National Laboratories, Albuquerque, NM. WPO 23548.

ABSTRACT;

" Pore-pressure and fluid-flow tests were performed in 15 boreholes drilled into the bedded evaporites of the Salado Formation from within the Waste Isolation Pilot Plant (WIPP). The tests measured fluid flow and pore pressure within the Salado. The boreholes were drilled into the previously undisturbed host rock around a proposed cylindrical test room, Room Q, located on the west side of the facility about 655 m below ground surface. The boreholes were about 23 m deep and ranged over 27.5 m of stratigraphy. They were completed and instrumented before excavation of Room Q. Tests were conducted in isolated zones at the end of each borehole. Three groups of 5 isolated zones extend above, below, and to the north of Room Q at increasing distances from the room axis. Measurements recorded before, during, and after the mining of the circular test room provided data about borehole closure, pressure, temperature, and brine seepage into the isolated zones. The effects of the circular excavation were recorded. This data report presents the data collected from the borehole test zones between April 25, 1989 and November 25, 1991. The report also describes test development, test equipment, and borehole drilling operations."



Hunter, R.L., 1985. A Regional Water Balance for the Waste Isolation Pilot Plant (WIPP) Site and Surrounding Area. SAND84-2233. Sandia National Laboratories, Albuquerque, NM. WPO 27628.

ABSTRACT, p. 3;

" The WIPP water-balance study area defined here comprises ~2000 mi<sup>2</sup> in Eddy and Lea Counties, southeastern New Mexico. Inflows to the study area are precipitation (roughly  $1.47 \times 10^6$  ac-ft/yr), surface water (roughly  $1.1 \times 10^5$  ac-ft/yr), water imported by municipalities and industries (roughly  $3 \times 10^4$  ac-ft/yr), and ground water (volume not estimated). Outflows from the area are evapotranspiration (roughly  $1.5 \times 10^6$  ac-ft/yr), surface water (roughly  $1.2 \times 10^5$  ac-ft/yr), and possibly some ground water. The volume of surface and ground water in storage in Nash Draw has increased since the beginning of potash refining. Regional ground water flow in aquifers above the Salado Formation is from the northeast to the southwest, although this pattern is interrupted by Clayton Basin, Nash Draw, and San Simon Swale. The Pecos River is the only important perennial stream. Most of the area has no integrated surface-water drainage.

The available data suggest that ~1600 mi<sup>2</sup> of the study area are hydrologically separate from Nash Draw and the WIPP site. Ground water north of Highway 180 apparently discharges into Clayton Basin and evaporates. Water in San Simon Swale apparently percolates downward and flows to the southeast. Data are inadequate to create a water budget for the Nash Draw-WIPP site hydrologic system alone, although an attempt to do so can provide guidance for further study."

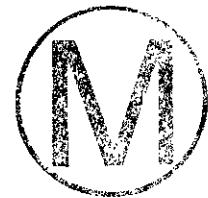


Hunter, R.L., Cranwell, R.M., and Chu, M.S.Y. 1986. Assessing Compliance with the EPA High-Level Waste Standard: An Overview. SAND86-0121, NUREG/CR-4510. Sandia National Laboratories, Albuquerque, NM. WPO 28435.

ABSTRACT, p iii;

" The US Environmental Protection Agency has set a standard for the performance of geologic repositories for the disposal of high-level radioactive waste. The standard is divided into several sections, including a section on containment requirements. The containment requirement is probabilistic, in that it allows certain small amounts of radioactive waste to be released at high probabilities and larger amounts to be released at lower probabilities. The US Nuclear Regulatory Commission is responsible for implementing the standard. Implementation of the standard will probably involve development and screening of scenarios, assignment of probabilities to the scenarios, determination of consequences of the scenarios, and analysis of uncertainties.

Scenario development consists of first, identifying events and processes that could initiate waste releases or affect waste transport, and second, combining the events and processes in physically reasonable ways. Scenarios can be screened on the basis of low probabilities or consequences. Consequences of scenarios are estimated using a series of models that simulate the movement of radionuclides out of the waste package and underground facility and the transport of the radionuclides by ground water or other means to the accessible environment. Sensitivity and uncertainty analysis examines the sources and effects of uncertainties on the calculations. This document uses a simple example to illustrate techniques for the implementation of the standard."



IAEA (International Atomic Energy Agency). 1989. Evaluating the Reliability of Predictions Made Using Environmental Transfer Models. Safety Series Report No. 100. International Atomic Energy Agency, Vienna.

FOREWORD;

" The development and application of mathematical models for predicting the consequences of releases of radionuclides into the environment from normal operations in the nuclear fuel cycle and hypothetical accident conditions has increased dramatically in the last two decades. Along with this development has come the recognition that it is not enough to have results presented as single value estimates of radiation dose or of environmental concentrations of radionuclides. Models are only approximations to real environmental systems and therefore there will always be some uncertainty associated with predictions obtained from their use. A model prediction without some estimate of the associated uncertainty is of little value to decision makers.

This Safety Practice publication has been prepared to provide guidance on the available methods for evaluating the reliability of environmental transfer model predictions. It provides a practical introduction to the subject and particular emphasis has been given to worked examples in the text, It is intended to supplement existing IAEA publications on environmental assessment methodology.

Although the book addresses the subject of environmental dose assessment, the methods described in it are of general application and are equally useful in other areas where modelling techniques are applied.

The text of this publication was produced through a series of consultants meetings and one Advisory Group Meeting. The IAEA wishes to acknowledge . . ."



Imbrie, J. 1985. "A Theoretical Framework for the Pleistocene Ice Ages," *Journal of the Geological Society*. Vol. 142, 417-432.

SUMMARY, p 417;

" This paper reviews 150 years of progress towards understanding the succession of Pleistocene ice ages. Emphasis is placed on the process of explaining *forced variations* in climate which occur in the *Milankovitch band* (periods from 10000 to 400000 years), where astronomical forcing functions are clearly identified and where the amplitudes of climatic change are large. An hierarchy of explanatory models is employed, including a statistical model that uses gain and phase terms to parameterize the climatic response to orbital forcing in several narrow frequency bands. This type of model accounts for a substantial fraction of the observed temporal variations of  $\delta^{18}\text{O}$  over the past 800000 years. Experiments using the model suggest that a change in the system response occurred about 400000 years ago. The problem of explaining climatic variations in other frequency bands is broadly reviewed. In the *decadal band* (10-400 years), there is good evidence of volcanic forcing, solar forcing, and tidal forcing, but much of the observed pattern is presumed to reflect *free variations*. In the *millenium band* (400 to 10000 years), significant climatic changes occur at periods ranging from 1000 to 3000 years. Their cause remains a challenging problem. Over the *tectonic band* (more than 400000 years), volcanic fluxes, continental elevation, and continental position are the most likely forcing functions of the observed climatic changes."



Compliance Certification Application Reference Expansion

---

Imbrie, J. and Imbrie, J.Z. 1980. "Modeling the Climatic Response to Orbital Variations," Science. Vol. 207, no. 4434, 943-953.

SUMMARY, p 943;

" According to the astronomical theory of climate, variations in the earth's orbit are the fundamental cause of the succession of Pleistocene ice ages. This article summarizes how the theory has evolved since the pioneer studies of James Croll and Milutin Milankovitch, reviews recent evidence that supports the theory, and argues that a major opportunity is at hand to investigate the physical mechanisms by which the climate system responds to orbital forcing. After a survey of the kinds of models that have been applied to this problem, a strategy is suggested for building simple, physically motivated models, and a time-dependent model is developed that simulates the history of planetary glaciation for the past 500,000 years. Ignoring anthropogenic and other possible sources of variation acting at frequencies higher than one cycle per 19,000 years, this model predicts that the long-term cooling trend which began some 6000 years ago will continue for the next 23,000 years."



Compliance Certification Application Reference Expansion

---

Imbrie J., Hays, J.D., Martinson, D.G., McIntyre, A., Mix, A.C., Morley, J.J., Pisias, N.G., Prell, W.L., and Shackleton, J.J. 1984. "The Orbital Theory of Pleistocene Climate: Support from a Revised Chronology of the Marine  $^{18}\text{O}$  Record," in Milankovitch and Climate, Understanding the Response to Astronomical Forcing, Proceedings of the NATO Advanced Research Workshop on Milankovitch and Climate, Palisades, NY, November 30-December 4, 1982, A. Berger, J. Imbrie, J. Hays, G. Kukla, and B. Saltzman, eds. Pt. 1, pp. 269-305. D. Reidel, Boston, MA.

NOTE: The above listed document was not available for inclusion in the Reference Expansion as of the printing date. Page changes will be provided as the above document becomes available for inclusion.





Imbrie, J., McIntyre, A., and Mix, A. 1989. "Oceanic Response to Orbital Forcing in the Late Quaternary: Observational and Experimental Strategies," *Climate and Geo-sciences*. Eds. A. Berger, S. Schneider, and J.C. Duplessy. 121-164. Kluwer, Boston, MA.

ABSTRACT, p 121;

" Observations on deep-sea cores demonstrate that late Pleistocene climate is determined by three broad-band cycles centered near periods of 23 ky, 41 ky, and 100 ky. These cycles permeate the global system, and include changes in the atmosphere, cryosphere, surface ocean, and deep ocean. The periods of these climatic cycles match orbital cycles of precession, obliquity, and eccentricity; and each orbit-climate pair is significantly correlated (coherent). These observations may be explained in different ways. We review various models and conclude that the climatic styles can be explained as an interaction between orbitally forced and internally driven oscillations of the climate system. Depending on the cycle and model, the external forcing may influence climate either as part of a driving mechanism which determines both the amplitude and phase of the cycle, or as a pacing mechanism which sets the phase of an internal oscillation. Our goal is to search climatic data for clues about the mechanisms which operate within the climate system on orbital time scales. Our strategy is patterned after previous investigations which partition the climatic record into cyclic components, record the phase of system responses in each cycle, and examine these phase sequences for clues about the chain of causal mechanisms.

We review the stratigraphic, chronologic, and statistical methods adopted to achieve these objectives, and then apply the strategy to two sets of data: (1) time series with local implications about conditions at the sea surface at 17 sites ranging from 54°N in the Atlantic to 44°S in the Indian Ocean (faunal estimates of sea-surface temperature, SST); and (2) time series with global implications about ice volume and ocean chemistry ( $\delta^{18}\text{O}$ ,  $\Delta\delta^{13}\text{C}$ , and Cd/Ca). The spatial pattern of SST response in each cycle is documented by mapping its amplitude and phase. Each cycle has a characteristic pattern, but all cycles show an early response near 40°S. Information drawn from both data sets is then combined to form a preliminary phase portrait of the entire system. In each cycle, responses occur over a wide range of phases centered on the point of minimum ice, and include indicators which lead and those which lag ice volume. Each cycle is characterized by the same three leading indicators: Cd/Ca,  $\Delta\delta^{13}\text{C}$ , and SST at ~40°S (with the addition of equatorial SST at 23 ky). Lagging indicators include North Atlantic SST at 23 ky.

Data on SST and  $\delta^{18}\text{O}$  phases are used to test simple models of radiation forcing in the 23 ky and 41 ky bands, and limited to explaining the observations of  $\delta^{18}\text{O}$ , and SST near 50°N and 40°S. The simplest model that fits our data assumes that summer radiation forces the system in the Northern Hemisphere, and that the response at high latitudes is transmitted rapidly to the Southern Hemisphere by modulation of the North Atlantic sources of deep water. In the 100 ky band we assume that the phase of an internally generated cycle is set by the amplitude of the 23 ky radiation cycle.

We conclude that the strategy developed here can guide the acquisition of new data, serve as a framework for synthesizing information on different parts of the climate system,

**Compliance Certification Application Reference Expansion**

---

and stimulate interactions between data and models. Opportunities now exist for comparing the predicted sequence of system response with the observed sequence."

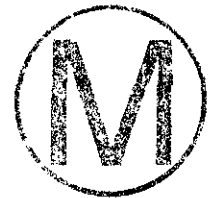


Izett, G.A., and Wilcox, R.E. 1982. Map Showing Localities and Inferred Distribution of the Huckleberry Ridge, Mesa Falls, and Lava Creek Ash Beds in the Western United States and Southern Canada. Misc. Investigations Map I-1325, scale 1:4,000,000. U.S. Geological Survey.

DISCUSSION;

" During the past 10 years there has been increasing interest among earth scientists for tephrochronological data useful for establishing volcanic ash beds as time-stratigraphic markers. When tephrochronological data are combined with other geological information such as stratigraphic position, faunal age, paleomagnetic direction, and isotopic age, the result is a multipronged analytical device with a combined resolving power far greater than that of any individual geologic technique. Correct identification of an isotopically dated volcanic ash bed can provide critical information to help resolve problems such as (1) the correlation (over long distances) of sedimentary deposits of diverse origins (marine, lacustrine, fluvial, paludal, glacial, periglacial, and eolian); (2) the determination of the times and rates of fault movements and other types of crustal deformation; (3) the determination of the average rates of deposition of sediments; (4) the evaluation of geologic hazards such as volcanic eruptions and earthquakes; (5) the calibration of paleomagnetic stratigraphies and faunal chronologies; (6) the calibration of experimental dating methods such as uranium-trend dating; (7) the identification of tephra sources; and (8) the evolution of silicic magma bodies and related tephra ejection mechanics, transportation, and deposition. Several upper Cenozoic volcanic ash beds of the western United States have been studied in considerable detail including tephra of Holocene age from Mount St. Helens volcano in Washington (Fryxell, 1965; Mullineaux and others, 1975; Westgate, 1977) in Washington; the Mazama ash bed of Holocene age (Powers and Wilcox, 1964); the Glacier Peak ash bed of latest Pleistocene age (Powers and Wilcox, 1964; Westgate and Evans, 1978); and the Bishop ash bed of middle Pleistocene age (Izett and others, 1970; Borchardt and others, 1972; Merriam and Bischoff, 1975; Sama-Wojcicki and others, 1980). These volcanic ashes are found interbedded in various types of fluvial, colluvial, and lacustrine Holocene and Pleistocene sedimentary deposits scattered from the West Coast of the United States to as far east as central Nebraska. Another set of volcanic ashes, the Pearlette family ash beds, also has been extensively studied and used for long range correlations of the enclosing sediments and their contained fossil materials. These ash beds are the main subject of this report.

The Pliocene and Pleistocene boundary . . . "



Compliance Certification Application Reference Expansion

---

Jones, C.L., 1978. Test Drilling for Potash Resources: Waste Isolation Pilot Plant Site, Eddy County, New Mexico, Open-File Report 78-592, Vols. 1 and 2. U.S. Geological Survey Denver, CO.

ABSTRACT, p 1;

" Twenty-one borings to augment existing information on potash resources at the proposed site for a waste isolation pilot plant in eastern Eddy County, N. Mex., were drilled and logged in an 11-week period, mid-August to November 1976. The basic data developed from the borings are tabulated in the present report. The tabulation includes lithologic and geophysical logs of all the borings, as well as the results of chemical analyses, X-ray determinations, and calculations to establish a modal mineralogical composition of core samples from potash ore zones and mineralized salt beds."



Jones, T.L., Kelley, V.A., Pickens, J.F., Upton, D.T., Beauheim, R.L., and Davies, P.B. 1992. Integration of Interpretation Results of Tracer Tests Performed in the Culebra Dolomite at the Waste Isolation Pilot Plant Site. SAND92-1579. Sandia National Laboratories, Albuquerque, NM. WPO 23504.



ABSTRACT, p i;

" Conservative tracer tests have been conducted within the Culebra Dolomite Member of the Rustler Formation at the H-2, H-3, H-4, H-6, and H-11 hydropads for transport scales ranging from approximately 20 to 40 m. Convergent-flow and two-well recirculating tracer tests provide data that is used to quantitatively characterize flow and transport processes. The observed long time period required for initial (detectable) tracer breakthrough (74 to 316 days) in the H-2 and H-4 tracer tests suggest the prevalence of single-porosity, matrix-only transport at these locations. Hydraulic-test responses at these two hydropads also indicate single-porosity, matrix-only conditions. The relatively poor quality of data defining the breakthrough curves from the H-2 and H-4 tracer tests precluded a detailed, quantitative analysis of transport parameter values from these tests. Interpretations of pumping tests and tracer tests at the H-3, H-6, and H-11 hydropads indicated that the Culebra dolomite behaves as a double-porosity (fracture-plus-matrix) medium at these locations. Both the H-3 and H-11 hydropads are located along the offsite transport pathways southeast of the Waste Isolation Pilot Plant waste-panel area. Significant fracture participation in transport is evidenced by rapid initial tracer breakthrough (1 to 21 hrs) on one travel path at each of these hydropads. The H-3, H-6, and H-11 convergent-flow tracer tests were analyzed using the SWIFT II model with the Culebra fracture/matrix system idealized as three, orthogonal, intersecting fracture sets equally spaced in all three directions. Input values and ranges for the assigned transport parameters (effective thickness, well spacing, pumping rate, free-water diffusion coefficient, longitudinal dispersivity, and matrix porosity) were specified based on field measurements, laboratory measurements on Culebra core, and scientific judgement. Measurement and/or calculated uncertainties were also defined for the assigned parameters. Two approaches were used to model double-porosity transport. The first approach assumed that differences in tracer breakthrough behavior at a single hydropad were caused by differences (heterogeneity) in matrix-block length (fracture spacing) between different travel paths. The second approach assumed that differences in tracer breakthrough behavior were caused by horizontal anisotropy in the flow field. Interpretations based on the heterogeneous-analysis approach yielded matrix-block lengths ranging from 0.11 to 1.23 m and fracture porosities ranging from  $5.0 \times 10^{-4}$  to  $1.0 \times 10^{-3}$ . Interpretations based on the anisotropic-analysis approach yielded matrix-block lengths ranging from 0.15 to 0.48 m, fracture porosities ranging from  $1.0 \times 10^{-3}$  to  $3.0 \times 10^{-3}$ , and anisotropy ratios ranging from 3:1 to 7:1. Sensitivity analyses were conducted to provide insight into the relative impact of varying individual transport parameters and to provide estimates of fitted-parameter uncertainty. These analyses yielded minimum and maximum matrix-block lengths for all hydropads that ranged from 0.02 to 3.22 m. Sensitivity analyses also showed that neither single-porosity, fracture-only transport nor single-porosity, matrix-only transport can

**Compliance Certification Application Reference Expansion**

---

reproduce the observed transport behavior at the H-3, H-6, and H-11 hydropads."





Compliance Certification Application Reference Expansion

---

Jung, Y., Ibrahim, A., and Borns, D.J. 1991. Mapping Fracture Zones in Salt; High Resolution Cross-Gallery Seismic Tomography, Geophysics: The Leading Edge of Exploration, Vol. 10, No. 4, pp. 37-39.

ABSTRACT p 37;

" The purpose of this article is to demonstrate the feasibility of high-resolution seismic tomography to identify fracture zones in salt at the Waste Isolation Pilot Plant (WIPP) located approximately 23 miles east of Carlsbad, New Mexico. The WIPP was established by the Department of Energy as an experimental facility to study the feasibility of using salt as a repository for transuranic nuclear wastes. The underground excavations, lying 2100 ft below the surface, were completed in the Salado formation (primarily a halite sequence of Permian age). The underground facility is composed of rooms and passageways developed within salt. Salt pillars separate the rooms and support the mine roof. Usually they have three faces forming walls for rooms and hallways. The fourth face does not exist because of the presence of unmined salt in the back of the pillar. Brine occurrences, which have been observed in excavations and drilling, are thought to be related to either sedimentary-related brine inclusions in the salt itself, or fractures in the marker beds created as a result of stress adjustments caused by the excavations.

Understanding the process of fracture development at the WIPP site is essential in predicting future changes in formation brine movement. Because a major groundwater unit in this area (the Rustler formation) exists above the salt sequence, the presence of fractures in the salt is of major interest in relation to the solubility of the salt as a safe disposal medium for radioactive waste. Fractures may create a hydrologic connection between the water-bearing unit and the underlying disposal area through shafts and boreholes. Another problem at the WIPP site is the development of a disturbed rock zone (DRZ) around underground excavations in the salt. The development of fractures and resultant dehydration of the pore fluid mark the growth of the DRZ. There is a concern that fracturing within the pillars will occur at a high enough rate to create unsafe conditions underground and reduce the planned operational lifetime of the project.

This study aims at developing high-resolution techniques to map fracture zones in salt. Preliminary studies suggest that fracture zones are identifiable through their linear lower seismic velocity pattern. As a means of mapping the seismic velocity in the salt pillar, several seismic techniques are under study. This paper focuses on the seismic tomographic study. To monitor changes in fracture patterns with time, the tomographic study should be done at time intervals on the same pillar. However, this is a lengthy process. Instead, two salt pillars excavated at different times were chosen for this study."

Kazemi, H., Merrill, Jr., L.S., Porterfield, K.L., and Zeman, P.R. 1976. Numerical Simulation of Water-Oil Flow in Naturally Fractured Reservoirs, Society of Petroleum Engineers Journal, Vol. 16, No. 6, pp. 317-326.

ABSTRACT, p 317;

" A three-dimensional, multiple-well, numerical simulator for simulating single- or two-phase flow of water and oil is developed for fractured reservoirs. The simulator equations are two-phase flow extensions of the single-phase flow equations derived by Warren and Root.<sup>1</sup> The simulator accounts for relative fluid mobilities, gravity force, imbibition, and variation in reservoir properties. The simulator handles uniformly and nonuniformly distributed fractures and/or no fractures at all. The simulator can be used to simulate the water-oil displacement process and in the transient testing of fractured reservoirs.

The simulator was used on the conceptual models of two naturally fractured reservoirs: a quadrant of a five-spot reservoir and a five-well dipping reservoir with water drive. These results show the significance of imbibition in recovering oil from the reservoir rock in reservoirs with an interconnected fracture network."





Kelley, V.A., and Saulnier, Jr., G.J. 1990. Core Analyses for Selected Samples from the Culebra Dolomite at the Waste Isolation Pilot Plant. SAND90-7011. Sandia National Laboratories, Albuquerque, NM. pp. 4-10. WPO 28629.

ABSTRACT, p. i;

" Two groups of core samples from the Culebra Dolomite Member of the Rustler Formation at and near the Waste Isolation Pilot Plant were analyzed to provide estimates of hydrologic parameters for use in flow-and-transport modeling. Whole-core and core-plug samples were analyzed by helium porosimetry, resaturation porosimetry, mercury-intrusion porosimetry, electrical-resistivity techniques, and gas-permeability methods.

Seventy-nine (79) helium-porosity determinations indicated that the distribution of Culebra porosities was skewed toward lower porosity values with an arithmetic mean and standard deviation of 0.153 and 0.053, respectively.

The vertical heterogeneity of porosity was indicated by 21 pairs of helium-porosity determinations where each sample of the pair was separated by approximately 5 cm. The porosity differences between the samples in the pairs varied from 0.050 to 0.093.

Water-resaturation-porosimetry results showed a near 1-to-1 correlation with the results from helium-porosity determinations. In some cases, the resaturation porosities were slightly larger than the helium porosities, possibly due to mineral dissolution by the resaturation fluid (deionized water) or to the experimental reproducibility of the two measuring techniques.

Endpoint mercury pore-volume saturations for 25 samples ranged from 66.7% to 99.9%, with an average endpoint pore-volume saturation of 95.4%. The endpoint pressure was 207 MPa. The median pore-throat radius varied over an order of magnitude from 0.077  $\mu\text{m}$  to 0.588  $\mu\text{m}$ , with an arithmetic average value of 0.315  $\mu\text{m}$ . Eighty-four percent of the pore-throat radii in the samples analyzed were between 0.1  $\mu\text{m}$  and 0.5  $\mu\text{m}$ . The average mercury-intrusion porosity was 0.148, as compared with the helium-porosity average of 0.154.

Seventy-three (73) grain-density measurements indicated a skewed distribution toward larger values of grain density with an arithmetic average of 2.82  $\text{g}/\text{cm}^3$  and a standard deviation of 0.19  $\text{g}/\text{cm}^3$ . The most common value of grain density was 2.83  $\text{g}/\text{cm}^3$ , which was also the median of the distribution.

Electrical-resistivity measurements of 15 saturated core plugs were used to calculate estimates of formation factor and tortuosity. Formation-factor values were log-normally distributed and values ranged from 12 to 407, with a geometric mean of 58.8. Tortuosity ranged from 0.04 to 0.33, with an arithmetic average of 0.14 and a median of 0.12. The results show a general trend of increasing tortuosity with increasing porosity. The diffusion porosities and diffusion tortuosities determined by Dykhuizen and Casey (1989) agree with the lower range of the values determined by this core-analysis study.

Sixty-six (66) horizontal-permeability measurements ranged from 7.9E-18  $\text{m}^2$  to 3.6E-13  $\text{m}^2$ , and the distribution had an arithmetic average of 6.2E-15  $\text{m}^2$ , a geometric mean of 4.5E-16  $\text{m}^2$ , and a median of 2.7E-16  $\text{m}^2$ . Twenty-six (26) vertical-permeability

## Compliance Certification Application Reference Expansion

---

measurements ranged from  $8.4\text{E-}18 \text{ m}^2$  to  $5.2\text{E-}14 \text{ m}^2$ , with an arithmetic mean of  $5.1\text{E-}15 \text{ m}^2$ , a geometric mean of  $9.0\text{E-}16 \text{ m}^2$ , and a median of  $3.5\text{E-}16 \text{ m}^2$ . Plots of the  $\log_{10}$  of permeability versus porosity indicated a weak correlation between the  $\log_{10}$  of permeability and porosity. A plot of  $\log_{10}$  of horizontal permeability versus the median pore-throat radii determined for the same samples indicated that the  $\log_{10}$  horizontal permeability is directly related to median pore-throat radius. "



Kim, J.I. 1991. "Actinide Colloid Generation in Groundwater," *Radiochimica Acta*. Vol. 52/53, Pt. 1, pp. 71-81.

**ABSTRACT;**

" The progress made in the investigation of actinide colloid generation in groundwaters is summarized and discussed with particular examples relevant to an understanding of the migration behavior of actinides in natural aquifer systems. The first part deals with the characterization of colloids: groundwater colloids, actinide real-colloids and actinide pseudocolloids. The second part concentrates on the generation processes and migration behavior of actinide pseudocolloids, which are discussed with some notable experimental examples. Importance is stressed more on the chemical aspects of the actinide colloid generation in groundwater. This work is a contribution to the CEC project MIRAGE II, particularly, to research area: complexation and colloids."



Lambert, S.J., 1983. Dissolution of Evaporites in and Around the Delaware Basin, Southeastern New Mexico and West Texas. SAND82-0461. Sandia National Laboratories, Albuquerque, NM. WPO 27520.

ABSTRACT, p 3;

" Permian evaporites in the Ochoan Castile, Salado, and Rustler Formations in the Delaware Basin of southeastern New Mexico and west Texas have been subjected to various degrees of dissolution (notably of halite and gypsum) through geologic time. Eastward tilting of the Delaware Basin has resulted in the exhumation and erosion of Ochoan rocks in the western part of the basin. Waters in the Capitan, Rustler, Castile, and Bell Canyon Formations have previously been proposed as agents or consequences of evaporite dissolution according to four principle models; solution-and-fill, phreatic dissolution, brine density flow, and stratabound dissolution (along bedding planes). Several geomorphological features of positive and negative relief have previously been cited as indicators of evaporite dissolution. Brine density flow has been used to explain the selective dissolution of certain evaporite horizons during the late Cenozoic. A review of available geological data has revealed that

- Halite deposition was probably not so extensive as formerly believed
- Waters with potential to dissolve evaporites are in the Rustler and Capitan, but not in the Bell Canyon, Salado mine seeps, or the Castile brine reservoirs
- Brine density flow has not been active in removing most of the 'missing' halite, nor are 'point-source' dissolution features likely to have their roots at the Bell Canyon
- Major evaporite dissolution has not been confined to the late Cenozoic, but much of it took place during the Permian, Triassic, Jurassic, and Tertiary periods
- The Bell Canyon Formation has not been a sink for dissolution-derived brine

Stratabound dissolution is an efficient process for the removal of evaporites and is well exemplified in Nash Draw. This process entails downdip migration of meteoric water within beds of competent fractured rock, with upward and downward excursions of the water into adjacent halite-bearing beds. The chief weakness in the stratabound model for dissolution is the as-yet-unidentified sink for dissolution brine. If the stratabound model of dissolution is active in removal of lower Salado halite, the threat of dissolution to the WIPP in the next 250,000 yr is comparable to the threat to the same area posed by the growth of Nash Draw during the past 600,000 yr. The regional geological history showed the past threat to be negligible."



Compliance Certification Application Reference Expansion

---

Lambert, S.J. 1987. "Stable-Isotope Studies of groundwaters in Southeastern New Mexico," In *The Rustler Formation at the WIPP Site, Report of a Workshop on the Geology and Hydrology of the Rustler Formation as it relates to the WIPP Project*. Ed. L. Chaturvedi. SAND85-1978C, EEG-34, pp. 36-57. Environmental Evaluation Group, Santa Fe, NM. WPO 28418.

ABSTRACT, p 36;

" Oxygen-18/16 and deuterium/hydrogen ratio measurements have been made on groundwaters sampled according to specific field criteria applied during pump tests of the Rustler Formation (the uppermost Permian evaporite unit) in Nash Draw, a solution-subsidence valley west of the WIPP site in the northern Delaware Basin of southeastern New Mexico. Comparison of these data with similar measurements on other groundwaters from the northern Delaware Basin indicates two nonoverlapping populations of meteoric groundwaters in delta-O-18/ delta-D space. Most of the Rustler waters in Nash Draw and at the WIPP site and older waters from the eastern two-thirds of the Capitan Limestone constitute one population, while unconfined groundwaters originating as observable modern surface recharge to alluvium, the near-surface Rustler in southwestern Nash Draw, and the Capitan in the Guadalupe Mountains (Carlsbad Caverns) constitute the other. The isotopic distinction suggests that Rustler groundwater in most of Nash Draw and at the WIPP site is not receiving significant modern meteoric recharge. A likely explanation for this distinction is that meteoric recharge to most of the Rustler and Capitan took place in the geologic past under climatic conditions significantly different from the present."



Compliance Certification Application Reference Expansion

---

Lenhardt, W.A. 1988. "Damage Studies at a Deep Level African Gold Mine." In Rockbursts & Seismicity In Mines, Proceedings of the Second International Symposium, Minneapolis, MN, June 8-10, 1988, C. Fairhurst, ed., 1990, pp. 391-393. A.A. Balkema, Brookfield, VT

ABSTRACT, p. 391;

" The effect of seismic event magnitude on damage at Western Deep Levels Limited, a deep level gold mine in South Africa, is evaluated. Relationships between length of face affected, number of panel shifts lost and seismic event magnitude were determined. Theoretical studies and observations elsewhere lend confidence to the validity of the results. Some insight was gained into the spread of truly damaging events across the seismic event magnitude spectrum. It is believed that the results will allow improved assessment of seismic related lossess (sic), thus facilitating the cost-benefit evaluation of regional support type, depth and other factors."



Lieser, K.H., Gleitsmann, B., and Steinkopff, T. 1986. "Sorption of Trace Elements or Radionuclides in Natural Systems Containing Groundwater and Sediments," *Radiochimica Acta*. Vol. 40, no. 1, 33-37.

ABSTRACT, p. 33;

" A general formula for the sorption ratio that is observed experimentally in natural systems is presented taking into account three kinds of processes: sorption at the outer surface of the solid particles, sorption in porous particles and one-directional processes such as precipitation or coprecipitation. These various processes as well as the mechanisms and the kinetics of sorption are discussed.

The sorption of radioactive  $Cs^+$ ,  $Sr^{2+}$  and  $Ce^{3+}$  is studied in two selected natural sediment/groundwater systems, one of low and one of high salinity, under various conditions.  $Cs^+$  ions are mainly sorbed in clay minerals that are suspended in the groundwater with relatively high sorption ratios,  $Sr^{2+}$  ions are mainly sorbed on the sediments with relatively low sorption ratios, and  $Ce^{3+}$  is mainly found in form of colloids or in suspended particles or in coprecipitates. Coprecipitation leads to very high sorption ratios for  $Ce^{3+}$ . The behavior of  $Cs^+$ ,  $Sr^{2+}$  and  $Ce^{3+}$  is typical for all elements with similar properties."



Lieser, K.H., Gleitsmann, B., Peschke, S., and Steinkopff, T. 1986. Colloid Formation and Sorption of Radionuclides in Natural Systems. *Radiochimica Acta*, Vol. 40, No. 1, pp. 39-47.

ABSTRACT, p39;

" Natural systems comprising sediments and groundwaters of low and of high salinity are investigated with respect to the formation and the influence of coarsely dispersed particles and finely dispersed particles (colloids). Equations are derived for the sorption equilibria in such systems and it is shown that the efficiencies of mutual separation of coarsely dispersed particles, finely dispersed particles and sediments (efficiencies of filtering) strongly influence the sorption ratios that are observed.

In groundwater without sediments the formation of colloids of radioactive  $Ce^{3+}$  is demonstrated, whereas  $Cs^+$  and  $Sr^{2+}$  do not form colloids under these conditions, as expected.

The amount of elements and of colloids given off by the sediments into the groundwaters are measured for the samples of low and of high salinity and the influence of agitation is shown. Sorption ratios of radioactive  $Cs^+$ ,  $Sr^{2+}$ , and  $Ce^{3+}$  are investigated as function of the ratio of the groundwater volume to the mass of the sediment without filtration, after filtration through  $0.45 \mu m$  filters and after ultrafiltration. The results are discussed on the basis of the equations derived. It is shown that  $Cs^+$  ions are sorbed mainly on the clay particles and that the larger amount of these clay particles has grain sizes greater than  $0.45 \mu m$  under the experimental conditions of smooth shaking.  $Sr^{2+}$  ions are mainly sorbed on the sediments with a relatively low sorption ratio.  $Ce^{3+}$  ions form colloids ("Eigenkolloide") that are retained by ultrafiltration."

Lieser, K.H., Ament, A., Hill, R., Singh, R.N., Stingl, U. and Thybusch, B.. 1990. Colloids in Groundwater and Their Influence on Migration of Trace Elements and Radionuclides. Radiochimica Acta, Vol. 49, No. 2, pp.83-100.

ABSTRACT, p 83;

" A survey on colloid and radiocolloid formation in groundwaters is given. Three groundwaters are analyzed after standing at rest for several months and after equilibration with the corresponding sediments. The partition of radioactive Cs, Sr, Pb, Ac and Th on the coarse particle fraction ( $>0.45 \mu\text{m}$ ), the fine particle fraction ( $0.002$  to  $0.45 \mu\text{m}$ ) and the molecular fraction ( $<0.002 \mu\text{m}$ ) in these groundwaters is investigated. Thereafter the groundwaters are passed through columns filled with the corresponding sediments from the same sites as the groundwaters at a linear flow rate of about 10 cm per day and the relative concentrations as well as the partition of the radionuclides on the three fractions in the effluent groundwaters are measured.

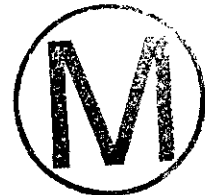
Strong retention of Cs, Pb, Ac and Th and to a smaller extent Sr in the columns is observed which is mainly due to sorption by ion exchange (Cs, Sr) or hydrolytic adsorption (Pb, Ac, Th) on the sediments as well as on the coarse and fine particles in the groundwaters. These particles serve as carriers. Comparison of column and batch experiments show that size filtration of coarse particles is very important with respect to retention."



Litvak, B.L. 1986. "Simulation and Characterization of Naturally Fractured Reservoirs." In Reservoir Characterization Technical Conference, Dallas, TX, April 29-May 1, 1985, L.W. Lake and H.B. Carroll, Jr., eds. pp. 561-584. Academic Press, Orlando, FL.

ABSTRACT, p 561;

" A three-dimensional, three-phase numerical simulator with rigorous treatment of matrix/fracture flow is developed for modeling naturally fractured reservoirs. A new method was developed in the simulator for description of capillary pressure and gravity forces in the matrix/fracture media. The simulator is designed for the solution of field reservoir problems. At the same time it considers physical processes in a single matrix block surrounded by fractures. A significant effect of different treatment of capillary and gravity forces in fractured reservoirs is demonstrated in an example problem."





Lowenstein, T.K. 1987 Post Burial Alteration of the Permian Rustler Formation Evaporites, WIPP Site, New Mexico: Textural, Stratigraphic and Chemical Evidence. EEG-36, DOE/AL/10752-36, Environmental Evaluation Group, Santa Fe, NM.

PREFACE, p vii;

" A repository for permanent isolation of defense transuranic wastes is being excavated in southeastern New Mexico, about 40 km (25 miles) east of Carlsbad. The Waste Isolation Pilot Plant (WIPP) repository has been designed for the disposal of waste in the lower part of the Salado (salt) Formation at a depth of 655 meters (2150 ft). The water-bearing zones of the Rustler Formation, which overlies the Salado, are considered to be the main pathway for the transport of radionuclides to the biosphere, if the repository is breached.

The Rustler Formation is 150 meters (490 feet) thick, 6.4 Km (4 miles) east of the center of the WIPP site. The thickness reduces drastically to the west so that it is only 91 meters (300 ft) thick in the western part of the WIPP site. At its thickest location, the Rustler consists of siltstone and anhydrite with two dolomite beds and both clear and clayey halite. Halite is progressively missing from deeper layers from east to west in the Rustler cross-section across the WIPP site. These observations were interpreted by Powers et al (1978), Mercer (1983), Lambert (1983), Chaturvedi and Rehfeldt (1984), Bachman (1984), Snyder (1985), Chaturvedi and Channell (1985) and others as indicating post-burial dissolution of halite and increased gypsification of anhydrite further west. Increased permeability of the water-bearing dolomites from east to west also was thought to result from the increased fracturing as a result of dissolution.

In 1984, Powers and Holt (1984) and Holt and Powers (1984) expressed doubts about the concept of post-burial dissolution of Rustler evaporites, on the basis of detailed mapping in the WIPP Waste Handling Shaft, and stated the following:

'Post-depositional dissolution features were not observed in any stratigraphic horizons in the Waste Shaft. In fact, several zones previously identified as dissolution residues in nearby boreholes (e.g. ERDA-9) contain pronounced primary sedimentary features. This is of great significance since dissolution has, historically, been considered as an important process that has greatly modified the Rustler Formation in this area.'

(Holt and Powers, 1984)

This statement was based on the first detailed sedimentological study of the Rustler stratigraphy, but only at one location, albeit in situ, in a shaft. It clearly signaled the need for further work on the lateral variations in the stratigraphy of the Rustler Formation across the WIPP site. Since the interpretation by Powers and Holt was based on sedimentary features, the need was for a sedimentological study of the Rustler Formation.

To resolve this issue, the Environmental Evaluation Group (EEG) asked Dr. Tim K. Lowenstein to perform a sedimentological study of the available cores of the Rustler Formation. Dr. Lowenstein is a sedimentologist with special interest in the study of evaporites and has studied the Ochoan evaporites of the Delaware Basin (Lowenstein, 1982,

## Compliance Certification Application Reference Expansion

---

1985). For this study, he performed a detailed sedimentological analysis of the Rustler cores from four wells, viz. DOE-2, W-19, H-11 and H-12. This included visual examination of the cores, preparation and petrographic analyses of 52 thin sections from selected locations of the cores, and x-ray diffraction analyses of 40 samples from selected locations of the cores. In addition, descriptive data on the rock cuttings and geophysical logs of borehole P-18 were used for correlation purposes. This report is a result of these analyses and correlation of sedimentary features between the drill-holes.

This study was confined to a miniscule area (only about 0.05%) of the total extent of the Rustler Formation and therefore cannot be considered to be a study of post-burial alteration of the Rustler Formation as a whole. Within the confines of this area, however, detailed stratigraphic correlations by Dr. Lowenstein based on sedimentary structures and textures indicate overall uniformity of depositional setting. Further, the physical and chemical alteration features, based on crosscutting relations, represent the last processes which have operated on these rocks. Four distinct dissolution zones in the Rustler Formation have been interpreted by Dr. Lowenstein. Although the strata above and below the inferred dissolution zones are chemically and physically altered, they contain abundant sedimentary structures and internal stratigraphy that can easily be matched from well to well. Dr. Lowenstein does not see a contradiction between post depositional dissolution and the survival of sedimentary structures. His interpretation is that the dissolved species produced by solution are removed from the site of reaction and the zones in which the effects of dissolution are now seen were at the periphery of main dissolution activity and therefore may exhibit some alteration as well as primary sedimentary structures."

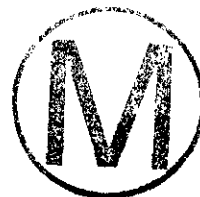


Lowenstein, T.K. 1988. Origin of Depositional Cycles in a Permian "Saline Giant": The Salado (McNutt Zone) Evaporites of New Mexico and Texas. Geological Society of America Bulletin, Vol. 100, No. 4, pp. 592-608.

ABSTRACT, p 592, col 1;

" Two types of metre-scale depositional cycles have been recognized within the McNutt Potash Zone of the Permian Salado evaporites. The cycles record progressive drawdown and concentration of brine in a shallow, marginal marine basin. 'Type I' cycles, made of basal carbonate-siliciclastic mudstone, then anhydrite-polyhalite pseudomorphous after primary gypsum, overlain by halite and capped by muddy halite, are interpreted as marine sea water dominated. They formed by massive spillover of sea water through a connection with the Permian Ocean at high relative sea-level stands (lagoonal mudstone and anhydrite-polyhalite after subaqueous gypsum), followed by relative lowering of sea level and gradual basin restriction (shallow saline-lake and salt-pan halite) and ending with a desiccated basin, isolated from the Permian Ocean (salt-pan halite and saline mudflat muddy halite cycle cap). 'Type II' cycles occur between the Type I cycles and contain halite overlain transitionally by muddy halite. They record a temporal evolution of environments from a shallow saline lake to an ephemeral salt-pan-saline mudflat complex and are interpreted as continental-dominated sequences sourced by meteoric inflow from surrounding land areas that mixed with variable amounts of sea water, either residual or introduced into the Salado basin by seepage.

The vertical stacking of Type I cycles is best explained by periodic invasions of sea water into the Salado basin coincident with eustatic sea-level rises. The continental-dominated Type II cycles formed during intervening periods of eustatic sea-level fall and low stands. The *maximum* time interval between major marine incursions is an average of  $10^5$  yr. "



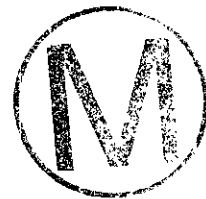
Compliance Certification Application Reference Expansion

---

Lyklema, J. 1978. Surface Chemistry of Colloids in Connection with Stability. The Scientific Basis of Flocculation. K.J. Ives, Ed., pp. 3-36. Sijthoff and Noordhoff: Dordrecht.

ABSTRACT, p. 3;

" A review is given of the fundamental features of the interfacial electrochemistry of colloid particles, emphasizing its role in colloid stability. The discussion includes a description of double layers in the presence of simple electrolytes and with polymers.



Compliance Certification Application Reference Expansion

---

Lyon, M.L. 1989 Annual Water Quality Data Report for the Waste Isolation Pilot Plant. DOE/WIPP 89-001. Westinghouse Electric Corporation, Carlsbad, NM.

1.1 SAMPLING PROGRAM SCOPE, p 1-5;

" The WIPP Water Quality Sampling Program (WQSP) was initiated in January 1985. The program's goals are to collect reproducible and representative ground-water samples from water-bearing zones in the WIPP vicinity. The Waste Isolation Pilot Plant Water Quality Sampling Manual WP 7-2, Revision 1 (October 1987) was the governing document for the program in 1988. This manual details the WQSP wells to be sampled and lists the types of analyses required for the program. Procedures detailing sample collection techniques and methods for field analyses accompany WP 7-2 are located in the Waste Isolation Pilot Plant Geotechnical and Geosciences Procedure Manual.

The water quality analytical data obtained by the WQSP directly support four major programs at the WIPP. These programs include site characterization, performance assessment (compliance with 40 CFR 191), the Radiological Baseline Program, and the Ecological Monitoring Program. Additionally, the State of New Mexico Environmental Evaluation Group is provided with water samples from each sampling location for independent analysis. Each of these programs requires a unique set of analyses and data, but overlap of analytical needs does occur. The particular set of water sample analyses supporting a given program are defined by that program and not by the WQSP. A brief description of each program is given below to illustrate the role of the WQSP at the WIPP."



Compliance Certification Application Reference Expansion

---

Machette, M.N. 1985. "Calcic Soils of the Southwestern United States." In Soils and Quaternary Geology of the Southwestern United States. D.L. Weide and M.L. Faber, eds., Special Paper Vol. 203, pp. 1-21. Geological Society of America, Denver, CO.

ABSTRACT, p 1;

" Calcic soils are commonly developed in Quaternary sediments throughout the arid and semiarid parts of the southwestern United States. In alluvial chronosequences, these soils have regional variations in their content of secondary calcium carbonate ( $\text{CaCO}_3$ ) because of (1) the combined effects of the age of the soil, (2) the amount, seasonal distribution, and concentration of  $\text{Ca}^{++}$  in rainfall, and (3) the  $\text{CaCO}_3$  content and net influx of airborne dust, silt, and sand. This study shows that the morphology and amount of secondary  $\text{CaCO}_3$  (cS) are valuable correlation tools that can also be used to date calcic soils.

The structures in calcic soils are clues to their age and . . ."



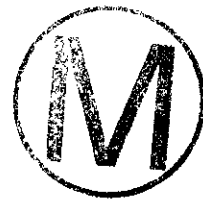
Compliance Certification Application Reference Expansion

---

Maiti, T.C., Smith, M.R., and Laul, J.C. 1989. Colloid Formation Study of U, Th, Ra, Pb, Po, Sr, Rb, and Cs in Briny (High Ionic Strength) Groundwaters: Analog Study for Waste Disposal. Nuclear Technology. Vol. 84, No. 1, pp. 82-87.

ABSTRACT, p. 82;

" Colloid formation of uranium, thorium, radium, lead, polonium, strontium, rubidium, and cesium in briny (high ionic strength) groundwaters is studied to predict their capability as vectors for transporting radionuclides. This knowledge is essential in developing models to infer the transport of radionuclides from the source region to the surrounding environment. Except polonium, based on the experimental results, colloid formation of uranium, thorium, radium, lead, strontium, rubidium, and cesium is unlikely in brines with compositions similar to the synthetic Palo Duro Basin brine. This observation of no colloid formation is explained by electrokinetic theory and inorganic solution chemistry."



## Compliance Certification Application Reference Expansion

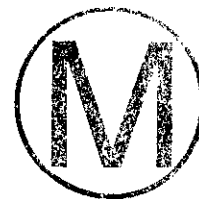
---

Mansure, A. and Reiter, M. 1977. An Accurate Equilibrium Temperature Log in AEC No. 8, A Drill Test in the Vicinity of the Proposed Carlsbad Disposal Site. Open File Report 80. New Mexico Bureau of Mines and Mineral Resources, Socorro, NM. WPO 21200.

" On February 24, 1977 an accurate, equilibrium log was run in drill test AEC #8, which is in the vicinity of the Carlsbad disposal site. The log was run from 50 feet to 4810 feet. Temperature data were taken at varying depth intervals with the sonde continuously moving. At 50 ft, 1000 ft, 2000 ft, 3000 ft, 4000 ft, 4500 ft, and 4810 ft the sonde was stopped to examine tool response and wellbore stability. The sonde is a thermistor device which is connected to Mueller bridge electronics at the surface. The measurements are believed to be accurate to  $\pm .03^{\circ}\text{F}$ . Data are printed out in this report and shown graphically.

From the graph it is evident that there are three distinct gradient zones. They are approximately : 1) 50 ft to 1035 ft, 2) 1056 ft to 4247 ft, and 3) 4306 ft to 4810 ft. The temperature gradients in these zones are respectively: 1)  $.85^{\circ}\text{F}/100\text{ ft}$ , 2)  $.43^{\circ}\text{F}/100\text{ ft}$ , and 3)  $.91^{\circ}\text{F}/100\text{ ft}$ .

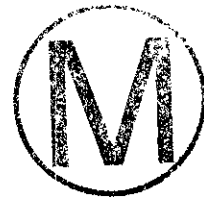
Sandia lab supplied thermal conductivity data (taken by Russel U. Acton, Sandia Lab tech. doc. in prep.) applicable to the middle gradient zone. The apparent average of these values is  $5.5\text{ W/M-}^{\circ}\text{K}$  or  $13.7\text{ mcal/cm-sec-}^{\circ}\text{C}$ . The product of the temperature gradient and the thermal conductivity mean in the middle zone yields an estimate of the geothermal heat flux at AEC #8; this is  $1.07\text{ }\mu\text{cal/cm}^2\text{-sec}$ ."



Marietta, M.G., Bertram-Howery, S.G., Anderson, D.R., Brinster, K.F., Guzowski, R.V., Iuzzolino, H., and Rechar, R.P. 1989. Performance Assessment Methodology Demonstration: Methodology Development for Evaluating Compliance With EPA 40 CFR Part 191, Subpart B, for the Waste Isolation Pilot Plant. SAND89-2027. Sandia National Laboratories, Albuquerque, NM. WPO 25952.

ABSTRACT;

" This report describes a demonstration of the performance assessment methodology for the Waste Isolation Pilot Plant (WIPP) to be used in assessing compliance with the Environmental Protection Agency's Standard, *Environmental Radiation Protection Standards for the Management and Disposal of Spent Nuclear Fuel, High-Level and Transuranic Radioactive Wastes* (40 CFR Part 191, Subpart B). This demonstration incorporates development and screening of potentially disruptive scenarios. A preliminary analysis of the WIPP disposal system's response to human intrusion scenarios produces preliminary complementary cumulative distribution functions (CCDFs) similar to those that will ultimately be used to assess the compliance of the WIPP with the Containment Requirements of the Standard. Preliminary estimates of scenario probabilities are used to construct two demonstration CCDFs. The conceptual model of the disposal system consists of geologic, hydrologic, and disposal system subsystems along with the physical and chemical processes associated with these subsystems. Parameter values defining the systems contain uncertainties and modeling approximations of such a disposal system contributes to those uncertainties. The WIPP compliance assessment methodology consists of a system of techniques and computer codes that estimate releases of radionuclides from the disposal system, incorporating analysis of the parameter uncertainties in the estimates. Demonstration CCDFs are presented, but are not yet credible enough to judge the probability of compliance of the WIPP with the EPA Standard. One CCDF, based primarily on conservative reference data and conservative conceptual models, exceeds EPA limits, and another CCDF that represents effects of possible engineered alternatives does not exceed EPA limits."



McGrath E.J., and Irving, D.C. 1975. Techniques for Efficient Monte Carlo Simulation. Volume III. Variance Reduction. ORNL-RSIC-38, Vol. 3. Oak Ridge National Laboratory, Oak Ridge, TN.

ABSTRACT, p v;

" Many Monte Carlo simulation problems lend themselves readily to the application of variance reduction techniques. These techniques can result in great improvements in simulation efficiency. This document describes the basic concepts of various reduction (Part I), and a methodology for application of variance reduction techniques is presented in Part II. Appendices include the basic analytical expressions for application of variance reduction schemes as well as an abstracted bibliography.

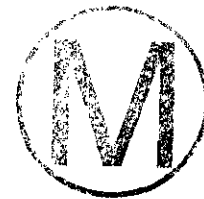
The techniques considered here include importance sampling, Russian roulette and splitting, systematic sampling, stratified sampling, expected values, statistical estimation, correlated sampling, history reanalysis, control variates, antithetic variates, regression, sequential sampling, adjoint formulation, transformations, orthonormal and conditional Monte Carlo. Emphasis has been placed on presentation of the material for application by the general user. This has been accomplished by presenting a step by step procedure for selection and application of the appropriate technique(s) for a given problem."



McGrath E.J., and Irving, D.C. 1975. Techniques for Efficient Monte Carlo Simulation. Volume II. Random Number Generation for Selected Probability Distributions. ORNL-RSIC-38 Vol. 2. Oak Ridge National Laboratory, Oak Ridge, TN.

ABSTRACT, p v;

" Algorithms for efficient generation of random numbers from various probability distributions are presented, in both a flowchart form and as a sample Fortran subroutine. Twenty-two different distributions, including all commonly encountered discrete and continuous functions, the Weibull, Johnson, and Pearson families of empirical distributions, and histogram distributions, are covered. The general techniques to apply in deriving a random number selection scheme for an arbitrary distribution are discussed. A machine-independent subroutine for generating uniform random numbers is also described."



McGrath E.J., Basin, S.L., Burton, R.W., Irving, D.C., and Jaquette, S.C. 1975. Techniques for Efficient Monte Carlo Simulation. Volume I. Selecting Probability Distributions. ORNL-RSIC-38 Vol. 1. Oak Ridge National Laboratory, Oak Ridge, TN.

ABSTRACT, p vii;

" This document is the first of three volumes which present techniques and methods for developing efficient Monte Carlo simulations: Each volume presents techniques for reducing computational effort in one of the following areas: Vol. I - Selecting Probability Distributions, Vol II - Random Number Generation For Selected Probability Distributions, and Vol. III - Variance Reduction.

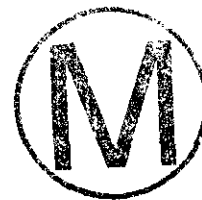
This volume provides a straightforward approach and associated techniques for selecting the most appropriate probability distributions for use in Monte Carlo simulations. Part I, BASIC CONSIDERATIONS, presents the underlying concepts and principles for selecting probability distributions. Part II, SELECTION OF DISTRIBUTIONS, gives the mathematical models representing stochastic processes and presents step-by-step procedures for identification and selection of the appropriate probability distributions based upon the degree of knowledge and available data for the random variable under study."



McKay, M.D., Beckman, R.J., and Conover, W.J. 1979. A Comparison of Three Methods for Selecting Values of Input Variables in the Analysis of Output from a Computer Code. Technometrics, Vol. 21, No. 2, pp. 239-245.

p 239;

" Two types of sampling plans are examined as alternatives to simple random sampling in Monte Carlo studies. These plans are shown to be improvements over simple random sampling with respect to variance for a class of estimators which includes the sample mean and the empirical distribution function."



Mercer, J.W., and Snyder, R.P. 1990. Basic Data Report for Drillholes at the H-11 Complex (Waste Isolation Pilot Plant--WIPP). SAND89-0200. Sandia National Laboratories, Albuquerque, NM. WPO 27705.

ABSTRACT, p iii;

" Drillholes H-11b1, H-11b2, and H-11b3 were drilled from August to December 1983 for site characterization and hydrologic studies of the Culebra Dolomite Member of the Upper Permian Rustler Formation at the Waste Isolation Pilot Plant (WIPP) site in southeastern New Mexico. In October 1984, the three wells were subjected to a series of pumping tests designed to develop the wells, provide information on hydraulic communication between the wells, provide hydraulic properties information, and to obtain water samples for quality of water measurements. Based on these tests, it was determined that this location would provide an excellent pad to conduct a convergent-flow non-sorbing tracer test in the Culebra dolomite. In 1988, a fourth hole (H-11b4) was drilled at this complex to provide a tracer-injection hole for the H-11 convergent-flow tracer test and to provide an additional point at which the hydraulic response of the Culebra H-11 multipad pumping test could be monitored.

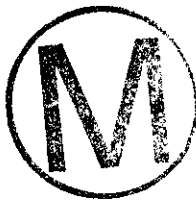
The geologic units penetrated in H-11b1 are surficial deposits (0-12.5 feet) of Holocene age, the Dockum Group (undifferentiated) (12.5-63 feet) of Upper Triassic age, the Dewey Lake Redbeds (63-558 feet) and the Rustler Formation (558-785+ feet) of Upper Permian age. There was evidence of Rustler halite in the core at 763 feet, which was 7 feet into the unnamed lower member).

The geologic units penetrated in H-11b2 are surficial deposits (0-11 feet) of Holocene age, the Dockum Group (undifferentiated) (11-62 feet) of Triassic age, the Dewey Lake Redbeds (62-560 feet) and the Rustler Formation (560-776+ feet) of Permian age. There was evidence of Rustler halite in place in the core at 764 feet, which was 7 feet into the unnamed lower member).

The geologic units penetrated in H-11b3 are surficial deposits (0-11 feet) of Holocene age, the Dockum Group (undifferentiated) (11-59.5 feet) of Upper Triassic age, the Dewey Lake Redbeds (59.5-560.2 feet) and the Rustler Formation (560.2-788.7+ feet) of Permian age. There was evidence of Rustler halite in the core at 777.7 feet, which was 17.7 feet into the unnamed lower member).

The geologic units penetrated in H-11b4 are surficial deposits (0-11 feet) of Holocene age, the Dockum Group (undifferentiated) (11-60 feet) of Upper Triassic age, the Dewey Lake Redbeds (60-554 feet) and the Rustler Formation (564-765.3+ feet) of Upper Permian age. There was no evidence of Rustler halite in the core to 765.3 feet, which was 19.2 feet into the unnamed lower member).

A suite of geophysical logs was run on the drillholes and was used to identify different lithologies and aided in interpretation of the hydraulic tests."



Mercer, J.W., Beauheim, R.L., Snyder, R.P., and Fairer, G.M. 1987. *Basic Data Report For Drilling and Hydrologic Testing of Drillhole DOE-2 at the Waste Isolation Pilot Plant (WIPP) Site.* SAND86-0611. Sandia National Laboratories, Albuquerque, NM.

**ABSTRACT;**

" Drillhole DOE-2 was drilled to investigate a structural depression marked by the downward displacement of stratigraphic markers in the Salado formation ~2 mi north of the center of the WIPP site. This depression was named informally after the shallow borehole FC-92 in which the structure was described. The presence of the depression was confirmed by drilling. Contrary to several hypotheses, halite layers were thicker in the lower part of the Salado, not thinner as a result of any removal of halite. The upper Castile anhydrite in Drillhole DOE-2 is anomalously thick and is strongly deformed relative to the anhydrite in adjacent drillholes. In contrast, the halite was <8 ft thick and significantly thinner than usually encountered. The lower Castile anhydrite appears to be normal. The depression within the correlated marker beds in the Salado Formation in Drillhole DOE-2 is interpreted as a result of gravity-driven deformation of the underlying Castile Formation.

Several stratigraphic units were hydrologically tested in Drillhole DOE-2. Testing of the unsaturated lower portion of the Dewey Lake Red Beds was unsuccessful because of exceptionally small rates of fluid intake. Drill-stem tests were conducted in five intervals in the Rustler Formation, over the Marker Bed 138-139 interval in the Salado Formation, and over three sandstone members of the Bell Canyon Formation. A pumping test was conducted in the Culebra Dolomite Member of the Rustler Formation. Pressure-pulse tests were conducted over the entire Salado Formation. Fluid samples were collected from the Culebra Dolomite Member and from the Hays Member of the Bell Canyon Formation."

Mitchell, J.F.B. 1989. The "Greenhouse" Effect and Climate Change. *Reviews of Geophysics*. Vol. 27, No. 1, pp. 115-139.

ABSTRACT, p. 115;

" The presence of radioactively active gases in the Earth's atmosphere (water vapor, carbon dioxide, and ozone) raises its global mean surface temperature by 30 K, making our planet habitable by life as we know it. There has been an increase in carbon dioxide and other trace gases since the Industrial revolution, largely as a result of man's activities, increasing the radiative heating of the troposphere and surface by about  $2 \text{ W m}^{-2}$ . This heating is likely to be enhanced by resulting changes in water vapor, snow and sea ice, and cloud. The associated equilibrium temperature rise is estimated to be between 1 and 2 K, there being uncertainties in the strength of climate feedbacks, particularly those due to cloud. The large thermal inertia of the oceans will slow the rate of warming, so that the expected temperature rise will be smaller than the equilibrium rise. This increases the uncertainty in the expected warming to date, with estimates ranging from less than 0.5 K to over 1 K. The observed increase of 0.5 K since 1900 is consistent with the lower range of these estimates, but the variability in the observed record is such that one cannot necessarily conclude that the observed temperature change is due to increases in trace gases. The prediction of changes in temperature over the next 50 years depends on assumptions concerning future changes in trace gas concentrations, the sensitivity of climate, and the effective thermal inertia of the oceans. On the basis of our current understanding a further warming of at least 1 K seems likely. Numerical models of climate indicate that the changes will not be uniform, nor will they be confined to temperature. The simulated warming is largest in high latitudes in winter and smallest over sea ice in summer, with little seasonal variation in the tropics. Annual mean precipitation and runoff increase in high latitudes, and most simulations indicate a drier land surface in northern mid-latitudes in summer. The agreement between different models is much better for temperature than for changes in the hydrological cycle. Priorities for future research include developing an improved representation of cloud in numerical models, obtaining a better understanding of vertical mixing in the deep ocean, and determining the inherent variability of the ocean-atmosphere system. Progress in these areas should enable detection of a man-made 'greenhouse' warming within the next two decades.



Molecke, M.A., Argüello, J.G., and Beraún, R. 1993. Waste Isolation Pilot Plant Simulated RH-TRU Waste Experiments: Data and Interpretation Report. SAND88-1314. Sandia National Laboratories, Albuquerque, NM. WPO 24906.

ABSTRACT, p. i;

" The simulated, i.e., nonradioactive remote-handled transuranic waste (RH TRU) experiments being conducted underground in the Waste Isolation Pilot Plant (WIPP) were emplaced in mid-1986 and have been in heated test operation since 9/23/86. These experiments involved the in situ, waste package performance testing of eight full-size, reference RH TRU containers emplaced in horizontal, unlined test holes in the rock salt ribs (walls) of WIPP Room T. All of the test containers have internal electrical heaters; four of the test emplacements were filled with bentonite and silica sand backfill materials. We designed test conditions to be 'near-reference' with respect to anticipated thermal outputs of RH TRU canisters and their geometrical spacing or layout in WIPP repository rooms, with RH TRU waste reference conditions current as of the start date of this test program. We also conducted some thermal overtest evaluations. This paper provides a: detailed test overview; comprehensive data update for the first 5 years of test operations; summary of experiment observations; initial data interpretations; and, several recommendations for future RH TRU waste emplacements in the WIPP. Details included are: current test status; experimental objectives -- how these tests support WIPP TRU waste acceptance, performance assessment studies, underground operations, and the overall WIPP mission; and, in situ performance evaluations of RH TRU waste package materials plus design details and options. We provide instrument data and results for in situ waste container and borehole temperatures, pressures exerted on test containers through the backfill materials, and vertical and horizontal borehole-closure measurements and rates. The effects of heat on borehole closure, fracturing, and near-field materials (metals, backfills, rock salt, and intruding brine) interactions were closely monitored and are summarized, as are assorted test observations. Predictive 3-dimensional thermal and structural modeling studies of borehole and room closures and temperature fields were also performed. Computed and measured borehole closure results indicate greater closure occurs near the middle- and back-end of the holes than at the (open) rib-end. Computed vertical closure results provide an upper bound estimate on borehole closure that is 1.5 - 2.5 times larger than the measured in situ values, but are in qualitative agreement. Based on our current data, results, observations, and interpretations, RH TRU waste packages, materials, and emplacement geometry in unlined salt boreholes appear to be quite adequate and safe for repository-phase isolation at WIPP. There should be no restrictions on RH TRU waste acceptance at WIPP due to observed waste package behavior."



Muehlberger, W.R., Belcher, R.C., and Goetz, L.K. 1978. Quaternary Faulting on Trans-Pecos Texas. *Geology*, Vol. 6, No. 6, pp. 337-340.

ABSTRACT, p 337;

" Faults that displace Quaternary units can be observed in scarps in Trans-Pecos Texas and are restricted to two north-trending zones in contrast to late Tertiary faults that cover the region and strike north, northwest, and west. The western zone of Quaternary faults, near El Paso, is usually included as the southern part of the Rio Grande rift. The eastern zone of Quaternary faults extends for 300 km from southern New Mexico along the Salt Basin graben through Van Horn, Texas; its probable extensions and subparallel associates extend southward to Presidio, Texas. This belt of faults is parallel to the Rio Grande rift zone and should be considered a southeast extension of that zone.

These fault zones die out southward into the edge of the Chihuahua tectonic belt, a region underlain by a thick Mesozoic carbonate and clastic section that in turn rests on a thick layer of evaporites. The evaporite zone may mask Cenozoic normal faulting and thus may define a zone of no data rather than a southern limit of basin-and-range or Rio Grande graben tectonics.

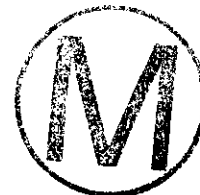
All Quaternary and most Tertiary faults trend parallel to pre-existing structures. The map pattern of Quaternary scarps suggest a maximum extension oriented about S80°W; however, first-motion studies of the 1931 Valentine, Texas earthquake show a maximum elongation direction of S50° to 55°W. This difference may be unique to this one earthquake or may be due to the pre-existing lines of weakness that control the location of presently active faults."

Myers, J., Derz, P., and James. 1991. "Chapter 6: The Redox State and the Occurrence and Influence of Organics in the Culebra." In *Hydrogeochemical Studies of the Rustler Formation and Related Rocks in the Waste Isolation Pilot Plant Area, Southeastern New Mexico*, M.D. Siegel, S.J. Lambert, and K.L. Robinson, eds. SAND88-0196. Sandia National Laboratories, Albuquerque, NM. In WPO 25624 (Chapter 6) pp. 6-1 through 6-35.

ABSTRACT, p i;

" Chemical, mineralogical, isotopic, and hydrological studies of the Culebra dolomite member of the Rustler Formation and related rocks are used to delineate hydrochemical facies and form the basis for a conceptual model for post-Pleistocene groundwater flow and chemical evolution. Modern flow within the Culebra in the Waste Isolation Pilot Plant (WIPP) area appears to be largely north-to-south; however, these flow directions under confined conditions are not consistent with the salinity distribution in the region surrounding the WIPP Site. Isotopic, mineralogical, and hydrological data suggest that vertical recharge to the Culebra in the WIPP area and to the immediate east and south has not occurred for several thousand years. Eastward increasing  $^{234}\text{U}/^{238}\text{U}$  activity ratios suggest recharge from a near-surface Pleistocene infiltration zone flowing from the west-northwest and imply a change in flow direction in the last 30,000 to 12,000 years.

Culebra groundwaters are in chemical equilibrium with gypsum and are undersaturated with halite and anhydrite. A partial-equilibrium model for the chemical evolution of the groundwater suggests that Na, Cl, Mg, K, and  $\text{SO}_4$  are added to the Culebra by dissolution of evaporite salts in adjacent strata. Equilibrium is maintained with gypsum and calcite, but dolomite supersaturation increases as the salinity of the water increases. Stable-isotope compositions of carbonates are consistent with this model and indicate that no recrystallization of dolomite in equilibrium with the groundwater has occurred. Major and minor element correlations are consistent with several plausible mechanisms of water/rock interaction, including sorption of lithium and boron by clays and dissolution of Mg-rich clays."



## Compliance Certification Application Reference Expansion

---

Nicholson, Jr., A., and Clebsch, Jr., A. 1961. Geology and Ground-Water Conditions in Southern Lea County, New Mexico. Ground-Water Report 6. State Bureau of Mines and Mineral Resources, Socorro, NM.

ABSTRACT, p 1;

" Southern Lea County is at the southeastern corner of New Mexico. Most of the area is in the Pecos Valley section of the Great Plains physiographic province; it also includes the southern margin of the Llano Estacado. There are no perennial streams and no throughgoing surface drainage.

Rocks of Quaternary, Tertiary, and Triassic age are exposed and contain the principle aquifers. The most important aquifer is the Ogallala formation, which underlies the Llano Estacado and forms outliers south of it. In large parts of southern Lea County, however, the Ogallala has been removed by erosion and in the low-lying areas Quaternary alluvium, derived principally from the Ogallala formation, has been deposited and is the main aquifer. The two aquifers are continuous in the eastern part of the area. Below the Cenozoic rocks are sandstones and shales of the Dockum group of Late Triassic age, from which small quantities of water are obtained. No usable ground water is obtained from rocks older than the Triassic, but highly saline water is produced along with oil from Paleozoic rocks.

In 1954 about 6,000 acre-feet of ground water were used. Most of this quantity was needed for irrigation and for gasoline plants, in about equal amounts. Economic growth from a rapidly developing petroleum industry has brought about a demand for water for industrial and public supplies that is expected to continue. Development of adequate supplies is hindered by restricted occurrence and low transmissibility of the sediments. Because of the low recharge rate, most of the water pumped is being removed from storage.

The chemical quality of the ground water from the principal aquifers is generally fair to good. Production of large quantities of oil-field brine (3,700 acre-feet in 1955) has created a waste-disposal problem of major importance. Most of the brine has been discharged into surface pits. Leakage from the pits has caused contamination of the shallow water in some areas and unless other disposal methods are used, the problem will spread."



Nowak, E.J., Tillerson, J.R., and Torres, T.M. 1990. Initial Reference Seal System Design: Waste Isolation Pilot Plant. SAND90-0355. Sandia National Laboratories, Albuquerque, NM. WPO 23981.

ABSTRACT, p i;

" Waste Isolation Pilot Plant (WIPP) sealing program results are embodied in the initial seal system strategy and reference design. The design provides a common basis for calculations and analyses so that results can be compared directly. The sealing strategy combines both long- and short-term seal components. Crushed salt, consolidated by creep closure of the excavations, is the principle long-term barrier to fluid flow. Short-term seal components are used until creep consolidation is sufficient. Concretes developed specifically for WIPP seals and a swelling clay material that exhibits low permeability to WIPP groundwater and brine have been chosen for the short-term components. A body of evidence exists showing the stability of these materials for the length of time they are required to function. Reference designs are described and drawings are shown for each of the principle multi-component seals. Confidence in the sealing strategy and the reference designs resulted from a combination of laboratory tests, numerical modeling, and in situ demonstrations. The sealing strategy, materials, and designs for the WIPP repository are consistent with the concepts and designs proposed previously for other national and international waste management programs. Past accomplishments and planned activities in the sealing program will produce a detailed conceptual design for the seal system and a seal system performance model. Additional design, analysis, laboratory testing, and in situ testing are needed to assure the performance of the seal system."

**Compliance Certification Application Reference Expansion**

---

OECD Nuclear Energy Agency. 1995. Future Human Actions at Disposal Sites: A Report of the NEA Working Group on Assessment of Future Human Actions at Radioactive Waste Disposal Sites. Organisation for Economic Co-Operation and Development, Paris, France.

NOTE: The above listed document was not available for inclusion in the Reference Expansion as of the printing date. Page changes will be provided as the above document becomes available for inclusion.



Parry, G.W. 1988. On the Meaning of Probability in Probabilistic Safety Assessment. Reliability Engineering and System Safety. Vol. 23, No. 4, pp. 309-314.

ABSTRACT, p. 309;

" The paper addresses the meaning of the term probability as it is used in Probabilistic Safety Assessment (PSA). The use of two different interpretations of probability, the classical interpretation to describe random physical processes, and the subjectivist interpretation to represent uncertainty, is discussed within the context of the PSA framework. Possible sources of confusion, largely resulting from a lack of clear definition of the scope and meaning of the analysis, are identified."



Paté-Cornell, M.E. 1986. Probability and Uncertainty in Nuclear Safety Decisions. Nuclear Engineering and Design. Vol. 93, No. 2-3, pp. 319-327.

ABSTRACT, p. 319;

" In this paper, we examine some problems posed by the use of probabilities in Nuclear Safety decisions. We discuss some of the theoretical difficulties due to the collective nature of regulatory decisions, and, in particular, the calibration and the aggregation of risk information (e.g., experts opinions). We argue that, if one chooses numerical safety goals as a regulatory basis, one can reduce the constraints to an individual safety goal and a cost-benefit criterion. We show the relevance of risk uncertainties in this kind of regulatory framework. We conclude that, whereas expected values of future failure frequencies are adequate to show compliance with economic constraints, the use of a fractile (e.g., 95%) to be specified by the regulatory agency is justified to treat hazard uncertainties for the individual safety goal."



Compliance Certification Application Reference Expansion

---

Pfeifer, M.C., Borns, D.J., Skokan, C.K., Andersen, H.T., and Starett, J.M. 1989. "Geophysical Methods to Monitor the Development of the Disturbed Rock Zone Around Underground Excavations in Bedded Salt." In Proceedings of the Symposium on the Application of Geophysics to Engineering and Environmental Problems, Golden, CO, March 13-16, 1989. SAND89-7055A. Vol. 2, pp. 400-411. WPO 29630.

SUMMARY, p. 400;

" A zone of disturbed rock develops around underground excavations. The manner and rate of degradation has direct implications on the intended long-term use of the excavations. The rate and manner of deformation is dependant on the time after interval since removal supporting room or tunnel material.

Several geophysical methods can be employed to monitor and characterize the zone of deformation as there is a change in the physical rock properties. Electrical methods have been used to monitor the change in moisture content and the development of voids in the excavation floor. Acoustic methods have been successfully used to both test the mechanical integrity of the pillars between excavations and the zone immediately around the underground opening."



Compliance Certification Application Reference Expansion

---

Powers, D.W. and Holt, R.M. 1990. "Sedimentology of the Rustler Formation near the Waste Isolation Pilot Plant (WIPP) Site." Geological and Hydrological Studies of Evaporites in the Northern Delaware Basin for the Waste Isolation Pilot Plant (WIPP), New Mexico. Field Trip #14 Guidebook, Geological Society of America 1990 Annual Meeting, October 29-November 1, 1990. pp. 79-106. Dallas Geological Society, Dallas, TX.

Section Regional Relationships, p 100, col 1, para 7;

" About 600 geophysical logs (natural gamma and acoustic) of the Rustler Formation were interpreted to understand the regional relationship between various units (Holt and Powers, 1988; Powers and Holt, in prep.). Geophysical logs near the site were carefully compared to lithofacies described from cores and shafts, easily relating many subdivisions. Several extended cross-sections were drafted to show lateral relationships in some detail (Holt and Powers, 1988). Structure contour and isopach maps for different units were drafted and compared. . . ."



Powers, D.W., and Holt, R.M. 1993. "The Upper Cenozoic Gatuña Formation of Southeastern New Mexico." In Carlsbad Region, New Mexico and West Texas, D.W. Love, J.W. Hawley, B.S. Kues, J.W. Adams, G.S. Austin, and J.M. Barker, eds., Forty-Fourth Annual Field Conference, October 6-9, 1993, pp. 271-282. New Mexico Geological Society, Socorro, NM.

ABSTRACT, p 271;

" The Gatuña Formation of southeastern New Mexico has been studied in the field for two landfill projects and the Waste Isolation Pilot Plant project. Shafts, drilling and field mapping reveal the distribution, thickness and sedimentary features of the unit in an area where it was poorly known or assigned to other units. The Gatuña is at least 300 ft thick in the study area. The formation was deposited in the north and east as clastic beds ranging from conglomerates to laminar claystones. Fining upward cycles are common, though depositional features and facies associations are consistent with braided river/stream environments, not meandering rivers. Laminar and thinly bedded siltstones to claystones were deposited in flood plain to playa environments. Pedogenic features superimposed on many fining upward cycles include soil fractures, slickensides, MnO<sub>2</sub>, illuviated clay, bioturbation, probable ped structures and desiccation cracks. The upper Gatuña more consistently includes pedogenic development. Beds of poorly indurated 'orange' sand, consisting of rounded and well-sorted grains, are interpreted as eolian deposits. From southern Nash Draw to Orla, the Gatuña is fine-grained and gypsoferous, including displacive crystals and probable subaqueous deposits. These outcrops represent low energy environments, including playas, which were near local base level. The age of the upper Gatuña is reasonably constrained by the Lava Creek B ash (0.6 Ma) within the Gatuña along Livingston Ridge. The age of basal deposits is poorly or not constrained. An ash within probable Gatuña near Orla, TX, is about 13 Ma based on both radiometric and geochemical data. The Gatuña represents an important piece of the geological history of southeastern New Mexico. Further studies could include efforts to better determine the age of the formation; to obtain paleontological data; and to map Gatuña structural relationships to older and younger beds in detail to determine the timing of and spatial evidence for, dissolution of evaporites and collapse of overlying beds, including the Gatuña."



Rechard, R.P., 1989. Review and Discussion of Code Linkage and Data Flow in Nuclear Waste Compliance Assessments. SAND87-2833. Sandia National Laboratories, Albuquerque, NM. WPO 25675.

ABSTRACT;

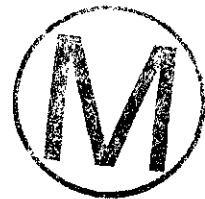
" This report presents a review and discussion of data flow in a compliance assessment for high-level and transuranic waste, primarily the Containment Requirement of the Environmental Protection Agency (EPA) regulations, 40 CFR 191, *Environmental Standards for the Management and Disposal of Spent Nuclear Fuel, High-Level and Transuranic Radioactive Wastes*. Two major points concerning data flow are presented. First, assuring the quality of a compliance assessment requires that the flow of data and linkage of computer codes be well defined and precisely controlled during execution. Second, the need to analyze many different scenarios using different computer codes requires a flexible data linkage. The manner of linking codes to simultaneously provide quality assurance and flexibility is emphasized, rather than specific computer codes used. Thus, this report is not a user's guide, but a description of how a compliance assessment system was implemented in accordance with EPA regulatory guidance. Although the methods described are general, all examples pertain to the Waste Isolation Pilot Plant (WIPP) project, which prompted development of the concepts."



Rechard, R.P., ed, 1992. User's Reference Manual for CAMCON: Compliance Assessment Methodology Controller Version 3.0. SAND90-1983. Sandia National Laboratories, Albuquerque, NM. WPO 25628.

Section 2. CAMCON General Description, 2.1 Purpose, p 2-1;

" A performance assessment (PA) for a nuclear waste repository such as WIPP can be viewed as a complex process (or composite function) that provides a prediction of performance. Within the complex process, the CAMCON system (Rechard, 1991a) has two important functions. First, the CAMCON system provides the analyst with flexibility (specifically, a variety of software tools and flexibility in use) necessary to investigate various events and phenomena (combined into scenarios), perform simulations, and present the predicted results. (For 40 CFR 191, the results are presented as a complementary cumulative distribution function [CCDF] and compared with probabilistically-based limits [see Appendix A for more information].) Second, the CAMCON system directory structure and several of its procedures and utility programs assist in implementing quality assurance (QA) procedures (Rechard et. al., 1991). For example, CAMCON serves as a software management system providing configuration control, FORTRAN libraries of commonly used subroutines, and on-line documentation for each code. In other words, the CAMCON system allows the analyst flexibility in building various software into an analysis system while providing assurance the analysis system is properly built and executed."



Compliance Certification Application Reference Expansion

---

Richey, S.F. 1987. Water-level Data from Wells in the Vicinity of the Waste Isolation Pilot Plant, Southeastern New Mexico. Open-File Report 87-120. United States Geological Survey, Albuquerque, NM.

ABSTRACT, p 1;

" The U. S. Geological Survey monitored water levels in wells in the vicinity of the Waste Isolation Pilot Plant in southeastern New Mexico during 1977 to 1985. Water-level data are presented, as are brief descriptions of measurement methods used."

Compliance Certification Application Reference Expansion

---

Robinson, J.Q., and Powers, D.W. 1987. "A Clastic Deposit Within the Lower Castile Formation, Western Delaware Basin, New Mexico." In *Geology of the Western Delaware Basin, West Texas and Southeastern New Mexico*. D.W. Powers and W.C. James, eds. El Paso Geological Society Guidebook 18, pp. 69-79. El Paso Geological Society, El Paso, TX. WPO 37942.

ABSTRACT, p 69, col 1;

" In the vicinity of CP Hill, about 16 km south-southwest of Whites City, New Mexico, a brecciated sequence in the lower Castile Formation has been examined in detail. Four distinct units associated with the breccia sequence have been defined. Unit A is clast poor, structureless to thinly bedded, and contains kerogen. It occurs only over nodular anhydrite. Unit B is pseudo-bedded, with anhydrite matrix supporting tabular anhydrite clasts. Unit C contains abundant rounded polyclasts and is grain-rich. Unit D is similar to A, but clasts are finer in Unit D. These beds are arranged in vertical sequence and show lateral thinning in an apparent fan shape. The textures, grading, and vertical and lateral relationships suggest this breccia unit was deposited as a subaqueous debris flow."



Robinson, T.W., and Lang, W.B. 1938. Geology and Ground-Water Conditions of the Pecos River Valley in the Vicinity of Laguna Grande de la Sal, New Mexico, with Special Reference to the Salt Content of the River Water. Twelfth and Thirteenth Biennial Reports of the State Engineer of New Mexico for the 23rd, 24th, 25th, and 26th Fiscal Years, July 1, 1935 to July 30, 1938. State Engineer, Santa Fe, NM. WPO 37942.

INTRODUCTION, p 79;

" At the request and in cooperation with the State Engineer of New Mexico, a study of ground-water conditions in the Pecos River Valley southeast of Carlsbad, Eddy County, New Mexico, has been under way since the spring of 1937. The results of that study are presented in this report. The area involved lies largely in Townships 21, 22, 23 and 24 south, Ranges 26, 27, 28 and 29 east, New Mexico principle meridian. (See plate 1). Intensive work was done chiefly in the vicinity of the Laguna Grande de la Sal and the area lying between it and the Malaga Bend of the Pecos River, about five miles south. The area is crossed by the Pecos River flowing southeastward from Carlsbad. During the growing season, the entire flow of the Pecos River above Carlsbad is normally diverted for irrigation at Lake McMillan and Lake Avalon. During this period the Pecos River from Carlsbad south is fed chiefly by large springs. The largest spring, known as Carlsbad Spring, is located in the river channel just below Lake Avalon. The Black River enters the area from the west and flows eastward to its confluence with the Pecos River northeast of Malaga. It is also spring-fed, deriving most of its water from Blue Spring and Castle Spring, near Black River village. The drainage pattern is well developed on the west, and during rainy periods many normally dry arroyos and draws discharge flood water into the Pecos River. Drainage from the east is by poorly developed draws which carry water to the Pecos only during exceptionally heavy rainfall. A prominent feature east of the river is Laguna Grande de la Sal, which is a shallow salt lake in a playa covering about 3½ square miles.

Carlsbad, the largest town in the area and the county seat of Eddy County, had a population of 3,708 in 1930. However, owing largely to the development of the potash mines located about 20 miles east, the population in 1938 is about double that of 1930. Loving, located about 12 miles south, and Malaga, about 18 miles south of Carlsbad, each had less than 1,000 inhabitants in 1930. Carlsbad is served by the Atchison, Topeka, and Santa Fe Railroad and by main highways leading north to Roswell, New Mexico, southwest to El Paso, Texas, south to Pecos, Texas, and east to Hobbs, New Mexico.

Cotton and hay are raised in the irrigated section along the Pecos River, while cattle, sheep and goat raising predominate in the unirrigated upland areas to the east and west. The principle mineral industry is the mining and refining of potash. A large number of tourists are attracted annually to the famous Carlsbad Caverns, located about 25 miles southwest of Carlsbad, near the highway leading to El Paso, Texas.

A group of farmers who pump water from the river for irrigation report that in recent years the water, because of its salinity, has been injurious to their cotton crop. In September 1932 the U.S. Potash Company began operations, using the Laguna Grande de la Sal as a disposal area for the waste brine from their potash refining operations. The reported



Compliance Certification Application Reference Expansion

---

difficulty with salt, shortly after refinery operations began, naturally cast suspicion on the brine in the Laguna Grande. There is no visible outlet from the Laguna Grande, and therefore the problem arose as to whether the lake brine may be percolating underground to the Pecos River.

A study of the chemical character of the water of the Pecos River has been made by C.S. Howard and W.F. White, Jr., and numerous analyses were made of the surface and ground waters in this area (see report on chemical character of Pecos River under 'Quality of Water,' to be found elsewhere in this volume). The ground-water studies by T.W. Robinson were begun on April 13, 1937, and the geologic studies by W.B. Lang on October 15, 1937."



Rosholt, J.N., and McKinney, C.R. 1980. Uranium Series Disequilibrium Investigations Related to the WIPP Site, New Mexico (USA). Part II Uranium Trend Dating of Surficial Deposits and Gypsum Spring Deposit Near WIPP Site, New Mexico. Open-File Report 80-879. U.S. Geological Survey, Denver, CO.

INTRODUCTION, p. 1;

" Just how suitable salt beds are for permanent disposal of radioactive wastes has been the subject of extensive studies covering diverse aspects over the past decade. The proposed site of the Waste Isolation Pilot Plant (WIPP) is located in southeastern New Mexico, about 42 km east of Carlsbad, where plans are to construct the storage facility in rock salt beds of the Permian Salado Formation. Detailed surface and subsurface geology at the site and of the surrounding area has been discussed previously (Bachman, 1976; Powers and others, 1978).

A basic concern for waste repositories in salt beds is their high solubility in ground waters. Different kinds of dissolution features are known in most evaporite basins including the Delaware Basin, the region of the proposed WIPP site. Some primary questions that can be posed are: 1. Is there active dissolution of salt at or near the site of WIPP? 2. Is the process of salt dissolution continuous or episodic? 3. If episodic, what is the correlation between time and depth? 4. When did the last salt dissolution cycle occur? 5. What is the rate of dissolution?

Rosholt and others (1966) and Rosholt (1978) demonstrated that a process of isotopic evolution of uranium and thorium occurs in most types of sediments, altered volcanic ashes and deeply buried granites provided that some groundwater is allowed to migrate through the porous zones of these materials during their geologic history. Often the analyses of the isotopes of the  $^{238}\text{U}$ - $^{234}\text{U}$ - $^{230}\text{Th}$ - $^{232}\text{Th}$  system yield an estimated age for the time of deposition (uranium-trend age estimate) over the range of the method from 2,000 to about 800,000 years ago (Rosholt, 1978). Accordingly, it was felt that a preliminary study of salt dissolution residue samples near the WIPP site may yield insight into the dissolution processes and/or it may provide a uranium-trend age estimate for the most recent salt dissolution that produced clay residuum and bands of gypsum. The application of uranium trend dating in the investigation of the age of surficial deposits in the area east of Carlsbad, New Mexico, is included in Part II of this report."

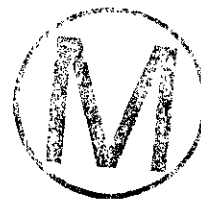
## Compliance Certification Application Reference Expansion

---

Sandia National Laboratories. 1992. Long-Term Gas and Brine Migration at the Waste Isolation Pilot Plant, Preliminary Sensitivity Analyses for Post-Closure 40 CFR 268 (RCRA), May 1992. SAND92-1933. Sandia National Laboratories, WIPP Performance Assessment Department, Albuquerque, NM. WPO 23513.

### ABSTRACT;

" This report describes preliminary probabilistic sensitivity analyses of long-term gas and brine migration at the Waste Isolation Pilot Plant (WIPP). Because gas and brine are potential transport media for organic compounds and heavy metals, understanding two-phase flow in the repository and the surrounding Salado Formation is essential to evaluating long-term compliance with 40 CFR 268.6, which is the portion of the Land Disposal Restrictions of the Hazardous and Solid Waste Amendments to the Resource Conservation and Recovery Act that states the conditions for disposal of specified hazardous wastes. Calculations described here are designed to provide guidance to the WIPP Project by identifying important parameters and helping to recognize processes not yet modeled that may affect compliance. Based on these analyses, performance is sensitive to shaft-seal permeabilities, parameters affecting gas generation, and the conceptual model used for the disturbed rock zone surrounding the excavation. Brine migration is less likely to affect compliance with 40 CFR 268.6 than gas migration. However, results are preliminary, and additional iterations of uncertainty and sensitivity analyses will be required to provide the confidence needed for a defensible compliance evaluation. Specifically, subsequent analyses will explicitly include effects of salt creep and, when conceptual and computational models are available, pressure-dependent fracturing of anhydrite marker beds."



Saulnier, G.J., Jr., 1987. Analysis of Pumping Tests of the Culebra Dolomite Conducted at the H-11 Hydropad at the Waste Isolation Pilot Plant (WIPP) Site. SAND87-7124. Sandia National Laboratories, Albuquerque, NM. WPO 28520.

ABSTRACT, p ii;

" The Culebra Dolomite Member of the Permian Rustler Formation was hydrologically evaluated in a series of pumping tests conducted at the H-11 hydropad at the Waste Isolation Pilot Plant (WIPP) site in 1984 and 1985. The H-11 hydropad was constructed in 1983 and consists of three wells, H-11b1, H-11b2, and H-11b3, each completed open-hole to the Culebra dolomite. At H-11, the Culebra dolomite is a 25-ft thick argillaceous dolomite with 0.1- to 0.5-foot thick layers with a high density of vugs. The vugs range in size from 0.1 to 0.5 inches in diameter; most are 0.1 to 0.2 inches in diameter. The thin vuggy layers alternate with thicker, more competent layers which have few vugs, but which do contain high-angle fractures. Some of the vugs and fractures are gypsum-filled.

The three pumping tests performed in 1984 consisted of 12- to 21-hour pumping periods at each of the three wells, while using the other two wells at the hydropad as observation wells. The 1985 pumping test was conducted at H-11b3 with H-11b1 and H-11b2 as observation wells. The 1985 test was a 32-day multirate test with four pumping and recovery periods. The 1984 tests were conducted by lowering a submersible pump and pressure transducers in the boreholes. The 1985 test added a downhole packer with feed-through assembly designed to isolate the test interval and reduce or minimize the effect of wellbore storage. The data from all tests were recorded and stored on floppy disks.

The pumping tests at the H-11 hydropad were analyzed with the INTERPRET reservoir-analysis software developed by Scientific Software-Intercomp. The analysis of the test data from both test periods indicates that at H-11, the Culebra dolomite behaves as a multilayered, double-porosity reservoir with slab-type geometry. The INTERPRET analysis of the H-11 pumping tests provided estimates of the double-porosity parameters  $\omega$  and  $\lambda$ .  $\omega$  is defined as the ratio of the storage capacity of the secondary-porosity system of the producing formation, usually considered to be fractures, to the storage capacity of the combined primary- and secondary-porosity systems.

The range of values calculated for the double-porosity parameter  $\omega$  in the observation wells was 0.30 to 0.43 for the 1984 tests and 0.07 for the 1985 test. The lower value for 1985 is probably due to the fact that the Culebra in all wells for this testing period was packer-isolated. The  $\omega$  values for the type curves used to analyze the 1985 H-11 test suggest that the primary-porosity part of this double-porosity reservoir provides 93% of the storage capacity of the formation. The double-porosity parameters  $\lambda$  (also called the interporosity flow parameter) describes the ability of fluid to flow from the primary-porosity system to the secondary-porosity system (e.g., from matrix to fractures). The definition includes the ratio of the permeability of the primary-porosity system to the permeability of the secondary-porosity system. The average  $\lambda$  value for the H-11 tests was  $3.0 \times 10^{-6}$ , with an effective range of  $3.73 \times 10^{-7}$  to  $1.25 \times 10^{-6}$ . Analysis of the  $\lambda$  values determined for the H-11 test data indicates a permeability contrast between the

primary- and secondary-porosity systems of about  $1.0 \times 10^{-6}$  with a characteristic slab-block dimension of 1 to 2 feet.

Using INTERPRET, the average transmissivity of the Culebra was calculated to be 23.2 ft<sup>2</sup>/day for the 1984 tests, 26.2 ft<sup>2</sup>/day for the 1985 test, and 24.0 ft<sup>2</sup>/day using the results of all the tests. The storativity of the Culebra, as determined from the pumping tests, is between  $2.9 \times 10^{-3}$  and  $4.5 \times 10^{-4}$ . The skin factors calculated from the pumping-well data range from -3.3 to -4.6, indicating that these wells behave as stimulated wells. The 1985 test at H-11b3 had both the highest transmissivity and the most negative skin factor, possibly implying that H-11b3 had undergone development during and after its 1984 test.

The results of the 1984 series of tests were also analyzed to determine the degree of anisotropy at the H-11 hydropad. The storage coefficient was estimated to be  $6.3 \times 10^{-4}$ . The average maximum transmissivity vector was 31.1 ft<sup>2</sup>/day oriented 5.8° north of east and the average minimum transmissivity vector was 19.3 ft<sup>2</sup>/day oriented 5.8° west of north. The ratio of the maximum to the minimum transmissivity vectors was calculated to be 1.6, indicating a low degree of anisotropy at H-11, although the degree of anisotropy may be dependent on fracture orientation and locations of the wells."



Saulnier, Jr., G.J., Domski, P.S., Palmer, J.B., Roberts, R.M., and Stensrud, W.A. 1991. WIPP Salado Hydrology Program Data Report #1. SAND90-7000. Sandia National Laboratories, Albuquerque, NM. WPO 25746.

**ABSTRACT;**

" WIPP Salado Hydrology Program Data Report #1 presents hydrologic data collected during permeability tests of the Salado Formation performed from August 1988 through December 1989. Analysis and interpretation of the test data are presented in a separate report. The report presents the results of the drilling and testing of six boreholes drilled from the WIPP underground facility 655 m below ground surface in the Salado Formation. Permeability tests were conducted using multipacker test tools with inflatable packers to isolate borehole intervals to allow formation pore-pressure buildup and subsequent pulse-withdrawal tests. Test data include pressures and temperatures in brine-filled, packer-isolated test intervals and borehole-closure and axial test-tool-movement measurements. The test boreholes are 4.0-inch (10.2-cm) in diameter, and were cored in halite and associated anhydrite interbeds and clay seams. The boreholes are oriented vertically downward, angled downward, and horizontal. The boreholes were drilled and cored using compressed air to remove drill cuttings. Three boreholes were drilled in Room C2:C2H01, C2H02, and C2H03. Borehole C2H01 was initially drilled to a depth of 5.68m below the floor of Room C2 and later deepened to 8.97 m to include Marker Bed 139 in the test interval. Borehole C2H02 was drilled to a depth of 10.86 m (7.68 m vertical projection from the floor of Room C2) at a 45° downward angle from the junction of the west wall and floor of Room C2. Marker bed 139 was included in the test interval in borehole C2H02. Borehole C2H03 was drilled horizontally into the west wall of Room C2. Vertically downward boreholes were drilled from the floor in the North 1420 drift (borehole N4P50); the South 1300 drift (borehole S0P01); and in Room 7, Waste Panel 1 in the waste-storage area (borehole S1P71).

Permeability tests were performed after installing multipacker test tools in test boreholes, inflating the packers, and allowing pressures to build up in the isolated intervals. Pulse-withdrawal tests were performed after buildup pressures approached the apparent formation pore pressure. Pulse injections were sometimes performed to increase the fluid pressures in isolated intervals.

Compliance tests were conducted in lengths of steel and stainless-steel casings to evaluate the mechanical performance of the multipacker test tools. The stainless-steel compliance-test chamber was installed with externally mounted thermocouples in a downward-angled borehole in Experimental Room 4. Compliance tests included leak tests and simulated pulse-injection and pulse-withdrawal sequences."



Schiel, K.A. 1988. The Dewey Lake Formation: End Stage Deposit of a Peripheral Foreland Basin [M.S. thesis]. University of Texas at El Paso, El Paso, TX.

ABSTRACT, p iv;

" The red siltstones and fine grained sandstones of the Dewey Lake Formation (Late Permian?) have always been relegated to a rather insignificant role in the geologic history of the Permian Basin. The present study suggests that they are, in fact, an important key to understanding the tectonic evolution of the southwestern United States.

Field work, in southeastern New Mexico, reveals that the Dewey Lake is fluvial in origin. Broad, shallow channels filled with thin horizontal laminations and flanked by laterally thinning wings comprise a large portion of the formation. Floodplain deposits, consisting of interbedded siltstone and silty claystone, are also very common.

The Dewey Lake displays many of the sedimentologic and morphologic characteristics associated with ephemeral fluvial systems. Some of these characteristics are an abundance of horizontal laminations and silty claystone drapes, the existence of interbedded siltstone and silty claystone interpreted to be the distal portion of sheet floods, and the presence of broad channels with laterally thinning wings. The Dewey Lake is, therefore, believed to have been deposited on a very extensive northwest sloping fluvial plain. Movement of sediment across this plain occurred only sporadically, during brief and localized flash floods.

It has previously been theorized that the Dewey Lake was extensively eroded prior to the deposition of the Santa Rosa Formation (Middle to Late Triassic). The results of the present study suggest that the thickness variations in the Dewey Lake are not a reflection of post depositional erosion but syndepositional differences in the subsidence rates of the Central Basin Platform and Delaware Basin. Increased subsidence of the Delaware Basin is reflected by the fact that the base of the Dewey Lake Formation is offset 100 m (300 ft) along the major northwest trending fault zone separating the Delaware Basin and Central Basin Platform. The Delaware Basin, therefore, appears to have been tectonically active throughout the deposition of the Dewey Lake Formation.

If the thickness variations in the Dewey Lake are due to subsidence rather than erosion then the contact between the Dewey Lake and the overlying Santa Rosa Formation is conformable. The Santa Rosa has been dated as Middle to Late Triassic in northeastern New Mexico; if this date is applicable to the Santa Rosa in southeastern New Mexico it dictates that the deposition of the Dewey Lake Formation continued into the Early Triassic.

A major unconformity separates Lower Permian and Cretaceous strata in the Fort Worth, Val Verde and Marfa Basin of Texas. This unconformity, which also exists in northwestern Chihuahua, clearly indicates that a large region of central Texas and northern Mexico was uplifted and eroded during the latest Permian ? and early Mesozoic. The location and timing of this uplift suggests that it was the source of the silt and fine sand comprising the Dewey Lake Formation. A close geographic and temporal relationship between this uplift and Late Triassic rift basins suggests that it originated as a pre-rift bulge.

The very extensive nature of this uplift suggests that the alluvial plain to the north (i.e. the Dewey Lake and Quartermaster Formations) extended significantly beyond the area

**Compliance Certification Application Reference Expansion**

---

of west Texas and eastern New Mexico. The western portion of this plain is theorized to be the redbed facies of the Moenkopi Formation (Early Triassic). Apparent similarities in age, stratigraphic position, lithology and paleoslope all support the concept that the Dewey Lake and Moenkopi Formations are components of a single lithologic unit."



Schlesinger, M.E., and Mitchell, J.F.B. 1987. Climate Model Simulations of the Equilibrium Climatic Response to Increased Carbon Dioxide. *Reviews of Geophysics*. Vol. 25, No. 4, pp. 760-798.

ABSTRACT, p. 760;

" The first assessments of the potential climatic effects of increased CO<sub>2</sub> were performed using simplified climate models, namely, energy balance models (EBMs) and radiative-convective models (RCMs). A wide range of surface temperature warming has been obtained by surface EBMs as a result of the inherent difficulty of these models in specifying the behavior of the climate system away from the energy balance level. RCMs have given estimates of  $\Delta T_a$  for a CO<sub>2</sub> doubling that range from 0.48° to 4.2°C. This response can be characterized by  $\Delta T_R = \Delta R_T G_0 / (1-f)$ , where  $\Delta R_T$  is the radiative forcing at the tropopause due to the CO<sub>2</sub> doubling ( $\sim 4 \text{ W m}^{-2}$ ),  $G_0$  is the gain of the climate system without feedbacks ( $\sim 0.3^\circ\text{C}/(\text{W m}^{-2})$ ), and  $f$  is the feedback. The feedback processes in RCMs include water vapor feedback ( $f$  is 0.3 to 0.4), moist adiabatic lapse rate feedback ( $f$  is -0.25 to -0.4), cloud altitude feedback ( $f$  is 0.15 to 0.30), cloud cover feedback ( $f$  is unknown), cloud optical depth feedback ( $f$  is 0 to -1.32), and surface albedo feedback ( $f$  is 0.14 to 0.19). However, these feedbacks can be predicted credibly only by physically based models that include the essential dynamics and thermodynamics of the feedback processes. Such physically based models are the general circulation models (GCMs). The earliest GCM simulations of CO<sub>2</sub>-induced climate change were performed without the annual insolation cycle. These 'annual mean' simulations gave for a CO<sub>2</sub> doubling a global mean surface air temperature warming of 1.3° to 3.9°C, an increase in the global mean precipitation rate of 2.7 to 7.8%, and an indication of a soil moisture drying in the middle latitudes. The first GCM simulation of the seasonal variation of CO<sub>2</sub>-induced climate change was performed for a CO<sub>2</sub> quadrupling and obtained annual global mean surface temperature and precipitation changes of 4.1°C and 6.7%, respectively. Substantial seasonal differences in the CO<sub>2</sub>-induced climate changes were found, especially in polar latitudes where the warming was maximum in winter and in the middle latitudes of the northern hemisphere where a soil moisture desiccation was found in summer. Recently, three CO<sub>2</sub>-doubling experiments have been performed with GCMs that include the annual insolation cycle. These seasonal simulations give an annual global mean warming of 3.5° to 4.2°C and precipitation increases of 7.1 to 11%. These changes are approximately twice as large as those implied for a CO<sub>2</sub> doubling by the earliest seasonal simulation, apparently as a result of a positive cloud feedback. The geographical distributions of the CO<sub>2</sub>-induced warming obtained by the recent simulations agree qualitatively but not quantitatively. Furthermore, the precipitation and soil moisture changes do not agree quantitatively and even show qualitative differences. In particular, the summertime soil moisture drying in middle-latitudes is simulated by only one of the CGMs. In order to improve the state of the art in simulating the equilibrium climatic change induced by increased CO<sub>2</sub> concentrations, it is recommended first that the contemporary GCM simulations be analyzed to determine the feedback processes responsible for their differences and second that the parameterization of these processes in the GCMs be



validated against highly detailed models and observations."



Sewards, T., Glenn, R., and Keil, K. 1991. Mineralogy of the Rustler Formation in the WIPP-19 Core. SAND87-7036. Sandia National Laboratories, Albuquerque, NM. WPO 24140

ABSTRACT, p i;

" The mineralogy of the Rustler Formation is a critical element in many of the radionuclide release models for the Waste Isolation Pilot Plant (WIPP), and it is necessary to know the abundances of the various minerals present, their compositions, their textures and locations with respect to water-bearing features, and their interrelationships. Clay mineralogy in particular is of vital importance because of the ability of clay minerals to sorb contaminant cations. Furthermore, the minerals present in the different units of the Rustler Formation are possible sources for solutes present in waters taken from various boreholes in the vicinity of the WIPP site.

This report characterizes the mineralogy of the Rustler Formation as represented in core from borehole WIPP-19. The major components, as determined by x-ray diffraction (XRD), are halite, anhydrite, gypsum, dolomite, magnesite, quartz, and clay. Minor components include calcite, pyrite, feldspar and phyllosilicates of metamorphic origin (muscovite, biotite, and chlorite). Clay minerals, identified by XRD, include illite, serpentine, chlorite, and mixed-layer chlorite/smectite (including corrensite).

Quartz and clay, with some halite and anhydrite, dominate the lower member; the Culebra and Magenta units are primarily dolomite with some quartz and clay, while the Forty-niner Member consists of quartz, clay, and sulfates (anhydrite and gypsum).

Halite occurs in four textural styles: bedded, recrystallized halite; displacive halite; as a cement in mud/siltstones; and as a fracture filling, and is largely restricted to the lower member. Anhydrite occurs primarily as a massive, crudely banded nodular structure, although there is often evidence of partial alteration to gypsum. Gypsum also is usually massive, in a crudely banded form. The massive areas consist of fine-grained irregular crystals ('patchy' gypsum); these areas are separated by veins of 'fibrous' gypsum, usually parallel to bedding. Fibrous gypsum vein filling in other lithologies is very common. Dolomite is unfossiliferous, laminated, and very fine-grained; it contains numerous vugs and fractures these are usually lined with clay, gypsum, and powdery dolomite. Magnesite, a relatively minor component, occurs as microcrystalline nodules and as euhedral elongated platy crystals included in halite. Quartz and clay always occur together with minor amounts of feldspar and detrital phyllosilicate grains. Calcite is restricted to a thin bed above the Culebra Dolomite in the samples studied.

In general, this study should be considered a detailed analysis of the Rustler section mineralogy. It is unlikely that any other minerals are present elsewhere in the Rustler Formation in any great quantity. Abundances of individual minerals may vary considerably in other areas of the formation."



Shinta, A.A., and Kazemi, H. 1993. "Tracer Transport in Characterization of Dual-Porosity Reservoirs." In Reservoir Engineering Proceedings, SPE Annual Technical Conference and Exhibition, Houston, TX, October 3-6, 1993. SPE 26636, pp. 285-299. Society of Petroleum Engineers, Richardson, TX.

ABSTRACT, p 285;

" A single-porosity model (SPM) for the tracer response analysis in fractured reservoirs is developed in this paper. This new technique is useful in characterizing fractures in terms of flow anisotropy and quantifying fractures properties such as porosity and permeability. Specifically, tracer response has good resolution and, therefore, its analysis can determine the orientation and conductivity of high permeability fractured systems in the reservoir. This information is highly desirable in improved oil recovery planning and management. The simulator used here is five-point, nine-point finite-difference, two-dimension and two-phase (oil and water) model. In addition to SPM, the simulator conducts a single block simulation (SBS) and conventional dual-porosity calculations. Several options to eliminate or minimize grid orientation effect (GOE) in fractured and unfractured reservoirs are included. These nine-point options appropriately account for the permeability tensor and flow channeling. The SPM is used successfully to characterize an anisotropic confined five-spot pattern in an actual field test."





Silva, M. 1994. Implications of the Presence of Petroleum Resources on the Integrity of the WIPP. EEG-55, DOE/AL/58309-55. Environmental Evaluation Group, Albuquerque, NM. WPO 9607.

**EXECUTIVE SUMMARY;**

" The Waste Isolation Pilot Plant (WIPP) is a facility of the U.S. Department of Energy (DOE), designed and constructed for the permanent disposal of transuranic (TRU) defense waste. The WIPP is surrounded by reserves of potash, crude oil, and natural gas. These are attractive targets for exploratory drilling which could disrupt the integrity of the transuranic waste repository. To proceed with disposal, the U.S. Environmental Protection Agency (EPA) Administrator must certify that the probabilities and fraction of the repository's release of radionuclides to the biosphere over the next 10,000 years will be less than those allowed by the EPA standards (U.S. EPA, 1993). The performance assessment calculations published to date have identified future drilling for oil and gas reserves as an event that may disrupt the repository and may release radionuclides in excess of the standards (SNL, 1992, vol. 1, Section 4.1.2). Therefore, the probability of inadvertent human intrusion into the repository by drilling and its impact on the integrity of the repository must be carefully assessed.

While the DOE funded a number of studies and reviews on the possibility of oil and gas reserves in the vicinity of the WIPP, the recent production of crude oil in the WIPP vicinity indicates that the 1974 study by Foster was correct. However, the DOE decided to rely on the reports which indicated or strongly suggested that crude oil was not considered economically recoverable.

The 1974 New Mexico Bureau of Mines and Mineral Resources (Foster, 1974) estimated crude oil reserves would range from 550,000 to 1,200,000 barrels per section in the vicinity of the WIPP Site. The Environmental Evaluation Group (Neill et al., 1983, p. 98) agreed with the Geologic Characterization Report (Powers et al., 1978) and commented that "since Foster's study used a regional statistical approach, there may be considerably more or less than the average quantity of hydrocarbons if the site were actually drilled." But the Environmental Evaluation Group also concluded that "it is possible that significant reserves of oil also exist within the site." The New Mexico Energy and Minerals Department (NMEMD, 1984) Task Force on natural resources relied on Foster's (1974) estimates of petroleum reserves.

However, four other studies and several reviews commissioned and used by the DOE stated or suggested that there were little or no economically recoverable crude oil reserves in the immediate vicinity of the WIPP. These include the studies of Netherland et al. (1974) and Keesey (1976, 1977, 1979) and the reviews of Griswold (1977), Powers et al. (1978), the DOE WIPP Final Environmental Impact Statement (U.S. DOE, 1980), Brausch et al. (1982), Weart (1983), and Weart et al. (1991).

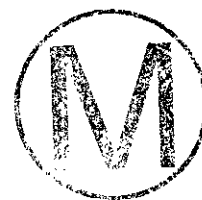
The Department of Energy acknowledged that the statistical study of the New Mexico Bureau of Mines and Mineral Resources indicated the presence of crude oil, but the DOE decided that later studies had discounted the existence of economically attractive quantities at

the site. (McGough, 1983a, p. 4). With respect to the impact of secondary recovery methods on the integrity of the repository, Brausch et al (1982) did not evaluate such production methods because they argued that there was a minimal amount of crude oil likely to exist within the WIPP Site. The report of Brausch et al. (1982) served as the basis for the major decision to relinquish control of a one mile buffer zone (Weart, 1983; McGough, 1983b) initially intended to provide DOE control of natural resource production methods (U.S. DOE, 1980). Less than ten years later, the WIPP area was confirmed by the oil and gas industry to be "extremely high in oil and gas reserves...." (Nibert, 1992).

The DOE position of minimal or no crude oil reserves persists in guiding assumptions on other major issues including demonstration of compliance with EPA disposal standards. For example, participants in two expert elicitation exercises conducted by Sandia National Laboratories (SNL) were asked to provide information with which to estimate oil and gas drilling rates in the WIPP vicinity over the next 10,000 years (Hora, 1992). Participants in the first elicitation were asked to identify the activities of future societies that would disrupt the integrity of the repository and to assign probabilities to events such as exploratory drilling.

Participants in the second elicitation were asked to design a marker that would discourage human intrusion and to evaluate the effectiveness of the markers they recommended. However, the participants in both exercises were provided outdated and incorrect information on the two issues that were most important to their discussions -- the actual drilling intensity and the crude oil reserves in the immediate vicinity of the WIPP Site. The effective drilling intensities, inferred from the elicitations, were consistently and substantially less than the EPA recommended maximum value of 30 boreholes per km<sup>2</sup> over 10,000 years (Hora, 1992).

The WIPP Project's experience indicates that allowing credit for institutional control in the performance assessment calculations may be difficult to justify. Experts from each of the four teams in the future societies elicitation exercise expressed reservations about the ability of the project to maintain active control for even a very short period of time (Hora et al., 1991). Two active oil and gas leases within the WIPP Site Boundary and a producing gas well were overlooked in several important DOE documents (Silva and Channell, 1992). Records indicate that DOE and the Department of Interior's Bureau of Land Management (DOI/BLM) did not implement required review, comment, and approval procedures in twenty-two of the twenty-five (88%) drilling applications filed during the first two years a Memorandum of Understanding was in effect and while the WIPP facility was in a state of full readiness to receive waste. The DOE review of the interface with the BLM failed to detect the problem. There is no plan nor commitment by DOE to active institutional control. The DOE intends to negotiate the extent of active institutional control with the State of New Mexico just prior to decommissioning of the facility or approximately 30 years after having taken full credit for active institutional control in the performance assessment calculations. Some components of passive institutional control, such as government ownership of the site, public records, and markers, failed to communicate the existence and location of oil and gas wells, a salt water disposal well, and a pipeline crossover in the WIPP area to WIPP project



employees.

The WIPP facility will be subjected to the actual exploration, production, and abandonment practices of the petroleum industry on adjacent properties. The potential problems due to secondary recovery have not yet been addressed because the project assumed that there were minimal crude oil reserves. Primary production of crude oil immediately adjacent to the WIPP is underway. The feasibility of secondary recovery or tertiary recovery for adjacent oil fields needs to be investigated. Of particular concern is the potential migration of injected water from adjacent properties through the Salado Formation (Ramey, 1976; Bailey, 1990, LaVenue, 1991; Hartman, 1993).

The leakage of existing and future oil, gas, and salt water injection wells appears to have a potential impact on the regional hydrology. In addition to faulty cement emplacement, leakage can result from rapid corrosion of well casings in the highly corrosive saline environment (LaVenue, 1991). There are several salt water disposal wells operating in the vicinity of the WIPP Site.

The performance assessment effort needs to address the problems associated with inadequate borehole sealing and abandonment practices on Bureau of Land Management properties (U.S. DOI, 1989, U.S. DOI, 1990, Baier, 1990). ~ The Bureau of Land Management's (BLM) existing guidelines on well completions, workovers and abandonments have never been formalized and published" (U.S. DOI, 1991, p. 20568). The potential impact of abandoned wells on the regional hydrology and on the performance of the repository has yet to be determined."

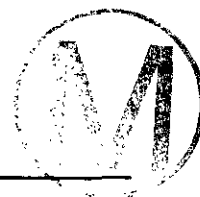


**Compliance Certification Application Reference Expansion**

---

Slezak, S., and Lappin, A. 1990. "Potential for and Possible Impacts of Generation of Flammable and/or Detonable Gas Mixtures during the WIPP Transportation, Test, and Operational Phases," In Memorandum to D. Mercer and C., Fredrickson, January 5, 1990. Sandia National Laboratories, Albuquerque, NM. WPO 21224.

NOTE: The above listed document was not available for inclusion in the Reference Expansion as of the printing date. Page changes will be provided as the above document becomes available for inclusion.



Snyder, R.P., Gard, Jr., L.M., and Mercer, J.W. 1982. Evaluation of Breccia Pipes In Southeastern New Mexico and Their Relation to the Waste Isolation Pilot Plant (WIPP) Site. Open-File Report 82-968. U.S. Geological Survey, Denver, CO.

INTRODUCTION, p. 1;

" The Waste Isolation Pilot Plant (WIPP) site is located about 40 km (25 mi) east of Carlsbad, N. Mex. (fig. 1). The site geography has been described in detail by Powers and others (1978) and U.S. Department of Energy (1980, 1981). Site selection was based principally on the existence of a thick section of Permian evaporites, mainly halite. The purpose of establishing this site is to demonstrate whether or not an evaporite environment is acceptable for the disposal of trans-uranic waste generated by the Nation's defense programs.

The primary concern regarding safe disposal of nuclear waste is to isolate the waste from the biosphere until it is no longer a danger to mankind. One of the most probable methods of accidental release of radiation from nuclear waste isolated in a geologic medium is leaching and transport of the waste by moving ground water. It is therefore of primary importance to identify any potential channelways that might allow water to enter a repository site located on bedded salt of the Salado Formation of southeastern New Mexico. The presence of the thick Permian (225 m.y.) rocks attests to the fact that major dissolution of the halite by unsaturated ground water has not occurred at the WIPP site.

#### Focus of Current Study

This report describes several dissolution features in the Delaware Basin and elsewhere that have been referred to as breccia pipes. Breccia pipes (also called breccia chimneys) as they occur in evaporites are vertical cylindrical pipes or chimneys that may or may not involve more than one geologic formation. The chimneys are filled with downward-displaced brecciated rock. In this context, the rock is brecciated by having collapsed into a void at depth that was probably created by ground-water solution and removal of deep-lying evaporite or carbonate rocks in an underlying aquifer system (Anderson and Kirkland, 1980; Bachman, 1980). Such features have been described in evaporite deposits in many areas of the world.

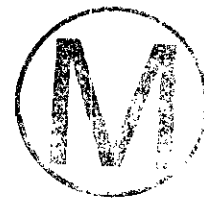
The current study was done for the U.S. Department of Energy (DOE) in response to a suggestion that because breccia pipes are thought to be the result of deep dissolution, they may represent channelways for future ingress of ground water, and that they should be considered in risk assessment programs for the evaluation of proposed waste repositories in bedded evaporite rocks. To this end, features referred to as breccia pipes in southeastern New Mexico have been assessed in relation to the integrity of the WIPP site. Reports by Anderson (1978), Bachman (1980), and Vine (1960) described dissolution and karst features in the Pecos region of southeastern New Mexico and discussed the origin and history of breccia pipes. The present report is intended to supplement these studies and provide detail that was not available to them at the time their reports were written.

Using the data from exploratory work, answers may be found to the following questions concerning breccia pipes:

## Compliance Certification Application Reference Expansion

---

1. Do breccia pipes penetrate through the evaporite section?
2. What is the physical description of a pipe?
3. How are they formed?
4. How deep do they go?
5. When are they formed, and are they forming at present?
6. Are they permeable?
7. Where are they formed, can they form at the WIPP site?
8. Do they represent a threat to the WIPP site?"



## Compliance Certification Application Reference Expansion

---

Stensrud, W.A., Bame, M.A., Lantz, K.D., Caufmann T.L., Palmer, J.B., and Saulnier, Jr., G.J. 1988. WIPP Hydrology Program, Waste Isolation Pilot Plant, Southeastern New Mexico, Hydrologic Data Report #6. SAND87-7166. Sandia National Laboratories, Albuquerque, NM. WPO 29674.

Foreword, p xxvii;

" Hydrologic Data Report #6, the sixth of a series of basic data reports, contains data from hydrologic testing and water-level measurements conducted at the Waste Isolation Pilot Plant (WIPP) site over the period May through October 1987. The purpose of these reports is to disseminate basic hydrologic data to interested parties in a timely manner, often before data interpretation has been performed. Performance of the field investigations was carried out by or under the direction of Sandia National Laboratories, Albuquerque, New Mexico. This report includes recent hydrologic data collected by INTERA Technologies, Inc. of Austin, Texas.

Hydrologic Data Report #6 contains descriptions of: permeability tests conducted from July to August 1987 in six sub-horizontal boreholes drilled from the waste-handling shaft (Part A); well development and slug testing conducted at wells H-1, H-12, and P-15 (Part B); a pumping test performed from July to September 1987 in conjunction with water-quality sampling at the H-2 hydropad (Part C); and drill-stem, slug, and pulse testing conducted by Sandia at wells H-16, H-17, and H-18 (Part D). Part E has been produced by INTERA from water-level and fluid-pressure data collected by INTERA and Sandia from May to October 1987.

The report is organized into five parts with sub-sections internally numbered without letter designations. The pages in each part are numbered consecutively with the letter prefixes A through E. The table of contents should be consulted for overall organizational details and content. For ease of reading, all Figures and Tables are grouped together at the end of the corresponding part, prior to the Appendixes."



Compliance Certification Application Reference Expansion

---

Stensrud, W.A., Dale, T.F., Domski, P.S., Palmer, J.B., Roberts, R.M., Fort, M.D., and Saulnier, Jr., G.J. 1992. Waste Isolation Pilot Plant Salado Hydrology Program Data Report #2. SAND92-7072. Sandia National Laboratories, Albuquerque, NM. WPO 26432.

ABSTRACT;

" WIPP Salado Hydrology Program Data Report #2 presents hydrologic data collected during permeability testing of the Salado Formation performed from August 1989 through July 1992. The report presents the results of the drilling and testing of six boreholes drilled from the WIPP underground facility 655 m below ground surface in the Salado Formation. Permeability tests were conducted using multipacker test tools with inflatable packers to isolate borehole intervals to allow formation pore-pressure buildup and subsequent pressure-pulse and constant-pressure-withdrawal tests. The tests performed in boreholes LAP51, LAP52, SCP01, S1P71, S1P72, and S1P73 involved Marker Beds 138 and 139, anhydrites 'a,' 'b,' and 'c,' clays B, D, E, G, H, J, and K, and several halitic strata. Test data include pressure and temperature from the brine-filled, packer-isolated test intervals, fluid and gas production during constant-pressure-withdrawal tests, and borehole-closure and axial test-tool-movement measurements. The boreholes were drilled and/or cored to nominal 10.2-cm diameters using compressed air to remove drill cuttings. Compliance tests were conducted in lengths of steel and stainless-steel casing to evaluate the mechanical performance of the multipacker test tools. Compliance tests included leak tests and pulse-injection and pulse-withdrawal sequences. Following permeability testing, fluid pressures were monitored in packer-isolated sections of test boreholes C2H01, C2H02, SCP01, S1P71, S1P72, DPD01, DPD02, and DPD03."



Stone, C.M., Krieg, R.D., and Beisinger, Z.E. 1985. SANCHO, A Finite Element Computer Program for the Quasistatic, Large Deformation, Inelastic Response of Two-Dimensional Solids. SAND84-2618. Sandia National Laboratories, Albuquerque, NM. WPO 24658.

ABSTRACT, p 3;

" SANCHO is a finite element computer program designed to compute the quasistatic, large deformation, inelastic response of planar or axisymmetric solids. Finite strain constitutive theories for plasticity, volumetric plasticity, and metallic creep behavior are included. A constant bulk strain, bilinear displacement isoparametric finite element is employed for the spatial discretization. The solution strategy used to generate the sequence of equilibrium solutions is a self-adaptive dynamic relaxation scheme which is based on explicit central difference pseudo-time integration and artificial damping. A master-slave algorithm for sliding interfaces is also implemented. A theoretical development of the appropriate governing equations and a description of the numerical algorithms are presented along with a user's guide which includes several sample problems and their solution."

Compliance Certification Application Reference Expansion

---

Stormont, J.C. 1990. Discontinuous Behavior Near Excavations in a Bedded Salt Formation. International Journal of Mining and Geological Engineering, SAND89-2403J, Vol. 8, No. 1, pp. 35-56. WPO 29472.

Behavior of overlying strata, page 4, para 1, Line 1;

" Limited tracer gas measurements indicate the flow paths are larger in the vertical direction than the horizontal direction in the center of the drift."

Behavior of underlying strata, p 5, para 10, line 4;

" Tracer gas measurements made in various size drifts have shown that the 1 m thick layer of salt has larger vertical than horizontal flow paths (equivalent apertures), and that the dimension of these flow paths increase an order of magnitude from about  $2E-5$  m to  $2E-4$  m as the drift span increases from 6.6 m to 11 m (Borns and Stormont, 1988)."



Stormont, J.C., Peterson, E.W., and Lagus, P.L. 1987. Summary and Observations About WIPP Facility Horizon Flow Measurements Through 1986. SAND87-0176. Sandia National Laboratories, Albuquerque, NM. WPO 27053.

ABSTRACT;

" Numerous gas flow measurements have been made at the Waste Isolation Pilot Plant (WIPP) facility horizon from 1984 through 1986. Almost all tests have been constant-pressure or pressure-decay tests from single boreholes drilled in the underground excavations. Results indicate that beyond about 2 m from an excavation, both halite and interbeds (anhydrite and clay layers) allowed very low gas flows, and calculated permeabilities are below 1 microdarcy. In regions within 2 m of an excavation, very high flow rates were measured in the interbeds immediately above and below an excavation when the test hole was drilled from near the center of the excavation. The halite also permits substantially greater gas flow within about 1 m of the excavations. Limited tracer measurements reveal that flow paths in both the halite and interbeds in the near field region are significantly larger than those in the presumed undisturbed condition. The gas flow measurements are consistent with the development of a (perhaps partially-saturated) dilutant zone (increased porosity) around the excavations. Considerable uncertainty is associated with permeabilities calculated from these flow measurements, due to unknowns of rock saturation, entry pressure effects, flow homogeneity, etc.

Observations based on these gas flow measurements will aid in understanding the behavior and response of rocks surrounding the WIPP Facility excavations. The implications of these measurements for seal design are useful, particularly in assessing the degree of seal bypass to expect in adjacent rock. Results suggest that seal be emplaced as soon as possible after excavation and in as narrow drifts as possible to minimize potential bypass. These data are also useful in separate studies of brine influx and gas generation/dissipation. Future measurements will focus on the development and extent of the disturbed zone, and on obtaining data which will make conversion of flow data to intrinsic permeabilities more defensible."



Stormont, J.C., Howard, C.L., and Daemen, J.J.K. 1991. In Situ Measurements of Rock Salt Permeability Changes due to a Nearby Excavation. SAND90-3134. Sandia National Laboratories, Albuquerque, NM. WPO 26166.

**ABSTRACT;**

" The Small-Scale Mine-By was an in situ experiment to measure changes in brine and gas permeability of rock salt as a result of nearby excavation. A series of small-volume pressurize brine- and gas-filled test intervals were established 8 m beneath the floor of Room L1 in the WIPP underground. The test intervals were isolated in the bottom of the 4.8-cm diameter monitoring boreholes with inflatable rubber packers, and are initially pressurized to about 2 MPa. Both brine- and gas-filled test intervals were located 1.25, 1.5, 2, 3, and 4 r from the center of a planned large-diameter hole, where r is the radius of the large-diameter hole. Prior to the drilling of the large-diameter borehole, the responses of both the brine- and gas-filled test intervals were consistent with the formation modeled as a very low permeability, low porosity porous medium with a significant pore (brine) pressure and no measurable gas permeability. The drilling of the mine-by borehole created a zone of dilated, partially saturated rock out to about 1.5 r. The formation pressure increases from near zero at 1.5 r to the pre-excavation value at 4 r. Injection tests reveal a gradient of brine permeabilities from  $5 \times 10^{-18} \text{ m}^2$  at 1.25 r to about the pre-excavation value ( $10^{-21} \text{ m}^2$ ) by 3 r. Gas-injection tests reveal measurable gas permeability is limited to within 1.5 r."

Telander, M.R., and Westerman, R.E. 1993. Hydrogen Generation by Metal Corrosion in Simulated Waste Isolation Pilot Plant Environments: Progress Report for the Period November 1989 through December 1992. SAND92-7347. Sandia National Laboratories, Albuquerque, NM. pp. 6-14 to 6-27. WPO 23456.

ABSTRACT, p i;

" The corrosion and gas-generation characteristics of three material types: low-carbon steel (the current waste packaging material for the Waste Isolation Pilot Plant), Cu-base materials, and Ti-base materials were determined in both the liquid and vapor phase of Brine A, a brine representative of an intergranular Salado Formation brine. Test environments included anoxic brine and anoxic brine with overpressures of CO<sub>2</sub>, H<sub>2</sub>S, and H<sub>2</sub>. Low-carbon steel reacted at a slow, measurable rate with anoxic brine, liberating H<sub>2</sub> on an equimolar basis with Fe reacted. Presence of CO<sub>2</sub> caused the initial reaction to proceed more rapidly, but CO<sub>2</sub>-induced passivation stopped the reaction if the CO<sub>2</sub> were present in sufficient quantities. Low-carbon steel immersed in brine with H<sub>2</sub>S showed no reaction, apparently because of passivation of the steel by formation of a protective iron sulfide reaction product. Cu- and Ti-base materials showed essentially no corrosion when exposed to brine and overpressures of N<sub>2</sub>, CO<sub>2</sub>, and H<sub>2</sub>S except for the rapid and complete reaction between Cu-base materials and H<sub>2</sub>S. No significant reaction took place on any material in any environment in the vapor-phase exposures."



Compliance Certification Application Reference Expansion

---

Thorne, B.J, and Rudeen, D.K. 1980. Regional Effects of TRU Repository Heat. SAND80-7161. Sandia National Laboratories, Albuquerque, NM. WPO 10281.

INTRODUCTION, p 1;

" A modification of a calculation reported in reference 1 was used to estimate the impact of heat from a 730,000 m<sup>2</sup> (180 acre) 0.69 W/m<sup>2</sup> (2.8 kW/acre) RH TRU repository at the WIPP site. The original calculation, reported in SAI-FR-145, was designed to estimate the effect of a 81,000 m<sup>2</sup> (20 acre) 7.4 kW/m<sup>2</sup> (30 kW/acre) spent fuel repository. This calculation is on much too coarse a scale to accurately predict details of the response. However, estimates obtained by this method are accurate enough to determine whether or not heat effects are large enough to justify more finely zoned calculations.

COMPUTATIONAL SETUP

All materials models, boundary conditions, initial conditions and computing techniques were identical to those described in Reference 1. ...

<sup>1</sup>D.E. Maxwell, K.K. Wahi, B. Dial, The Thermomechanical Response of WIPP Repositories, Science Applications, Inc., SAI-FR-145, Sandia National Laboratories, SAND 79-7111, May 1980."



Tierney, M.S. 1993. "PA Methodology Overview." In Initial Performance Assessment of the Disposal of Spent Nuclear Fuel and High-Level Waste Stored at Idaho National Engineering Laboratory. Volume 1: Methodology and Results. R.P. Rechard, ed. SAND93-2330/1. Sandia National Laboratories, Albuquerque, NM. 3-1 through 3-28. Chapter 3 of WPO 26694.



3.1 Introduction; p 3-1;

" The U. S. Environmental Protection Agency (EPA's) guidance and intentions concerning the nature and purpose of performance assessment (see Chapter 2) suggests that PA is ideally a *stochastic simulation* (Section 3.2.4) of possible long-term behaviors of a real system with a computer-implemented mathematical model of that system. In this respect performance assessment is similar to other large-scale simulations (e.g., the *Reactor Safety Study*[Rasmussen, 1975]) that have been used by federal agencies in the past to explore policy options and develop regulations. Performance assessments of systems for the disposal of radioactive and toxic wastes may nevertheless differ from most simulations with 'regulatory models' (Morgan et al., 1990, p. 292) in two significant and related ways: the way results of a performance assessment are to be used; and the nature of the real system that is being simulated.

In contrast with past simulations with federally sponsored models, PA results are ultimately used to test compliance of a real system with an existing environmental standard, not merely to gain insight into the behavior of the system with the purpose of discovering a rational basis for new standards. Furthermore, a quantitative treatment of uncertainty in PA calculations is not merely good analytical practice but is mandated by the explicitly probabilistic statement of the Standard in which all results are to be combined in an 'overall probability distribution' whenever practicable. As will be seen later, such a quantitative treatment of uncertainty forces the development of two categories of models of the same system; the usual, deterministic phenomenological models (called 'consequence' models in PA; Section 3.2.1), and probability models (Section 3.2.3) that can provide quantitative estimates of the degree of uncertainty associated with parameters that specify the possible configuration of the consequence models.

The problems arising from direct use of PA results in testing compliance and a mandated quantitative treatment of uncertainty are compounded by the nature of the focal system in PA: geological waste-disposal systems are built up largely from natural components (as opposed, for example, to the man-made components of a nuclear reactor), the physical and chemical characteristics of which are usually inhomogeneous and distributed in space and time. There is little published work on efficient methods for conducting sensitivity and uncertainty analyses of such distributed-parameter systems; objective methods for the assignment of the parametric uncertainty associated with such systems are also lacking. Indeed, in building methodologies for PA, investigators have in the past drawn heavily upon ideas and analytical techniques developed primarily for the study of 'lumped parameter' systems and have largely ignored the special needs of PA that arise from the problems mentioned above.

## Compliance Certification Application Reference Expansion

---

With the hope that a firm understanding of the structure of a PA will help in meeting PA's special needs, this overview offers a description of current PA methodologies in terms and concepts taken from the broader context in which they are imbedded, i.e., the general theory of stochastic simulation, as it is applied to the study of natural systems that may change or 'fail' over long periods of time. To minimize misunderstanding among investigators with diverse backgrounds, terminology developed for PA will be maintained throughout the overview, but PA terms will be matched with their mathematical counterparts whenever possible. Discussion of each topic proceeds from generalities to specifics, and from theory to practical applications. The structure of a PA is summarized in Section 3.2, where emphasis is upon the correspondence of PA concepts such as consequence models, probability models, and performance measures, with concepts from the general theory of stochastic simulation. Section 3.3 is a technical treatment of certain topics of special interest to PA practitioners; in particular, the confusing topic of 'scenarios' is treated. Applications and examples are taken from the initial performance assessment described in this report and from an assessment of the performance of the Waste Isolation Pilot Plant (WIPP), a research and development facility located in southeastern New Mexico for the purpose of demonstrating safe disposal of defense-generated transuranic wastes (WIPP PA Division, 1991a, 1991b; WIPP PA Department, 1992b).



Tiller, C.L., and O'Melia, C.R. 1993. "Natural Organic Matter and Colloidal Stability. Models and Measurements." In *Colloids in the Aquatic Environment. Colloids and Surfaces A: Physiochemical and Engineering Aspects*, T.F. Tadros and J. Gregory, eds., pp. 89-102. Elsevier Applied Science, London.

ABSTRACT, p 89;

" Laboratory and field observations by several investigators indicate that natural organic matter (NOM) affects and probably controls the colloidal stability of particles in aquatic systems. The enhanced stability of particles in aquatic systems containing NOM is a consistent observation without a clear cause. In this work, the potential importance of the macromolecular nature of NOM was investigated using model systems. A mathematical model for the adsorption of linear, flexible polyelectrolytes was used to examine the effects of molecular weight, pH, and ionic strength on the conformations of these surrogates for NOM at interfaces in natural waters. Laboratory experiments involving submicron hematite particles, two anionic polyelectrolytes, and an aquatic NOM were used to examine the effects of solution composition on colloidal stability. Together, the results of the mathematical simulations and the laboratory experiments indicate that electrostatic effects dominate particle-particle interactions, but that the macromolecular nature of NOM can have direct influence under certain conditions. At low ionic strength, anionic polyelectrolytes affect the coagulation of positively charged particles by altering net surface charge in a way similar to specifically adsorbing, multivalent, monomeric anions. At high ionic strength ( $I > 0.1$ ), the conformational characteristics of adsorbed polyelectrolytics at the solid/water interface directly affect coagulation by expanding the effective distance of electrostatic repulsion between approaching particles, as well as by altering net surface charge. Non-electrostatic steric repulsion plays little or no role in the stabilization of hematite particles by the organic macromolecules used in this work. Calcium acts to destabilize hematite particles in the presence of the organic macromolecules, perhaps through a combination of special chemical and charge effects."



Tipping, E. 1993. "Modeling Ion Binding by Humic Acids." In Colloids in the Aquatic Environment. Colloids and Surfaces A: Physicochemical and Engineering Aspects, T.F. Tadros and J. Gregory, eds., pp. 117-131. Elsevier Applied Science, London.

ABSTRACT, p 117;

" Humic ion-binding Model V is a discrete site/electrostatic model of ion binding by humic matter that describes competition amongst interacting species (protons and metal species) and the effects on binding of ionic strength. Six adjustable parameters are required to describe proton binding. These are  $n_A$  (equivalent acid groups per gram),  $pK_A$  and  $pK_B$  (midrange intrinsic proton disassociation constants),  $\Delta pK_A$  and  $\Delta pK_B$  (ranges of pK values), and  $P$  (empirical constant for electrostatics). For each metal species, two further parameters are required; these are intrinsic equilibrium constants for metal-proton exchanges ( $pK_{MHA}$  and  $pK_{MHB}$ ). Both monodentate and bidentate binding sites for metal species are included, and binding for non-specific accumulation of counterions is taken into account. In this study, Model V parameter values are derived from published results for humic acids (acid base titrations and binding studies with 15 metals). It is found that an approximate relationship between  $pK_{MHA}$  and  $pK_{MHB}$  can be derived, which eliminates an adjustable parameter and allows useful rationalization of the different data sets. Electrostatic effects with humic acids are greater than those with fulvic acids, and the two types of humic material also differ in the affinities of their discrete binding sites for protons and metal ions."

Tóth, L.M., Friedman, H.A., and Osborne, M.M. 1981. Polymerization of Pu(IV) in Aqueous Nitric Acid Solutions. *Journal of Inorganic and Nuclear Chemistry*, Vol. 43, No. 11, pp. 2929-2934.

ABSTRACT, p 2929;

" The polymerization of Pu(IV) in aqueous nitric acid solutions has been studied spectrophotometrically both to determine the effects of large  $\text{UO}_2(\text{NO}_3)_2$  concentrations on the polymerization rates and, more generally, to review the influence of other major parameters on the polymer reaction. Typically, experiments have been performed at  $50^\circ\text{C}$  and at 0.05M Pu in aqueous solutions of  $\text{HNO}_3$  at concentrations ranging from 0.07 to 0.4M. An induction period usually precedes the polymer growth stage, during which time it is believed that primary hydrolysis products form and begin to aggregate. Uranyl nitrate retards the polymerization reaction by approximately 35% despite the counteracting influence of the nitrate ions associated with this solute. The rate of polymer formation at  $50^\circ\text{C}$  has been shown to be third order in Pu(IV) concentration."



Van der Lee, J., de Marsily, G. and Ledoux, E. 1993. "Are Colloids Important for Transport Rate Assessment of Radionuclides? A Microscopic Modeling Approach," In High Level Radioactive Waste Management, Proceedings of the Fourth Annual International Conference, Las Vegas, NV, April 26-30, 1993, pp. 646-652. American Society of Civil Engineers. New York, NY.

ABSTRACT, p 646;

" Understanding the transport phenomena of radionuclides migrating through weakly-permeable rock forms an essential part of far-field safety assessment studies. Colloidal matter can be important in view of the solubility of radioactive waste, and as a potential rapid carrier of the radionuclides in far-field migration. When estimating the influence of colloids on the fate of radionuclides, a key aspect is the understanding of the interaction mechanisms of the phases involved, i.e. aqueous, solute and colloidal phase and the solid medium, because they define the retardation and hence the arrival time of the pollutant in the human environment.

The present study is an attempt to quantify interaction phenomena according to a microscopic modeling approach, based on a combination of chemical and electro-physical considerations. In order to define the state of the surface of colloids and medium, a model based upon the surface complexation theory was developed. Migration from the inner pore-space towards the surface is governed by diffusion, gravitation and, very close to the surface, electrostatic forces. Colloidal fixation is electrochemically as well as physically bounded by a maximum adsorption capacity and it is expected that electrostatic surface properties change when the surface becomes progressively saturated by colloids. Therefore, the model includes surface reactions with parameters depending on the maximum concentration at the surface.

The result is a microscopic model which includes chemical speciation, electrochemical characteristics of the medium and colloids, pH, ionic strength and surface boundary-layer phenomena. The model can be used for predictive purposes in laboratory experiments, using simple hydrogeological geometries and organic colloids. Effects of radionuclide concentration (e.g. Am(III)), pH and surface potential are quantified.



Van Sambeek, L.L., Luo, D.D., Lin, M.S., Ostrowski, W., and Oyenuga, D. 1993. Seal Design Alternatives Study. SAND92-7340. Sandia National Laboratories, Albuquerque, NM. WPO 23445.

**ABSTRACT;**

" This report presents the results from a study of various sealing alternatives for the WIPP sealing system. Overall, the sealing system has the purpose of reducing to the extent possible the potential for fluids (either gas or liquid) from entering or leaving the repository. The sealing system is divided into three subsystems: drifts and panel seals within the repository horizon, shaft seals in each of the four shafts, and borehole seals.

Alternatives to the baseline configuration for the WIPP seal system design included evaluating different geometries and schedules for seal component installations and the use of different materials for seal components. Order-of-magnitude costs for the various alternatives were prepared as part of the study. Firm recommendations are not presented, but the advantages and disadvantages of the alternatives are discussed. Technical information deficiencies are identified and studies are outlined which can provide required information."



Vesely, W.E., and Rasmuson, D.M. 1984. Uncertainties in Nuclear Probabilistic Risk Analyses. Risk Analysis, Vol. 4, No. 4, pp. 313-322.

p 313;

" There are many uncertainties in a probabilistic risk analysis (PRA). We identify the different types of uncertainties and describe their implications. We then summarize the uncertainty analyses which have been performed in current PRAs and characterize results which have been obtained. We draw conclusions regarding interpretations of uncertainties, areas having largest uncertainties, and needs which exist in uncertainty analysis. We finally characterize the robustness of various utilizations of PRA results."



Vilks, P. 1994. The Role of Colloids and Suspended Particles in Radionuclide Transport in the Canadian Concept for Nuclear Fuel Waste Disposal. AECL-10280. Whiteshell Laboratories, Atomic Energy of Canada, Ltd., Pinawa, Manitoba. Yucca Mt #. MOL.19950202.0067.

**ABSTRACT;**

" AECL Research is developing a concept for the permanent disposal of nuclear fuel waste in a deep engineered vault in plutonic rock of the Canadian Shield and is preparing an Environmental Impact Statement (EIS) to document its case for the acceptability of the disposal concept. This report, one in a series of supporting documents for the EIS, addresses the role of particles in radionuclide transport. It summarizes our studies of natural particles in groundwater and presents the arguments used to justify the omission of particle-facilitated transport in the geosphere model that is based on the Whiteshell Research Area (WRA) and used in the postclosure assessment study case.

Because radionuclides formed in the vault will not be able to migrate through the clay buffer, radiocolloid formation in the geosphere will be determined by the sorption of radionuclides onto particles in groundwater. These particles consist of typical fracture-lining minerals, such as clays, micas and quartz; precipitated particles such as colloidal silica and Fe-Si oxyhydroxides; and organic particles. In groundwater from the WRA, the average concentrations of colloids and suspended particles are 0.34 and 1.4 mg/L respectively. Particle-facilitated transport is not included in the geosphere model because the concentrations of particles in groundwater from the WRA are too low to have significant impact on radionuclide transport."





Vine, J.D., 1963. Surface Geology of the Nash Draw Quadrangle, Eddy County, New Mexico. U.S. Geological Survey Bulletin, 1141-B. WPO 39558.

ABSTRACT, p B1;

" Outcropping rocks and surficial deposits of the Nash Draw quadrangle were mapped to provide geologic information for the U.S. Atomic Energy Commission's Plowshare program. The quadrangle is near the north margin of the Delaware basin and about 15 miles east of Carlsbad, N. Mex. The region is sparsely inhabited and has an arid climate.

As much as 4,000 feet of salt and anhydrite of Permian age is present below the surface, but does not crop out in normal thickness in this area or elsewhere because of their high solubility. These rocks have been divided into the Castile formation below and the Salado formation above. Rocks exposed at the surface overlie these soluble rocks and include the Rustler formation of Late Permian age, the Pierce Canyon redbeds of Permian or Triassic age, the Santa Rosa sandstone of Late Triassic age, and the Gatuna formation, caliche, and a variety of unconsolidated deposits of late Cenozoic age.

The Rustler formation of Late Permian age is subdivided into four easily distinguishable members, excluding about 120 feet of the lower part, which is not exposed at the surface in this area. The oldest member exposed is the Culebra dolomite member, about 30 feet thick, identified only in erratically distributed outcrops in collapse areas. The Culebra consists of microcrystalline gray dolomite or dolomitic limestone characterized by numerous spherical cavities 1 to 10 mm in diameter. It is conformably overlain by the Tamarisk member, named herein for exposures directly east of Tamarisk Flat. It consists of about 115 feet of massive gypsum at the surface, changing to anhydrite in the subsurface, and a bed, 5 feet thick, of siltstone near the base. Surficial deformation caused by hydration and solution are characteristic of all the outcrops. The Tamarisk member is conformably overlain by the Magenta member, about 20 feet thick and consisting of alternating wavy laminae of pale-red dolomite and pale yellowish-green anhydrite or gypsum. The top member of the Rustler formation conformably overlies the Magenta and is here named the Forty-niner member after Forty-niner Ridge, where it crops out. In surface exposures it consists of about 40 to 65 feet of broken and slumped massive gypsum and a bed of siltstone in the lower part. The siltstone beds in the Tamarisk and Forty-niner members probably represent the insoluble residue of salt beds reported from the subsurface to the east."

Overlying the Rustler formation with apparent conformity are the Pierce Canyon redbeds of Permian or Triassic age. These rocks consist of about 200 to 250 feet of laminated or minutely cross-laminated moderate reddish-brown siltstone. The contact between the Pierce Canyon redbeds and the overlying Santa Rosa sandstone is a disconformity, at least locally.

The Santa Rosa sandstone of Late Triassic age consists of pale-red sandstone and conglomerate lenses crossbedded in sets 3 to 15 feet thick separated locally by moderate reddish-brown siltstone and claystone. Only the lower 50 to 70 feet of Santa Rosa was recognized in the area.

The Gatuna formation of Pleistocene (?) age unconformably overlies all older rocks.

## Compliance Certification Application Reference Expansion

---

In much of the area it consists of 3 to 5 feet of moderate reddish-orange sandstone, siltstone, and conglomerate. Locally, in karst depressions, the Gatuna attains a thickness of at least 100 feet. In some areas the lithology closely resembles the Pierce Canyon rebeds or the Santa Rosa sandstone.

Caliche forms a resistant layer at the ground surface, 5 to 10 feet thick, that protects older rocks from erosion in many areas. The caliche consists of calcareous material with a variable amount of imbedded sand grains, pebbles, and rock fragments. Caliche mounds and broken flexure ridges, 10 to 15 feet high, have formed narrow zones 50 to several hundred feet long.

Quaternary alluvium has been deposited along the sides of depressions. It is overlain by playa lake deposits, which are in turn overlain by conspicuous sand dunes as much as 100 feet high.

The regional structure is relatively simple and consists of a dip of a few feet per mile to the east and southeast.

Normally flat-lying strata are tilted, warped, and locally distorted at the surface by hydration and solution of the evaporite rocks in the subsurface. Nash Draw, a depression 4 to 6 miles wide and about 18 miles long, has resulted from the solution of salt in the Rustler and Salado formations and collapse of the overlying relatively insoluble rocks. Topography and surface structure conform in some areas with the configuration of the underlying solution surface at the top of the massive salt in the Salado formation; however, locally there is an inverse correspondence. Many circular karst features 1/10 to 1/2 mile in diameter are in the area. Some of these features are structural domes, but they contain a core of tilted or brecciated rock. These karst features result from the formation and collapse of sinkholes, differential solution at the top of the massive salt, and hydration of the anhydrite beds."



Vlassopoulos, D., Wood, S.A., and Mucci, A. 1990. Gold Speciation in Natural Waters: II. The Importance of Organic Complexing--Experiments with Some Simple Model Ligands. *Geochimica et Cosmochimica Acta*, Vol. 54, No. 6, pp. 1575-1586.

NOTE:portions of the following text were not clear on the document that they were copied from and have been interpreted for content by the typist.

ABSTRACT, P 1575;

" The solubility of Au has been measured at 25°C in aqueous solutions in the presence of various organic ligands (acetate, benzoate, oxalate, phthalate, salicylate, and thiosalicylate). These ligands were chosen as sample analogs of humic acid moieties in order to model the complexation of AU by humic and fulvic acids in natural waters. With the first five ligands ( $\Sigma L = 0.1$  M), solubilities were generally below 25  $\mu\text{g/l}$ , whereas in the thiosalicylate solutions ( $\Sigma L = 0.45$  M), a maximum Au concentration of 680 mg/l was measured. Acetate and benzoate complexes are too weak to detect by the solubility method. Oxalate appears to have a reducing effect on Au in solution, and both oxalate and phthalate complexes of Au(I) may be coordinatively unfavorable. It was only possible to identify one salicylate complex ( $\log \beta_2 = 17.5 \pm 0.5$ ) and two thiosalicylate species ( $\log \beta_1 = 29.9 \pm 0.3$  and  $\log \beta_2 = 31.7 \pm 0.3$ ). In addition, stability constants for a number of O-, N-, and S-donor complexes of Au(I) were estimated from linear free energy relationships with Cu(I), Ag(I), and Hg(II).

General trends in stability constants of Au-organic complexes with various donor atoms are  $S \gg N \geq O$ . Calculations based on a simple model of a fulvic acid suggest that Au is almost exclusively bound to S-donor sites under reducing conditions, but  $\text{AuOH}(\text{H}_2\text{O})^6$  and complexing by organic O-donors are more important in oxidizing environments."



Wallner, M. 1981. "Critical Examination of Conditions for Ductile Fracture in Rock Salt." In Proceedings of the Workshop on Near-Field Phenomena in Geologic Repositories for Radioactive Waste, Seattle, WA, August 31-September 3, 1981, pp. 243-253. Organisation for Economic Co-Operation and Development, Paris, France.

ABSTRACT, p. 243;

" Rock salt because of its ductility in general prevents the presence of open cracks. This favorable property is derived from the capability of the material to reduce deviatoric stresses by means of creep deformations. Ductile fracture of halite under in situ stress conditions therefore is only possible under certain circumstance. The condition to initiate and propogate fractures in a salt formation on one hand and the fracture healing process on the other are discussed.

An extensive experimental programme was performed to ascertain the fracture strength of rock salt. A summary of results from these tests are given and a proposed criterion for creep fracture in compression is explained."



Warrick, R. and Oerlemans, J. 1990. "Sea Level Rise." In *Climate Change: The IPCC Scientific Assessment*, J.T. Houghton, G.J. Jenkins, and J.J. Ephraums, eds., pp. 257-281. Intergovernmental Panel on Climate Change, Sweden.

Section 9.5 **HOW MIGHT SEA LEVEL CHANGE IN THE FUTURE?**, p. 278, col. 1;

" Various estimates of future sea level rise are noted in Table 9.9. Such estimates are very difficult to compare because different time periods are chosen, and because assumptions regarding future greenhouse gas concentrations, changes in climate, response times, etc., are either different or not clearly stated. In general, most of the studies in Table 9.9 foresee a sea level rise of somewhere between 10cm and 30 cm over the next four decades. This represents a rate of rise that is significantly faster than that experienced, on average, over the last 100 years."





Washington, W.M., and Meehl, G.A. 1984. Seasonal Cycle Experiment on the Climate Sensitivity Due to Doubling of CO<sub>2</sub> with an Atmospheric General Circulation Model Coupled to a Simple Mixed-Layer Ocean Model. *Journal of Geophysical Research*, Vol. 89, No. D6, pp. 9475-9503.

ABSTRACT, p. 9475;

" A simple slab ocean of 50 m depth, which allows for seasonal ocean heat storage but no ocean heat transport, is coupled to a global special general circulation model with global domain, realistic geography, and computed clouds. Globally averaged, the annual mean surface air temperature increase computed over the last 3 years of an integration with a full annual cycle for 2 x CO<sub>2</sub> compared to the control for 1 x CO<sub>2</sub> is 3.5°C. Zonal mean air temperature differences indicate stratospheric cooling and tropospheric warming as seen in other CO<sub>2</sub> modeling studies. Greatest increases of surface air temperature in the 2 x CO<sub>2</sub> case, compared to the control, occur the sea ice margins. Retreat of sea ice in the 2 x CO<sub>2</sub> case is associated with changes in the positions of the cloud maxima. Ice-free areas of ocean in the 2 x CO<sub>2</sub> case, which are ice covered in the 1 x CO<sub>2</sub> case, store relatively more heat during the summer season. Warmer surface air temperatures then occur in areas that are much colder in the control case because of the lack of the insulating effect of the sea ice, especially in winter. Increases of zonal mean precipitation are evident at most latitudes as a result of increases of available moisture evaporated from the warmer oceans. In the tropics this is associated with a strengthening of the mean meridional circulation and with intensification of the upper level zonal-component winds in the subtropics. Warming near the surface associated with the retreat of the ice line in the 2 x CO<sub>2</sub> case slackens the meridional temperature gradient and results in weaker upper level zonal-component winds in the mid-latitudes. Three-year seasonal means of soil moisture show decreases in tropical and subtropical continental areas and increases at high latitudes, but at mid-latitudes the change depends on the season. An analysis of the statistical significance of the geographical distribution of 7-year seasonal means of surface air temperature and soil moisture differences is given for the 2 x CO<sub>2</sub> case compared to the control. Areas of significant differences correspond to similar regions of large differences seen in the 3-year seasonal means. Certain regions experience summer drying seen in other studies, but zonal mean soil moisture differences show increases of soil moisture at mid and high latitudes of the northern hemisphere year-round, with a relative minimum of increase in late summer. These differences are attributed to large increases of soil moisture in late spring that persist into summer and cause a positive feedback with precipitation and low clouds. This inhibits continental warming and limits summer drying seen in the zonal mean as a result of the doubling of CO<sub>2</sub>. A comparison of the present experiment with the previous swamp model experiment is consistent with other studies in that the extent of sea ice in the control case critically influences the climatic response to increased CO<sub>2</sub> such that more extensive sea ice is associated with a larger response. The seasonal cycle along with ocean heat storage in the mixed layer model are shown to be important in producing a more realistic simulation of the present climate than does the swamp experiment and, presumably, a more credible response

**Compliance Certification Application Reference Expansion**

---

to increased CO<sub>2</sub>. However, in the context of recent studies the overextensive sea ice in the present mixed layer model suggests that the inclusion of ocean heat transport from a fully computed ocean model and a resulting sea ice distribution closer to the observed would possibly produce less of a response to increased CO<sub>2</sub>."



Weatherby, J.R., Brown, W.T., and Butcher, B.M. 1991. "The Closure of WIPP Disposal Rooms Filled with Various Waste and Backfill Combinations." In *Rock Mechanics as a Multidisciplinary Science*, Proceedings of the 32nd U.S. Symposium, University of Oklahoma, Norman, OK, July 10-12, 1991, J.C. Roegiers, ed. SAND90-2399C, pp. 919-928. A.A. Balkema, Brookfield, VT. WPO 28617.

ABSTRACT p. 1;

" Two-dimensional finite element analyses were used to investigate the closure of WIPP disposal rooms filled with backfill and rooms filled with a combination of waste and backfill. Two different backfill materials were considered. The analyses provide estimates of the porosity in the disposal room as a function of time. These results have been used to help evaluate the suitability of the backfill materials for use in the repository."



Compliance Certification Application Reference Expansion

---

Westinghouse Electric Corporation. 1994. Backfill Engineering Analysis Report, Waste Isolation Pilot Plant. Westinghouse Electric Corporation, Waste Isolation Division, Carlsbad, NM. WPO 37909.

Executive Summary, Scope, p i;

" The Waste Isolation Pilot Plant (WIPP), located in southeastern New Mexico 26 miles east of Carlsbad, is a facility designed for the permanent disposal of transuranic waste generated at U. S. Department of Energy (DOE) facilities across the United States. The primary purpose of this report is to determine if there is a geomechanical need or advantage to backfilling the WIPP underground. The concept of backfilling the WIPP underground is usually associated with the final sealing of the repository. Since WIPP was designed to be a permanent waste disposal facility, sealing is a part of the decommissioning process, which can include backfilling some or all of the underground workings. The main focus of this report is on the various proposed geomechanical uses for backfill in the WIPP underground: operational and long-term performance uses are also discussed briefly. (Information on the validity of each backfill use is presented, when available.) The primary geomechanical effect explored in this report is subsidence, which could affect the stability of the facilities at the surface and in the shafts and could potentially disturb the Culebra Dolomite or other water-bearing units of the Rustler Formation above the WIPP underground facility."



Wilson, C.A., and Mitchell, J.F.B. 1987. A Doubled CO<sub>2</sub> Climate Sensitivity Experiment with a Global Climate Model Including a Simple Ocean. *Journal of Geophysical Research*, Vol. 92, No. D11, pp. 13,315-13,343.

ABSTRACT, p 13,315;

" The sensitivity of a global climate to increased atmospheric CO<sub>2</sub> concentrations is presented, assessed, and compared with earlier studies. The ocean is represented by a 50-m slab in which the heat convergence due to oceanic dynamics is prescribed, producing an accurate simulation of sea surface temperatures, sea-ice extents, and associated features in the control simulation. Changes in surface temperature are qualitatively similar to those found in earlier studies using models with similar or lower horizontal resolution, although the global warming is slightly larger. The simulated changes in hydrology agree broadly with those in studies made with higher horizontal resolution and prescribed changes in sea surface temperatures and include a drying over the northern mid-latitude continents. Many of the discrepancies in the responses of different models can be traced to differences in the simulations of present-day climate. The choice of convective parametrization appears to influence the sensitivity of the simulated response in the tropics."



Wolery, T.J. 1992. EQ3NR, A Computer Program for Geochemical Aqueous Speciation-Solubility Calculations: Theoretical Manual, Users guide, and Related Documentation (Version 7.0). UCRL-MA-110662 PT 3. Lawrence Livermore National Laboratory, Livermore, CA.

ABSTRACT; p. 1, para. 1;

" EQ3NR is an aqueous solution speciation-solubility modeling code. It is part of the EQ3/6 software package for geochemical modeling. It computes the thermodynamic state of an aqueous solution by determining the distribution of chemical species, including simple ions, ion pairs, and complexes, using standard state thermodynamic data and various equations which describe the thermodynamic activity coefficients of these species. The input to the code describes the aqueous solution in terms of analytical data, including total (analytical) concentrations of dissolved components and such other parameters as the  $pH$ ,  $pHCl$ ,  $Eh$ ,  $pe$ , and oxygen fugacity. The input may also include a desired electrical balancing adjustment and various constraints which impose equilibrium with specified pure minerals, solid solution end-member components (of specified mole fractions), and gases (of specified fugacities). The code evaluates the degree of disequilibrium in terms of the saturation index ( $SI = \log Q/K$ ) and the thermodynamic affinity ( $A = -2.303 RT \log Q/K$ ) for various reaction, such as mineral dissolution or oxidation-reduction in the aqueous solution itself. Individual values of  $Eh$ ,  $pe$ , oxygen fugacity, and  $Ah$  (redox affinity) are computed for aqueous redox couples. Equilibrium fugacities are computed for gas species. The code is highly flexible in dealing with various parameters as either model inputs or outputs. The user can specify modification or substitution of equilibrium constants at run time by using options on the input file. The output consists of an output file and a pickup file, which can be used to initialize an EQ6 reaction path calculation. The chief numerical method employed is a hybrid Newton-Raphson technique. This is supported by a set of algorithms which create and optimize starting values. EQ3NR reads a secondary unformatted data file (data1) that is created from a primary formatted data file (data0) by EQPT, the EQ3/6 data file preprocessor. There is currently a set of five data (data0) files. Three of these may be used with either the Davies equation or the B-dot equation to describe the activity coefficients of the aqueous species. Their use is restricted to modeling dilute solutions. The other two of these use Pitzer's equations and are suitable for modeling solutions to high concentrations, though with fewer chemical components. The temperature range of the thermodynamic data on the data files varies from 25°C only to 0-300°C. EQ3NR may be used by itself or to initialize a a (sic) reaction path calculation by EQ6, its companion code in the EQ3/6 package. EQ3NR and the other codes in the EQ3/6 package are written in FORTRAN 77 and have been developed to run under the UNIX operating system on computers ranging from workstations to supercomputers."





Wolery, T.J., and Daveler, S.A., 1992. EQ6, A Computer Program for Reaction Path Modeling of Aqueous Geochemical Systems; Theoretical Manual, User's Guide and Related Documentation (Version 7.0). UCRL-MA-110662-Pt.4. Lawrence Livermore National Laboratory, Livermore, CA.

ABSTRACT; p. 1, para. 1;

" EQ6 is a FORTRAN computer program in the EQ3/6 software package (Wolery, 1979). It calculates reaction paths (chemical evolution) in reacting water-rock waste systems. Speciation in aqueous solution is an integral part of these calculations. EQ6 computes models of titration processes (including fluid mixing), irreversible reaction in closed systems, irreversible reaction in some simple kinds of open systems, and heating or cooling processes, as well as solve "single-point" thermodynamic equilibrium calculations. Chemical evolution is driven by a set of irreversible reactions (i.e., reactions out of equilibrium) and/or changes in temperature and/or pressure. These irreversible reactions usually represent the dissolution or precipitation of minerals or other solids. The code computes the appearance and disappearance of phases in solubility equilibrium with the water. It finds the identities of these phases automatically. The user may specify which potential phases are allowed to form and which are not. There is an option to fix the fugacities of specified gas species, simulating contact with a large external reservoir. Rate laws for irreversible reactions may be either relative rates or actual rates. If any actual rates are used, the calculation has a time frame. Several forms for actual rate laws are programmed into the code. EQ6 is presently able to model both mineral dissolution and growth kinetics. The user can specify modification or substitution of equilibrium constants at run time by using option on the input file. The output consists of an output file, a tab file (tables of output parameters), and a pickup file, which allows a restart capability. The chief numerical method employed for equilibrium calculations is a hybrid Newton-Raphson technique. This is supported by a set of algorithms which create and optimize starting values. When actual rate laws are used, EQ6 integrates them using a finite-difference based ordinary differential equation (ODE) solver. EQ6 reads a secondary unformatted data file (data1) that is created from a primary formatted data file (data0) by EQPT, the EQ3/6 data file preprocessor. There is currently a set of five data (data0) files. Three of these may be used with either the Davies equation or the B-dot equation to describe the activity coefficients, and their use is restricted to modeling dilute solution. The other two of these use Pitzer's equations and are suitable for modeling solution to high concentrations, though with fewer chemical components. The temperature range of the thermodynamic data on the data files varies from 25°C only to 0-300°C. The companion code EQ3NR must be used to initialize a a (sic) reaction path calculation by EQ6. EQ6 and the other codes in the EQ3/6 package are written in FORTRAN 77 and have been developed to run under the UNIX operating system on computers ranging from workstations to supercomputers."

Wood, B.J., Snow, R.E., Cosler, D.J., and Haji-Djafari, S. 1982. Delaware Mountain Group (DMG) Hydrology -- Salt Removal Potential, Waste Isolation Pilot Plant (WIPP) Project, Southeastern New Mexico. TME 3166. U.S. Department of Energy, Albuquerque, NM.

**INTRODUCTION AND SUMMARY, p. 1;**

" This report provides an account of studies performed to evaluate the potential for salt dissolution in the Castile Formation, removal of dissolved salt by fluids in the Bell Canyon aquifer within the Delaware Mountain Group (DMG), and the potential impact of this process on the long-term integrity of the Waste Isolation Pilot Plant (WIPP) facility.

The results of this study provide responses to the stipulated agreement of July 1, 1981 with the U.S. Department of Energy (DOE) and the state of New Mexico regarding the DMG hydrologic investigation. This study was performed and this report prepared by D'Appolonia Consulting Engineers, Inc. (D'Appolonia), under Subcontract S9-CJR-45451 with Westinghouse Electric Corporation, Advanced Energy Systems Division, under Contract DE-AC04-78-ET05346 with the DOE. The Westinghouse team is serving as the Technical Support Contractors (TSC) to the DOE for the WIPP project. ..."



Compliance Certification Application Reference Expansion

---

Zoback, M.D., and Zoback, M.L. State of Stress and Interplate Earthquakes in the United States. *Science*, Vol. 213, No. 4203, pp. 96-104.

SUMMARY, p 96, col 1;

" Recently compiled data on the state of stress have been used to define stress provinces in the conterminous United States in which the orientation and relative magnitude of the horizontal principle stresses are fairly uniform. The observed patterns of stress constrain mechanisms for generating interplate lithospheric stresses. Coupled with new information on geologic structure and tectonism in seismically active areas of the Midcontinent and East, these data help to define some characteristics common to these areas and to identify key questions regarding why certain faults seem to be seismically active."



## Compliance Certification Application Reference Expansion

### INDEX

- 102-579 (66)  
1141-B (344)  
40 CFR 191 (55), (66), (67), (138), (188),  
(222), (226), (241), (281),  
(304), (305)  
4339-4 (166)  
4339-8 (158)  
46 FR 9162 (220)  
74-194 (159)  
78-592 (262)  
79-98 (110)  
80-1099 (161)  
80-879 (310)  
81-31 (162)  
82-968 (325)  
87-120 (306)  
88-490 (216)  
89-001 (281)  
89-011 (222)  
90-051 (81)  
91-007 (223)  
94-008 (227)  
94-019 (226)  
96-164 (222)  
97-425 (66)  
Actinide (148), (209), (218), (269)  
Adams (153), (203), (208), (213), (303)  
AECL-10280 (343)  
AIM (186)  
Airborne (282)  
Alluvial (282), (315)  
Alpha (65)  
Ament (275)  
Andersen (198), (301)  
Anderson (154-156), (189), (201), (210), (285),  
(325)  
Anhydrite (4), (5), (10), (12-15), (17), (29),  
(45), (60), (69), (81), (116),  
(117), (118), (120), (124),  
(125), (128), (129), (156),  
(161), (163), (165), (181),  
(194), (196), (198), (235),  
(277), (279), (291), (295),  
(307), (311), (314), (319),  
(331), (344), (345)  
Anisotropic (45), (171), (263), (320)  
Anticlines (154)  
Aqueous (339), (340), (346), (354), (355)  
Aquifer (2), (50), (77), (81), (97), (118), (154),  
(161), (163), (171), (173),  
(199), (202), (212), (218),  
(269), (296),  
(325), (356)  
Argüello (157), (293)  
Ash (261), (303)  
Attenuation (248)  
Austin (203), (208), (213), (303), (327)  
Avis (181)  
Bachman (158-166), (277), (310), (325)  
Backfill (40), (112), (124), (224), (293), (351),  
(352)  
Baes (168)  
Baker (189)  
Bame (327)  
Barker (169), (203), (208), (213), (303)  
Barr (2)  
Basal (76), (156), (279), (303)  
Basin (47), (48), (82), (112), (116), (117),  
(120), (121), (153-156),  
(161), (163), (164), (166),  
(167), (178), (194), (195),  
(213), (215), (232), (253),  
(270), (271), (277), (279),  
(283), (288), (294), (302),  
(307), (310), (315), (325),  
(344)  
Bean (145), (189)  
Bear (46), (170), (173), (174), (245)  
Beauheim (4), (14), (29), (96), (116), (146),  
(175), (176-181), (263),  
(291)  
Bechtel (77), (182)  
Beckman (289)  
Beisinger (329)  
Belcher (294)  
Bell (62), (110), (154), (156), (179), (183),  
(184), (195), (270), (291),  
(356)  
Bentonite (40), (234), (293)  
Beraún (157), (293)  
Berger (186), (258), (259)  
Bertram-Howery (127), (131), (188), (189),  
(201), (285)  
Beyeler (189)  
Biggers (183), (184)  
Bird (191)  
Black (76), (77), (116), (211), (246), (308)  
Borehole (4), (11), (13), (52), (56), (71), (81),  
(97), (116), (128), (129),  
(135), (136), (164), (175),  
(179), (190), (198), (204),  
(235), (241), (242), (252),



**Compliance Certification Application Reference Expansion**

---

- (278), (291),
- (293), (314),
- (319), (323),
- (328), (332), (341)
- Borns (96), (194-198), (265), (301), (330)
- Brausch (321), (322)
- Breccia (69), (154), (156), (161), (163), (165),
- (208), (215), (307), (325),
- (326)
- Bredhoeft (199)
- brine (4), (11), (13), (45), (58), (59), (62),
- (69), (73), (96), (97), (99),
- (101), (102), (103), (105),
- (108), (112), (116-118),
- (120), (121), (124), (125),
- (127), (128), (136), (138),
- (148), (150), (151), (154),
- (155), (181), (190), (194),
- (196), (198), (205), (208),
- (216), (223), (224), (234),
- (235), (242), (252), (265),
- (270), (279), (283), (293),
- (296), (297), (308), (309),
- (311), (314), (328),
- (331-333)
- Brinster (146), (189), (201), (285)
- Brown (76), (82), (234), (344), (351)
- Brush (96), (147), (148), (150), (201)
- Buddemeier (202)
- Burton (203), (288)
- Butcher (30), (31), (35), (96), (99), (100),
- (105), (109), (133), (134),
- (147), (351)
- Cabin Baby-1 (4), (179)
- Calcic (282)
- CAMCON: (305)
- Campbell (49), (214)
- Capitan (120), (154), (161), (163), (215),
- (270), (271)
- Capitan Reef (120), (163), (215)
- Carbonate (60), (76), (81-83), (279), (282),
- (294), (325)
- Carroll (276)
- Case (2), (47), (50), (52), (64), (96), (97),
- (101), (108), (112), (115),
- (120), (135), (140), (150),
- (170), (171), (172), (217),
- (242), (343), (349)
- Castile (4), (62), (72), (96), (116-118), (120),
- (128), (154), (156), (161),
- (163), (194), (195), (205),
- (235), (270), (291), (307),
- (344), (356)
- Cations (168), (202), (319)
- Cauuffman (96), (204)
- Cenozoic (4), (158-161), (163), (261), (270),
- (294), (296), (303), (344)
- CH-TRU (33), (96), (228), (229)
- Channell (277), (322)
- Chapman (112), (141), (205)
- Chappell (207)
- Characterization (4), (66), (70), (77), (81),
- (99), (110), (116), (122),
- (123), (141), (188), (190),
- (205), (208), (219), (238),
- (269), (276), (281), (290),
- (320), (321)
- Chemical (1), (50), (70), (88), (111), (112),
- (114), (117), (118), (136),
- (138), (139), (168), (170),
- (171), (201), (202), (218),
- (227), (228), (243), (262),
- (269), (277), (278), (285),
- (295), (296), (309), (335),
- (337), (340), (354), (355)
- Cherry (236)
- Chloride (111), (140)
- Choppin (209)
- Chu (96), (254)
- Chugg (210)
- Circular 184 (163)
- Clebsch (296)
- Clements (34), (35)
- Climate (46), (113), (131), (132), (134), (135),
- (186), (187), (207), (213),
- (240), (251), (256-259),
- (292), (317), (344), (348),
- (349), (353)
- Closure (39), (40), (42), (44), (66), (73), (99),
- (112), (124), (142), (143),
- (147), (197), (231), (252),
- (293), (297), (311), (314),
- (328), (351)
- Coats (211)
- Coleman (183)
- colloid (202), (218), (245), (269), (274), (275),
- (280), (283)
- Compaction (31-33), (36), (37), (39), (42),
- (99), (100-102), (105),
- (108), (109), (117), (133),
- (134)
- Complexation (269), (340), (346)
- Compliance (55), (67-71), (122), (131), (138),
- (139), (188-190), (201),
- (214), (221), (223), (226),
- (227), (233), (254), (281),
- (285), (300), (304), (305),
- (311), (314), (322), (328), (335)



## Compliance Certification Application Reference Expansion

---

Conover (91), (289)  
 Consolidation (31), (37), (40), (42), (44), (297)  
 Containment (29), (46), (55), (64), (118),  
     (122), (138), (189), (201),  
     (223), (254), (285), (304)  
 Continental (88), (256), (279), (349)  
 Coons (116)  
 Cooper (199), (212)  
 Corbet (46), (146), (213)  
 Corrosion (58), (100), (108), (124), (135),  
     (147), (148-151), (223),  
     (242), (323), (333)  
 Cosler (356)  
 Costanzo (183), (184)  
 Coupled (29), (47), (349), (357)  
 Cox (127)  
 Cranwell (49), (139), (214), (254)  
 Creep (36), (73), (99), (125), (297), (311),  
     (329), (347)  
 Culebra (2-5), (10), (12), (14-17), (46-48),  
     (72), (76), (82), (96), (97),  
     (110), (111), (125), (128),  
     (131), (134), (135), (136),  
     (138), (175), (176), (177),  
     (180), (204), (212), (213),  
     (216), (217), (242), (243),  
     (263), (267), (290), (291),  
     (295), (312), (313), (319),  
     (344), (352)  
 D'Appolonia (116), (117), (121), (356)  
 Daemen (332)  
 Dale (57), (180), (328)  
 Davies (58), (73), (96), (215), (216), (263),  
     (354), (355)  
 de Marsily (46), (131), (174), (340)  
 Deal (67), (68), (174)  
 Dean (156)  
 Dearlove (218)  
 Deformation (31), (39), (73), (99), (102),  
     (108), (116), (120), (181),  
     (194), (198), (261), (291),  
     (301), (329), (344)  
 Degradation (52), (56), (58), (223), (234),  
     (301)  
 Delakowit (218)  
 Delaware Basin (116), (120), (121), (153),  
     (154), (155), (156), (161),  
     (163), (178), (194), (195),  
     (213), (215), (232), (270),  
     (271), (277), (302), (307),  
     (310), (315), (325), (344)  
 Delaware Mountain (118), (356)  
 density (33-37), (97), (99), (102), (105), (108),  
     (110), (154), (155), (179),  
     (204), (216),  
     (267), (270), (312)  
 Dewey Lake Red beds (4), (12-14), (162),  
     (163), (175), (291)  
 Diffusivity (191)  
 Dike (53)  
 Dissolution (14-16), (51), (52), (56), (76), (83),  
     (84), (111), (116), (154),  
     (155), (159-167), (195),  
     (208), (215), (267), (270),  
     (277), (278), (295), (303),  
     (310), (325), (354-356)  
 Dissolved (58), (59), (82), (110), (111), (117),  
     (154), (155), (156), (164),  
     (166), (201), (202), (278),  
     (354), (356)  
 Disturbed rock Zone (196-198), (265), (301),  
     (311)  
 Dockum (161), (162), (290), (296)  
 Doctor (219)  
 DOE-2 (14-16), (175), (176), (278), (291)  
 DOE/AL/10752-35 (205)  
 DOE/AL/10752-36 (277)  
 DOE/AL/58309-55 (321)  
 DOE/CAO-94-1005 (228)  
 DOE/EIS-0026 (220)  
 DOE/RW-0006 (33), (225)  
 DOE/WIPP-221 (182)  
 Dolomite (2), (4), (5), (11), (14), (15), (46),  
     (76), (96), (97), (110),  
     (111), (125), (131), (135),  
     (138), (175-177), (180),  
     (204), (212), (213), (216),  
     (242), (263), (267), (277),  
     (290), (291), (295), (312),  
     (319), (344), (352)  
 Domski (314), (328)  
 Drez (33-36), (149)  
 Drilling (5), (11), (14), (56), (96), (116-118),  
     (127), (135), (138), (232),  
     (235), (239), (241), (242),  
     (250), (252), (262), (265),  
     (291), (303), (314), (321),  
     (322), (328), (332)  
 dual-porosity (132), (135), (136), (138), (139),  
     (190), (211), (242), (243),  
     (320)  
 Dune (83), (164)  
 Dykhuizen (267)  
 Dynamics (170), (199), (317), (353)  
 Eager (232)  
 Earthquakes (199), (200), (231), (261), (357)  
 EEG-34 (271)  
 EEG-35 (205)



## Compliance Certification Application Reference Expansion

- EEG-36 (277)  
 EEG-55 (321)  
 Ellingson (116)  
 Engwall (203)  
 Ephraums (251), (348)  
 EQ3/6 (354), (355)  
 ERDA 9 (71)  
 ERDA-6 (116-118), (120)  
 ERDA-9 (4), (277)  
 Erosion (2), (55), (154), (158), (160), (166),  
     (194), (270), (296), (315),  
     (345)  
 Evaporite (111), (116), (117), (155), (156),  
     (160), (161), (165), (270),  
     (271), (294), (295), (310),  
     (325), (326), (345)  
 Evaporites (83), (116), (117), (153-155), (158),  
     (161), (162), (163), (165),  
     (178), (181), (252), (270),  
     (277), (279), (294), (302),  
     (303), (325)  
 Excavation (56), (58), (59), (125), (181),  
     (196), (197), (198), (250),  
     (252), (301), (311), (331),  
     (332)  
 Experimental (31), (36), (40), (148), (184),  
     (226), (227), (250), (259),  
     (261), (265), (267), (269),  
     (274), (283), (293), (314),  
     (347)  
 Expert Judgement (133), (138), (139), (142)  
 Exploratory (116), (138), (179), (235), (321),  
     (322), (325)  
 Fairer (291)  
 Fault (50), (52), (53), (200), (231), (261),  
     (294), (315)  
 Flocculation (245), (280)  
 flow (4), (10), (12), (14), (15), (45-48), (50),  
     (51), (53), (58), (59), (73),  
     (96), (97-99), (101-103),  
     (105), (108), (110), (112),  
     (113), (116), (117), (124),  
     (125), (128), (132),  
     (134-136), (154), (155),  
     (170-174), (177), (180),  
     (181), (185), (190), (191),  
     (196-198), (204), (213),  
     (216), (217), (242), (252),  
     (253), (263), (266), (267),  
     (270), (275), (276), (290),  
     (295), (297), (304), (307),  
     (308), (311), (312), (320),  
     (330), (331)  
 fluids (69), (97), (117), (170-172), (174),  
     (181), (196),  
     (235), (341), (356)  
 Flux (45), (97), (112), (131), (132), (134),  
     (216), (284)  
 Fort (315), (328)  
 Fossil (76), (261)  
 Foster (321)  
 fractured (29), (83), (116), (117), (174-176),  
     (211), (246), (266), (270),  
     (276), (320)  
 Francis (234)  
 Fredrickson (324)  
 Freeze (73), (236)  
 Friedman (339)  
 Frydrych (151)  
 Galloway (81)  
 Garber (96)  
 Gard (325)  
 Garner (145), (241), (242)  
 Garrick (92), (127), (139), (244)  
 Gas-Generation (45), (73), (147), (333)  
 Gatuña (81), (82), (164), (303)  
 geologic (14), (16), (49), (51-53), (59), (62),  
     (64), (71), (76), (77), (81),  
     (82), (88), (90), (91), (99),  
     (116), (120), (131), (159),  
     (167), (173), (189), (201),  
     (205), (208), (209), (214),  
     (215), (216), (219), (220),  
     (225), (238), (239), (244),  
     (254), (261), (270), (271),  
     (285), (290), (309), (310),  
     (315), (321), (325), (344),  
     (347), (357)  
 Geology (49), (69), (77), (81), (116), (117),  
     (155), (161-163), (174),  
     (178), (215), (236), (247),  
     (271), (282), (294), (296),  
     (307), (308), (310), (344)  
 geomorphic (164)  
 Geophysical (62), (69), (196-199), (232),  
     (235), (239), (262), (278),  
     (290), (301), (302), (349),  
     (353)  
 Gillow (234)  
 glacial (186), (217), (218), (240), (261)  
 Glanzman (212)  
 Gleitsmann (273), (274)  
 Glenn (319)  
 Gnome (212)  
 Goetz (294)  
 Gomez (96)  
 Gonzalez (2)  
 Gorleben (218)



## Compliance Certification Application Reference Expansion

- Gravity (11), (13), (120), (121), (124), (246), (266), (276), (291)
- Great Plains (296)
- Greenhouse (251), (292), (348)
- Gregory (169), (337), (338)
- Griswold (239), (321)
- groundwater (2), (10), (12), (14), (15), (46), (47), (48), (99), (112), (113), (124), (135), (136), (165), (166), (173), (180), (199), (202), (205), (213), (216), (218), (236), (241), (242), (243), (265), (269), (271), (273-275), (295), (297), (310), (343)
- Grout (224)
- Guadalupe (154), (271)
- Guadalupean (195)
- Guzowski (49), (96), (127), (139), (189), (201), (285)
- Haberman (151)
- Haji-Djafari (356)
- halite (4), (14-16), (45), (58), (59), (81-84), (117), (118), (120), (156), (161), (163), (164), (166), (181), (194), (196), (235), (265), (270), (277), (279), (290), (291), (295), (314), (319), (325), (331), (347)
- Hartman (323)
- Hassinger (179)
- Hawley (203), (208), (213), (303)
- Hays (179), (240), (258), (291)
- Helton (127), (189), (214), (241), (242), (244)
- Hicks (237)
- Hiemenz (245)
- Hill (246), (275), (307)
- Hills (247)
- Hobbs (308)
- Holcomb (248)
- Holocene (261), (290)
- Holt (15), (16), (76), (77), (81-83), (178), (277), (302), (303)
- Hora (132), (133), (139), (249), (250), (322)
- Houghton (251), (348)
- Howard (252), (309), (332)
- Huckleberry Ridge (261)
- Human Intrusion (71), (96), (138), (201), (223), (249), (250), (285), (321), (322)
- Humate (209)
- Humics (209)
- Hunt (202), (223)
- Hunter (96), (127), (188), (253), (254)
- Hydraulics (2)
- Hydrocarbon (116), (179)
- Hydrofracture (29)
- Hydrogen (116), (118), (271), (333)
- Hydrogeology (46), (69), (178)
- Hydrologic (56), (82), (96), (110), (118), (179), (196-198), (201), (215), (235), (238), (239), (253), (265), (267), (285), (290), (291), (314), (327), (328), (356)
- Hydrolysis (168), (339)
- Hydrostatic (39), (125), (179)
- Ibrahim (59), (265)
- Igneous (74), (166), (169), (220), (247)
- Iman (90), (91), (133), (139), (214)
- Imbrie (240), (256-259)
- Immiscible (172)
- Inelastic (329)
- Integrated (90), (117), (123), (132), (219), (225), (228), (253)
- Irving (286-288)
- Isotopes (205-207), (218), (310)
- Iuzzolino (96), (201), (285)
- Ivanovich (218)
- Ives (280)
- Izett (261)
- Jaquette (288)
- Jenkins (251), (348)
- Jensen (252)
- John (168)
- Johnson (74), (166), (287)
- Jones (120), (210), (252), (262), (263)
- Jung (265)
- Jurassic (160), (270)
- Kaplan (92), (127), (139), (244)
- Karst (161-166), (206), (325), (345)
- Kazemi (266), (320)
- Keesey (321)
- Keil (319)
- Kelley (96), (263), (267)
- Kelly (179), (235)
- Kenya Rift (169)
- Key (77), (81), (220), (223), (248), (315), (340), (357)
- Kinetics (149), (184), (273), (355)
- King (210)
- Kirkland (155), (156), (325)
- Klaiber (179)
- Knupp (46)
- Kottowski (247)
- Krieg (329)
- Kudera (34), (35)
- Kues (203), (208), (213), (303)

**Compliance Certification Application Reference Expansion**

---

Kukia (258)  
 Laguna Grande (308), (309)  
 Lagus (331)  
 Lake (4), (12-14), (47), (48), (72), (81-83),  
     (146), (162), (163), (175),  
     (213), (232), (276), (279),  
     (290), (291), (308), (309),  
     (315), (316), (345)  
 Lambert (96), (205), (270), (271), (277), (295)  
 Lang (308), (309)  
 Lantz (327)  
 Lappin (37), (96), (125), (127), (223), (324)  
 Larson (73)  
 Laul (283)  
 Lava Creek (261), (303)  
 LaVenue (97), (131), (204), (323)  
 Ledoux (340)  
 Lee (340)  
 Lenhardt (272)  
 Lie (42), (212), (239)  
 Lieser (273-275)  
 ligands (346)  
 Lightfoot (191)  
 Lin (341)  
 Lipponer (33)  
 Lithofacies (82-84), (302)  
 Little (2), (3), (11), (14), (15), (31), (39), (42),  
     (44), (47), (111), (118),  
     (134), (211), (255), (292),  
     (321), (335), (337)  
 Litvak (276)  
 Llano Estacado (296)  
 Long (1), (3), (12), (46), (58), (64), (67), (68),  
     (73), (96), (108), (110),  
     (111), (112), (114), (118),  
     (122), (127), (138), (147),  
     (166), (184), (186-189),  
     (196), (212), (213),  
     (215-217), (222), (223),  
     (226), (227), (231), (234),  
     (237), (240), (257), (261),  
     (263), (297), (301), (311),  
     (335), (336), (345), (352),  
     (356)  
 Longsine (214)  
 Longworth (218)  
 Lord (145)  
 Los Medaños (239)  
 Love (203), (208), (213), (303)  
 Lowenstein (82), (277-279)  
 Luker (99)  
 Luo (341)  
 Lyklema (280)  
 Lyon (281)

Machette (282)  
 Mackinnon (145)  
 Magenta (2-5), (10-13), (16), (17), (47), (48),  
     (72), (110), (111), (180),  
     (319), (344)  
 Magmatic (56), (169)  
 Magnetic (209), (240)  
 Maiti (283)  
 Malaga (308)  
 Mansure (284)  
 Marietta (96), (125), (127), (131), (189), (201),  
     (223), (244), (285)  
 Marine (258), (261), (279)  
 Marker Bed 139 (181), (194), (314)  
 Martinson (258)  
 McCord (204)  
 McCurley (189), (241)  
 McGrath (286-288)  
 McIntyre (258), (259)  
 McKay (289)  
 McKinney (310)  
 McNutt (72), (279)  
 Mechanical (31), (37), (39), (50), (57), (99),  
     (101), (109), (133), (134),  
     (196), (197), (301), (314),  
     (328)  
 media (60), (170-172), (174), (176), (209),  
     (220), (276), (311)  
 Meehl (349)  
 Mercer (14), (16), (96), (110), (277), (290),  
     (291), (324), (325)  
 Merrill (266)  
 Mesa Falls (261)  
 Mesmer (168)  
 meteoric (83), (117), (154), (205), (270),  
     (271), (279)  
 microbial (58), (124), (135), (147-149), (223),  
     (234), (242)  
 Milankovitch (186), (256-258)  
 Miller (2), (112)  
 Mineral (163), (198), (267), (284), (296),  
     (308), (321), (354), (355)  
 Mitchell (292), (317), (353)  
 Modeling (2), (10), (12), (45), (73), (96), (99),  
     (112), (122), (128), (131),  
     (132), (138), (139), (142),  
     (173), (176), (180), (186),  
     (189), (201), (204), (211),  
     (219), (250), (257), (267),  
     (276), (285), (293), (297),  
     (338), (340), (349), (354), (355)  
 Molecke (157), (293)  
 Monte Carlo (91), (123), (136), (139), (185),  
     (241), (286-289)



**Compliance Certification Application Reference Expansion**

---

Morgan (335) (117), (125),  
 Morley (258) (127), (128),  
 Mucci (346) (133), (134),  
 Muehlberger (294) (136), (144),  
 Myers (295) (154), (172),  
 Nash Draw (3), (15), (16), (111), (159), (162), (174), (175),  
 (164), (176), (205), (216), (177), (181),  
 (253), (270), (271), (303), (190), (196),  
 (344), (345) (198), (199),  
 (223), (242),  
 Neill (321) (246), (267),  
 Newton (354), (355) (268), (277),  
 Nicholson (296) (297), (312),  
 Nowak (96), (297) (314), (320),  
 NUREG/CR-1667 (49) (327), (328), (332)  
 NUREG/CR-2452 (214)  
 NUREG/CR-4510 (254)  
 O'Melia (337)  
 Oceanic (259), (353)  
 Ochoa (153)  
 Ochoan (161-163), (195), (270), (277)  
 OECD (75), (115), (298)  
 Oerlemans (348)  
 Ogallala (158), (160), (166), (296)  
 Oil (140), (171), (173), (211), (232), (246), (266), (296), (320-323)  
 Olsen (116)  
 Orbit (186), (240), (257), (259)  
 Orbital (186), (187), (240), (256-259)  
 Organic (35), (120), (147), (156), (168), (218), (229), (234), (311), (337), (340), (343), (346)  
 ORNL (286-288)  
 ORNL-RSIC-38 (286-288)  
 Orr (110)  
 Ortiz (49), (214)  
 Osborne (339)  
 Ostrowski (341)  
 Oxidation (354)  
 Oxygen (117), (207), (271), (354)  
 Oyenuga (341)  
 Paleohydrology (216)  
 Palmer (314), (327), (328)  
 Palo Duro (283)  
 pan (82-84), (194), (279)  
 Parker (45)  
 Parry (299)  
 Paté-Cornell (300)  
 Patti (31), (109), (133), (134)  
 Pecos (158), (161), (163), (165), (169), (212), (216), (253), (294), (296), (308), (309), (325)  
 Permeability (10), (14), (29), (42), (45), (58), (59), (60), (69), (99-103), (105), (108), (110), (112), (117), (125), (127), (128), (133), (134), (136), (144), (154), (172), (174), (175), (177), (181), (190), (196), (198), (199), (223), (242), (246), (267), (268), (277), (297), (312), (314), (320), (327), (328), (332)  
 Permian (46), (110), (117), (153), (156), (158), (159), (160-163), (165), (166), (167), (195), (212), (232), (265), (270), (271), (277), (279), (290), (310), (312), (315), (325), (344)  
 Peschke (274)  
 Peterson (252), (331)  
 petrographic (278)  
 Pfeifer (198), (301)  
 Phenomena (49-53), (55), (75), (115), (142), (143), (170), (171), (191), (227), (305), (340), (347)  
 Physiographic (296)  
 Pickens (96), (180), (204), (263)  
 Pierce Canyon (344), (345)  
 Pipes (69), (84), (154), (163), (165), (215), (325), (326)  
 Piasis (258)  
 Pitzer (354), (355)  
 pleistocene (46), (83), (159-162), (164), (165), (213), (217), (240), (256), (257), (258), (259), (261), (295), (344)  
 Pliocene (158), (160), (166), (261)  
 Plutonium (183), (184)  
 Polyhalite (194), (198), (279)  
 polymer (183), (184), (245), (339)  
 polymerization (183), (184), (339)  
 Popielak (116)  
 porous (2), (60), (117), (170-172), (174), (176), (185), (273), (310), (332)  
 Porterfield (266)  
 postclosure (74), (219), (343)  
 Potash (71), (72), (140), (163), (239), (253), (262), (279), (308), (321)  
 Potassium (118)  
 Powers (15), (16), (76), (77), (81-83), (178),



## Compliance Certification Application Reference Expansion

- (261), (277),  
 (302), (303),  
 (307), (310),  
 (321), (325)  
 precipitation (117), (134), (135), (183), (206),  
 (253), (273), (292), (317),  
 (349), (355)  
 Prell (258)  
 probabilities (51), (55), (122), (124), (128),  
 (138), (139), (189), (201),  
 (241), (244), (249), (250),  
 (254), (285), (300), (321),  
 (322)  
 Quasistatic (329)  
 Quaternary (162), (186), (212), (259), (282),  
 (294), (296), (345)  
 Radar (196)  
 Radioactive (1), (31), (49), (64-67), (69), (71),  
 (75), (77), (88), (90), (91),  
 (99), (112), (114-116),  
 (122), (127), (138), (142),  
 (155), (173), (174), (188),  
 (189), (201), (208),  
 (214-216), (219), (220),  
 (222), (223), (225), (241),  
 (244), (254), (265), (273),  
 (274), (275), (285), (298),  
 (304), (310), (335), (340),  
 (347)  
 Radiocolloid (275), (343)  
 Radiological (70), (142), (143), (281)  
 Radiolysis (223)  
 radiometric (303)  
 radionuclides (46), (50-53), (65), (70), (96),  
 (114), (124), (125), (136),  
 (138), (201), (202), (205),  
 (208), (209), (216), (218),  
 (223), (227), (242), (254),  
 (255), (273-275), (277),  
 (283), (285), (321), (340),  
 (343)  
 Railroad (308)  
 Ramey (323)  
 Read (124)  
 Rechar (96), (189), (201), (242), (244), (285),  
 (304), (305), (335)  
 Recharge (14), (46), (47), (118), (131), (132),  
 (134), (135), (165), (173),  
 (205), (206), (217), (271),  
 (295), (296)  
 Reeves (96), (97)  
 Regional (2), (46), (55), (83), (131), (154),  
 (161), (163), (195), (213),  
 (216), (253), (270), (272),  
 (282), (302),  
 (321), (323),  
 (334), (345)  
 Register (64), (66), (67), (69), (71)  
 Rehfeldt (277)  
 Reiter (284)  
 Repositories (64), (75), (88), (90), (173),  
 (174), (196), (254), (310),  
 (325), (334), (347)  
 reservoirs (116-118), (174), (198), (208),  
 (211), (246), (266), (270),  
 (276), (320)  
 Resistivity (62), (196), (198), (267)  
 Resource (143), (173), (212), (239), (311),  
 (322)  
 Reynolds (171)  
 RH-TRU (228), (229), (293)  
 Richardson (211), (246), (320)  
 Richey (306)  
 Riley (199)  
 Rio Grande (294)  
 Risk (49), (51), (55), (92-94), (122), (123),  
 (127), (136), (137), (139),  
 (142), (155), (214), (219),  
 (221), (241), (244), (300),  
 (325), (342)  
 Roberts (29), (314), (328)  
 Robinson (96), (295), (307-309)  
 Roeloffs (199)  
 Room (31), (37), (40), (42), (44), (45), (73),  
 (124), (147), (248), (252),  
 (293), (301), (314), (332),  
 (351)  
 Rosholt (310)  
 Rubidium (283)  
 Rudeen (189), (241), (242), (334)  
 Runkle (214)  
 Rustler (2), (4), (5), (10), (12-17), (46), (48),  
 (72), (76), (81-83), (110),  
 (111), (118), (131), (135),  
 (138), (161-164), (175),  
 (176), (177), (180), (195),  
 (205), (208), (212), (213),  
 (216), (232), (242), (263),  
 (265), (267), (270), (271),  
 (277), (278), (290), (291),  
 (295), (302), (312), (319),  
 (344), (345), (352)  
 Salado (4), (15), (16), (45), (46), (58), (59),  
 (61), (62), (72), (76), (77),  
 (81), (82), (110), (111),  
 (116), (127-129), (136),  
 (154), (156), (161), (163),  
 (175), (179), (181), (194),



## Compliance Certification Application Reference Expansion

---

<p>(195), (205),          (208), (212),          (232), (239),          (242), (252),          (253), (265),          (270), (277),          (279), (291),          (310), (311),          (314), (323),          (325), (328),          (333), (344), (345)</p> <p>saline (81), (82), (212), (218), (279), (296),          (323)</p> <p>Salt/Bentonite (40)          Saltzman (258)          SANCHO (40), (73), (329)          SAND77-0946 (239)          SAND80-1429 (49)          SAND80-7161 (334)          SAND81-2573 (214)          SAND82-0461 (270)          SAND83-0391 (2)          SAND83-1798 (195)          SAND84-2233 (253)          SAND84-2618 (329)          SAND84-7178 (164)          SAND85-0023 (194)          SAND86-0121 (254)          SAND86-0611 (291)          SAND86-1364 (175)          SAND86-2311 (177)          SAND86-7078 (165)          SAND87-0039 (4)          SAND87-0176 (331)          SAND87-1375 (196)          SAND87-2456 (176)          SAND87-2833 (304)          SAND87-7036 (319)          SAND87-7124 (312)          SAND87-7144 (62)          SAND87-7166 (327)          SAND88-0196 (295)          SAND88-1065 (238)          SAND88-1314 (293)          SAND88-2230c (197)          SAND89-0178 (188)          SAND89-0200 (290)          SAND89-0462 (96)          SAND89-2027 (201), (285)          SAND89-7055A (301)          SAND89-7068 (204)          SAND90-0083 (181)          SAND90-0355 (297)          SAND90-1206 (31), (133), (134)</p>	<p>SAND90-1685A (198)          SAND90-1983 (305)          SAND90-2347 (189)          SAND90-2368C (99)          SAND90-2399C (351)          SAND90-3063 (250)          SAND90-3134 (332)          SAND90-3246 (58)          SAND90-7000 (314)          SAND90-7011 (267)          SAND90-7103 (241)          SAND91-0893 (122), (242)          SAND92-0700 (138), (249)          SAND92-1172 (252)          SAND92-1579 (263)          SAND92-1933 (311)          SAND92-2285 (244)          SAND92-7072 (328)          SAND92-7340 (341)          SAND92-7347 (333)          SAND93-1318J (213)          SAND93-2330 (335)          SAND93-7036 (234)          Saulnier (14), (181), (267), (312), (314), (327),          (328)          Schiel (81), (315)          Schlesinger (317)          Schreiber (145), (189)          Sea Level (55), (120), (121), (207), (251),          (279), (348)          Sedimentary (15), (76), (82), (160), (166),          (261), (265), (277), (278),          (303)          Sedimentation (55), (81), (117), (156), (194)          Sedimentology (302)          Sediments (64), (76), (220), (261), (273-275),          (282), (296), (310)          Seismicity (272)          Senseny (120)          Swards (319)          Shackelton (207)          Shaffer (195)          Shinta (145), (320)          Shortencarier (214)          Siegel (96), (295)          Siliciclastic (279)          Silva (321), (322)          Simulated (31), (32), (39), (46), (47), (73),          (99), (100), (101), (109),          (128), (133), (134), (180),          (213), (217), (292), (293),          (314), (317), (333), (335),          (353)          Singh (275)</p>
---	---



## Compliance Certification Application Reference Expansion

- single-porosity (4-6), (11-13), (132), (136),  
(139), (180), (211), (242),  
(263), (320)
- SITE-94 (141)
- Skokan (198), (301)
- Slezak (324)
- Smith (283)
- Snider (156)
- Snow (292), (356)
- Snyder (15), (16), (277), (290), (291), (325)
- Soils (59), (60), (172), (209), (229), (282)
- Solado (4), (124), (125)
- Solubility (148), (183), (241), (265), (310),  
(340), (344), (346), (354),  
(355)
- Solutes (185), (319)
- Spatial (4), (97), (128), (131), (185), (245),  
(259), (303), (329)
- SPE 13537 (246)
- SPE 18427 (211)
- SPE 26636 (320)
- Stability (40), (112), (117), (166), (186), (280),  
(284), (297), (337), (346),  
(352)
- Starett (301)
- Steinkopff (273), (274)
- Stenhouse (141)
- Stensrud (10-13), (314), (327), (328)
- Stewart (191)
- Stingl (275)
- Stone (40), (73), (329)
- Stormont (196), (197), (330-332)
- stratigraphy (45), (179), (195), (235), (247),  
(252), (277), (278)
- Stress (15), (31), (32), (36), (37), (39), (40),  
(42), (56), (99), (101),  
(102), (105), (108), (154),  
(157), (159), (176), (194),  
(198), (265), (347), (357)
- strontium (283)
- Structures (15), (76), (82), (120), (154), (155),  
(195), (209), (215), (231),  
(245), (278), (282), (294),  
(303)
- Subpart B (64-68), (122), (138), (188), (189),  
(201), (242), (244), (285)
- subsidence (15), (55), (56), (71), (111), (158),  
(159), (166), (173), (215),  
(271), (315), (352)
- Sulfur (192)
- Sumerling (75), (141)
- Surface Water (253)
- Surficial (55), (158), (164), (234), (290), (310),  
(344)
- Swenson (166)
- Swift (134), (189), (237), (242), (263)
- Tadros (337), (338)
- TDEM (62)
- tectonic (118), (166), (169), (256), (294), (315)
- Tectonism (166), (357)
- Telander (148), (149), (151), (333)
- Terrestrial (88)
- Textures (81-84), (278), (307), (319)
- Thomas (59), (246)
- Thompson (31), (99), (109), (133), (134)
- Thorium (218), (283), (310)
- Thorne (142), (334)
- Thybusch (275)
- Tierney (30), (335)
- Tiller (337)
- Tillerson (297)
- Tipping (338)
- TME 3166 (356)
- Tomography (265)
- Tornado (221)
- Torres (297)
- Tóth (339)
- Tracer (174), (263), (290), (320), (330), (331)
- Trachyte (169)
- trans-Pecos (169), (294)
- Transient (46), (47), (97), (204), (217), (266)
- Transmissivity (4-6), (10-17), (110), (111),  
(131), (175-177), (180),  
(313)
- transport (2), (14), (48), (50-53), (55), (69),  
(96), (97), (98), (112),  
(124), (132), (135), (136),  
(138), (139), (174), (185),  
(190), (191), (196), (202),  
(205), (216), (218), (241),  
(242), (243), (254), (263),  
(264), (267), (277), (283),  
(311), (320), (325), (340),  
(343), (349), (350)
- Transuranic (31), (46), (58), (64-66), (69),  
(71), (77), (99), (101),  
(122), (127), (138), (148),  
(178), (188), (189), (201),  
(208), (222), (223), (225),  
(226), (228), (234), (244),  
(265), (277), (285), (293),  
(304), (321), (336), (352)
- Transverse (185)
- Trauth (250)
- Triassic (46-48), (83), (159), (161), (162),  
(212), (270), (290), (296),  
(315), (316), (344)
- Tsang (174)



## Compliance Certification Application Reference Expansion

---

Two-Phase (45), (128), (266), (311), (320)  
UCRL-MA-110662 (354), (355)  
Upton (263)  
Uranium (64), (218), (225), (261), (283), (310)  
USGS (2), (199)  
van der Lee (340)  
Van Horn (294)  
VanBuskirk (31)  
Variable-Density (216)  
varved (156)  
Vaughn (145), (189)  
Velocity (97), (120), (191), (216), (248), (265)  
Vertical (4), (5), (10), (15), (32), (40), (46),  
(47), (48), (71), (82), (110),  
(111), (120), (213), (216),  
(238), (247), (267), (279),  
(292), (293), (295), (307),  
(314), (325), (330)  
Vilks (343)  
Vine (325), (344)  
Vlassopoulos (346)  
von Winterfeldt (250)  
Wallace (146), (213)  
Wallner (347)  
Warrant (37), (135)  
Warrick (348)  
Washington (64), (66), (69), (71), (203), (210),  
(212), (220), (233), (261),  
(349)  
Washington Ranch (203)  
water (2), (5), (12), (14), (17), (30), (32), (35),  
(46), (47), (48), (50), (53),  
(58), (64), (66-68), (70),  
(81), (83), (96), (97), (101),  
(110), (111), (118), (120),  
(121), (124), (135), (140),  
(154), (155), (161), (163),  
(164), (167), (168), (170),  
(171), (172-174), (176),  
(185), (190), (196), (199),  
(204), (205), (206), (208),  
(210), (212), (213), (216),  
(231), (246), (253), (254),  
(259), (263), (265-267),  
(270), (277), (279), (281),  
(290), (292), (295), (296),  
(306), (308), (309), (317),  
(319), (320), (322), (323),  
(325), (327), (337), (352),  
(355)  
Wawersik (29)  
Weart (321), (322)  
Weatherby (42), (124), (351)  
Webb (45)  
Wells (2), (4), (5), (10-12), (17), (56), (110),  
(117), (118), (131), (140),  
(173), (175-177), (180),  
(195), (199), (212), (238),  
(278), (281), (290), (306),  
(312), (313), (322), (323),  
(327)  
West (3), (15), (111), (131), (153), (156),  
(157), (164), (169), (175),  
(176), (203), (208), (213),  
(216), (218), (252), (261),  
(270), (271), (277), (294),  
(295), (303), (307), (308),  
(313), (314), (316)  
Westerman (148), (149), (151), (333)  
Westgate (261)  
Wilcox (261)  
Wilson (353)  
Wind (221)  
Wolery (354), (355)  
Wood (35), (99), (100), (346), (356)  
WTSD-TME-020 (179)  
WTSD-TME-038 (76)  
Yucca (219), (343)  
Zeh (218)  
Zeman (266)  
Zoback (357)

